

Metabolic efficiency in remodeled failing hearts

by

Waleed Gameel Tawfeek Masoud

A thesis submitted in partial fulfillment of the requirements for the degree of

Doctor of Philosophy

Department of Pharmacology
University of Alberta

© Waleed Gameel Tawfeek Masoud, 2015

Abstract

Heart failure is a serious cardiovascular disease that develops following a variety of insults to the heart including hypertrophy and myocardial infarction. While it is clear that heart failure is associated with changes in cardiac energy metabolism, it remains unclear if, and how, such changes might contribute to left ventricular (LV) contractile dysfunction. Two distinct hypotheses have been advanced to link changes in energy metabolism with heart failure: 1) there is a state of energetic crisis / starvation, where rates of energy metabolism decrease and thereby cause LV failure, or 2) there is inefficiency in energy utilization where more energy is required to produce external work. Inefficiency may be due to mismatched rates of glycolysis and glucose oxidation that leads to intracellular proton accumulation resulting in Na^+ and Ca^{2+} overload. Recently, drug-induced modulation of rates of carbohydrate and fat metabolism has been proposed as a new approach for the treatment of LV dysfunction and heart failure. Such metabolic modulation can also be achieved experimentally by the use of genetically-modified experimental animals. This thesis compared the metabolic profile of remodeled post-infarction mouse hearts with normal hearts, studied the response of these hearts to *ex vivo* ischemia reperfusion (IR) and the ability of metabolic modulation to limit the deterioration of metabolic efficiency and LV dysfunction following myocardial infarction.

Using coronary artery ligation, we created a mouse model of post-infarction remodeled heart failure that we verified using *in vivo* echocardiographic examination. Using *ex vivo* heart perfusion in the isolated working mode, we

provided evidence that CAL hearts are metabolically inefficient rather than energy starved and that mismatched glucose metabolism is a possible contributor to metabolic inefficiency.

Using malonyl CoA decarboxylase deficient (MCD-KO) mice that are known to have better matching of glucose metabolism, we confirmed that this metabolic intervention improved glucose matching, metabolic efficiency and limited functional deterioration in CAL hearts.

We also studied the response of CAL hearts to *ex vivo* IR. We showed that CAL hearts have better functional recovery and limited functional deterioration following IR in comparison to SHAM hearts. This was associated with reduced ischemic glycogenolysis, lack of acceleration in fatty acid oxidation during reperfusion and increased triacylglycerol accumulation in reperfused CAL hearts. We provided evidence that mitochondrial mass, Ca²⁺ handling proteins and AMPK activity are unchanged and are unlikely to contribute to the observed response of CAL hearts to IR.

This thesis also studied the potential for further protection of CAL hearts after IR via pharmacologic improvement of the match of glucose oxidation using dichloroacetate (DCA). We showed that in presence of lactate, DCA did not stimulate glucose oxidation, improve functional recovery or improve the match of glucose metabolism. We also showed that in absence of lactate, DCA was able to stimulate glucose oxidation but this was not enough to improve the matching of glucose metabolism. This thesis also discussed differences between mouse and rat

heart metabolism that may explain the lack of response to DCA in mouse hearts. Similarly, we studied the possible improvement of metabolic efficiency in CAL hearts via acute *ex vivo* MCD inhibition but this acute intervention was not sufficient to produce benefit.

Preface

This thesis is an original work by Waleed GT. Masoud. The research projects, of which this thesis is a part, received research ethics approval from the University of Alberta Research Ethics Board as follows:

1. Study Title “Cardioprotective mechanisms in rat hearts”, Study ID: AUP00000239, Study Investigator: Alexander S. Clanachan.

2. Study title “Protection of the ischemic myocardium and Breeding Colony”, Study ID: AUP00000288, Study investigator: Gary D. Lopaschuk.

Dedication

This thesis is dedicated to my wife, Diana Masry, my two daughters Anastasya Masoud and Theodora Masoud, my mother Dr. Afifa AG. Alam and my father Dr. Gameel T. Masoud.

Acknowledgements

I would like to thank Dr. Alexander S. Clanachan for giving me the chance to pursue my graduate studies in his laboratory. Dr. Clanachan adopts an open-door policy. He was always there for me to discuss trends in research, my results or even personal issues. I enjoyed his excellent mentorship that gave me confidence that I can achieve my career goals.

Thanks also go to my co-supervisor, Dr. Gary D. Lopaschuk. I was able to attend his weekly laboratory meetings and to be part of active scientific discussions about relevant research trends. Dr. Lopaschuk opened the door for me to take part of many volunteer activities that enriched my experience.

I would also like to thank the members of my supervisory committee, Dr. Peter E. Light and Dr. Zamaneh Kassiri for their constructive advice, encouragement and feedback during my graduate studies.

Thanks to Dr. Fikry H. Osman from the Department of Pharmacology, Faculty of Medicine, Assiut University, Egypt who encouraged me to apply for graduate studies at University of Alberta. His sincere advice and extensive experience helped me prepare for the study in Canada.

Thanks to my colleague Dr. Manoj Gandhi who taught me how to master isolated working mouse heart perfusions, metabolic assays and to calculate all the derived metabolic and functional parameters. He was a role-model for accuracy and being meticulous in doing experiments.

Thanks to the current and previous members of Dr. Clanachan and Dr. Lopaschuk's laboratories. Special thanks go to Dr. Mohamed A. Omar for

teaching me how to perform immunoblots. Thanks also to Dr. Wei Wang for teaching me how to master coronary artery ligation surgery in mice.

Thanks to my wife, Diana RN. Masry for her sincere love and support, for always supporting and encouraging me, for her active listening to my complaints about results that were not expected, experiments that did not work and studentship applications that were not accepted, for being patient and supportive when I had to work weekends and to stay late evenings to finish my experiments. Thanks to my two daughters, Anastasya Masoud and Theodora Masoud for the joy and cheer they gave to me and for being a big motivation for me to finish my studies to be able to spend more time with them.

Thanks to My father, Dr. Gameel T. Masoud and my mother, Dr. Afifa AG. Alam for their continuous support and prayers, for always believing in me and for rooting in me the principals and values that formed the person I am today.

Thanks to all the teachers, professors and friends here in Edmonton and back in Assiut, Egypt who motivating me to learn and achieve my goals.

Thanks to the Coptic Orthodox Christian Church back in Egypt and here in Canada for rooting the fundamentals of faith in me that helped me come over all the difficult times while doing my graduate studies.

Thanks to the funding agencies that provided financial support so that I can complete my graduate studies: Mazankowski Alberta Heart Institute, Queen Elizabeth Doctoral Studentship, Faculty of Graduate Studies and Research and the Department of Pharmacology, Faculty of Medicine and Dentistry.

Table of contents

1	Introduction	1
1.1	Heart failure.....	2
1.1.1	Definition, different etiologies and compensatory mechanisms.....	2
1.1.2	The frequently used animal models of heart failure	2
1.2	Cardiac metabolism.....	3
1.2.1	Normal cardiac metabolism	3
1.2.1.1	Cardiac energy demand.....	3
1.2.1.2	Energy substrate utilization and generation of ATP	4
1.2.1.2.1	Energy substrate delivery	5
1.2.1.2.1.1	Glucose delivery.....	5
1.2.1.2.1.2	Fatty acid delivery.....	5
1.2.1.2.2	Energy substrate utilization	6
1.2.1.2.2.1	Glycolysis.....	7
1.2.1.2.2.2	Fatty acid β -oxidation.....	8
1.2.1.2.2.3	Glucose oxidation.....	11
1.2.1.2.2.4	Mutual regulation between fatty acid oxidation and glucose oxidation: The Randle cycle.....	12
1.2.1.2.3	Oxidative phosphorylation for ATP production	14
1.2.1.2.4	ATP transfer and phosphocreatine/creatine kinase shuttle	14
1.2.2	Metabolic phenotype in heart failure	16

1.2.2.1	Metabolic inefficiency in heart failure	16
1.2.2.1.1	Contributors to metabolic inefficiency in heart failure.....	17
1.2.2.1.1.1	Increased oxygen cost of ATP production due to an increased dependence on fatty acids.....	17
1.2.2.1.1.2	Uncoupled oxidation-phosphorylation at TCA cycle.....	19
1.2.2.1.1.3	Futile cycling in the heart.....	20
1.2.2.1.1.4	Reversion to fetal glycolytic metabolism favors mismatched glucose metabolism and the subsequent higher energy cost of ionic homeostasis	22
1.2.2.1.1.5	Impaired energy transfer to myofibrils: consequences of compromised phosphocreatine/creatine kinase shuttle.....	25
1.2.2.1.2	Proof of principle for cardiac metabolic inefficiency	27
1.2.2.2	Energy starvation in heart failure	30
1.2.2.2.1	Reduced oxygen and energy substrate supply to the heart	30
1.2.2.2.2	Reduced energy substrate uptake and utilization.....	31
1.2.2.2.3	Reduced oxidative phosphorylation	34
1.3	Cardiac ischemia reperfusion injury	35
1.3.1	Definition, causes and mechanisms	35
1.3.2	Metabolic profile in IR.....	36
1.3.2.1	Anaerobic glycolysis and disturbed intracellular ionic homeostasis	36
1.3.2.2	Mitochondrial oxidative metabolism	39

1.3.2.3	Response of remodeled hearts to IR.....	40
1.3.3	Pharmacologic metabolic interventions to improve cardiac metabolic inefficiency	41
1.3.3.1	MCD inhibition limits metabolic inefficiency and functional deterioration in heart failure.....	42
1.3.3.2	DCA as a protective agent against ischemia reperfusion injury and heart failure	43
1.3.3.2.1	Linking DCA-induced glucose oxidation to changes in fatty acid oxidation and glycolytic flux rates	47
1.3.4	Conclusion	47
1.3.5	Hypothesis and Objectives.....	49
1.3.5.1	Hypothesis.....	49
1.3.5.1.1	Specific Objectives	50
2	Materials and Methods	58
2.1	Materials.....	59
2.2	Methods.....	61
2.2.1	Mouse model of post-infarction heart failure:	61
2.2.2	<i>In vivo</i> evaluation of heart function by echocardiography:	62
2.2.3	<i>Ex vivo</i> isolated working heart perfusions:	63
2.2.4	Measurement of LV function.....	64
2.2.5	Measurement of rates of energy substrate metabolism and calculation of ATP production rates:.....	65

2.2.6	Measurements of glycogen content and turnover:	67
2.2.7	Measurements of TG content and turnover:	68
2.2.8	Immunoblot analysis of protein expression:	69
2.2.9	Measurement of adenine nucleotide and creatine content in frozen heart tissue:	70
2.2.10	Statistical analysis:	71
3	Failing mouse hearts utilize energy inefficiently and benefit from improved coupling of glycolysis and glucose oxidation	74
3.1	Introduction	75
3.2	Methods	76
3.3	Results	76
3.3.1	CAL hearts have lower mechanical function	76
3.3.2	CAL hearts are not energetically starved	77
3.3.3	CAL hearts are inefficient	78
3.3.4	MCD-KO CAL hearts have better function than WT CAL hearts .	79
3.3.5	Inefficiency is lessened in MCD-KO CAL hearts	80
3.4	Discussion	82
	Conclusion	87
4	Tolerance to ischemic injury in remodeled mouse hearts: less ischemic glycogenolysis and preserved metabolic efficiency	109
4.1	Introduction	110
4.2	Methods	112

4.3	Results	112
4.3.1	CAL hearts have lower <i>in vivo</i> function	112
4.3.2	CAL hearts are not energy starved during post-ischemic reperfusion.....	113
4.3.3	CAL hearts undergo less deterioration in metabolic efficiency during reperfusion.....	114
4.3.4	Endogenous substrate utilization during ischemia and reperfusion.....	115
4.3.5	Abundance of mitochondrial markers and key metabolic enzymes.....	115
4.4	Discussion	116
4.5	Conclusion.....	122
5	Study of the possible cardioprotective effect of pharmacologic modulation of cardiac energy substrate metabolism	143
5.1	Introduction	144
5.2	Methods.....	147
5.2.1	Measurement of short chain CoA esters in heart tissues	148
5.3	Results	149
5.3.1	Treatment with DCA at reperfusion	149
5.3.1.1	Pre- and post-ischemic function of untreated remodeled hearts	149
5.3.1.2	The effect of reperfusion DCA treatment on SHAM and CAL hearts.....	150

5.3.1.2.1	Post-ischemic functional recovery.....	150
5.3.1.2.2	Energy substrate metabolism and ATP production	150
5.3.1.2.3	Reperfusion metabolic efficiency	151
5.3.1.3	The effect of reperfusion DCA treatment on healthy (non-SHAM) hearts	153
5.3.1.3.1	Post-ischemic functional recovery.....	153
5.3.1.3.2	Energy substrate metabolism and ATP production	153
5.3.1.3.3	Reperfusion metabolic efficiency	153
5.3.1.4	Effect of absence of lactate on response to DCA treatment of healthy hearts	154
5.3.2	Treatment with MCDi during aerobic perfusion	155
5.3.2.1	LV function:	155
5.3.2.2	Metabolic rates:	155
5.3.2.3	Malonyl CoA content:	155
5.4	Discussion	156
5.4.1	Response to reperfusion with DCA treatment	156
5.4.1.1	Contribution of the chemical composition of the perfusate to the sensitivity of mouse hearts to DCA	158
5.4.1.2	Species-dependent difference in the sensitivity to DCA.....	160
5.4.2	Response to aerobic MCD inhibition.....	161
5.5	Conclusion.....	165

6	General Discussion and Conclusions	194
6.1	Experimental model and methods	197
6.1.1	Coronary artery ligation in the mouse	197
6.1.2	Isolated working mouse heart perfusions	200
6.1.3	Measurement of energy substrate metabolism.....	204
6.1.4	Pros and cons of the use of ³ H- and ¹⁴ C- radiolabeled substrates .	205
6.2	Aerobic metabolic profiling of CAL hearts	207
6.3	Improved coupling of glucose metabolism limits metabolic inefficiency and mechanical dysfunction in CAL hearts	209
6.4	Remodeled hearts exhibit no further deterioration of mechanical function and metabolic efficiency following <i>ex vivo</i> ischemia reperfusion	211
6.5	Reperfusion DCA administration does not stimulate glucose oxidation or improve functional recovery	214
6.5.1	Contribution of the chemical composition of the perfusate to the sensitivity of mouse hearts to DCA.....	215
6.5.2	Species-dependent difference in the sensitivity to DCA	216
6.6	Despite effective MCD inhibition, metabolic inefficiency is not improved in MCDi-treated CAL hearts	217
6.7	Conclusion.....	220
7	Future directions	222
7.1	Limiting metabolic inefficiency and mechanical dysfunction following CAL surgery via chronic MCD inhibition	223

7.2	Study of the acetylation control of fatty acid oxidation in remodeled hearts	224
7.3	Stimulation of pentose phosphate pathway to lessen cardiac post-infarction functional and metabolic deterioration	227
8	References	230

List of tables

Table 3.1 <i>In vivo</i> echocardiographic and <i>ex vivo</i> hemodynamic parameters of CAL and SHAM hearts.....	105
Table 3.2 <i>In vivo</i> echocardiographic and <i>ex vivo</i> hemodynamic parameters of WT-CAL and MCD-KO CAL hearts.....	106
Table 3.3 Adenine nucleotide, inosine and creatine content in CAL and SHAM hearts.....	107
Table 3.4 Immunoblot analysis of protein expression of mitochondrial abundance and key metabolic regulatory enzymes.....	108
Table 4.1 Detailed echocardiographic parameters of SHAM and CAL hearts...	139
Table 4.2 Detailed <i>ex vivo</i> hemodynamic parameters of SHAM and CAL hearts.	141
Table 4.3 End reperfusion nucleotide, nucleoside and creatine contents.	142
Table 5.1 <i>In vivo</i> echocardiographic assessment of function of SHAM and CAL hearts.	188
Table 5.2 <i>Ex vivo</i> hemodynamic parameters of SHAM and CAL hearts.	190
Table 5.3 <i>Ex vivo</i> hemodynamic parameters of normal healthy hearts.	191
Table 5.4 <i>Ex vivo</i> hemodynamic parameters of aerobically-perfused normal healthy hearts.	192
Table 5.5 <i>Ex vivo</i> hemodynamic parameters of aerobically-perfused SHAM and CAL hearts: Effect of MCDi.....	193

List of figures

Figure 1.1 Relationship between glycolysis, glucose oxidation and fatty acid oxidation	51
Figure 1.2 Energy metabolic changes in heart failure.	54
Figure 1.3 Normal versus mismatched glucose metabolism.	56
Figure 2.1 Schematic representation of methods	72
Figure 3.1 Assessment of mechanical function of CAL and SHAM hearts.	89
Figure 3.2 Rates of exogenous energy substrate metabolism in SHAM and CAL hearts.	91
Figure 3.3 Rates of exogenous energy substrate metabolism in SHAM and CAL hearts normalized for LV work.....	93
Figure 3.4 Rates of endogenous energy substrate metabolism in SHAM and CAL hearts.	95
Figure 3.5 Rates of endogenous energy substrate metabolism in SHAM and CAL hearts normalized for LV work.....	97
Figure 3.6 Assessment of cardiac function of WT CAL and MCD-KO CAL hearts.	99
Figure 3.7 Rates of exogenous energy substrate metabolism in WT CAL and MCD-KO CAL hearts.....	101
Figure 3.8 Rates of exogenous energy substrate metabolism in WT CAL and MCD-KO CAL hearts normalized for LV work.....	103
Figure 4.1 In vivo echocardiographic functional assessment.	123

Figure 4.2 <i>Ex vivo</i> assessment of mechanical function and hemodynamic parameters.....	125
Figure 4.3 Rates of energy substrate metabolism in SHAM and CAL hearts.	127
Figure 4.4 Metabolic rates per LV work of SHAM and CAL hearts.	129
Figure 4.5 Contents and change of endogenous energy substrates in SHAM and CAL hearts.....	131
Figure 4.6 Phosphorylation status (pAMPK/tAMPK) of AMPK.....	133
Figure 4.7 Protein expression of markers of mitochondrial biogenesis and abundance and calcium handling proteins.....	135
Figure 4.8 Protein expression of key metabolic enzymes.....	137
Figure 5.1 <i>In vivo</i> echocardiographic assessment of LV function in SHAM and CAL hearts.....	167
Figure 5.2 <i>Ex vivo</i> assessment of LV mechanical function of SHAM and CAL hearts.....	169
Figure 5.3 Rates of energy substrate metabolism in SHAM and CAL hearts.	171
Figure 5.4 Metabolic rates per LV work of SHAM and CAL hearts.	173
Figure 5.5 <i>Ex vivo</i> assessment of LV mechanical function of normal healthy hearts.....	175
Figure 5.6 Rates of energy substrate metabolism in unremodeled hearts treated by DCA at reperfusion.....	177
Figure 5.7 Rates of energy substrate metabolism per LV work in normal healthy hearts.....	179

Figure 5.8 <i>Ex vivo</i> assessment of LV mechanical function and metabolic rates of aerobically-perfused normal healthy hearts: Effect of DCA in presence or absence of lactate.....	181
Figure 5.9 <i>Ex vivo</i> assessment of LV mechanical function of aerobically-perfused CAL and SHAM hearts: Effect of MCDi.	183
Figure 5.10 Rates of energy substrate metabolism SHAM and CAL hearts: Effect of MCDi.....	185
Figure 5.11 Change in cardiac malonyl CoA content in SHAM and CAL hearts: Effect of MCDi.	187

List of abbreviations

Term	Meaning
A	Late mitral inflow velocities
ACBP	Acyl CoA binding protein
ACC	Acetyl CoA carboxylase
ACC2 KO	Acetyl CoA carboxylase 2 knockout
ADP	Adenosine diphosphate
AMP	Adenosine monophosphate
AMPK	AMP-dependent kinase
ANOVA	Analysis of variance
ATP	Adenosine triphosphate
BPG	Bisphosphoglycerate
BSA	Bovine serum albumin
CAL	Coronary artery ligation
CAMKII	Ca ²⁺ /calmodulin-dependent protein kinase II
CAT	Carnitine acetyl transferase
CK	Creatine kinase
CPT1	Carnitine palmitoyl transferase I
Cr	Creatine
CT	Carnitine translocase
CVC	Coronary vascular conductance
DCA	Dichloroacetate

List of abbreviations (cont.)

Term	Meaning
E'	Mitral annular early diastolic velocity
EF	Ejection fraction
ET	Ejection time
F-2,6-bp	Fructose-2,6-bisphosphate
F-6-P	Fructose-6-phosphate
FABP	Fatty acid binding protein
FAC	Fractional area change
FACS	Fatty acyl CoA synthase
FADH ₂	Flavine adenine dinucleotide
FFA	Free fatty acids
GAPDH	Glyceraldehyde 3-phosphate dehydrogenase
GI	Global no flow ischemia
GLUT1	Glucose transporter1
GLUT4	Glucose transporter4
GSK3 β	Glycogen synthase kinase β
GTP	Guanosine triphosphate
G-6-PD	Glucose-6-phosphate dehydrogenase
HK	Hexose kinase
IP	Intraperitoneal
IR	Ischemia reperfusion injury

List of abbreviations (cont.)

Term	Meaning
IVCT	Isovolumetric contraction time
IVRT	Isovolumetric relaxation time
IVSd	Interventricular septal thickness at the end of diastole
IVSs	Interventricular septal thickness at the end of systole
LCAD	Long chain fatty acyl CoA dehydrogenase
LDH	Lactate dehydrogenase
LDH-A	Lactate dehydrogenase-A
LV	Left ventricle
LVIDd	Left ventricular internal dimension at the end of diastole
LVIDs	Left ventricular internal dimension at the end of systole
LVPWd	Left ventricular posterior wall thickness at the end of diastole
LVPWs	Left ventricular posterior wall thickness at the end of systole
MCD	Malonyl CoA decaeboxylase
MCDi	MCD inhibitor (CMB-0000382)
MCD-KO	Malonyl CoA decarboxylase knock out
MCT	Monocarboxylic acid transporter
miCK	Mitochondrial creatine kinase
MM-CK	Myofibrillar creatine kinase
mPTP	Mitochondrial permeability transition pore
MV DT	Mitral valve deceleration time

List of abbreviations (cont.)

Term	Meaning
MVO ₂	Oxygen consumption
NADH	Nicotinamide adenine dinucleotide
NBC	Na ⁺ -HCO ₃ ⁻ cotransporter
NDUFB6	NADH dehydrogenase [ubiquinone] 1 beta subcomplex subunit 6
NEFA	Non-esterified fatty acids
NHE	Na ⁺ hydrogen exchanger
NKA	Na ⁺ -K ⁺ ATPase
NK-κB	Nuclear factor kappa-light-chain-enhancer of activated B cells
NMR	Nuclear magnetic resonance
p-ACC	Phosphorylated ACC
p-AMPK ^{Thr172}	Phosphorylated AMPK at threonine residue number 172
p-CAMKII ^{Thr286}	Phosphorylated CAMKII at threonine residue number 286
PCr	Phosphocreatine
PDH	Pyruvate dehydrogenase
PDHP	PDH phosphatase
PDK	Pyruvate dehydrogenase kinase
PDK4	Pyruvate dehydrogenase kinase isoforms 4
PEP	Phosphoenol pyruvate
PFK1	6-phosphofructo-1-kinase
PFK2	6-phosphofructo-2-kinase

List of abbreviations (cont.)

Term	Meaning
PG	Phosphoglycerate
PGC1- α	PPAR gamma co-activator 1-alpha
PGI	Phosphoglucose isomerase
PGM	Phosphoglycerate mutase
p-GSK3 β	Phosphorylated glycogen synthase kinase β
PK	Pyruvate kinase
PPAR	Peroxisome proliferator activated receptor
PPP	Pentose phosphate pathway
RAAS	Renin-angiotensin-aldosterone system
rmNCX	Reverse mode Na ⁺ - Ca ²⁺ exchanger
SERCA	Sarco/endoplasmic reticulum ATPase
SHAM	Sham-operated
TBA	Tetrabutyl ammonium
TCA	Tricarboxylic acid
TG	Triacylglycerol
UCP	Uncoupling proteins
UPLC	Ultra performance liquid chromatography
VDAC	Voltage dependent anion channel
WT	Wild type litterate
β -HAD	β -hydroxyacyl-CoA dehydrogenase

1 Introduction

Part of this section has been published as a chapter In: Jugdutt BI, Dhalla NS, eds. Cardiac Remodeling. : Springer New York, Masoud WT, Clanachan AS, Lopaschuk GD. The Failing Heart: Is it an Inefficient Engine or an Engine Out of Fuel? 2013:65-84.

1.1 Heart failure

1.1.1 Definition, different etiologies and compensatory mechanisms

Heart failure is defined as failure of the heart to pump an adequate amount of blood to meet the peripheral needs of the body. It develops following various insults to the heart including, but not limited to, ischemic insults, hypertrophy following longstanding untreated hypertension, genetic or acquired cardiomyopathies, glycogen storage diseases, or hyperdynamic circulation such as severe anemia or hyperthyroidism [1]. During the progression to heart failure adaptive changes occur in the heart, including structural and metabolic remodeling. Systemic neurohumoral compensatory mechanisms develop to maintain adequate cardiac output. This includes activation of renin-angiotensin-aldosterone system (RAAS) and sympathetic system [2]. However as heart failure progresses, these initially adaptive mechanisms become maladaptive leading to increased workloads and energy demand of the heart as well as energy cost of work ending in decompensation [3].

1.1.2 The frequently used animal models of heart failure

The study of mechanisms contributing to heart failure is complicated by the many causes of heart failure. However, numerous animal models of heart failure have been studied, with each mimicking a subtype such as pressure overload (e.g. transverse aortic constriction and abdominal aortic constriction),

volume overload (e.g. aortocaval shunt), stress overload (e.g. rapid ventricular pacing), genetic alterations (transgenic animals), or post-infarction (coronary artery ligation, CAL) (see [4] for excellent review). As will be discussed, each of these experimental models, as well as complementary human studies, has provided valuable information as to how alterations in energy metabolism contribute to severity of heart failure.

1.2 Cardiac metabolism

As mentioned above, development of heart failure is associated with changes in cardiac metabolism. To better understand these changes, it is warranted to shed light on the major metabolic pathways in the heart.

1.2.1 Normal cardiac metabolism

1.2.1.1 Cardiac energy demand

The heart is a continuously contracting organ with a great need for energy. This is illustrated by the high turnover rates of adenosine triphosphate (ATP) in the heart. Although cardiac ATP content is very low (5 $\mu\text{mol/g}$ wet wt), the heart has high ATP hydrolysis rates ($\sim 30 \mu\text{mol/g}$ wet wt/min). Thus, the heart has virtually no energy reserves and the ATP pool of the heart is essentially turned over every 10 beats [5-8]. To secure the energy needed to perform its tasks (such as mechanical work, ionic homeostasis, cardiac signaling, and synthetic function) the heart is flexible in which energy substrates it utilizes. Many different energy substrates can be used, which include fatty acids, glucose, lactate, pyruvate,

ketone bodies, and amino acids. The relative contribution of each of these energy substrates to overall cardiac ATP production depends on substrate availability, the workload of the heart, circulating hormones (such as insulin and catecholamines), age, oxygen availability, and pathophysiologic changes that accompany various diseases including heart failure [9, 10], hypertrophy [11], cardiomyopathy [12] and ischemia-reperfusion (IR) injuries [13]. However, under physiologic conditions, the adult heart normally derives most (80% in rats and 50% in mice) of its ATP from fatty acid oxidation, with the remainder primarily being derived from the oxidation of carbohydrates (glucose, lactate and pyruvate) [14-18].

1.2.1.2 Energy substrate utilization and generation of ATP

The heart is a highly dynamic organ. The human heart pumps about 10 tons of blood on a daily basis and beats about 100,000 times a day [19]. To accomplish this task, the heart uses multiple energy substrates to generate the needed work. In this regard, the heart is the highest energy substrate consumer in the body on a gram weight basis [19]. The process of energy substrate utilization in the heart involves several processes namely, energy substrate delivery, energy substrate utilization, mitochondrial oxidative phosphorylation (tricarboxylic acid (TCA) cycle) and electron transfer chain for ATP generation), and transfer of the high energy phosphates to the contracting myofilaments. In addition, ATP is used for work-unrelated housekeeping activities such as ionic homeostasis and regeneration of organelles.

1.2.1.2.1 Energy substrate delivery

This process entails the uptake of various energy substrates by the cardiomyocytes followed by subsequent metabolism.

1.2.1.2.1.1 Glucose delivery

Glucose is delivered to cardiomyocytes via activity of insulin-dependent glucose transporter 4 (GLUT4) and insulin-independent glucose transporter 1 (GLUT1). Through the activity of hexokinase (HK) enzyme, glucose is phosphorylated into glucose-6-phosphate (G-6-P) and is trapped in the cytosol. In states of energy abundance in the heart, G-6-P can be relatively partitioned towards glycogen synthesis for storage. In contrast, in conditions of increased energy demand, G-6-P preferentially undergoes glycolysis, where each mole of glucose yields 2 moles of pyruvate or lactate in aerobic or anaerobic conditions, respectively. This pathway yields 2 moles of ATP per each mole of glucose [20-23]. Pyruvate is then transported into the mitochondria and activated into acetyl CoA via the activity pyruvate dehydrogenase (PDH) complex. Oxidation of acetyl CoA through activity of TCA cycle yields most of ATP (See Fig 1.1 for details of glucose metabolism). Normally, TCA cycle activity is coupled to oxidative phosphorylation for ATP production [19, 21].

1.2.1.2.1.2 Fatty acid delivery

Fatty acids are primarily delivered to the heart either as free fatty acids (FFA) bound to albumin, or as triacylglycerols (TGs) present in chylomicrons and very low density lipoproteins [5, 21, 24]. The free fatty acids are then activated

into fatty acyl CoA via the activity of fatty acyl CoA synthase (FACS). In the cytosol, acyl CoA molecules bound to acyl CoA binding protein (ACBP) undergo a number of different metabolic pathways including phospholipid and TG synthesis, signal transduction, or mitochondrial fatty acid β -oxidation [21]. Since the inner mitochondrial membrane is impermeable to fatty acyl CoA, mitochondrial uptake of fatty acyl CoAs is thus mediated by a complex of proteins utilizing carnitine as a shuttle mechanism [25-29]. Carnitine palmitoyl-transferase 1 (CPT1) is localized to the outer mitochondrial membrane and converts fatty acyl-CoA molecules to their respective fatty acylcarnitine moieties [25, 29, 30], which are subsequently shuttled into the mitochondrial matrix space by carnitine translocase (CT), and reconverted back to a fatty acyl-CoA moiety by carnitine palmitoyl-transferase 2 (CPT2), which is localized to the inner leaflet of the inner mitochondrial membrane [31-35].

Similarly, other energy substrates such as ketone bodies and amino acids contribute to overall cardiac ATP generation and become of extreme importance in heart failure and during IR but they are out of the scope of this thesis (see references [36-39] for review).

1.2.1.2.2 Energy substrate utilization

This includes glycolysis, glucose oxidation and fatty acid oxidation. Different types of fatty acid oxidation exist such as peroxisomal ω -oxidation [40, 41] in brain [42], leucocytes [43] and liver [44] and peroxisomal α -oxidation [45, 46] but this thesis will focus on mitochondrial β -oxidation.

1.2.1.2.2.1 Glycolysis

Once inside the cardiomyocytes, glucose is phosphorylated to G-6-P by the activity of HK, which will then be directed to either storage via glycogen synthesis pathway or catabolism via glycolysis to eventually produce pyruvate or lactate in aerobic or anaerobic conditions, respectively [20-23]. The advantage of glycolysis is that it produces ATP without the requirement for oxygen. However, the amount of ATP generated is small in comparison to the amount produced by mitochondrial oxidative phosphorylation, and as a result, glycolysis normally produces less than 5% of the total ATP requirements of the heart [5]. However, as will be discussed below, this proportion can change in the failing heart and in conditions of IR.

Glycolysis is regulated via multiple check points. The enzyme 6-phosphofructo-1-kinase (PFK1) is the first regulatory site that shuttles glucose to glycolysis [47] (see Fig 1.1). Flux through PFK1 is allosterically inhibited by ATP, citrate, and protons and is allosterically stimulated by fructose-2,6-bisphosphate (F-2,6-bp), a product of PFK2 (Fig 1.1) [47]. Glyceraldehyde-3-phosphate dehydrogenase (GAPDH), the first enzyme of the ATP generating stage of glycolysis, controls the feed forward of glycolysis via the oxidation and phosphorylation of glyceraldehyde phosphate coupled to the production of reduced nicotinamide adenine dinucleotide (NADH) from oxidized NAD (NAD⁺) [20, 47, 48]. To ensure that flux through GAPDH is not limited, NADH must be continually reoxidized to NAD⁺, which can be accomplished by one of two routes. In the absence of oxygen (O₂), NADH is reoxidized by the enzyme lactate

dehydrogenase (LDH), which converts pyruvate to lactate, whereas in the presence of O₂, NADH is reoxidized by the malate/aspartate shuttle and mitochondrial electron transport chain.

1.2.1.2.2.2 Fatty acid β -oxidation

Oxidation of fatty acids in the mitochondria via β -oxidation produces more ATP per mole of fatty acid than any other energy substrate (e.g. 104 moles of ATP per mole of palmitate). The sequential release of acetyl CoA moieties from fatty acids requires sequential carboxylation of the long fatty acid molecules through energy-consuming activation by fatty acid CoA synthase. Thus, fatty acid oxidation consumes more O₂ as compared to glucose oxidation hence fatty acids are an inefficient source of energy (see section 1.2.2.1.1.1 for details). The contribution of fatty acid oxidation to cardiac energy generation varies from being a predominant source of energy to being a minimal source. This depends on fatty acid availability, energy demand, cardiac pathologic status and competition with the other energy substrates (see [21] for review). In addition, data from our lab indicate varying overall contribution of fatty acid oxidation to ATP production in different species. For example, in our hands, fatty acid oxidation contributes almost 80% of ATP production in rat heart versus 50% in a mouse heart. The section below describes details of fatty acid oxidation and different levels of its regulation.

As mentioned above, fatty acids are delivered to the heart as free fatty acids (FFAs) bound to albumin or liberated from TGs by the activity of

lipoprotein lipase [5, 20, 21, 24, 49]. In the cytosol, FFAs are esterified to fatty acyl CoA through an ATP utilizing process catalyzed by FACS. The portion of fatty acyl CoA that undergoes subsequent β -oxidation is transported to the mitochondria via the activity of CPT1 and CPT2 as mentioned above.

In the mitochondrial matrix, fatty acyl CoA molecules are progressively shortened by 2 carbons each cycle of β -oxidation by the sequential action of the enzymes acyl CoA dehydrogenase, enoyl-CoA hydratase, 3-L-hydroxyacyl CoA dehydrogenase and 3-ketoacyl CoA thiolase acting on the saturated skeleton of these fatty acids. Polyunsaturated and monounsaturated fatty acids (e.g. oleate) require auxiliary enzymes including 2,4-dienoyl-CoA reductase and enoyl CoA isomerase which facilitate the generation of a trans double-bond [20, 21, 49, 50], a prerequisite for fatty acid β -oxidation by the four major enzymes described above. Each cycle of β -oxidation liberates an acetyl CoA moiety that feeds into the TCA cycle. It also generates reducing equivalents (NADH and reduced flavine adenine dinucleotide (FADH₂)) that act as electron donors in the electron transport chain that produces ATP in the final steps of oxidative phosphorylation.

The rate of β -oxidation is regulated by the level of plasma FFA, activity of the key enzymes of fatty acid oxidation and the intracellular level of malonyl CoA [51-54]. Plasma FFA concentration depends on both dietary intake and hormonal factors. Fasting increases circulating plasma FFA while feeding decreases FFA concentrations secondary to carbohydrate-induced insulin secretion which in turn exerts anabolic and anti-lipolytic effects [55-57]. Similarly, increased catecholamine release during stressful conditions such as surgeries, IR or during

early adaptive hormonal changes that accompany the developing heart failure also increase circulating FFA via increased lipolysis through stimulation of β_3 -adrenoceptors in adipose tissue [58].

The second factor that regulates fatty acid oxidation is the activities of the enzymes of mitochondrial β -oxidation [20, 21, 49]. The acyl-CoA dehydrogenase and 3-hydroxyacyl-CoA dehydrogenase enzymes are both sensitive to the ratios of FAD/FADH₂ and NAD⁺/NADH in the mitochondrial matrix, and the enzyme 3-ketoacyl-CoA thiolase is sensitive to the mitochondrial acetyl-CoA/CoA ratio.

The third regulator of fatty acid oxidation is the malonyl-CoA level [51-53, 59-69]. The intracellular levels of malonyl-CoA are determined by energy demand and its rates of synthesis and degradation. Malonyl-CoA is synthesized from cytosolic acetyl CoA via acetyl-CoA carboxylase (ACC). It is degraded via malonyl-CoA decarboxylase (MCD) [51-53, 59-69]. The activity of ACC is under phosphorylation control by 5'-AMP activated protein kinase (AMPK), a kinase that modifies the activity of a number of metabolic enzymes involved in regulating both fatty acid and glucose metabolism [70-86]. In addition, AMPK is also implicated in upregulating various energy producing processes, thus, is central in the regulation of energy substrate metabolism [84-90]. It is important to mention that regulation of fatty acid oxidation is multi-factorial. Thus, absence of one regulator might not be enough to sufficiently alter fatty acid oxidation. This can be illustrated by the finding that lack of AMPK-induced inhibitory phosphorylation of ACC that results in accumulation of malonyl CoA does not inhibit fatty acid oxidation [91]. Another regulatory factor is citrate which

influences malonyl CoA levels. A proportion of citrate that escapes oxidation in the mitochondrial matrix by the TCA cycle, can utilize the mitochondrial tricarboxylate transporter to translocate to the cytosolic compartment, where it can allosterically activate ACC or serve as a contributor to cytosolic acetyl-CoA synthesis via the ATP citrate lyase reaction [92, 93]. Malonyl CoA regulates fatty acid β -oxidation by inhibiting the activity of CPT1, the rate limiting enzyme of mitochondrial fatty acid uptake, thereby controlling the entry of fatty acids into the mitochondria for subsequent oxidation [51-53, 59-62, 64-68, 94-97] (Fig 1.1).

1.2.1.2.2.3 Glucose oxidation

Glucose oxidation (oxidation of the 2 moles of pyruvate produced from each mole of glucose via glycolysis) requires pyruvate transport into the mitochondria via a monocarboxylate transporter (MCT) [98] (Fig 1.1) that is recently identified as mitochondrial pyruvate carrier (MPC) [99]. In the mitochondrial matrix, the majority of pyruvate undergoes oxidative decarboxylation by the pyruvate dehydrogenase (PDH) complex producing acetyl CoA [20, 100-102]. The PDH complex consists of PDH itself, PDH kinase (PDK), and PDH phosphatase (PDHP), and is regulated both by substrate/product ratio and by covalent modification [103-109]. Generally only a small fraction (~20%) of PDH is in the active form, and this proportion is increased in response to an increase in glycolytic flux (and hence an increased generation of pyruvate), or in response to increased cardiac workload or catecholamine stimulation. PDH is also sensitive to inhibition by its products, as an increase in either the ratio of NADH/NAD⁺ and/or acetyl-CoA/CoA decreases the rate of pyruvate

decarboxylation [103, 110-121]. With respect to covalent modification, PDHP dephosphorylates and activates PDH, whereas PDK, in response to acetyl-CoA and NADH phosphorylates and inhibits PDH, thereby restricting the oxidation of carbon units derived from glycolysis [103, 110-122].

In addition to glycolysis-derived pyruvate, pyruvate can also be produced from lactate via the activity of LDH to feed into the TCA cycle as discussed above. Glucose oxidation produces less ATP per mole of glucose (36 moles) than fatty acid oxidation (108 moles of ATP per mole of palmitate). However, glucose oxidation consumes less O₂ per mole of ATP generated; hence it is considered a more efficient energy substrate (see [6, 8, 15, 123] for review).

1.2.1.2.2.4 Mutual regulation between fatty acid oxidation and glucose oxidation:

The Randle cycle

Fatty acid oxidation and glucose oxidation exhibit a reciprocal relationship. That is to say when fatty acid oxidation increases, it causes glucose oxidation to decrease and *vice versa*. This is known as glucose/fatty acid or Randle cycle. It was originally described by Randle et al. in 1963 [57]. This reciprocal control occurs at various levels of both metabolic pathways. Acetyl CoA and NADH produced from fatty acid β -oxidation inhibit the PDH complex. Citrate derived from β -oxidation-derived acetyl CoA can inhibit PFK1 which in turn can lead to an inhibition of HK by G-6-P [56]. However, as PDH inhibition by β -oxidation-derived acetyl CoA and NADH dominates over the inhibition of glycolysis, the overall effect of fatty acid oxidation stimulation is a mismatch

between glucose oxidation and glycolysis resulting in a relative accumulation of pyruvate.

Under normal conditions, the negatively-charged pyruvate requires co-transport of protons in a 1:1 stoichiometric manner [124-126] to the mitochondrial matrix for subsequent activation by PDH complex. Thus, in conditions of mismatch, the relative accumulation of pyruvate is accompanied by accumulation of protons derived from hydrolysis of glycolysis-derived ATP resulting in intracellular acidosis [20, 127, 128]. Under conditions of low coronary flow such as ischemia or in low cardiac output heart failure, the limited clearing of metabolic byproducts results in intracellular acidosis, activation of the sodium-hydrogen exchanger (NHE) which exchanges intracellular protons with Na^+ . The accumulating Na^+ stimulates the reverse mode $\text{Na}^+ - \text{Ca}^{2+}$ exchanger (rmNCX) resulting in Ca^{2+} overload. These effects collectively result in a dysregulation of ionic homeostasis (See below and Fig 1.2, Fig 1.3).

In contrast, increasing the contribution of glucose oxidation to the generation of acetyl CoA inhibits fatty acid oxidation via feedback inhibition of 3-ketoacyl CoA thiolase, while NADH derived from glucose oxidation can decrease fatty acid oxidation via feedback inhibition of both acyl CoA dehydrogenase and 3-hydroxyacyl CoA dehydrogenase. Furthermore, an increase in glucose-derived acetyl CoA, via the actions of the enzymes carnitine acetyl transferase (CAT) [20, 21, 49, 129, 130] and ACC can increase the synthesis of cytosolic malonyl-CoA. Also, increasing glucose oxidation improves the coupling of glucose metabolism, and hence decreases proton production (Fig 1.1).

1.2.1.2.3 Oxidative phosphorylation for ATP production

Under aerobic conditions about 95% of the hearts ATP requirements are met through the mitochondrial oxidative phosphorylation of ADP. The reducing equivalents produced in TCA cycle are transferred to the mitochondria via FADH₂ and NADH, which are generated via dehydrogenase reactions in fatty acid β -oxidation, TCA cycle, the glycolytic pathway, and from the oxidation of pyruvate derived from glucose or lactate. The relative contribution of the various energy substrates to ATP production is affected by many factors including the developmental stage of the heart, cardiac workload (pre- and afterload), heart rate and force of contraction, and the presence of various cardiac pathologies (e.g., hypertrophy, failure or ischemia-reperfusion injury) [19-21, 131].

1.2.1.2.4 ATP transfer and phosphocreatine/creatine kinase shuttle

Transfer of the high energy phosphate bond in ATP that is generated inside the mitochondria (via oxidative phosphorylation) to the site of ATPases (i.e. the myofibrils, sarcoplasmic reticulum, and sarcolemma) is facilitated by the creatine kinase shuttle system. Creatine kinase (CK) is a reversible kinase that initially phosphorylates creatine to phosphocreatine (PCr) using the high energy phosphate bond in ATP [132]. The CK shuttle is facilitated by mitochondrial and cytoplasmic CKs, which eventually results in the rephosphorylation of ADP to ATP in the cytoplasm.

In cardiomyocytes, about two thirds of creatine are phosphorylated and act as a reservoir for ATP. Thus, when energy production declines, PCr levels decline while ATP levels are initially maintained. This is accompanied by an increase in ADP levels [133, 134]. Because of this, total creatine levels and PCr/ATP ratio can be used as indices of cardiac energetic status. In general, both indices decline in early phases of heart failure before an actual decline in total ATP levels occurs [132-134].

Since creatine is not synthesized *de novo* in cardiac muscle [135], the activity of creatine transporters plays a regulatory role on the intracellular availability of creatine in cardiomyocytes. Reduction of creatine transporter expression and/or activity can be one of the contributing factors to the deterioration of PCr/CK shuttle observed in many cardiac diseases, including heart failure [132-134].

The association of various isoforms of CK with subcellular structures ensures adequate transfer of ATP-derived energy for adequate coupling of energy generation and utilization. For example, the tight association of myofibrillar CK (MM-CK) with sarco/endoplasmic reticulum ATPase (SERCA) is thought to enable efficient energy transfer for Ca^{2+} uptake [136]. Similarly, the mitochondrial CK (miCK) being located in the inner mitochondrial membrane near the adenine nucleotide translocase is thought to help export the high energy phosphate of ATP through the formation of ADP and PCr thus maintaining mitochondrial respiration by prevention of intramitochondrial ATP accumulation [137] (for further review see [138]).

1.2.2 Metabolic phenotype in heart failure

Heart failure is associated with a number of changes in energy metabolism [19, 21, 138-140]. Whether these changes contribute to the contractile failure of these hearts, hence considered as maladaptive and should be discouraged [141, 142], or whether they represent an adaptive response that should be encouraged is not yet firmly established [143]. Moreover, there is no agreement regarding the actual nature of the energy metabolic changes that occur in heart failure and two main concepts have emerged (Fig. 1.2). The first concept is that the failing heart is energetically starved, similar to an engine out of fuel [19, 144]. This implies lower rates of energy metabolism and lower rates of production of the energy currency; ATP. The second concept is that the failing heart may not necessarily be energy starved, but rather is inefficient in its use of energy for contractile function [145].

1.2.2.1 Metabolic inefficiency in heart failure

Cardiac energy stores are expended for mechanical work generation, ionic homeostasis and other vital cellular functions, such as synthesis and degradation of various intracellular molecules and their trafficking to various cellular compartments or to the extracellular compartment [146-148]. In 1949 Bing *et al* [149] defined cardiac mechanical efficiency as the “cardiac work generated per energy consumed”. Since most of cardiac energy generated (about 95% under aerobic conditions) is derived from fatty acid and carbohydrate metabolism [123], and the fact that metabolic rates in cardiac muscle are tightly coupled with energy

demand [150, 151], oxygen consumption (MVO_2) by the cardiac muscle can be used as a measure of energy production. A decrease in cardiac efficiency occurs when more energy substrates are utilized without a corresponding increase in external work generation. A decrease in the efficiency in utilizing energy for mechanical function has the potential to be a major contributor to cardiac dysfunction in heart failure [123, 152-158]. This cardiac inefficiency can develop primarily at three different levels: 1) increased oxygen cost of acetyl CoA and ATP production, 2) increased ATP consumption for non-contractile homeostatic activities, and 3) impaired energy transfer to myofibrils.

1.2.2.1.1 Contributors to metabolic inefficiency in heart failure

1.2.2.1.1.1 Increased oxygen cost of ATP production due to an increased dependence on fatty acids

As mentioned, under aerobic conditions the heart derives most of its energy requirements from fatty acids [123, 152-158]. Moreover, the activated neurohumoral mechanisms during early stages of heart failure favor lipolysis leading to increased circulating fatty acids and exposure of the cardiomyocytes to greater concentrations of fatty acids [2]. When one molecule of palmitate is fully metabolized, it yields 104 ATP molecules, compared to the metabolism of glucose where only 31 ATP molecules are produced. However, despite this higher ATP yield of palmitate, a higher MVO_2 is also needed [21]. This is because while the initial cytoplasmic metabolism of glucose (i.e. glycolysis) produces 2 ATP, the initial cytoplasmic metabolism of fatty acids (i.e. the

formation of long chain acyl CoA from fatty acids and CoA) actually consumes two high energy phosphates (i.e. ATP to AMP). Also, the fact that palmitate oxidation yields both FADH₂ and NADH, as compared to only NADH produced during glucose metabolism, contributes to palmitate being an inefficient source of energy. Because FADH₂ bypasses complex I of the electron transfer chain, it pumps less protons and generates less ATP than NADH (reviewed in [21]). This means that a preferential dependence on fatty acids for energy generation in early stages of hearts failure could lead to more MVO₂ for the same energy yield; hence causing inefficiency in ATP generation. This effect was shown many years ago when increasing FFA supply to the heart secondary to adrenergic stimulation-induced lipolysis was found to increase cardiac MVO₂ without changing cardiac external work [155, 158]. In theory, a complete dependence on fatty acids for energy generation leads to 10-13% reduction in the calculated efficiency. However, the observed differences in efficiency are even higher; indicative of involvement of other mechanisms [20, 21].

In heart failure, there is not a uniform consensus as to what happens to cardiac fatty acid oxidation rates. Both human and experimental studies have shown an increase in fatty acid oxidation rates, a decrease in fatty acid oxidation rates, or no change in fatty acid oxidation rates (see references [15, 20, 21] for reviews). As a result, it cannot be conclusively stated as to whether the heart is more inefficient due to an increased reliance on fatty acid as an energy source. Similarly, there are no consensus regarding whether inhibiting or stimulating fatty acid oxidation is beneficial in heart failure [15, 19-21]. This is probably

dependent on the stage of heart failure and the availability of other energy substrates.

1.2.2.1.1.2 Uncoupled oxidation-phosphorylation at TCA cycle

The mitochondrial electron transfer chain (also known as the mitochondrial respiratory chain) utilizes reducing equivalents in the mitochondrial matrix to generate ATP. The electrochemical gradient of protons across the inner mitochondrial membrane is essential for this process. This gradient is generated by the movement of protons from the mitochondrial matrix to the intermembrane space by complexes I, III and IV. The protons then move down their electrochemical gradient to the mitochondrial matrix to provide the energy needed for ATP synthase activity, with the subsequent phosphorylation of ADP to ATP [21, 159, 160].

The uncoupling proteins (UCP) provide a potential alternative route for transport of protons across the inner mitochondrial membrane without the involvement in ATP synthesis [160]. These UCPs were originally discovered in brown adipose tissue where they help oxidatively-generated energy to dissipate in the form of heat, secondary to failure of coupling with phosphorylation of ADP for ATP generation [161, 162]. In the heart UCP2 and UCP3 are preferentially expressed [163]. UCP3 has been suggested to mediate fatty acid-induced uncoupling of oxidation-phosphorylation [164]. Moreover, high circulating fatty acid levels increase UCP3 expression in the heart [165]. The aforementioned observation provides a potential explanation why the reported difference in

efficiency due to dependence on fatty acid oxidation is higher than the theoretically-calculated difference. Several reports from animal models of heart failure describe overexpression of UCPs (see [166] for review). In an abdominal aorta constriction model of heart failure in the rat, decreases in ATP, ADP, AMP and PCr contents in the failing heart were associated with a significant increase in UCP2 expression [167]. Adenovirus-mediated overexpression of UCP2 in neonatal cardiomyocytes was also found to increase basal oxygen consumption without affecting total ATP content [168], indicative of an increase in cardiac inefficiency. Moreover, UCP2 overexpression disrupted mitochondrial membrane potential secondary to failure to control Ca^{2+} -induced Ca^{2+} release from SERCA [168]. In cardiac mitochondria isolated 10 weeks following CAL surgery in rats, UPC3 was also shown to be up-regulated, mitochondria were less coupled (lower ADP/oxygen ratio), and a significant reduction of efficiency was observed [169]. Furthermore a positive correlation between UPC3 levels and circulating non-fasting fatty acid levels was observed, an observation which supports the regulatory role of circulating fatty acids on cardiac UPC3 expression and thus increased inefficiency [169].

1.2.2.1.1.3 Futile cycling in the heart

Normally, the heart consumes generated ATP for mechanical work, ionic homeostasis and synthesis of various cellular molecules [146, 148, 170]. However, utilization of ATP can be preferentially directed to additional homeostatic activities leading to further deterioration of inefficiency in heart failure.

As fatty acid supply to the myocardium increases early in the disease progression secondary to increased sympathetic activity, excess fatty acyl CoA has the potential to accumulate in the mitochondrial matrix. A mitochondrial thioesterase has been identified, which may cleave this unneeded fatty acyl CoA into fatty acid anion and free CoA [171, 172]. This process maintains the CoA pool in the mitochondria for further activation of fatty acids for β -oxidation. However, not only is the high energy CoA bond lost due to the thioesterase activity, the resulting fatty acid anions have been proposed to be exported to the cytosolic compartment via the activity of UCP3 [173, 174]. While this process prevents intramitochondrial accumulation of potentially harmful fatty acid anions, it increases the futile utilization of ATP for the subsequent esterification of these fatty anions prior to subsequent β -oxidation [20, 21].

Another source of futile ATP utilization is glycerolipid/TG cycling which is another fate for fatty acids taken up by the heart. In this case, fatty acids cycle between the intracellular TG pool and the free fatty acid state. Excess ATP is thus utilized at the esterification step prior to incorporation of fatty acids into the TG pool or prior to β -oxidation [175].

Whether these two pathways of futile fatty acid cycling are involved in the cardiac inefficiency in heart failure is not yet clear. However, as indicated above, the increased sympathetic activity in heart failure is expected to mobilize fatty acids from adipose tissue increasing the circulating levels of fatty acids and increased exposure of the heart to fatty acids [3].

1.2.2.1.1.4 Reversion to fetal glycolytic metabolism favors mismatched glucose metabolism and the subsequent higher energy cost of ionic homeostasis

It is known that the fetal heart is largely glycolytic [176]. Studies with newborn rabbit hearts have shown that after birth, the expression of fatty acid oxidation regulating enzymes such as peroxisome proliferator activated receptor α (PPAR α) rapidly increases while those regulating glycolysis decline. These changes mark the conversion from glycolysis to fatty acid oxidation as the main source of energy [21, 177-179]

In experimental models of heart failure in which an initial pathologic hypertrophy develops (such as salt-sensitive hypertensive rats [180], pressure overload models such as transverse aortic constriction [181], and volume overload models such as aortocaval fistula [176, 182, 183]), reversion to a fetal glycolytic metabolism occurs. Proteomic analysis of mitochondrial proteins also confirms this shift to glycolytic metabolism in rats 8 weeks after CAL surgery [184].

The reversion to glycolytic metabolism that is associated with a decline in mitochondrial oxidative capacity is thought to help produce energy from a substrate that utilizes less oxygen per ATP, hence efficiency is improved. On the other hand, this increase in glycolysis without a parallel increase in glucose oxidation can favour mismatched glucose metabolism, whereby increased hydrolysis of glycolytically-derived ATP accelerates proton production with the development of intracellular acidosis [185]. This can subsequently lead to an

increase in Na^+ and Ca^{2+} accumulation [185], resulting in an impaired contractility (Fig. 2). Correction of intracellular accumulation of Na^+ and Ca^{2+} increases ATP utilization for ionic homeostasis, rather than for contractile activity (see below for mechanisms and consequences of disturbed ionic homeostasis during IR).

Reversion to fetal glycolytic metabolism is associated with changes in the expression of gene and protein levels and activity of enzymes known to regulate glycolysis as well as fatty acid oxidation. Members of the PPAR family are specifically involved. PPAR α , which is predominantly expressed in the heart and skeletal muscles, is known to regulate fatty acid oxidation and thus its inhibition can be responsible for the reversion to fetal glycolytic metabolism [186]. In this regard, genetic deletion of PPAR α results in hypertrophy and inhibition of fatty acid oxidation in mice exposed to transverse aortic constriction [187]. This is associated with decreased expression of fatty acid oxidation genes [188] and a decline of fatty acid oxidation rates accompanied by stimulation of glucose oxidation [189]. Previous findings led to the notion that stimulating PPAR α in failing hearts could improve function through prevention of the development of fetal glycolytic metabolic profile via inhibition of the downregulation of fatty acid oxidation [190]. As a result, pharmacologic approaches to activate PPAR α (e.g., with the use of fenofibrate) were used in an attempt to decrease the severity of heart failure. This was found to produce a uniform up-regulation of PPAR α -regulated genes but variable results regarding heart function [191, 192]. A worsening of *ex vivo* LV function was observed in hypertrophied hearts derived

from rats exposed to transverse aortic constriction [191]. In post-infarct rat hearts [192] and in dogs with heart failure due to pacing-induced tachycardia [193], there was no improvement of LV function and no reduction in chamber volume following chronic fenofibrate treatment. On the other hand, the use of fenofibrate in a porcine tachycardia model of heart failure resulted in less deterioration of LV function [194]. The variability in the reported functional consequences of PPAR α activation hints at the lower likelihood of PPAR α involvement in progression to heart failure. However, these findings should not concern heart failure patients who are already using fenofibrate to reduce cholesterol. In fact, fenofibrate may possess cardioprotective effects mediated by non-metabolic pathways. For example, it was reported that fenofibrate lessens cardiac fibrosis and diastolic dysfunction in salt-sensitive hypertensive rats, probably via non-metabolic effects involving the suppression of inflammation via inhibiting nuclear factor kappa-light-chain-enhancer of activated B cells (NF- κ B) [195].

PPAR β/δ is another member of the PPAR family which may be involved in the reversion of the heart to a fetal glycolytic metabolism. Although not specific for cardiac muscle, it is expressed in high amounts in the heart [196]. The role of PPAR β/δ in cardiac metabolism has been studied by cardiac-specific deletion of PPAR β/δ in mice. These mice develop severe cardiomyopathy ending in heart failure and premature death associated with decreased cardiac expression of genes responsible for fatty acid oxidation, decreased cardiac fatty acid oxidation rates, and increased cardiac lipid deposition [197]. In contrast, cardiac-specific PPAR β/δ overexpression increases expression of genes involved in fatty

acid oxidation. However, fatty acid oxidation rates in these mice are normal, indicative of possible post-translational modifications. Neither genes involved in TG synthesis nor those involved in fatty acid uptake are increased. Surprisingly, cardiac-specific overexpression of PPAR β/δ is associated with increased expression of genes involved in glucose uptake (such as GLUT4 and the key regulatory enzyme PFK), which is associated with an increase in cardiac glucose uptake and oxidation [186, 198-200]. Despite the fact that both PPAR α and PPAR β/δ share overlapping pathways for control of fatty acid oxidation [186], cardiomyocyte PPAR β/δ restriction in PPAR α null mice results in no further inhibition of fatty acid oxidation, but rather a pronounced inhibition of mitochondrial biogenesis [201]. Whether the reversion to fetal glycolytic phenotype is associated with increased PPAR β/δ expression in the failing heart is yet to be studied.

1.2.2.1.1.5 Impaired energy transfer to myofibrils: consequences of compromised phosphocreatine/creatine kinase shuttle

Failure of the PCr/CK shuttle may also be a contributing factor to the development of inefficiency in heart failure. PCr acts as a reservoir to replenish ATP content via the activity of creatine kinase, a reaction that is capable of producing ATP 10 times faster than the rate of ATP synthesis from oxidative phosphorylation, under conditions of energy demand [202]. This fact is confirmed in various models of heart failure. For example, Hearse et al [203] observed a rapid decline in myocardial PCr levels and contractility in isolated working rat hearts during post-ischemic reperfusion. Similar results were

reported by Whitman et al [204] using isolated perfused rabbit hearts. The same concept was further confirmed in a porcine model of transverse aortic constriction-induced cardiac hypertrophy and failure [205].

PCr/ATP ratio is usually used as an index of the energy status of the heart [206, 207], that can also predict possible protection against supervening ischemic insults and the subsequent development of heart failure. Changes in PCr levels have been reported in many heart failure patient studies. Winter et al [208] reported an earlier decline in PCr levels in non-ischemic heart failure patients using magnetic resonance spectroscopy, where a significant reduction in cardiac creatine levels was shown by a significant reduction of water/creatine index. This decrease in PCr was also reported early in patients with dilated cardiomyopathy [209]. These findings conform to the studies of Neubauer et al [210], who used ³¹P-NMR spectroscopy and found a 70% reduction in PCr levels in heart failure patients with dilated cardiomyopathy while ATP levels were unaltered. The PCr/ATP ratio was thus markedly reduced in these patients. The authors found that the decline of PCr/ATP ratio correlates with the severity of heart failure and that the ratio improves by recompensation. The authors also found that PCr/ATP ratio is a valid predictor of mortality in these patients. They found that patients with normal PCr/ATP (more than 1.6) had an all-cause mortality of 10% following a 2.5-year surveillance. On the other hand, patients with low PCr/ATP ratio had 40% all-cause mortality [210].

Not only do PCr levels decline in heart failure, but the ability of the failing heart to maintain adequate ATP levels in response to exercise challenge is also

compromised to various degrees depending on heart failure etiology. Using the hand grip exercise, Weiss et al [211] observed that PCr/ATP ratio in the left ventricular wall is maintained in non-ischemic heart failure patients, but is greatly reduced in patients with heart failure due to coronary artery disease. Similar changes were also observed by Yabe et al [212] at the level of subendocardium.

1.2.2.1.2 Proof of principle for cardiac metabolic inefficiency

As mentioned below, supporters of the energy starvation theory refer to the generalized decline in metabolic rates seen in advanced cases of heart failure [9, 213]. They also refer to the observation that mechanical function in advanced heart failure can be improved by stimulating energy substrate metabolism. The following few lines will summarize evidence commonly presented by supporters of energy starvation theory. First, stimulation of glucose oxidation (e.g., by dichloroacetate (DCA)), in patients with congestive heart failure was found to improve mechanical efficiency and hemodynamic parameters [214]. Also intracoronary infusion of pyruvate can induce a short-term functional improvement in heart failure patients [215]. Furthermore, cardiac-specific overexpression of GLUT1, expected to increase intracellular glucose transport for subsequent utilization, was found to prevent the development of LV dysfunction after transverse aortic banding [216]. Finally, induction of mitochondrial biogenesis can prevent cardiomyopathy in mice [144]. On the one hand, treatments that limit the energy demand of the failing heart by reducing mechanical work such as β -adrenoceptor antagonists are also known to be useful adjuncts to traditional heart failure therapy [217-220].

Indeed, the aforementioned evidence supports the metabolic inefficiency theory. The observed improvement of mechanical function in patients with congestive heart failure with the use of glucose oxidation stimulators such as DCA [214] can be explained on basis of improved matching between glucose oxidation and the upregulated rates of glycolytic flux observed in various stages of heart failure [9, 178, 179, 221]. In addition, this mismatch can be accentuated by a concurrent reduction of glucose oxidation despite increased glycolytic flux [9]. Thus, stimulation of glucose oxidation is expected to lessen the mismatch between glycolytic flux rates and glucose oxidation rates.

Further support for cardiac metabolic inefficiency in heart failure is gained from the beneficial effect of fatty acid oxidation inhibitors, a fact that clearly contradicts the concept of energy starvation [see [15, 19, 21, 170] for reviews). A number of approaches to inhibit fatty acid oxidation have been used, which include: 1) reduction of circulating fatty acids levels with β -adrenoceptor antagonists such as nebivolol that inhibit lipolysis [218, 219], 2) the use of PPAR γ agonists such as thiazolidinediones that favor sequestration of fatty acids in adipose tissue [222-224], 3) inhibition of mitochondrial fatty acid uptake by etomoxir [225] or perhexiline [226-228], and 4) inhibition of mitochondrial β -oxidation with agents such as trimetazidine [229-234]). The resulting indirect stimulation of glucose oxidation as a consequence of lower rates of fatty acid oxidation (Randle cycle) improves the coupling of glycolysis to glucose oxidation leading to reduced proton production from the hydrolysis of glycolytically-derived ATP (Fig. 1.2). Also, shifting substrate preference from fatty acid

oxidation is expected to increase efficiency of energy production without changes in MVO_2 .

Reports from Kolwicz et al [235] apparently contradict this approach where acetyl CoA carboxylase 2 knockout (ACC2 KO) mice, expected to exhibit increased fatty acid oxidation rates, were protected against metabolic remodeling following pressure overload. However, thorough interpretation of their results is, in fact, in support of metabolic inefficiency. Contrary to the authors' assumption, ACC2 KO did not result in increased fatty acid oxidation possibly due to compensatory mechanisms arising from chronic ACC2 deficiency. Moreover, the authors did not show the actual metabolic rates. Rather, they expressed relative contribution to overall oxidation rates which makes it difficult to understand the actual change in metabolic rates. More importantly, they showed that ACC2 KO mice did not exhibit an increase in glycolytic rates, and in contrast to the common finding of accelerated glycolysis in hypertrophied hearts following pressure overload [176, 179, 236]. The lack of upregulation of glycolytic rates in those mice indicates better matching with their unaltered glucose oxidation minimizing inefficiency of glucose metabolism, hence, the observed better function. It is thus very important to carefully interpret changes in metabolic rates and the metabolic efficiency consequences in studies that use stimulation of energy substrate metabolic to improve mechanical function in failing hearts as an evidence to support energy starvation theory.

1.2.2.2 Energy starvation in heart failure

The energy starvation theory was initially proposed by Hermann in 1939 [237], who reviewed the chemical nature of heart failure and addressed the reduction of myocardial creatine in the heart. From this perspective, the failing heart can be described as an engine out of fuel [19]. This implies an ability to improve, or at least prevent further deterioration of, cardiac function by stimulating the various stages of high energy generation [144]. Because this theory gained much interest and is described in detail elsewhere, we will only briefly highlight this concept (refer to [19] for review) and the accumulating evidence against this theory.

Energy starvation generally develops only in advanced cases of heart failure and may result from reduced oxygen and energy substrate supply to the heart, reduced energy substrate uptake and utilization and finally, reduced oxidative phosphorylation resulting in reduced ATP production.

1.2.2.2.1 Reduced oxygen and energy substrate supply to the heart

As heart failure progresses, the pumping action of the heart declines. This is initially compensated by the neurohumoral responses (increased sympathetic tone and stimulation of the RAAS) that maintain near normal cardiac output. However, with further progression of heart failure, the compensatory responses fail to maintain adequate cardiac output and eventually cardiac output declines. This in turn, reduces blood supply to all organs including the heart itself. The reduced tissue perfusion leads to reduced oxygen and nutrient supply. This is

further complicated by the associated development of pulmonary congestion that reduces oxygen saturation leading to further deterioration of oxygen supply. In general, reduced intracellular oxygen availability does not limit peak oxygen utilization. However, as heart failure progresses, the workload increases and cardiac MVO_2 can reach a maximum and becomes limiting leading to subsequent deficiency of energy generation and utilization [238]. Moreover, as heart failure advances, the increasing afterload increases energy demand to maintain an acceptable cardiac output. This creates a state of relative energy starvation.

1.2.2.2.2 Reduced energy substrate uptake and utilization

Supporters of the energy starvation theory believe that early in the development of heart failure, metabolic rates are not markedly changed. In fact fatty acid utilization is either unchanged or slightly increased [123, 221, 239, 240]. This may be due to increased expression of fatty acid transport protein (CD36) and intracellular fatty acid binding protein (FABP) [241]. They report that as heart failure advances, fatty acid utilization declines significantly out of proportion with the decline in mechanical function [10, 21]. A similar trend is also observed for glucose utilization where rates of glucose oxidation are unchanged early in heart failure [221, 242] with a compensatory increase in the rates of glycolysis [240, 243]. Similarly, in hearts with advanced failure, there is a decline in glucose utilization [244-246]. The latter may be partially explained by the development of insulin resistance in advanced heart failure [247, 248] which may be a protective mechanism to protect the failing heart from the energy substrate overload induced by the upregulated sympathetic tone [249]. Moreover,

membrane expression of the insulin-sensitive glucose transporter GLUT4 is reduced in advanced heart failure [250] contributing to the observed reduction in glucose uptake and subsequent utilization.

In support of their hypothesis, some experimental models of severe end stage heart failure showed a depression in overall oxidative metabolism. For example, twenty weeks following pressure overload-induced heart failure, secondary to transverse aortic constriction in rats, there is a decrease in mitochondrial state 3 respiration, as well as a decrease in both fatty acid (i.e. oleate) and glucose oxidation [251-253]. These findings are not universal in different models of severe heart failure. In canine model of severe heart failure induced by rapid ventricular pacing, the rate of fatty acid oxidation is decreased while glucose oxidation rate increases [254, 255]. However, protein expression of PDH is decreased, while that of its negative regulator, PDK4 is increased, indicative of an inhibitory response [255]. Interestingly, the metabolic phenotype observed in pacing-induced heart failure is reversible, as the rates of fatty acid oxidation and glucose oxidation return to near baseline values during a recovery phase following discontinuation of rapid ventricular pacing [254].

Support to the energy starvation theory comes also from the clinical setting. For example, rates of both fatty acid uptake and oxidation are decreased in patients with dilated cardiomyopathy (ejection fraction ~32%), while the rates of glucose uptake are increased [256]. Furthermore fatty acid uptake and glucose uptake do not increase in response to pacing stress, which contributes to their metabolic inefficiency [256]. Marked and acute reductions in circulating fatty

acid levels in response to acipimox (an inhibitor of lipolysis) treatment are accompanied by large reductions in fatty acid uptake, and decreased cardiac efficiency, although fractional fatty acid oxidation remains unchanged, indicative of the potential contribution to metabolic inefficiency in those hearts [257].

However, the metabolic alterations in heart failure are not homogeneous throughout different models and the various stages of heart failure development. Contrary to the aforementioned evidence of energy starvation in heart failure, ventricular homogenates obtained from hearts subjected to pressure overload with preserved ejection fraction had similar rates of fatty acid oxidation to homogenates obtained from normal hearts, whereas the rates of glycolysis are accelerated [258, 259]. Furthermore, as LV hypertrophy advances to congestive heart failure, glucose uptake increases even further and fatty acid uptake is decreased [259]. The authors in that study did not comment of the actual changes in glucose oxidation and fatty acid oxidation rates [256, 258, 259][256, 258, 258, 259, 259][256, 258, 258, 259, 259]. Similar patterns are described in different models of heart failure. For example, fatty acid oxidation rates are also similar in ventricular homogenates obtained from hearts subjected to myocardial infarction and subsequent heart failure at a time point when there is a downregulation in genes encoding enzymes involved in fatty acid oxidation including acyl CoA synthase and CPT1 [260]. Similarly, whole heart fatty acid oxidation does not differ in acute heart failure secondary to aortic banding in rats [261], or in the canine microembolization model, where glucose uptake and oxidation are also preserved relative to the normal heart [239]. These animal findings can be

extrapolated to human patients. Previous studies indicate that patients with asymptomatic hypertrophic cardiomyopathy have decreased fatty acid uptake and exogenous glucose utilization, possibly due to flow limitations or regional differences in systolic function [262] but cardiac fatty acid oxidation remains normal [263]. Similarly, NYHA functional class III patients have enhanced fatty acid utilization secondary to enhanced lipolysis associated with elevated plasma lactate concentrations, indicative of fatty acid-induced mismatch of glucose oxidation with relatively higher glycolysis rates [264]. Interestingly, in clinically stable NYHA functional class II and III patients, cardiac fatty acid uptake [265, 266] and fatty acid oxidation [265] were greater than healthy controls, while glucose uptake [266] and oxidation were lower [265]. The above animal and patient evidence is at least against a universal energy starvation in heart failure.

1.2.2.2.3 Reduced oxidative phosphorylation

Supporters of energy starvation claim that heart failure is associated with reduced mitochondrial oxidative phosphorylation [267]. This is due in part to reduced TCA activity [268]. In addition, the activity of electron transport chain and ATP synthase are reduced [269-271]. The increased expression of uncoupling proteins increases uncoupling of oxidation and phosphorylation resulting in reduced ATP generation [169, 272]. In addition, flexibility in substrate utilization is lost [273]. However, reduced glucose oxidation can be seen as a source of mismatched glucose metabolism especially when glycolysis rates are increased.

1.3 Cardiac ischemia reperfusion injury

1.3.1 Definition, causes and mechanisms

Myocardial ischemia reperfusion (IR) injury involves a two-step myocardial injury. The first one is caused by ischemic insult and the second one accompanies the reperfusion. Myocardial ischemia occurs due to partial or complete derangement of coronary blood flow resulting in reduced oxygen and nutrient supply to the area supplied by this blocked coronary artery which becomes inadequate to maintain normal heart function. Myocardial ischemia results mostly from coronary thrombosis on top of atheromatous lesions [274]. Other causes include coronary artery embolic obstruction following bypass grafts [275], transient coronary spasm (vasospastic angina - Prinzmetal's angina) [276] of coronary artery and anomalous left coronary artery originating from pulmonary artery which results in early onset angina or even infarction [277-279]. Currently, approaches to restore the disrupted coronary flow include medications that dissolve the occluding thrombus (thrombolytics, e.g., tissue plasminogen activator), procedural interventions that reopen the blocked segment of the artery (angioplasty \pm stent placement) or urgent bypass grafting using venous graft (e.g., saphenous vein graft). However, restoration of the temporarily interrupted coronary flow can add further insult to the myocardium called reperfusion injury [280, 281]. Reperfusion injury is thought to be due to the reintroduction of oxygen and blood to myocardium in the area at risk and which results in cell death above and beyond that due to the preceding ischemia [282]. Reperfusion injury has been

attributed to many factors including, but not limited to, oxidative stress causing cell death [283], metabolic inefficiency secondary to mismatched glucose metabolism and subsequent proton accumulation and Na^+ and Ca^{2+} accumulation [284] and finally, uncontrolled opening of the mitochondrial permeability transition pore (mPTP) causing widespread depolarization of the inner mitochondrial membrane, hydrolysis of ATP, mitochondrial rupture and eventual necrotic cell death [285].

1.3.2 Metabolic profile in IR

1.3.2.1 Anaerobic glycolysis and disturbed intracellular ionic homeostasis

Ionic dysregulation during IR is initiated by events that occur during ischemia. This is then augmented by further events at the initiation of reperfusion. During ischemia, the decrease in glucose oxidation necessitates a rapid acceleration in the conversion of pyruvate to lactate via LDH in order to regenerate NAD^+ under anaerobic conditions, which is required to maintain glycolytic flux through GAPDH (Fig 1.1). The increased dependence on anaerobic glycolysis leads to reduced ATP production rate and a buildup of intracellular acidosis due to accumulation of lactate and protons generated from hydrolysis of glycolysis-derived ATP. These events collectively result in dysregulation of ionic homeostasis.

In response to the decreasing pH (acidosis), cardiomyocytes remove some of the accumulating protons generated during ischemia by extrusion of weak acids

such as lactic acid as well as via exchange of protons with Na^+ and HCO_3^- via the activity of NHE and $\text{Na}^+-\text{HCO}_3^-$ cotransporter (NBC), respectively. This, in turn, acidifies the extracellular space and limits further removal of intracellular protons [286]. Assessment of cardiomyocyte intracellular and extracellular pH during ischemia confirms acidification to final pH values of 5.9 and 5.5, respectively [287]. Furthermore, depletion of ATP during ischemia impairs ATP-dependent ion transport machinery such as Na^+-K^+ ATPase thereby limiting its ability to transport Na^+ to the extracellular space against its electrochemical gradient.

Meanwhile, influx of Na^+ into cardiomyocytes increases during ischemia thus aggravating Na^+ accumulation in the intracellular compartment. This inward movement of Na^+ depolarizes the membrane resting potential of cardiomyocytes [284, 288]. Different mechanisms contribute to increased Na^+ influx during ischemia. First, increased dependence on anaerobic glycolysis during ischemia and the hydrolysis of glycolytically-derived ATP increases intracellular proton concentration that activates Na^+ influx in exchange with protons via activity of NHE [289] and neutralization of protons using HCO_3^- via the activity of NBC [290]. Second, the activation of late Na^+ current via voltage-gated Na^+ channels during ischemia. During resting conditions, the rapid inactivation of voltage-gated Na^+ channels limits Na^+ influx. However, during ischemia, delayed inactivation of Na^+ channels augments late Na^+ current. Many factors collectively result in delayed Na^+ channel activation including AMPK [291], reactive oxygen species [292-294] and ischemic metabolites [295]. The increased intracellular Na^+

concentration, in turn, activates the rm-NCX to extrude 3 Na⁺ ions in exchange with 1 Ca²⁺ ion resulting in intracellular Ca²⁺ overload [296].

Despite the fact that reperfusion aims at restoration of normal blood flow to the ischemic myocardium, the initiation of reperfusion adds further insult and contributes to ionic dysregulation. The rapid restoration of extracellular pH and the persistence of intracellular acid pH create a marked pH gradient that favours the sequential activation of NHE and rmNCX (see above) and ends in Na⁺ and Ca²⁺ accumulation [286, 288].

The ultimate result of increasing Ca²⁺ overload is the activation of detrimental pathways such as triggering of arrhythmia, activation of enzymes, opening of mPTP, myocardial stunning and eventually cardiomyocyte death [297].

Thus, it is evident that the accumulation of protons during IR is the initiating event is the detrimental cascade of events that ends in cardiomyocyte death. It is also known that metabolic changes during ischemia, namely reliance on anaerobic glycolytic flux, constitute a major source of protons generated from hydrolysis of glycolytically derived ATP. Similar consequences are expected during post-ischemic heart failure where the mismatched rates of glycolytic flux and glucose oxidation result in preferential accumulation of protons that stimulate similar detrimental cascades adding to the deterioration of myocardial function and the developing metabolic inefficiency. This thesis studies the possibility to halt the initiating events of proton accumulation through favouring a better match

between glycolytic flux and glucose oxidation using several approaches to prevent ionic dysregulation during the developing post-ischemic heart failure or during further IR insult in remodeled hearts.

1.3.2.2 Mitochondrial oxidative metabolism

Increased catecholamine release is a known feature of the response to IR *in vivo*. Catecholamines favour insulin resistance, decrease insulin release and stimulate lipolysis [298-300]. Furthermore, the associated stress response involves increased corticosteroid hormone release which, in turn, induces insulin resistance and interferes with myocardial glucose utilization [301]. This response is usually transient but catecholamines can remain elevated up to 24 h depending on the severity of IR [302]. The overall response is increased circulating FFA and glucose levels. During reperfusion, the myocardium faces these increased levels resulting in increased glucose and FFA uptake. Since recovery of mitochondrial glucose oxidation is delayed relative to fatty acid oxidation [303], most of glucose undergoes glycolysis during reperfusion that is not matched to glucose oxidation rates resulting in further proton accumulation and subsequent deterioration of ionic homeostasis as mentioned above. Besides, fatty acid oxidation remains the predominant process for residual oxidative metabolism [303-308]. The increased dependence on fatty acid oxidation, being metabolically inefficient, adds to deterioration in mechanical function and metabolic inefficiency.

In the case of total ischemia, NADH, and FADH₂ can accumulate [309], and inhibit the acyl CoA dehydrogenase and 3-hydroxyacyl CoA dehydrogenase enzyme reactions of fatty acid oxidation [5, 20, 310, 311]. Also, acylcarnitines

can accumulate in the mitochondrial matrix and cytosolic compartments, while acyl CoA species can accumulate primarily in the mitochondrial matrix [312]. The accumulation of acylcarnitine and acyl-CoAs lead to the disruption of mitochondrial cristae, and the formation of amorphous intramitochondrial densities. These changes in mitochondrial ultrastructure may ultimately disrupt mitochondrial function [20, 313].

1.3.2.3 Response of remodeled hearts to IR

Based on their metabolic inefficiency, it might be expected that remodeled hearts would be more susceptible to subsequent IR injury than normal healthy hearts. However, several studies have provided evidence that remodeled hearts have a greater tolerance to ischemia [314-316]. In a comparison of normal and remodeled hearts perfused in the Langendorff mode, Kalkman *et al* [315] reported that remodeled hearts have a lower ischemia-induced release of lactate and purines. Similar tolerance to ischemic injury in remodeled hearts was confirmed by Pantos *et al* [314] who showed that the lower release of LDH was accompanied by less ischemic contracture, a higher expression of heat shock protein 70, as well as an improved recovery of mechanical function during post-ischemic reperfusion. Both studies employed non-working Langendorff preparations so metabolic mechanisms were not investigated. Less dysregulation of ion homeostasis has also been noted in remodeled hearts by Sharikabad and colleagues [316] who reported that cardiomyocytes derived from post-infarction remodeled rat hearts exhibit less Na⁺ and Ca²⁺ accumulation than cells from normal hearts. They also found lower release of LDH and less depletion of ATP

content during hypoxic challenge of remodeled cardiomyocytes, but the mechanistic basis of the increased tolerance has not yet been elucidated.

It is known that energy substrate metabolism and substrate preference during reperfusion affect recovery of LV mechanical function [13, 20, 317, 318]. For example, acceleration of fatty acid oxidation during reperfusion inhibits glucose oxidation (Randle effect) and thereby increases the uncoupling of rates of glycolysis and glucose oxidation leading to increased proton production. This slows the rate of recovery of intracellular pH and contributes to further accumulation of Na^+ and Ca^{2+} overload [317]. On the other hand, inhibition of glycolysis during early reperfusion limits Ca^{2+} overload and improves post-ischemic recovery of LV function secondary to improved matching with glucose oxidation that limits the subsequent events that leads to dysregulation of ionic homeostasis [318]. Thus optimizing energy substrate metabolism during IR can be a useful tool to minimize IR injury and promote functional recovery.

1.3.3 Pharmacologic metabolic interventions to improve cardiac metabolic inefficiency

As stated above, metabolic inefficiency is one of the two themes explaining metabolic changes in heart failure [19, 319]. Among the various contributors to metabolic inefficiency in heart failure (reviewed in Masoud et al [221]), mismatched glucose oxidation is of particular importance due to availability of pharmacologic and genetic intervention tools to lessen it.

One approach to restore a reasonable match between glycolytic flux rate and glucose oxidation rate is to stimulate glucose oxidation. This can be achieved either directly via PDH stimulation using metabolic modulators such as DCA or indirectly via inhibiting fatty acid oxidation (Randle cycle). In this regard, many approaches have been tried to inhibit fatty acid oxidation including trimetazidine, perhexiline and MCD inhibition [207, 226-228, 230, 232-234, 320-322]. While the other interventions have been reviewed in detail (Jaswal et al [20] and Fillmore et al [323]), MCD inhibition is an evolving promising approach to improve matching of glucose metabolism in models of heart failure, especially post-infarction heart failure [59].

1.3.3.1 MCD inhibition limits metabolic inefficiency and functional deterioration in heart failure

A recent study by Wu et al [60] reported that cardiac-specific MCD deletion via microRNA limits functional deterioration and preserves energy stores in post-infarction remodeled rat hearts [60]. Similarly, other studies highlighted the importance of MCD inhibition in the setting of ischemia, heart failure and insulin resistance [66, 67, 96, 221, 322, 324]. The ability of MCD inhibition to improve the matching of glucose oxidation through indirect stimulation of glucose oxidation secondary to inhibition of fatty acid oxidation (Randle effect) was shown to reduce lactate production in ischemic pig hearts following demand-induced ischemia [66]. Furthermore, MCD inhibition was shown to improve post-ischemic functional recovery in *ex vivo* perfused rat hearts [66, 67]. This was

associated with improved matching of glucose oxidation, due to stimulated glucose oxidation secondary to inhibition of fatty acid oxidation, resulting in less lactate production [66, 67].

It is known that genetic interventions such as MCD-KO can result in a myriad of compensatory mechanisms that can confound the results. In this regard, it was found that MCD-KO mouse hearts maintain comparable energy substrate metabolic rates under normal aerobic perfusion conditions despite an increase in malonyl CoA content [96]. The authors concluded that compensatory increase in the fatty acid carrier, CD36, uncoupling protein 3 (UCP3), creatine phosphate CPT1 or pyruvate PDK4 [96]. To dissect the effect of acute MCD inhibition in *ex vivo* perfused remodeled hearts from the confounding compensatory mechanisms seen in genetic MCD-KO hearts, we will study the consequences of *ex vivo* administration of an MCDi to remodeled hearts during post-ischemic perfusion.

1.3.3.2 DCA as a protective agent against ischemia reperfusion injury and heart failure

It has been shown that deterioration of post-ischemic LV function is associated with increased proton load due to dependence on glycolytic flux for ATP production [325-331]. This initiates events that activate NHE [332-335] and NCX [336-338] ending in Na⁺ and Ca²⁺ accumulation and contractile function deterioration. The details of metabolic changes that occur in IR injury have been previously described [13, 317, 328, 329, 331, 339-342].

An approach to minimize IR injury is to minimize the mismatch between glycolytic flux and glucose oxidation at the start of reperfusion. This can be achieved by either inhibiting glycolytic flux rates, using exogenous adenosine [328, 331, 340] or by limiting glucose-6-phosphate availability via its partitioning to glycogen synthesis [318], or via stimulating glucose oxidation rates either directly using DCA or indirectly via inhibiting fatty acid oxidation using trimetazidine [234, 320, 321, 343-349], etomoxir [350] or an MCD inhibitor [61, 64, 66, 322] (Randle cycle - Fig 1.1). The studies described in this thesis will examine the effect of DCA on remodeled hearts during post-ischemic reperfusion.

The reported protective effect of DCA against IR injury is due to its ability to rapidly reach the mitochondria after *in vivo* or *ex vivo* administration where it inhibits PDK. Thus, it prevents the inhibitory phosphorylation of PDH, the rate-limiting enzyme for pyruvate activation into acetyl CoA which is a common step for glucose, lactate and pyruvate oxidation [351-356]. The stimulation of glucose oxidation improves matching with glycolytic flux rates which prevents proton accumulation and minimizes acidosis. Both contribute to functional deterioration in IR injury [329, 330, 357-361].

The protective effect of DCA has been shown in many *ex vivo* models of heart disease. For instance, in hearts isolated from rats exposed to experimental endotoxemia, DCA improves functional parameters, namely stroke volume, cardiac output and peak systolic pressure, over a wide range of left atrial filling pressures associated with increased ATP production and stimulation of PDH [356, 362]. The metabolic effects of DCA that improve efficiency and limit proton

accumulation can explain the improvement of inotropic actions of amrinone and ouabain when given with DCA to hearts from rats exposed to experimental endotoxemia [363-365].

The response to DCA treatment varies significantly based on the timing of DCA addition. DCA added at reperfusion improves functional recovery in healthy hearts exposed to *ex vivo* IR [322, 329, 355, 366-370]. In contrast, addition of DCA to the perfusate before or at the start of reperfusion following global no-flow ischemia in isolated perfused working rat hearts does not limit LV functional deterioration at reperfusion and results in more lactate accumulation [368]. This may be due to the ability of DCA to stimulate glucose uptake secondary to inhibition of fatty acid oxidation as a consequence of stimulating glucose oxidation (Randle cycle - Fig 1.1) [310, 371-376]. This results in lowering of intracellular citrate [372, 373, 375] which normally inhibits fructose 1,6 biphosphate kinase (PFK1), the rate limiting enzyme in glycolysis. Consequently, glycolytic rates increase and offset the benefit of stimulating glucose oxidation with increased proton and lactic acid accumulation during ischemia. Similar experiments conducted by Ussher *et al* used DCA at reperfusion of hearts exposed to *ex vivo* IR resulted in improved functional recovery and decreased reperfusion proton production per unit LV work [322].

Similar protective effects of DCA have been described using *in vivo* models of IR and hearts failure. DCA administration to dogs 30 min before partial left anterior coronary (LAD) artery occlusion for 90 min reduced the depletion of myocardial ATP and creatine phosphate, prevented pH shift to acidic levels and

prevented rise in myocardial lactate [377]. Interestingly, DCA administration to open-chest dogs exposed to either partial or complete [374] LAD occlusion reduced the expected ST segment rise commonly seen in infarcted hearts without changing systemic hemodynamic parameters, coronary artery flow to the ischemic area, myocardial ATP or creatine phosphate content. The absence of changes in ATP or creatine phosphate contents can be explained on basis of a change in the source of ATP rather than a change in the amount of ATP produced. As stated above, DCA treatment improves matching of glucose oxidation and glycolytic rates secondary to stimulation of glucose oxidation. Consequently, fatty acid oxidation decreases (Randle cycle). Thus, total ATP production does not change but DCA enhances dependence on more efficient sources.

Results from clinical trials also support the experimental findings. DCA infusion in healthy male volunteers improved their cardiac index and reduced peripheral vascular resistance and blood lactate levels. These findings were not associated with increase in arterial oxygen saturation but cardiac output did increase, indicative of improved tissue oxygen delivery [378]. Similarly, intravenous DCA administration in normotensive patients with stable coronary artery disease [379] resulted in improvement of cardiac output, and stroke volume, decreased systemic lactate and peripheral vascular resistance while heart rate, coronary blood flow and MVO_2 did not decrease. The latter indicates improved cardiac efficiency in treated patients since LV work increased in those patients without increase in MVO_2 . DCA was also shown to have superior effects to pharmacologic inotropic medications such as dobutamine. Patients with severe

congestive heart failure treated with intravenous DCA had similar hemodynamic benefits to those treated with dobutamine [214]. In addition, MVO_2 increased in DCA-treated, but not dobutamine-treated, patients indicative of improvement of cardiac efficiency in the former.

1.3.3.2.1 Linking DCA-induced glucose oxidation to changes in fatty acid oxidation and glycolytic flux rates

DCA localizes in the helix bundle in the N-terminal domain of PDK. Bound DCA promotes local conformational changes that are communicated to both nucleotide-binding and lipoyl-binding pockets of PDK1, leading to the inactivation of kinase activity [380]. Thus, PDK fails to phosphorylate and inhibit PDH. Consequently, increased acetyl CoA stimulates ACC to produce malonyl CoA. Malonyl CoA, in turn, inhibits CPT1 on the outer mitochondrial membrane reducing fatty acyl CoA uptake resulting in inhibition of fatty acid oxidation. Hence, intracellular citrate levels decrease and PFK1 is no longer allosterically inhibited by citrate leading to stimulation of glycolysis. The shift from fatty acid oxidation to glucose metabolism increases metabolic efficiency as glucose produces more ATP units per oxygen as compared to fatty acids.

1.3.4 Conclusion

Both cardiac energy starvation and cardiac inefficiency may contribute to the severity of heart failure. These two contributing mechanisms are also not mutually exclusive, and may coexist. However, it is likely that energy starvation occurs later in the course of heart failure, while inefficiency may be present

throughout the course of heart failure, including the very early stages where metabolic interventions are expected to yield maximum benefit. It would thus be desirable to consider cardiac inefficiency when designing metabolic modulators to treat heart failure, since stimulation of substrate utilization may not always be beneficial. This is supported by reduced efficiency observed with acceleration of fatty acid oxidation or of glycolysis.

Cardiac inefficiency may be a contributor to the severity of ischemia reperfusion injury in remodeled hearts. However, many reports indicate that remodeled hearts have better tolerance to ischemia reperfusion injury. These observations included less release of lactate dehydrogenase, less buildup of intracellular pH and less accumulation of Na^+ and Ca^{2+} . None of these reports studies changes in metabolic efficiency before and after ischemia reperfusion injury in remodeled hearts as compared to normal hearts.

Several metabolic interventions have been tried to lessen functional deterioration following IR and the subsequent development of heart failure. These interventions include fatty acid oxidation inhibition, inhibition of glycolysis and stimulation of glucose oxidation. This thesis studies two pharmacologic interventions. The first intervention is the pharmacologic MCD inhibition during aerobic perfusion of remodeled hearts. This helps to study the potential for improvement of their metabolic inefficiency in remodelled hearts. The second intervention is *ex vivo* administration of DCA in reperfused remodeled hearts following *ex vivo* IR to study the potential for improving functional recovery and limiting deterioration of metabolic inefficiency.

1.3.5 Hypothesis and Objectives

Heart failure is associated with metabolic change the nature of which is not well characterized. The main two themes that explain these metabolic changes are energy starvation and metabolic inefficiency. These metabolic changes are expected to affect recovery of remodeled heart following a second IR. However, whether remodeled hearts are more susceptible or more protected against IR is also not agreed upon. Metabolic interventions such as inhibiting fatty acid oxidation, inhibiting glycolysis or stimulating glucose oxidation have been proposed to improve functioning of remodeled hearts.

1.3.5.1 Hypothesis

Post-infarction remodeled failing hearts are not energy starved. Rather they are metabolically inefficient and can benefit from interventions that aim to improve matching of glucose oxidation and glycolytic flux whether directly via stimulating glucose oxidation or indirectly via fatty acid oxidation inhibition (Randle cycle). These hearts are expected to suffer more deterioration in function and metabolic efficiency following *ex vivo* IR as compared to healthy unremodeled hearts. The state of metabolic inefficiency in remodeled hearts can be improved by metabolic interventions such MCD inhibition. Similarly, stimulating glucose oxidation during post-ischemic reperfusion in remodeled hearts is expected to improve their functional recovery secondary to lessened deterioration of metabolic inefficiency.

1.3.5.1.1 Specific Objectives

1. To characterize energy substrate metabolic changes in remodeled post-infarction hearts to study the nature of these changes and whether metabolic inefficiency or energy starvation dominates in our model.
2. To test whether chronic MCD deficiency and the subsequent improvement of glucose metabolism matching can limit post-infarction deterioration in LV function and metabolic efficiency in mouse hearts
3. To study response of post-infarction remodeled hearts to *ex vivo* IR and the associated changes in metabolic efficiency as compared to unremodeled mouse hearts.
4. To study whether MCD is a target for pharmacologic inhibition to improve metabolic inefficiency in remodeled failing hearts via *ex vivo* exposure to an MCDi during aerobic perfusion. Also to study potential for improvement of functional recovery and metabolic efficiency of remodeled hearts following *ex vivo* IR using DCA applied at reperfusion.

1.1 Relationship between glycolysis, glucose oxidation and fatty acid oxidation

Glucose is taken up by the cell via activity of glucose transporter 1 (GLUT1) and the insulin-dependent glucose transporter 4 (GLUT4). Glycolysis occurs in the cytosol and is composed of 3 main steps (priming, splitting and energy trapping). Priming of glucose occurs via consecutive steps where hexose kinase (HK) phosphorylates glucose at carbon 6 to produce glucose-6-phosphate (G-6-P) that is then isomerized into fructose-6-phosphate (F-6-P) via the activity of phosphoglucose isomerase (PGI). The rate limiting enzyme of glycolysis, phosphofructokinase-1 (PFK1) adds another phosphate group to carbon 1 producing fructose 1,6 bisphosphate (F-1,6 BP). The second stage of glycolysis is splitting of F-1,6 BP by aldolase into 2 molecules of glyceraldehydes 3 phosphate (G-3-P). The third stage is energy trapping where high energy molecules are produced. First each of G-3-P is converted into 1,3 bisphosphoglycerate (1,3 BPG) via glyceraldehydes 3 phosphate dehydrogenase (GAPD). Phosphoglycerate kinase (PGK) converts 1,3 BPG into 3 phosphoglycerate (3PG) that is isomerized into 2 PG via phosphoglycerate mutase (PGM). Enolase removes a molecule of H₂O to produce phosphoenol pyruvate (PEP) that is converted to pyruvate via pyruvate kinase (PK). Pyruvate can be reversibly converted into lactate via lactate dehydrogenase (LDH). For pyruvate to be oxidized in the mitochondria, it is transported into the mitochondria via pyruvate transporter (Monocarboxylate transporter 1 - MCT1). MCT cotransports protons with pyruvate inside the mitochondria. Pyruvate is then activated via pyruvate

dehydrogenase complex (PDH) into acetyl CoA which then enters tricarboxylic acid (TCA) cycle for pyruvate oxidation.

Fatty acyl CoA is transported into the mitochondria via the activity of carnitine palmitoyl transferase 1 and 2 (CPT1 and CPT2) where it undergoes β -oxidation to produce acetyl CoA that feeds into TCA cycle.

Glycolysis, glucose oxidation and fatty acid oxidation can alter the rate of each other in many ways such as:

1. PFK1, the rate limiting enzyme of glycolysis, which is allosterically activated by the products of PFK2 is suppressed by the increasing cytosolic citrate concentration secondary to increased TCA activity due to increased glucose or fatty acid oxidation.
2. PDH kinase (PDK) which inhibits PDH via phosphorylation, is activated by increased acetyl CoA production from either β -oxidation or pyruvate activation itself. Thus, glucose oxidation is inhibited.
3. Acetyl CoA from pyruvate activation is transported to cytosol via carnitine acetyl transferase (CAT) where it produces malonyl CoA, via acetyl CoA carboxylase (ACC), that competes with fatty acyl CoA for mitochondrial uptake, thus fatty acid oxidation inhibition.

Figure 1.1

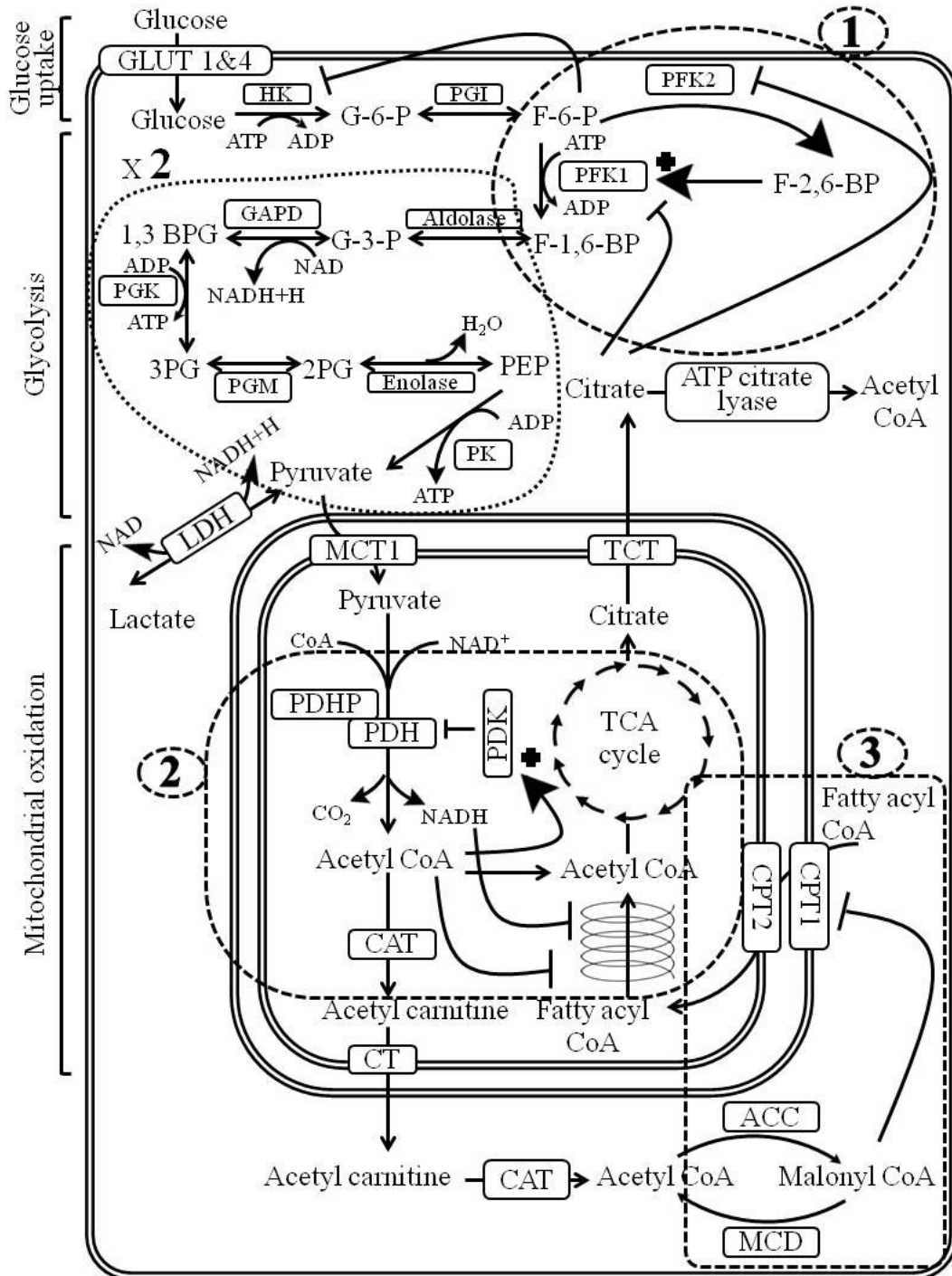
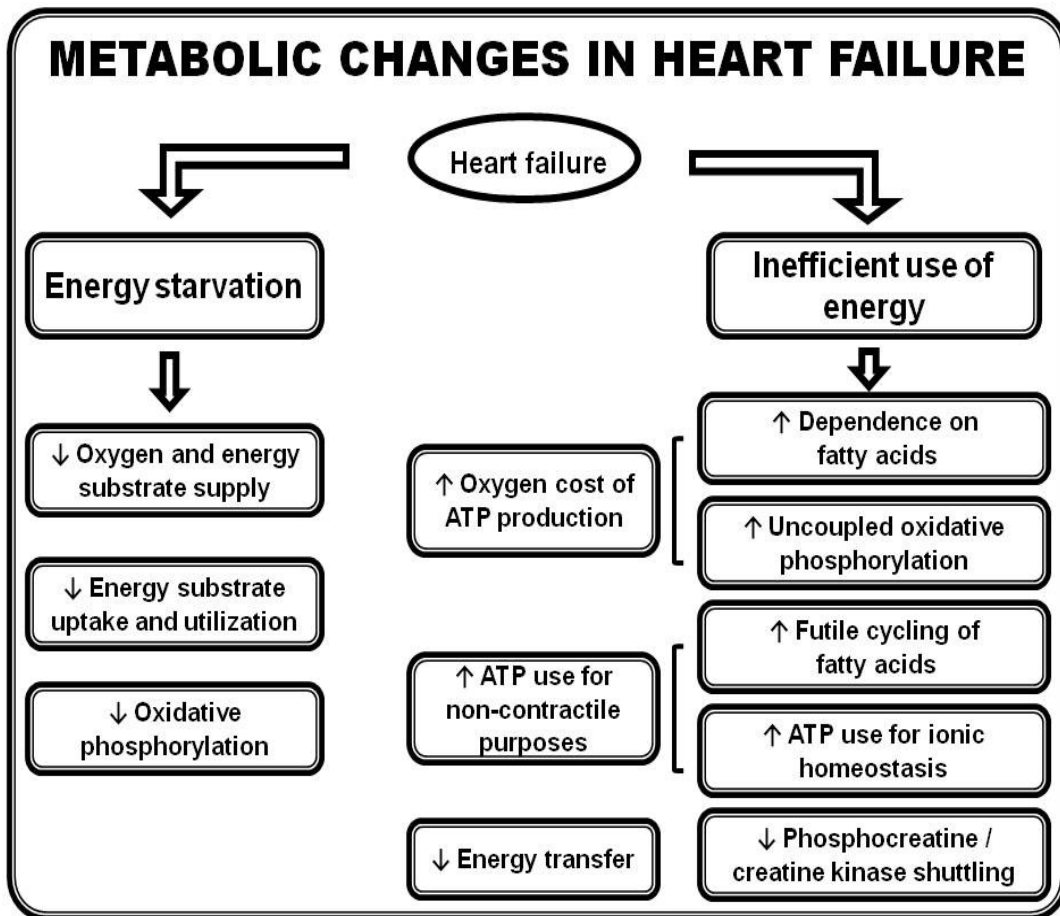


Figure 1.2 Energy metabolic changes in heart failure.

The energy starvation theory describes the failing heart as an engine out of fuel with: a) reduction of oxygen and substrate delivery to the heart, b) reduction in energy substrate uptake and utilization, and c) reduced mitochondrial oxidative phosphorylation. The cardiac inefficiency theory considers the inefficient energy utilization for mechanical work due to: a) increased oxygen cost of ATP production which in turn can be due to the preferential dependence on fatty acids or uncoupling of oxidation phosphorylation. b) increased use of ATP for homeostatic activities that include futile cycling of fatty acids and ionic homeostasis secondary to increased Na^+ and Ca^{2+} accumulation induced by mismatched glucose metabolism, c) reduced energy transfer to myofibrils due to impaired phosphocreatine/creatine kinase shuttle.

Figure 1.2

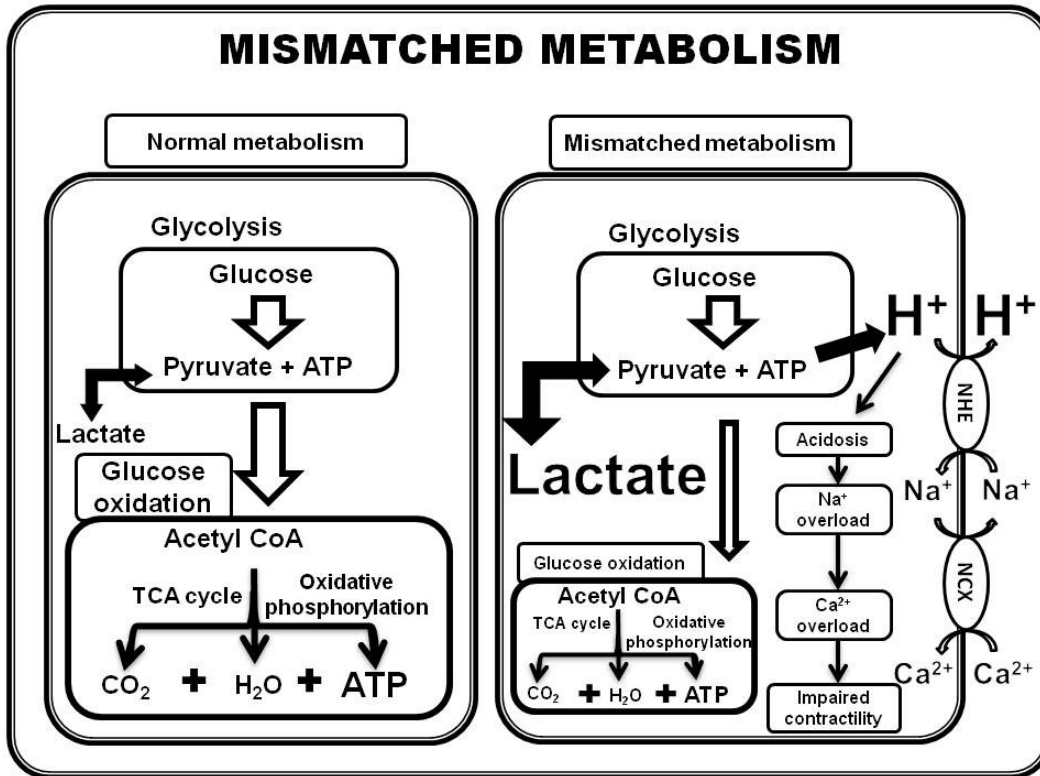


1.3 Normal versus mismatched glucose metabolism.

Intracellular proton production arises when the rate of glycolysis exceeds the rate of glucose oxidation. If glycolysis increases and / or glucose oxidation decreases (mismatched rates of glucose metabolism), proton production from the hydrolysis and glycolytically-derived ATP accelerates and causes intracellular acidosis.

Efflux of proton leads to Na^+ overload (activity of sodium-hydrogen exchanger (NHE)) and ultimately Ca^{2+} overload (activity of reverse mode sodium-calcium exchanger (NCX)) that causes cardiac mechanical dysfunction and inefficiency.

Figure 1.3



2 Materials and Methods

Part of this section is published in the online supplement of a paper in Cardiovasc Res; Masoud WG, Ussher JR, Wang W, Jaswal JS, Wagg CS, Dyck JR, et al. “Failing mouse hearts utilize energy inefficiently and benefit from improved coupling of glycolysis and glucose oxidation”. 2014;101:30-38

2.1 Materials

Bovine serum albumin (BSA fraction V, free fatty acid free) was purchased from Equitech-Bio, Inc. (Kerrville, Texas). [U-¹⁴C]glucose, D-[5-³H]glucose, [U-¹⁴C]lactate and [9,10-³H]palmitate were purchased from Perkin Elmer (Boston, Massachusetts, USA). Insulin (Novolin® ge Toronto) was purchased through the University of Alberta Hospital stores from Novo Nordisk (Mississauga, Ontario, CA). Euthanyl (pentobarbital sodium) was purchased from Bimeda-MTC Animal Health Inc. (Cambridge, Ontario, CA). Hyamine hydroxide (1 M in methanol solution) was purchased from J.T Baker (Phillipsburg, New Jersey, USA). Ecolite™ and Cytoscint™ Aqueous Counting Scintillation fluids were purchased from MP Biomedicals (Solon, Ohio, USA). AG® 1-X4 anion exchange resin, chloride form, 4% cross linkage, 200-400 dry mesh size was obtained from Bio-Rad Laboratories, Inc (Hercules, California, USA). Glucose assay kits were purchased from Sigma Diagnostics (St. Louis, Missouri, USA). Protease inhibitor cocktail was purchased from Sigma-Aldrich, Inc. (St. Louis, Missouri, USA). Phosphatase inhibitor cocktails 2 and 3 were purchased from Sigma-Aldrich, Inc. (St. Louis, Missouri, USA). Bio-Rad protein assay dye reagent concentrate, nitrocellulose membranes (Trans-Blot® Transfer Medium, 0.45 µm), Precision plus protein™ dual color molecular weight marker and Mini-Protean gel electrophoresis system were purchased from Bio-Rad Laboratories, Inc. (Hercules, California, USA). Kodak BioMax MR films were purchased from Care stream Health, Inc (Rochester, New York). Fuji medical X-ray films (Super RX) were purchased from FUJIFILM Europe GmbH (Düsseldorf, Germany).

Amersham™ ECL™ prime Western Blotting Detection Reagent was purchased from GE Healthcare (Buckinghamshire, UK). Monoclonal and polyclonal antibodies for phosphorylated AMP-dependent kinase (p-AMPK^{Thr172}), AMP-dependent kinase (AMPK), PPAR gamma co-activator 1-alpha (PGC1- α), pyruvate dehydrogenase (PDH), hexokinase, voltage dependent anion channel (VDAC), glucose transporter 4 (GLUT4), acetyl CoA carboxylase (ACC), Phosphorylated ACC (p-ACC), peroxisome proliferator activated receptor alpha (PPAR α), sarco/endoplasmic reticulum calcium ATPase-2 (SERCA2) and peroxidase-conjugated goat anti-rabbit secondary antibody were purchased from Cell Signaling Technology (Danvers, Massachusetts). Antibodies to Ca²⁺/calmodulin-dependent protein kinase II (CAMKII), phosphorylated CAMKII (p-CAMKII^{Thr286}), long chain fatty acyl CoA dehydrogenase (LCAD), β -hydroxy acyl CoA dehydrogenase (β -HAD) and Complex I subunit (NADH dehydrogenase [ubiquinone] 1 β subcomplex subunit 6 (NDUFB6)) were purchased from ABCAM, Inc. (Cambridge, Maryland, USA). Antibody to GLUT1 was purchased from FabGennix International, Inc. (Frisco, Texas, USA). ATX Ponceau S red staining solution and dichloroacetate were purchased from Sigma-Aldrich, Inc. (St. Louis, Missouri, USA). All other chemicals are purchased from Fischer Scientific, Inc. (New Jersey, USA).

Small animal intubation kit was purchased from Kent Scientific Co. (Connecticut, USA). Self-retaining chest retractor, dissecting forceps, surgical scissors (different sizes) and needle holders (different sizes) were purchased from Fine Science Tools, Inc. (California, USA). 7-0 non-absorbable sutures and 6-0

non-absorbable silk sutures were purchased from Ethicon Endo-Surgery, Inc. (Ohio, USA). C57/Bl6 mice were purchased from Charles River Laboratories, USA. The colony of MCD-KO mice was established by Dr. Lopaschuk's lab and Chugai Pharmaceuticals.

2.2 Methods

2.2.1 Mouse model of post-infarction heart failure:

All experimental procedures were approved by the Animal Care and Use Committee, University of Alberta. They also conform to guidelines of the Canadian Council of Animal Care, Alberta and the *Guide for the Care and Use of Laboratory Animals*; published by the National Institutes of Health (NIH Publication No. 85-23, Revised 1996). Male C57BL/6 mice aged 12 week were subjected to either coronary artery ligation (CAL) or sham (SHAM) procedure, as described previously [381, 382]. Briefly, animals were anesthetized with intraperitoneal pentobarbital sodium (60 mg/kg) and intubated with a 20-gauge plastic cannula and ventilated with 100% oxygen. Once the animal reached surgical plane anesthesia, as indicated by loss of withdrawal reflex, a left thoracotomy incision was made to expose the left ventricle (LV). Using 7-0 prolene threads, the left anterior descending coronary artery was permanently-ligated. The chest wall, muscle and skin, was closed in layers using 6-0 silk threads. At the end of the procedure, a dose of buprinorphine (0.05 mg/kg. IM) was given. Animals were monitored for pain, as described before [383], during the first 3 postsurgical days as indicated by piloerection, hunched posture, reduced activity, reduced appetite and reduced drinking. A second dose of

pubrinorphine was given if needed. A 4 week-postsurgical period was allowed to guarantee the development of a mature scar prior to *ex vivo* functional and metabolic evaluation of the animals.

2.2.2 *In vivo* evaluation of heart function by echocardiography:

LV wall thicknesses were measured using a modified version of the leading-edge method of the American Society for Echocardiography using three consecutive cycles of M-mode tracing[384, 385]. Myocardial peak velocities (systolic and diastolic) were derived at the mitral valve level and the ratio between early mitral inflow velocity and mitral annular early diastolic velocity (E/E') ratio was used as an indicator of LV filling pressure [384, 385]. Other indicators of diastolic function included isovolumetric relaxation time (IVRT), mitral valve deceleration time (MV DT), ratio of early (E) and late (A) mitral inflow velocities (E/A) and Tei index (calculated as sum of isovolumetric relaxation and contraction times (IVRT+IVCT) divided by ejection time (ET) were also calculated. Simpson's measurements were performed to obtain an averaged ejection fraction (%EF) and fractional area change (%FAC) of all CAL animals and representative samples of the SHAM group. Only a representative sample of SHAM hearts was required since wall motions were observed to have synchronous motion, whereas infarcted groups had asynchronous wall motion. Since both MCD-KO CAL and WT CAL mice were expected to have infarcts and

asynchronous wall motion, the averaged %EF and %FAC were calculated using Simpson's measurements.

2.2.3 *Ex vivo* isolated working heart perfusions:

Three days after echocardiography, animals were deeply anesthetized (pentobarbital, 480 mg/kg, ip) and hearts were excised and immediately placed in ice-cold Krebs-Henseleit solution. The aorta was cannulated and perfusion initiated (60 mmHg pressure and 37°C) while the left atrium was cannulated. Hearts were then perfused aerobically in working mode [69, 340] (50 mmHg afterload and 11.5 mmHg preload) using a recirculating perfusate (100 ml) composed of (in mM) 1.2 KH₂PO₄, 1.2 MgSO₄ · 7H₂O, 2.5 CaCl₂ · 2H₂O, 4.7 KCL, 25 NaHCO₃ and 118 NaCl. Palmitate (1.2 mM, prebound to 3% fatty acid free bovine serum albumin), glucose (11 mM) and lactate (1 mM) were added as energy substrates, as well as insulin (100 µU/mL. Thin film oxygenation of the perfusate was achieved using carbogen (95% O₂ and 5% CO₂) to maintain O₂ saturation and a pH of 7.4. Times of perfusion protocol depended on the study and details are provided in each corresponding Chapter. Normal healthy hearts were perfused under the same perfusion conditions and with the same energy substrate concentrations. MCD-KO CAL and SHAM hearts were perfused using a perfusate that contained glucose (5 mM), lactate (1 mM) and palmitate (0.4 mM) in an attempt to replicate the perfusion conditions of Ussher *et al* [322]. In that paper, the rate of proton production during reperfusion was shown to be lower in MCD-KO hearts due to improved matching of glucose metabolism. An additional group of WT CAL hearts was added as an appropriate control. Apart from the

change in energy substrate concentration, all other constituents of perfusate were comparable to that used in all other experiments. After perfusion, infarcts were excised and hearts were immediately frozen in liquid nitrogen (using Wollenberger clamps) and stored at -80°C . Infarct sizes were expressed as the percentage of infarct wet weight to total heart wet weight.

2.2.4 Measurement of LV function

Systolic and diastolic aortic pressures were measured during working heart perfusions using a Gould P21 pressure transducer attached to the aortic outflow line. Cardiac output (mL/min) and aortic flow (mL/min) were measured via ultrasonic flow probes (Transonic T206) placed in the left atrial inflow line and the aortic outflow line, respectively. The difference between cardiac output and aortic flow was used to calculate coronary flow. The ratio of coronary flow and mean aortic pressure normalized to heart dry wt was used to calculate coronary vascular conductance (CVC, mL/min/mmHg/g dry wt). The product of cardiac output and LV developed pressure (systolic pressure – preload pressure (11.5 mmHg)) normalized to the heart dry weight was used as an index of LV mechanical function and was termed LV work (Joule/min/g dry wt).

2.2.5 Measurement of rates of energy substrate

metabolism and calculation of ATP production

rates:

Rates of glycolysis, glucose oxidation, fatty acid oxidation, and lactate oxidation were measured and expressed per gram viable tissue ($\mu\text{mol}/\text{min}/\text{g}$ dry wt, where viable tissue in SHAM hearts is the whole ventricular tissue and in CAL is the ventricular tissue excluding the infarct) as described previously [386] using $[5\text{-}^3\text{H}]\text{glucose}$ and $[\text{U-}^{14}\text{C}]\text{glucose}$ to measure glycolysis and glucose oxidation, respectively. Another set of perfusions used $[9,10\text{-}^3\text{H}]\text{palmitate}$, and $[\text{U-}^{14}\text{C}]\text{lactate}$ to measure palmitate oxidation and lactate oxidation, respectively. These substrates were added to the Krebs-Henseleit solution at the start of working mode perfusion. Glycolytic rates were measured by the quantitative determination of the accumulation of $^3\text{H}_2\text{O}$ liberated from $[5\text{-}^3\text{H}]\text{glucose}$ by the glycolytic enzyme, enolase catalyzing the conversion of 2 phosphoglycerate into phosphoenol pyruvate.. Separation of $^3\text{H}_2\text{O}$ from $[5\text{-}^3\text{H}]\text{glucose}$ in the perfusate samples is achieved by passing 100 μL of perfusate through AG® 1-X 4 anion exchange resin (200-400 mesh) columns as described previously [171]. Thereafter, the columns were washed with 800 μL of distilled water. The eluted water was collected in 5 mL scintillation vials together with 4 mL of scintillation fluid (Ecolite, MP Biomedicals (Solon, Ohio)). This is followed by counting the radioactivity in a liquid scintillation counter.

Rates of glucose oxidation and lactate oxidation were determined by quantitative determination of $^{14}\text{CO}_2$ liberated at the level of pyruvate dehydrogenase and in the TCA cycle from [^{14}C]glucose and [^{14}C]lactate, respectively. This accounted for both the TCA cycle end product; $^{14}\text{CO}_2$ that is released during the experiment and captured in hyamine hydroxide trap as well as [^{14}C]HCO₃ retained in the perfusate and released as $^{14}\text{CO}_2$ via reaction with 9N H₂SO₄ and then trapped on hyamine-soaked filter papers. The trapped $^{14}\text{CO}_2$ is collected in 5 mL scintillation vials and 4 mL of scintillation fluid (Cytoscent, ICN) were added and the radioactivity was counted in a liquid scintillation counter [171].

Palmitate oxidation rates were determined by quantitative determination of $^3\text{H}_2\text{O}$ liberated from [9,10- ^3H]palmitate. A vapor transfer method was used to separate $^3\text{H}_2\text{O}$ from perfusate samples as described previously [387]. Briefly, 500 μL of water was put in a 5 mL scintillation vial, and then a lidless 1.5 mL micro-centrifuge tube containing 200 μL of the perfusate was placed inside the scintillation vial. The vials were then capped and stored overnight at 50 °C then stored at 4 °C for another 24 hours. After that, the micro-centrifuge tubes were removed, any water droplets on the outer surface of the micro-centrifuge tubes were wiped using filter papers (1 cm X 1 cm) that were placed inside the corresponding scintillation vials. Scintillation fluid was then added (Ecolite, MP Biomedicals (Solon, Ohio)) and the radioactivity was then counted using liquid scintillation counter. Perfusate samples were collected at the following time points: 5, 20, 35, 44, 60, 70, 80 and 90 min and metabolic rates ($\mu\text{mol}/\text{min}/\text{g}$ dry

wt) were calculated and were averaged for each phase of the perfusion protocol (aerobic and reperfusion).

ATP production rates from each substrate were calculated for each energy substrate by multiplying the metabolic rates by the corresponding ATP molecular yield expected from each substrate as follows: 104 for palmitate oxidation, 31 for glucose oxidation, 17 for lactate oxidation and 2 for glycolysis.

Proton production from glucose metabolism is derived from hydrolysis of glycolysis-derived ATP (2 ATP per 1 glucose molecule produce 2 protons) while TCA cycle utilizes 1 proton for each pyruvate molecule (2 protons for each glucose molecule oxidized) at the pyruvate carboxylation step. Thus, if the rate of glycolysis and glucose oxidation are mismatched, there is a net proton production, the rate of which is $2 \times (\text{glycolysis rate} - \text{glucose oxidation rate})$ [369]. This method was previously validated and compared to pH_i measurements using ^{31}P NMR [317].

2.2.6 Measurements of glycogen content and turnover:

Myocardial glycogen content ($\mu\text{mol glucosyl unit/g dry wt}$) was measured as described previously [369] via measurement of glucose content in samples of frozen powdered heart tissue subjected to alkaline extraction by 30% KOH, ethanol precipitation and acid hydrolysis (2 N H_2SO_4). The rate of glycogen synthesis ($\mu\text{mol/min/g dry wt}$) was calculated as described previously [388] from the rate of incorporation of radiolabeled glucose into myocardial glycogen assuming that glycogen is made up of homogenous glucosyl moieties. The net

glycogen degradation rate was measured from the change in the unlabeled myocardial glycogen pool over the 45 minute aerobic perfusion protocol [388]. ATP production from glycogen degradation was calculated based on the assumption that all glycogen-derived G-6-P undergoes glycolysis. The ATP produced from subsequent glucose oxidation was calculated using the observed glycolysis to glucose oxidation ratio in respective groups and the same yield used for ATP production from exogenous energy substrates (see previous section).

2.2.7 Measurements of TG content and turnover:

Frozen heart tissue (15-20 mg) was extracted in a 20-fold volume of 2:1 chloroform-methanol, following which an 0.2 mL volume of methanol was added, and the extract was vortexed for 30 s. The mixture was then centrifuged at 3500g for 10 min, and the supernatant was collected. A 0.2 volume of 0.04% CaCl₂ was added to the supernatant, which was then centrifuged at 2400g for 20 min. The upper phase was removed and the interface was washed with pure solvent upper phase consisting of 1.5 mL chloroform, 24.0 mL methanol, and 23.5 mL water. The previous step was repeated three times and the final wash was removed. After that, 50 µL of methanol was added to form one phase. The samples were then dried under N₂ at 60 °C and re-dissolved in 50 µL of 3:2 *tert*-butyl alcohol-Triton X-100/methyl alcohol. Cardiac TG was then quantified colorimetrically with an enzymatic assay (Wako Pure Chemical Industries) [389]. Rates of degradation were calculated based on the changes of cold TG content between time zero and 45 min. Rates of synthesis were calculated based on the incorporation of radiolabelled palmitate over the 45-min period assuming that TG

is made up of homogenous palmitoyl moieties. ATP production from unlabelled TG was calculated based on the assumption that TG fatty acids undergo complete β -oxidation.

2.2.8 Immunoblot analysis of protein expression:

Powdered heart tissue, maintained at the temperature of liquid nitrogen, was homogenized (10% w/v) in homogenization buffer that contains (mmol/L) 5 sodium pyrophosphate, 50 NaCl, 20 Tris·HCl, 50 NaF, 250 sucrose, phosphatase inhibitor cocktail 2 and 3, protease inhibitor cocktail (Sigma- Aldrich, Inc., St. Louis, Missouri) and 1 DTT. Tissue homogenates were centrifuged at 1000g for 10 min at 4 °C. The supernatant was aliquoted for storage at - 80 °C for further analysis. Protein levels in the supernatant were determined by Bio-Rad® protein assay. 30 μ g of homogenate protein (20 μ g in case of LDH-A and GAPDH) were run for SDS-polyacrylamide gel electrophoresis then transferred to nitrocellulose membranes as previously described [390]. After blocking (5% milk) for 1 hour at room temperature, membranes were incubated overnight with rabbit antibodies against phospho AMPK (p-AMPK^{Thr172}), AMPK, peroxisome proliferator-activated receptor gamma coactivator 1-alpha (PGC1- α), GLUT4, LDH, PDH, HK, GAPDH, voltage dependent anion channel (VDAC), glycogen synthase kinase-3 β (GSK3 β), phospho-glycogen synthase kinase-3 β (pGSK3 β) and PPAR α (1:1000 dilution - Cell Signaling Technology Inc., Danvers, Massachusetts, USA) and rabbit antibodies against phosphor CAMKII (p-CaMKII^{Thr286}), CaMKII, long chain acyl CoA dehydrogenase (LCAD), β -HAD, NDUFB6 and mouse antibodies against phospholamban (1:1000 dilution - ABCAM Inc., Cambridge, Maryland,

USA) and GLUT1 (1:1000 dilution - FabGennix Inc, Frisco, Texas, USA) in 5 % BSA (wt/vol) in TBS. After the membranes were extensively washed, they were incubated with a peroxidase-conjugated goat anti-rabbit secondary antibody (1:2000 dilution - Cell Signaling Technology Inc. Danvers, Massachusetts, USA) or goat anti-mouse (1:5000 dilution - Bio-Rad) in 5% skim milk powder (wt/vol) in TBS when appropriate. After 3 times wash each of 5 min, antibodies were visualized using the Amersham ECL Prime Western blotting detection system (GE Healthcare, Buckinghamshire, UK). Densitometric analyses of immunoblots were performed using ImageJ software (National Institute of Health, Bethesda, Maryland). Ponceau staining (Ponceau S staining solution, Sigma -Aldrich, Missouri, USA) was used as loading control as described previously [391]. Values are presented relative to SHAM heart values.

2.2.9 Measurement of adenine nucleotide and creatine content in frozen heart tissue:

Separation of nucleotides (ATP, ADP, AMP, GTP), inosine, creatine phosphate and creatine was achieved using ultra performance liquid chromatography (UPLC) as described previously [392], using a 2.1×100 mm ACQUITY UPLC HSS T3 column packed with $1.7 \mu\text{m}$ particles (Waters, Milford, MA, USA), by recording the optical density at 254 nm for adenine nucleotides and 210 nm for creatine and phosphocreatine. A $10 \mu\text{L}$ of each sample was injected using an autosampler. The mobile phase consisted of buffer A (mM) (3 tetrabutyl ammonium (TBA) bisulphate and 20 Na_2HPO_4) and buffer

B (10% (v/v) acetonitrile, 200 Na₂HPO₄ and 0.3 TBA bisulphate). The pH was adjusted to 5 using 2 M phosphoric acid. The elution was performed in buffer A for 2 min then 1:1 gradient elution with buffers A and B up to 8.5 min then with buffer B up to 10 min (all at a flow rate of 0.4 mL/min). After analysis, the column was re-equilibrated by washing for 1 min with water then 9 min with buffer A. Cleaning was done by washing with 80% methanol after every series of experiments. Calibration stock solution (0.1 M, pH 7) was prepared in 0.2 M Na₂HPO₄ and stored at - 40°C for a maximum of 3 days to minimize phosphocreatine and ATP degradation.

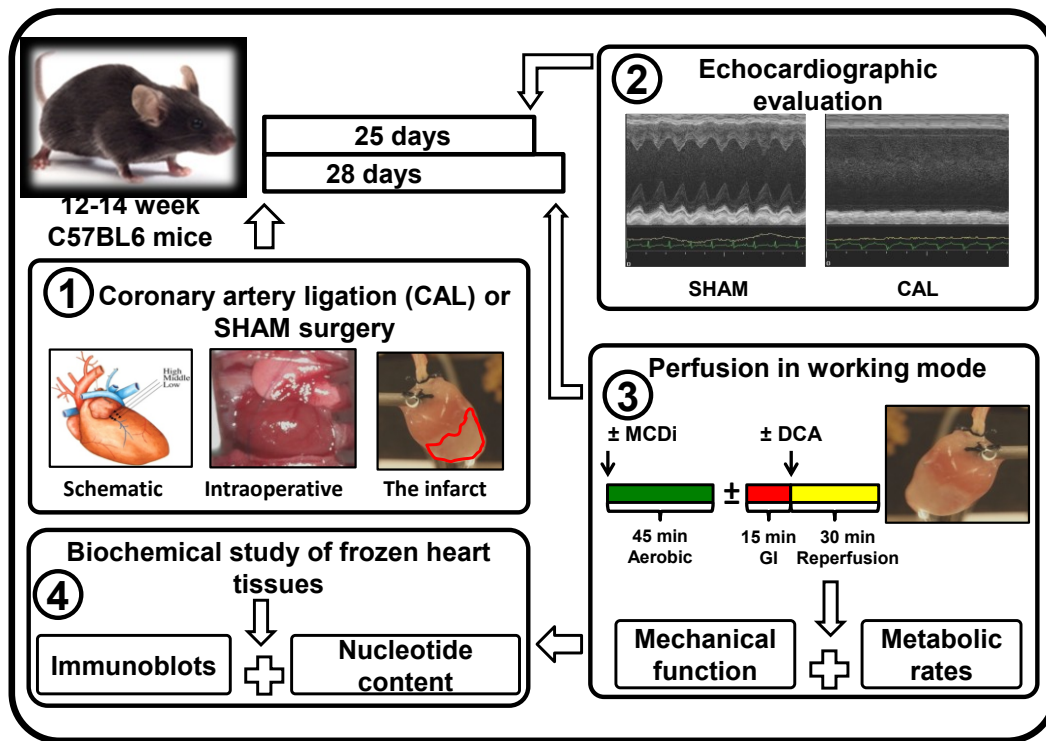
2.2.10 Statistical analysis:

Normality of data distribution was tested using Shapiro-Wilk normality test. Normally distributed data are expressed as mean \pm SEM for n independent experiments. Unpaired Student's t-test was used to compare differences between two groups and one way ANOVA was used to compare 3 or more groups. Two-way repeated measures ANOVA was used to compare time-dependent measurements. Bonferroni post-hoc test was used to provide comparison between selected pairs of data. If data were not normally distributed, data were presented as median \pm interquartile ranges (5% and 95%). Statistical analysis of differences was then made using non-parametric methods (Mann-Whitney test to compare 2 groups, or Kruskal-Wallis ANOVA to compare 3 or more groups followed by Dunn's post-hoc test. Differences were considered significant when $P < 0.05$. Statistical analyses were performed using GraphPad Prism 5 (Graphpad Software Inc., La Jolla, California, USA).

Figure 2.1 Schematic representation of methods

1. CAL or SHAM procedures were performed on 12-14 week old C57BL6 mice.
2. On the 25th-26th day post-surgical day, *in vivo* function was evaluated using echocardiography.
3. On the 28th day, hearts were perfused in the working mode. This included 45 min aerobic perfusion for aerobic perfusion protocol. In the ischemia reperfusion protocol, this was followed by 15 minute global no-flow ischemia (GI) followed by 30 minute aerobic reperfusion. Drugs, when used, were added at the start of aerobic perfusion (MCDi - Chapter 5-2) or aerobic reperfusion (DCA - Chapter 5-1). Assessment of mechanical function and collection of samples for measurement of metabolic rates were done at 5, 20, 35, 45, 60, 70, 80 and 90 min of the perfusion protocol as appropriate.
4. Frozen hearts were powdered and were used for biochemical studies which included immunoblotting for protein expression, HPLC detection of nucleotide, nucleoside and creatine contents. Glycogen and triacylglycerol (TG) contents were also measured.

Figure 2.1



3 Failing mouse hearts utilize energy inefficiently and benefit from improved coupling of glycolysis and glucose oxidation

HPLC analysis of nucleotides was performed by Ken Strynadka and echocardiographic examinations were performed by Donna Becker from the Cardiovascular Research Centre, University of Alberta.

A version of this Chapter has been published in Cardiovascular Research. Masoud WG, Ussher JR, Wang W, Jaswal JS, Wagg CS, Dyck JR, Lygate CA, Neubauer S, Clanachan AS, Lopaschuk GD. Failing mouse hearts utilize energy inefficiently and benefit from improved coupling of glycolysis and glucose oxidation. 2014 Jan;101:30-38.

3.1 Introduction

Heart failure develops following myocardial infarction (MI) [393] or following systemic diseases such as hypertension [394] or diabetes [395]. Heart failure is associated with changes in energy metabolism [139], but whether these contribute to contractile failure or whether they are adaptive is not established [143]. Currently there is no consensus on the nature of energy changes in heart failure. Two main concepts have emerged. One describes failing hearts as energetically-starved, comparable to an engine out of fuel [19]. This implies inadequate rates of energy substrate metabolism and ATP production. A second concept considers failing hearts use energy inefficiently [145], potentially due to mismatched glucose metabolism (glycolysis uncoupled from glucose oxidation), that accelerates proton production, leading to acidosis, intracellular Na^+ and Ca^{2+} overload, and impaired contractility [396].

Optimizing energy metabolism is a novel approach for heart failure pharmacotherapy, but knowledge of the relative contribution of inefficiency versus energy starvation to heart failure is key for development of optimal metabolic modulator therapy. If failing hearts are energetically-starved, then stimulation of mitochondrial oxidation [144] of fatty acids or carbohydrates is warranted. However, if failing hearts are inefficient, then optimizing energy substrate preference (inhibition of glycolysis and/or stimulation of glucose oxidation) is desirable. This study characterized energy substrate metabolism in post-infarction remodeled mouse hearts with LV dysfunction to examine whether hearts are energetically-starved or energetically-inefficient. We also examined

whether mechanical function and efficiency are affected by chronic deficiency of malonyl CoA decarboxylase (MCD), an enzyme that regulates fatty acid oxidation by producing malonyl CoA which slows fatty acid oxidation by inhibiting fatty acid uptake into mitochondria and whose inhibition is beneficial in ischemia-reperfusion (IR) [96, 397]. We hypothesize that: 1) post-MI remodeled hearts with LV dysfunction are not energetically starved but are inefficient, and 2) improved coupling of glycolysis and glucose oxidation via chronic deficiency of MCD lessens inefficiency and improves contractile function.

3.2 Methods

Male C57BL/6 mice, age 12-14 weeks, were subjected to permanent coronary artery ligation (CAL, n=17) or sham operation (SHAM, n=18). Please refer to Chapter 2 for details about the surgery, *in vivo* functional evaluation, isolated perfused working heart protocol, assessment of metabolic rates and other biochemical measurements.

3.3 Results

3.3.1 CAL hearts have lower mechanical function

Compared to SHAM, CAL mice have impaired *in vivo* LV systolic function 4 weeks after surgery, as indicated by reduced LV % ejection fraction (%EF) and LV % fractional area change (%FAC). CAL hearts have coexistent diastolic dysfunction (higher Tei index and IVRT) and marked dilatation as indicated by the significant increases in LV diastolic and systolic volumes. There is no difference in diastolic or systolic posterior wall or interventricular septal

thickness (LVPW and IVS - mm) (Table 3.1). The similarity in wall thickness was confirmed *in vitro* from dry weights of CAL and SHAM hearts (Fig 3.1E). *In vitro* function of CAL hearts (average LV work during perfusion, Joule/min/g dry wt), is 46% lower than SHAM hearts and confirms *in vivo* findings (Fig 3.1A-D). See Table 3.1 for other parameters.

3.3.2 CAL hearts are not energetically starved

Compared to SHAM hearts, CAL hearts have similar rates ($\mu\text{mol}/\text{min}/\text{g}$ dry wt) of glycolysis, glucose oxidation, proton production, a trend of lower fatty acid oxidation and lower lactate oxidation (Fig 3.2A-E). In contrast to the marked reduction in mechanical function in CAL hearts, total ATP production rate from exogenous substrate oxidation and glycolysis indicates that CAL hearts have only 25% reduction relative to SHAM hearts (Fig 3.3G). CAL and SHAM hearts have similar contents of ATP, ADP, AMP, GTP, creatine and creatine phosphate (Table 3.3), indicative of absence of energy starvation.

Compared to SHAM hearts, CAL hearts have similar rates of glycogen degradation (Fig 3.4B), glycogen synthesis (Fig 3.4C), TG degradation (Fig 3.4E) and TG synthesis (Fig 3.4F). Moreover, no differences in end-perfusion ($\mu\text{mol}/\text{g}$ dry wt) glycogen content (Fig 3.4A) and TG fatty acid content (Fig 3.4D) were observed.

Endogenous substrate metabolism from TG and glycogen contributes 29% of total ATP production for SHAM and 34% for CAL hearts (Fig 3.4G). Also, there is no difference in the % contribution of each energy substrate to the overall

ATP production (Fig 3.4H), or in the % contribution of fatty acid oxidation from both endogenous and exogenous sources (39 % in SHAM and 40% in CAL hearts - Fig 3.4H).

The protein expression of markers of mitochondrial abundance (VDAC, β -HAD, complex I subunit (NDUFB6)) as well as metabolic regulatory enzymes are similar in CAL and SHAM hearts (Table 3.4, details in Fig 4.7 and 4.8).

3.3.3 CAL hearts are inefficient

To examine efficiency of exogenous substrate utilization, rates of energy substrate metabolism were normalized for LV work ($\mu\text{mol}/\text{Joule}$). CAL hearts have higher glycolysis per unit LV work and higher glucose oxidation per unit LV work (Fig 3.3A-B). However, since accelerated rates of glucose oxidation and glycolysis are unmatched to a greater extent, proton production is significantly higher in CAL vs SHAM hearts (Fig 3.3C). Fatty acid oxidation per unit LV work is not different between groups (Fig 3.3D), and there is a trend of lower lactate oxidation per unit LV work (Fig 3.3E). Efficiency of exogenous substrate utilization, calculated by dividing average LV work by the rate of ATP production from exogenous substrates, is lower in CAL hearts (Fig 3.3F).

Similarly, rates of endogenous energy substrate degradation and synthesis were expressed per unit LV work ($\mu\text{mol}/\text{Joule}$). Groups have similar glycogen degradation rates (Fig 3.5A), glycogen synthesis rates (Fig 3.5B) and TG synthesis rates (Fig 3.5D), but CAL hearts have higher TG degradation rates (Fig 3.5C). The efficiency of endogenous substrate utilization, calculated by dividing

average LV work by ATP derived from endogenous sources, trended to be lower in CAL hearts but did not reach statistical significance (Fig 3.5E).

3.3.4 MCD-KO CAL hearts have better function than WT CAL hearts

Hearts in MCD-KO CAL mice show less *in vivo* functional deterioration compared to WT CAL littermates. There is a trend of higher %EF and %FAC. MCD-KO CAL hearts have comparable pre-surgical and 1 week post-surgical LVPW thickness. However, they show enhanced hypertrophic response 4 weeks post-surgery (Table 3.2). This was also evident following *in vitro* perfusion as MCD-KO CAL hearts have higher dry weights (Fig 3.6A). Despite the enhanced hypertrophic response in MCD-KO CAL hearts, they tend to be less dilated (Table 3.2). Both groups developed comparable infarct weights (mg) (0.024 ± 0.007 , n=8 vs 0.019 ± 0.003 , n=7, P=0.547) as were infarct weights as a percentage of total wet weight (13% vs 10% - Fig 3.6B). However, LV work, expressed per g dry wt, is similar in MCD-KO CAL and WT CAL hearts (Fig 3.6C-D), possibly due to the normalization of *in vitro* LV work to g dry weight, which masks any difference in work done by the whole heart. When LV work is expressed as Joule/min per whole heart, MCD-KO CAL hearts perform higher average work (Fig 3.6E-F). Hemodynamic parameters measured *ex vivo* and other *in vivo* echocardiographic parameters are shown in Table 3.2.

3.3.5 Inefficiency is lessened in MCD-KO CAL hearts

Since this subset of experiments was done under different perfusion conditions in an attempt to mimic conditions used by Ussher et al[322] where MCD-KO hearts had lower reperfusion proton production rates than WT littermates, we included an additional group of WT CAL hearts perfused under identical conditions to serve as controls. Thus, metabolic rates reported in this subset of experiments are not comparable to those reported in CAL and SHAM hearts due to the differences in energy substrate concentrations. Compared to WT CAL hearts, MCD-KO CAL hearts have significantly lower rates of glycolysis and glucose oxidation (Fig 3.7A-B). Thus, MCD-KO CAL hearts have an improved coupling of glucose metabolism and a lower proton production (Fig 3.7C). MCD-KO CAL hearts have comparable fatty acid oxidation rates to WT CAL hearts (Fig 3.7D), but decreased lactate oxidation rates (Fig 3.7E). The apparent increase in fatty acid oxidation contribution to total ATP is due to decreased contributions from glycolysis and glucose oxidation. ATP production from exogenous sources is significantly lower in MCD-KO CAL hearts (Fig 3.7G-H).

When expressed per unit LV work, MCD-KO CAL hearts have lower rates of glycolysis compared to WT CAL hearts (Fig 3.8A), as well as lower glucose oxidation rates (Fig 3.8B). However, the larger decrease in glycolysis versus glucose oxidation, results in lower proton production rates from glucose metabolism (Fig 3.8C). No difference between groups was observed in fatty acid oxidation normalized for LV work (Fig 3.8D), while lactate oxidation was

significantly lower in MCD-KO CAL hearts (Fig 3.8E). A significant improvement in the efficiency of exogenous substrate utilization (Joule/ μ mole) in MCD-KO CAL hearts was observed (Fig 3.8F).

3.4 Discussion

The important finding of this study is that post-infarction failing mouse hearts are not energetically starved, but are inefficient in energy utilization for mechanical function. The reduction in total ATP production rate in isolated failing mouse hearts (25%) is insufficient to account for the reduction in LV work (46%), and is clearly indicative of inefficient use of energy for external mechanical function. Meanwhile, CAL hearts have similar adenine nucleotide, inosine, creatine and creatine phosphate contents to SHAM, negating energy starvation. The observed mismatch between rates of glycolysis and glucose oxidation in failing hearts, that accelerates proton production from glucose metabolism, may be a significant contributor to observed inefficiency, as accelerated proton production may cause Na^+ and Ca^{2+} accumulation and a shift in ATP utilization from contractile function to ionic homeostasis [185, 396]. Our study also demonstrates that inefficient energy utilization post-infarction (causes reviewed in Introduction) is amenable to improvement by a metabolic intervention that reduces the uncoupling of glycolysis and glucose oxidation.

This study used a CAL model to mimic post-infarction LV dysfunction, as this is a common etiology of heart failure [382]. The demonstration by *in vivo* echocardiography that CAL hearts have lower %EF and %FAC clearly indicates LV dysfunction. This was confirmed *ex vivo* in isolated working hearts where total LV work, as well as LV work per g dry wt, is significantly depressed. Measurement of rates of energy substrate metabolism in SHAM and CAL hearts allowed direct assessment of efficiency of energy utilization for external work

(ratio of LV work per μmol ATP produced from substrate oxidation and glycolysis). CAL hearts maintained LVPW and IVS thickness *in vivo*, and dry weights *ex vivo* were identical despite conversion of a significant proportion of the LV into a fibrous infarct (removed before weighing). This indicates that surviving viable tissue was hypertrophied [398]. These results are consistent with previous findings, where following myocardial infarction cardiac hypertrophy contributes to maintaining the non-infarcted area comparable to SHAM hearts [398]. It should be noted, that although echocardiographically-calculated LV mass increases in CAL hearts compared to SHAM hearts (based on LV volumes rather than actual mass), it reflects total LV mass, including the portions of the LV which are converted to scar, and is thus not indicative of viable LV mass. Despite similar LV mass, total LV work decreased in CAL hearts, indicative of decompensation.

Energy starvation as an etiology of heart failure was introduced in 1939 with a description of the failing heart as a “slapped retired horse” [399], suggesting that LV mechanical dysfunction is due to deterioration in energy substrate uptake and utilization [245, 246], oxidative phosphorylation for ATP production [270, 271], and/or transfer of high energy phosphate to creatine, via creatine kinase (CK) activity [400].

However, a generalized decline in energy substrate metabolism is not a uniform finding in all heart failure models [239, 401] and suggests that alternate etiologies are involved. Our data indicate that CAL hearts do not have depressed rates of glycolysis, glucose oxidation or fatty acid oxidation. While lactate

oxidation rates declined, total rates of ATP production were only 25% lower in CAL hearts, much less than the marked depression in LV work (46%). Besides, CAL hearts have similar contents of ATP, AMP, creatine and creatine phosphate. These findings argue against energy starvation being the only contributing metabolic defect in CAL hearts, and support the notion that CAL hearts are inefficient in the utilization of energy for mechanical work. These results are consistent with the demonstration that in the setting of hypertrophy there is a greater requirement of MVO_2 for non-contractile purposes (e.g. excitation-contraction coupling and Ca^{2+} handling) [402], which may divert ATP available from contraction itself, and thus decrease metabolic efficiency. Alterations in energy substrate preference occur in hearts following acute ischemia [403] and have the potential to decrease efficiency [21, 319], but based on similar percentage contributions of energy substrates to overall ATP production in SHAM and CAL hearts (Fig 3.4H), it appears that substrate preference is unaltered in the infarct-remodeled heart.

To avoid any confounding effect of different LV work levels in CAL and SHAM hearts, rates of energy substrate metabolism were also expressed per unit LV work. Again, data do not support the concept of energy starvation as CAL hearts have higher rates of glycolysis and glucose oxidation, as well as unchanged rates of fatty acid oxidation and lactate oxidation. As the increase in glucose oxidation rate per unit LV work was insufficient to match the increase in glycolysis rate per unit LV work, this causes a significant increase in proton production per unit LV work and suggests that mismatched glucose metabolism

may be a contributor to inefficiency. This mismatch has also been reported in other HF models [9, 236, 325, 404].

To investigate potential differences in endogenous substrate metabolism, rates of synthesis and degradation of glycogen and TG were calculated. Endogenous substrates contributed a similar percentage to total ATP production (29% in SHAM and 34% in CAL hearts). Even after expression per unit LV work, glycogen degradation and synthesis rates were not different. TG synthesis expressed per unit LV work was also similar but TG degradation was higher in CAL. However, due to very low actual rates, no difference in total ATP production from endogenous sources was observed. CAL hearts trended to be inefficient in endogenous substrate utilization but this did not reach statistical significance ($P=0.07$).

Interestingly, evidence used to support the energy starvation theory can be subject to alternate interpretations that actually support the inefficiency concept. An inefficient heart uses more energy to perform an equivalent workload, so providing more ATP, whether via external supply of energy substrates, increasing rates of energy substrate metabolism, or enhancing ATP flux through CK, can improve contractility. Improved mechanical function in rats with heart failure by dichloroacetate-induced stimulation of glucose oxidation [214] reduces mismatched glucose metabolism. Thus, heart function improves, not only due to increased ATP generation, but also by less dysregulation of ionic homeostasis.

Since the contribution of endogenous substrate metabolism to overall energy production was not different in CAL hearts, we determined the metabolic and functional consequences of CAL-induced remodeling in hearts from MCD-KO mice. While these hearts have unaltered rates of glucose and fatty acid oxidation when perfused aerobically, when challenged by IR they show a preference for glucose oxidation over fatty acid oxidation. This improves coupling between glycolysis and glucose oxidation, lessens intracellular acidosis and improves recovery of contractility [322]. Using this model, we determined whether enhanced mechanical function could be achieved via improvement in the efficiency of exogenous substrate utilization. We studied the metabolic and functional consequences of CAL-induced remodeling in MCD-KO mice which was shown previously [322] to be protected from IR injury due to improved matching of glucose metabolism. As expected with the permanent CAL model, infarct weights (both actual and as % of whole heart weight) were similar in WT CAL and MCD-KO CAL hearts, and indicates that functional effects are due to actions on surviving viable tissue.

MCD-KO CAL hearts have improved cardiac function and have lower rates of glycolysis, glucose oxidation, lactate oxidation well as ATP production. Despite lower energy availability, function is improved, and clearly indicates improved efficiency. These changes persisted after normalization for LV work. In accordance with the study by Dyck *et al* [96], MCD-KO CAL hearts have unaltered fatty acid oxidation rates. The higher contribution of fatty acid oxidation to the overall ATP production appears to be due to reduced percentage

contribution from the other substrates. Our understanding is that fatty acid oxidation regulating genes that code for fatty acid transporter (CD36), carnitine palmitoyl transferase 1, acyl CoA thioesterase, and uncoupling protein-3 are upregulated in MCD-KO healthy hearts [96] resulting in maintained aerobic fatty acid oxidation despite the lack of MCD. We speculate that the upregulated genes are also responsible for the lack of significant change in fatty acid oxidation rates in remodeled MCD-KO CAL hearts. The improved metabolic efficiency and maintained fatty acid oxidation rates in these hearts may explain why lower rates of glucose metabolism were observed.

The demonstration that MCD-KO CAL hearts have improved coupling between glycolysis and glucose oxidation, lower proton production and improved total LV work, suggests that improvement in the matching of glucose metabolism has beneficial consequences in this model of heart failure. While this does not unequivocally prove a relationship between metabolic inefficiency and cardiac function, it is supportive of such a relationship.

Conclusion

Our study shows that post-infarction remodeled failing mouse hearts are inefficient in the utilization of energy substrates for mechanical work.

Mismatched glucose metabolism (glycolysis vs glucose oxidation) and the resulting accelerated proton production per unit LV work may be a contributor to inefficiency and the deterioration of LV mechanical function. The prevention of inefficiency by a metabolic intervention (chronic MCD deficiency) that lessens

mismatched glucose metabolism and improves mechanical function supports the view that inefficiency is a major contributor to heart failure in the infarct-remodeled heart and is amenable for improvement by metabolic interventions.

Figure 3.1 Assessment of mechanical function of CAL and SHAM hearts.

The time-courses of LV work per g dry wt (A, SHAM=18, CAL=17) and total LV work per whole heart (C) is shown, as well as average values for LV work per g dry wt (B), total LV work per whole heart (D) and heart dry weights (mg, F). Data are expressed as mean \pm SEM, N values represent independent hearts. * indicates $P < 0.05$.

Figure 3.1

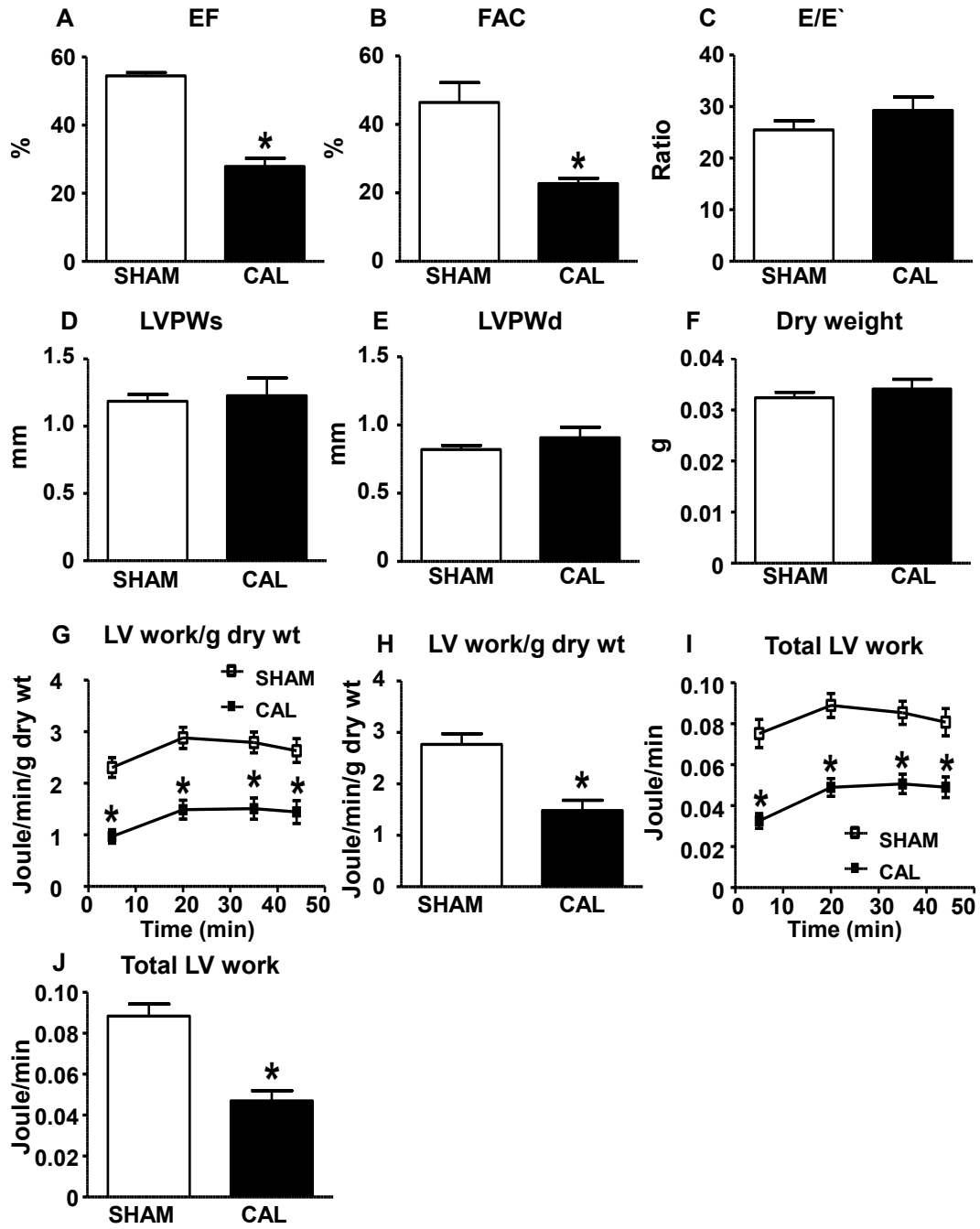


Figure 3.2 Rates of exogenous energy substrate metabolism in SHAM and CAL hearts.

Rates ($\mu\text{mol}/\text{min}/\text{g}$ dry wt) are shown for glycolysis (A, SHAM=11, CAL=6), glucose oxidation (B, SHAM=11, CAL=6) proton production (C, SHAM=11, CAL=6), fatty acid oxidation (D, SHAM=7, CAL=11) and lactate oxidation (E, SHAM=7, CAL=11). Data are expressed as mean \pm SEM, N values represent independent hearts. * indicates $P < 0.05$.

Figure 3.2

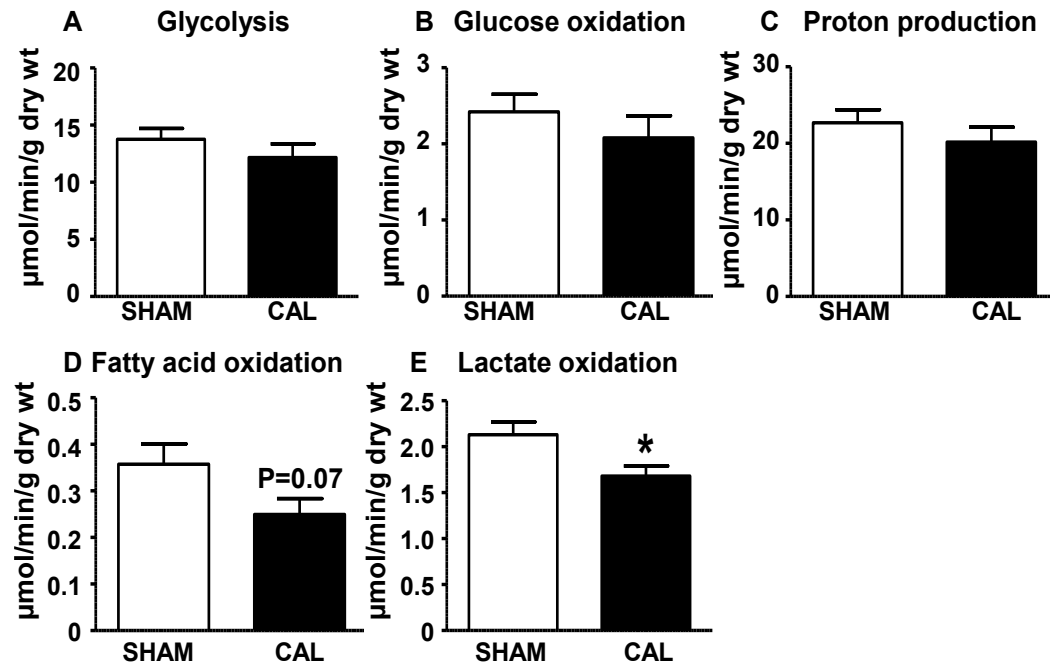


Figure 3.3 Rates of exogenous energy substrate metabolism in SHAM and CAL hearts normalized for LV work.

Metabolic rates (expressed per unit LV work) are shown for glycolysis (A, SHAM=11, CAL=6), glucose oxidation (B, SHAM=11, CAL=6), proton production (C, SHAM=11, CAL=6), fatty acid oxidation (D, SHAM=7, CAL=11) and lactate oxidation (E, SHAM=7, CAL=7). Cardiac efficiency, calculated as Joule per μ mole ATP (F, SHAM=7, CAL=6) and rates of ATP production (G, SHAM=7, CAL=6) are also shown. Data are expressed as mean \pm SEM, N values represent independent hearts. *indicates $P < 0.05$.

Figure 3.3

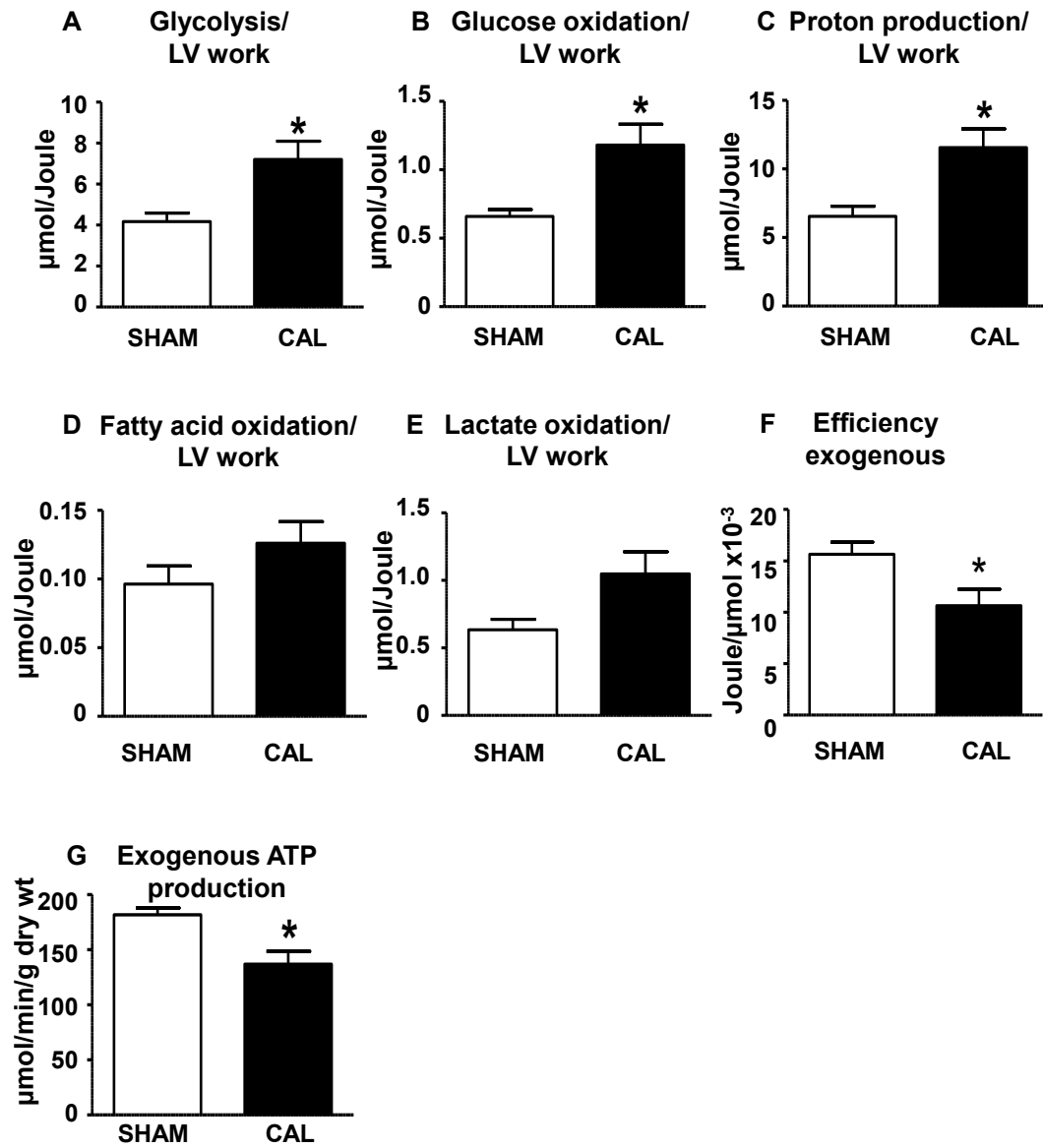


Figure 3.4 Rates of endogenous energy substrate metabolism in SHAM and CAL hearts.

Glycogen content at the end of perfusion ($\mu\text{mol/g dry wt}$) is shown (A) for SHAM (N=5) and CAL (N=5), as well as rates ($\mu\text{mol/min/g dry wt}$) of glycogen degradation (B) and glycogen synthesis (C). TG fatty acid content at the end of perfusion ($\mu\text{mol/g dry wt}$) (D), TG degradation rate ($\mu\text{mol/min/g dry wt}$) (E), TG synthesis rate (F), ATP production rate from the endogenous energy substrates, glycogen and TG (G), and percentage contribution to ATP production of the metabolism of exogenous and endogenous energy substrates (H) are also shown. Data are expressed as mean \pm SEM, N values represent independent hearts.

*indicates $P < 0.05$.

Figure 3.4

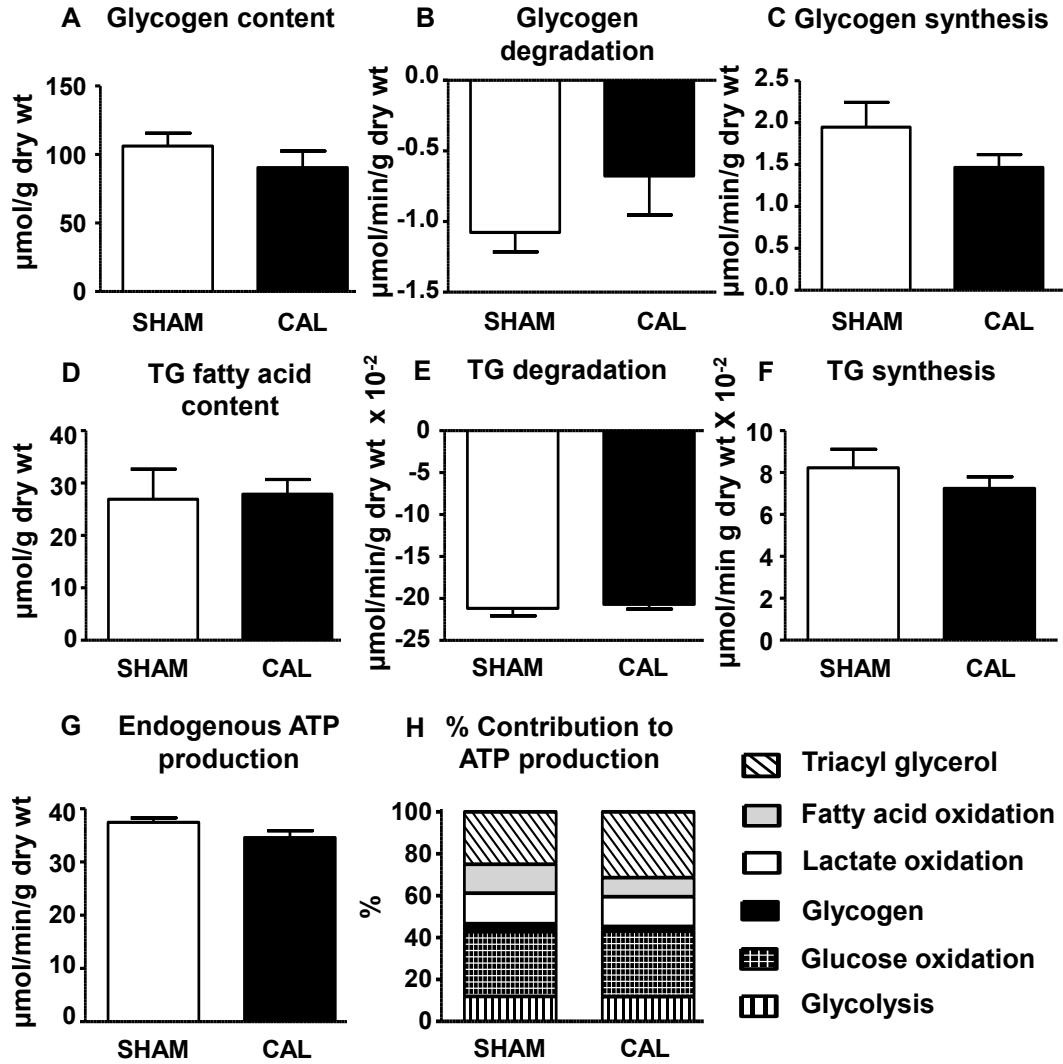


Figure 3.5 Rates of endogenous energy substrate metabolism in SHAM and CAL hearts normalized for LV work.

Metabolic rates (expressed per unit LV work, SHAM N=5, CAL N=5) for glycogen degradation (A), glycogen synthesis (B), TG degradation (C) and TG synthesis (D) are shown as well as efficiency of endogenous substrate utilization (E), calculated as Joule/ μ mol by dividing LV work by ATP generated from glycogen and TG degradation. Data are expressed as mean \pm SEM, N values represent independent hearts. * indicates $P < 0.05$.

Figure 3.5

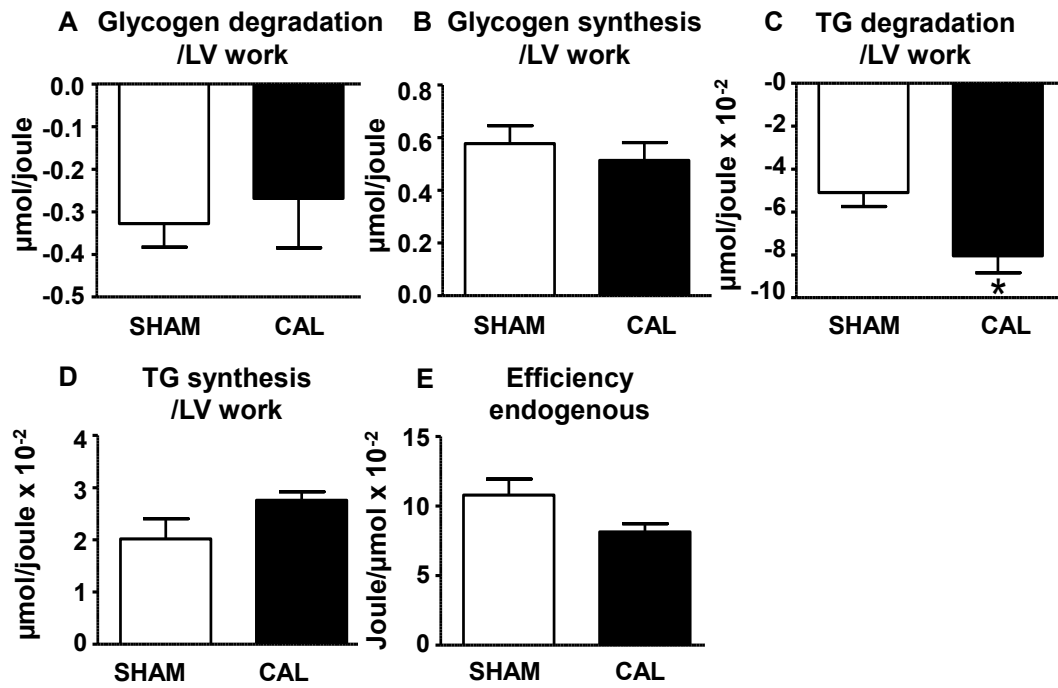


Figure 3.6 Assessment of cardiac function of WT CAL and MCD-KO CAL hearts.

Dry weights (mg, A, WT CAL=17, MCD-KO CAL=11) are shown for perfused hearts. Infarct size, expressed as percentage of the whole heart weight (B, WT CAL=7, MCD-KO CAL=8), as well as the time-courses of LV work per g dry wt (C, WT CAL=17, MCD-KO CAL=11) and total LV work per whole heart (E, WT CAL=17, MCD-KO CAL=11) are presented. Average values for LV work per g dry wt (D, WT CAL=17, MCD-KO CAL=11) and total LV work per whole heart (F, WT CAL=17, MCD-KO CAL=11) are also shown. Data are expressed as mean \pm SEM, N values represent independent hearts. * indicates $P < 0.05$.

Figure 3.6

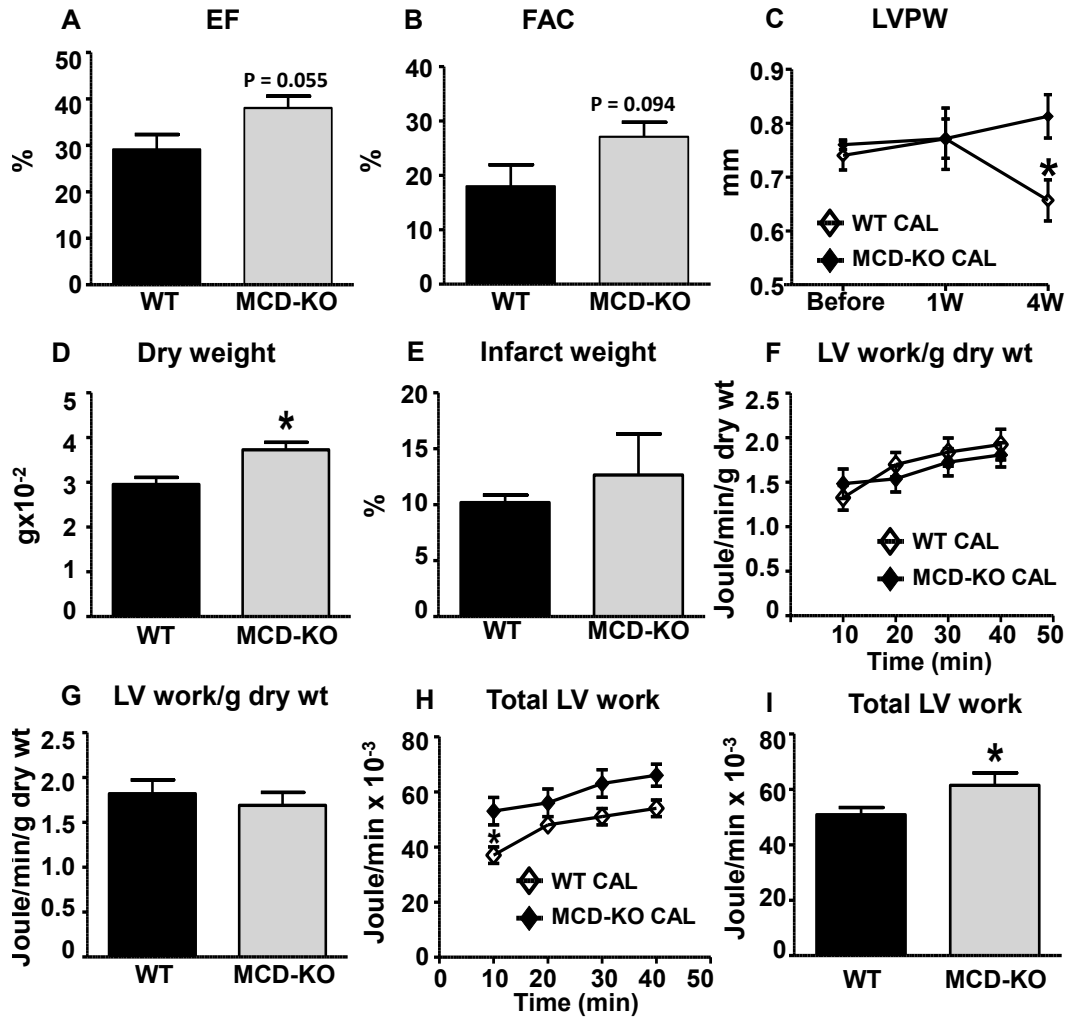


Figure 3.7 Rates of exogenous energy substrate metabolism in WT CAL and MCD-KO CAL hearts.

Rates ($\mu\text{mol}/\text{min}/\text{g}$ dry wt) are shown for glycolysis (A, WT CAL=5, MCD-KO CAL=4), glucose oxidation (B, WT CAL=12, MCD-KO CAL=7) proton production (C, WT CAL=5, MCD-KO CAL=4), fatty acid oxidation (D, WT CAL=12, MCD-KO CAL=6) and lactate oxidation (E, WT CAL=5, MCD-KO CAL=4). Data are expressed as mean \pm SEM, N values represent independent hearts. * indicates $P < 0.05$.

Figure 3.7

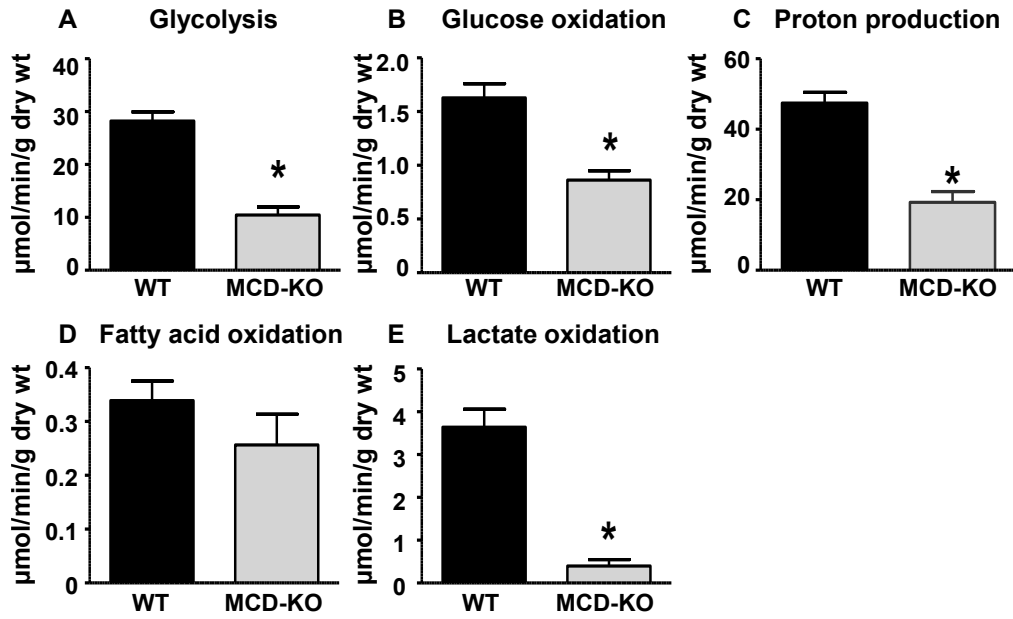


Figure 3.8 Rates of exogenous energy substrate metabolism in WT CAL and MCD-KO CAL hearts normalized for LV work.

Metabolic rates (expressed per unit LV work) are shown for glycolysis (A, WT CAL=5, MCD-KO CAL=4), glucose oxidation (B, WT CAL=12, MCD-KO CAL=7), proton production (C, WT CAL=5, MCD-KO CAL=4), fatty acid oxidation (D, WT CAL=12, MCD-KO CAL=6) and lactate oxidation (E, WT CAL=5, MCD-KO CAL=4). Cardiac efficiency of exogenous substrate utilization, calculated as Joule per μ mole ATP, (F, WT CAL=5, MCD-KO CAL=4), ATP production (G, WT CAL=5, MCD-KO CAL=4), % contribution of each energy substrate to ATP production (H, WT CAL=5, MCD-KO CAL=4) are also shown. Data are expressed as mean \pm SEM, N values represent independent hearts. *indicates $P < 0.05$.

Figure 3.8

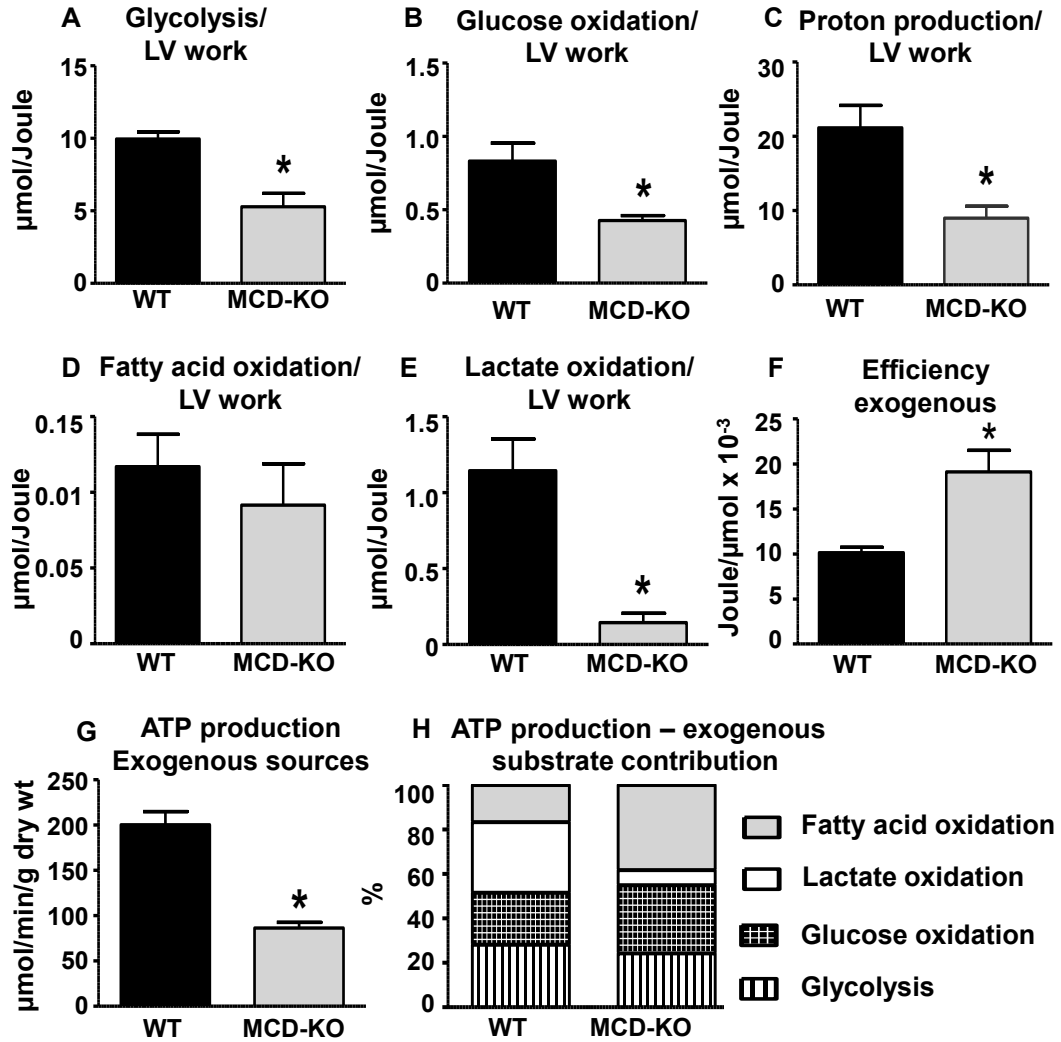


Table 3.1 *In vivo* echocardiographic and *ex vivo* hemodynamic parameters of CAL and SHAM hearts

Parameter (unit)	<i>In vivo</i>		
	SHAM (N=12)	CAL (N=11)	P value
Heart rate (beats/min)	437±14	440±19	0.84
Cardiac output (mL/min)	21.75±2.22	20.26±1.54	0.59
LV systolic volume (μL)	33.95±2.63	119.89±19	0.0001
LV diastolic volume (μL)	77.56±3.43	175.37±21.32	0.0001
LVIDs (mm)	2.94±0.10	4.90±0.32	<0.0001
LVIDd (mm)	4.17±0.08	5.84±0.30	<0.0001
Corrected LV mass	102.96±1.54	156.29±18.90	0.0015
LVPWs (mm)	1.19±0.05	1.23±0.13	0.76
LVPWd (mm)	0.82±0.03	0.91±0.08	0.30
IVSs (mm)	1.18±0.04	1.17±0.12	0.97
IVSd (mm)	0.81±0.01	0.84±0.06	0.97
EF (%)	54.47±0.98	27.89±2.38	<0.0001
FAC (%)	46.41±5.83	22.75±1.54	0.0001
IVCT (ms)	17.14±1.20	28.19±2.55	0.0005
Tei index (ratio)	0.76±0.03	1.24±0.09	<0.0001
E	768±92	643±50	0.03
E'	31.8±9.0	23.2±7.5	0.02
A	440±184	279±162	0.04
E/E' (ratio)	25.48±1.77	29.26±2.58	0.23
E/A (ratio)	2.01±0.24	4.59±2.27	0.23
IVRT (ms)	17.78±1.01	23.02±1.29	0.004
MV DT (ms)	16.92±0.95	15.18±2.47	0.45

Parameter (unit)	<i>Ex vivo</i>		
	SHAM (N=18)	CAL (N=17)	P value
Body weight (g)	26.99 ± 0.31	27.45 ± 0.37	0.34
Systolic pressure (mmHg)	77.2 ± 1.8	68.5 ± 1.0	0.0002
Diastolic pressure (mmHg)	20.4 ± 1.2	28.9 ± 1.4	<0.0001
Cardiac output (mL/min)	9.51 ± 0.46	5.84 ± 0.55	<0.0001
Aortic flow (mL/min)	7.04 ± 0.45	3.61 ± 0.41	<0.0001
Coronary flow (mL/min)	2.48 ± 0.33	2.23 ± 0.37	0.62

Abbreviations: LV= left ventricular, LVID=LV internal dimension, LVPW=LV posterior wall thickness, IVS=interventricular septal thickness, EF=ejection fraction, FAC=fraction area change, IVRT=isovolumetric relaxation time, IVCT=isovolumetric contraction time, MVDT=mitral valve deceleration time. All data are mean ± SEM. P values are shown beside each parameter and a value less than 0.05 is considered significant.

Table 3.2 *In vivo* echocardiographic and *ex vivo* hemodynamic parameters of WT-CAL and MCD-KO CAL hearts

Parameter (unit)	<i>In vivo</i>		P value
	WT CAL (N=9)	MCD-KO CAL (N=7)	
Heart rate (beats/min)	504±25	519±14	0.64
Cardiac output (mL/min)	18.24±1.74	20.80±1.26	0.28
LV systolic volume (μL)	78.98±15.71	54.47±11.88	0.26
LV diastolic volume (μL)	114.42±11.78	107.48±13.75	0.71
LVIDs (mm)	4.06±0.35	3.49±0.31	0.26
LVIDd (mm)	4.88±0.21	4.75±0.26	0.69
Corrected LV mass	103.77±9.51	118.98±6.78	0.24
LVPWs (mm)	0.83±0.08	1.14±0.05	0.007
LVPWd (mm)	0.66±0.04	0.81±0.04	0.014
IVSs (mm)	0.84±0.08	1.00±0.07	0.17
IVSd (mm)	0.66±0.04	0.73±0.03	0.19
EF (%)	29.16±3.20	38.08±2.50	0.055
FAC (%)	18.03±3.92	27.12±2.66	0.09
LVPWd (mm)-pre-op	0.74±0.03	0.76±0.01	>0.05
LVPWd (mm)-Week 1	0.77±0.06	0.77±0.04	>0.05
LVPWd (mm)-Week 4	0.66±0.04	0.81±0.04	<0.05
LV diastolic volume-pre-op (μL)	50.50±1.78	60.29±1.86	0.20
LV diastolic volume-Week1 (μL)	106.20±5.73	102.38±8.53	0.71
LV diastolic volume-Week 4 (μL)	130.44±11.29	107.58±7.72	0.14

Parameter (unit)	<i>Ex vivo</i>		P value
	WT CAL (N=17)	MCD-KO CAL (N=11)	
Body weight (g)	22.74 ± 0.47	23.92 ± 1.14	0.28
Systolic pressure (mmHg)	63.9 ± 1.2	67.8 ± 2.2	0.10
Diastolic pressure (mmHg)	41.9 ± 1.5	38.2 ± 2.1	0.16
Cardiac output (mL/min)	6.73 ± 0.31	7.95 ± 0.57	0.05
Aortic flow (mL/min)	4.76 ± 0.34	5.67 ± 0.44	0.11
Coronary flow (mL/min)	1.97 ± 0.23	2.28 ± 0.28	0.40

Abbreviations: LV= left ventricular, LVID=LV internal dimension, LVPW=LV posterior wall thickness, IVS=interventricular septal thickness, EF=ejection fraction, FAC=fraction area change. All data are mean ± SEM. P values are shown beside each parameter and a value less than 0.05 is considered significant.

Table 3.3 Adenine nucleotide, inosine and creatine content in CAL and SHAM hearts

Parameter ($\mu\text{mol/g}$ dry wt)	<i>In vivo</i>		P value
	SHAM (N=5)	CAL (N=5)	
ATP	31.02 \pm 2.09	22.96 \pm 3.40	0.08
ADP	5.90 \pm 0.53	5.13 \pm 0.81	0.45
AMP	0.78 \pm 0.08	0.98 \pm 0.26	0.49
GTP	1.63 \pm 0.12	1.43 \pm 0.18	0.21
Inosine	10.45 \pm 4.32	4.91 \pm 2.39	0.29
Creatine	27.93 \pm 2.01	20.75 \pm 2.87	0.07
Creatine phosphate	35.31 \pm 2.76	28.64 \pm 4.61	0.25

Abbreviations: ATP=adenosine triphosphate, ADP=adenosine diphosphate, AMP=adenosine monophosphate, GTP=guanosine triphosphate. All data are mean \pm SEM. P values are shown beside each parameter and a value less than 0.05 is considered significant.

Table 3.4 Immunoblot analysis of protein expression of mitochondrial abundance and key metabolic regulatory enzymes

Parameter (arbitrary units)	<i>In vivo</i>		P value
	SHAM (N)	CAL (N)	
VDAC	1.00±0.24 (3)	1.01±0.13 (3)	0.99
Complex I (NDUFB6)	1.00±0.06 (3)	1.05±0.07 (3)	0.56
β-HAD	1.00±0.16 (4)	1.06±0.10 (4)	0.76
LCAD	1.00±0.08 (3)	1.33±0.12 (3)	0.08
PDH	1.00±0.13 (3)	0.90±0.13 (3)	0.20
LDH-A	1.00±0.17 (6)	1.04±0.32 (6)	0.92
HK1	1.00±0.19 (3)	1.22±0.16 (3)	0.43
GAPDH	1.00±0.07 (6)	1.29±0.20 (6)	0.19

Abbreviations: VDAC= voltage-dependent anion channel, β-HAD = β-hydroxy acyl CoA dehydrogenase, LCAD=long chain acyl CoA dehydrogenase, PDH=pyruvate dehydrogenase, LDH-A=lactate dehydrogenase isozyme A, HK1=hexokinase 1, GAPDH=glyceraldehyde-3-phosphate dehydrogenase. All data are mean ± SEM. P values are shown beside each parameter and a value less than 0.05 is considered significant. See details in Fig 4.7 and 4.8.

4 Tolerance to ischemic injury in remodeled mouse hearts: less ischemic glycogenolysis and preserved metabolic efficiency

A version of this Chapter has been submitted to Cardiovascular Research. Masoud WGT, Abo Al-Rob O, Yang Y, Lopaschuk GD, Clanachan AS. . “Tolerance to ischemic injury in remodeled mouse hearts: less ischemic glycogenolysis and preserved metabolic efficiency”.

Nov 24th 2014. ID: *CVR-2014-414R1*

HPLC analysis of nucleotides was performed by Ken Strynadka and echocardiographic examinations were performed by Donna Becker from the Cardiovascular Research Centre, University of Alberta.

4.1 Introduction

Hearts that are remodeled following ischemia exhibit impaired mechanical function both *in vivo* and during *ex vivo* aerobic perfusion [221]. In Chapter 3, energy metabolic mechanisms that may contribute to the observed mechanical dysfunction were investigated and the data demonstrate that hearts remodeled following CAL surgery are not energetically starved as they maintain comparable rates of energy substrate oxidation, rates of ATP production and ATP contents despite lower mechanical function. Instead, post-infarction remodeled hearts are metabolically inefficient [221], that is, remodeled hearts have adequate rates of energy substrate metabolism and ATP production, but this energy is not translated into mechanical function as efficiently as in normal hearts. Although many factors may influence cardiac metabolic efficiency (reviewed in Chapter 1, Introduction), metabolic inefficiency in remodeled hearts may be related to higher rates of proton production from glucose metabolism. This increased proton production can increase the amount of energy used for the correction of acidosis-induced dysregulation of ion homeostasis, that includes Na^+ and Ca^{2+} overload.

Based on this metabolic inefficiency, it might be expected that remodeled hearts would be more susceptible to injury following a subsequent episode of ischemia compared to normal healthy hearts. However, several studies have provided evidence that remodeled hearts actually have a greater tolerance to ischemia [314-316]. In a comparison of normal and remodeled hearts perfused in the Langendorff mode, Kalkman *et al* [315] reported that remodeled hearts have a lower ischemia-induced release of lactate and purines. A similar improved

tolerance to ischemic injury in remodeled hearts was confirmed by Pantos *et al* [314] who showed that a lower release of lactate dehydrogenase was accompanied by less ischemic contracture, a higher expression of heat shock protein 70, as well as an improved recovery of mechanical function during post-ischemic reperfusion. Both studies employed non-working Langendorff preparations so energy metabolic mechanisms were not investigated. Less dysregulation of ion homeostasis has also been noted in remodeled hearts by Sharikabad and colleagues [316], who reported that cardiomyocytes derived from post-infarction remodeled rat hearts exhibit less Na^+ and Ca^{+2} accumulation than cells from normal hearts. These authors also found lower release of lactate dehydrogenase and less depletion of ATP content during a hypoxic challenge of remodeled cardiomyocytes, but the mechanistic basis of the increased tolerance has not yet been elucidated.

Energy substrate metabolic rates and energy substrate preference during reperfusion of ischemic hearts affects recovery of LV mechanical function [13, 140, 317, 318]. For example, acceleration of fatty acid oxidation during reperfusion inhibits glucose oxidation (the “Randle cycle”), thereby increasing the uncoupling of glycolysis and glucose oxidation leading to increased proton production. This slows the rate of recovery of intracellular pH and contributes to further accumulation of Na^+ and Ca^{2+} overload [317]. Moreover, inhibition of glycolysis during early reperfusion limits Ca^{2+} overload and improves post-ischemic recovery of LV function [318].

Experiments described in this Chapter were designed to compare post-ischemic mechanical function in normal and remodeled hearts, and to investigate the associated changes in cardiac energy substrate metabolism and metabolic efficiency. Studies were performed in mouse hearts that had undergone remodeling following coronary artery ligation or a sham procedure. Hearts were isolated and perfused as isolated working heart mode in the presence of relevant energy substrates (fatty acids, glucose, and lactate) and energy demand (workload), in order to assess LV mechanical work, rates of energy substrate metabolism and metabolic efficiency.

4.2 Methods

Male C57BL/6 mice (age 12 weeks) were subjected to either a coronary artery ligation (CAL, n=17) or a sham procedure (SHAM, n=33), as described previously [381, 382].

4.3 Results

4.3.1 CAL hearts have lower *in vivo* function

In accordance with data presented in Chapter 3, , echocardiographic evaluation of CAL mice revealed impaired LV function relative to the age-matched SHAM group (Fig 4.1 and Table 4.1). CAL mice have lower systolic function as indicated by reduced LV % ejection fraction (%EF) and LV % fractional area change (%FAC). CAL hearts have coexistent diastolic dysfunction (higher Tei index, E/E' and IVRT) and marked dilatation (as indicated by the significant increases in LV diastolic and systolic volumes and internal diameters).

CAL hearts are also mildly hypertrophied (higher diastolic interventricular septal thickness (IVSd) but unaltered LV posterior wall thickness).

Ex vivo mechanical function (average LV work during aerobic perfusion, Joule/min/g dry wt) is 36% lower in CAL hearts than in SHAM hearts, which confirms the *in vivo* findings of lower systolic function. However, CAL hearts recovered to aerobic levels of LV work during post-ischemic reperfusion, in contrast to SHAM hearts that show significant deterioration of LV work during post-ischemic reperfusion (Fig 4.2A-B). When LV work during reperfusion is expressed as a percent recovery of pre-ischemic values (Fig 4.2C), there is a significantly higher recovery of LV work in CAL hearts compared to SHAM hearts ($67\pm 5\%$ vs $49\pm 5\%$, $P<0.05$). A similar complete recovery of other hemodynamic parameters was also seen in CAL hearts post-ischemia (Table 4.2).

4.3.2 CAL hearts are not energy starved during post-ischemic reperfusion

As we reported in Chapter 3, CAL hearts, relative to SHAM hearts, are not energy starved during aerobic perfusion, as indicated by similar rates of glycolysis, glucose oxidation, fatty acid oxidation and lactate oxidation in the two groups (Fig 4.3A-E). Thus the rate of ATP production from these energy substrates is similar in CAL and SHAM hearts, indicating that CAL hearts are not deficient in energy availability (Fig 4.3F). Moreover, we now show that post-ischemic reperfused CAL hearts maintain similar rates of energy substrate

metabolism to SHAM hearts, which indicates that they are also not energy starved during reperfusion.

Similarly, CAL hearts maintain comparable ATP and creatine phosphate contents to SHAM hearts during post-ischemic reperfusion (Table 4.3), also indicative of a lack of energy starvation.

4.3.3 CAL hearts undergo less deterioration in metabolic efficiency during reperfusion

During aerobic perfusion, when normalized per unit LV work ($\mu\text{mol}/\text{Joule}$), CAL hearts have higher rates of glycolysis (Fig 4.4 A, $P < 0.05$, t-test) and similar rates of glucose oxidation (Fig 4.4B), a finding confirming data presented in Chapter 3. The greater mismatch in the rates of glycolysis and glucose oxidation in CAL hearts results in a higher rate of proton production (Fig 4.4C, $P < 0.05$). Fatty acid oxidation and lactate oxidation rates were similar in SHAM and CAL hearts (Fig 4.4D-E). CAL hearts have lower metabolic efficiency (LV work done per ATP produced, $\text{Joule}/\mu\text{mol}$) (Fig 4.4F, $P < 0.05$).

During reperfusion, as compared to aerobic perfusion, SHAM hearts exhibit a significantly higher glycolysis per LV work (Fig 4.4A) while glucose oxidation per LV work is unchanged (Fig 4.4B), yielding a significantly higher rate of proton production per LV work (Fig 4.4C). Rates of fatty acid oxidation per LV work significantly increase (Fig 4.4D) while lactate oxidation per LV work remain similar to aerobic rates (Fig 4.4E). Accordingly, metabolic efficiency is significantly lower in reperfused SHAM hearts (Fig 4.4F).

In contrast, reperfused CAL hearts exhibit no further changes in glucose metabolism (Fig 4.4A-B). Thus, proton production per LV work remains at similar levels to aerobic perfusion (Fig 4.4C). Similarly, fatty acid oxidation and lactate oxidation per LV work are comparable to values during aerobic perfusion (Fig 4.4D-E). Thus, in CAL hearts energy substrate preference is unaltered and metabolic efficiency does not further deteriorate during post-ischemic reperfusion (Fig 4.4F).

4.3.4 Endogenous substrate utilization during ischemia and reperfusion

Compared to SHAM hearts, CAL hearts utilize less glycogen during ischemia but accumulate less glycogen during reperfusion (Fig 4.5A-B). As a result, CAL hearts produced less protons during ischemia compared to SHAM hearts (Fig. 4.5C). TG utilization was similar in CAL and SHAM hearts during ischemia. While SHAM hearts continue to utilize TGs during reperfusion, CAL hearts accumulate TG (Fig 4.5d-E), which, together with comparable LV work levels, indicates a higher metabolic efficiency in reperfused CAL hearts.

4.3.5 Abundance of mitochondrial markers and key metabolic enzymes

CAL hearts have a significantly higher PGC-1 α protein expression (Fig 4.7A), indicative of a higher stimulus for mitochondrial biogenesis. However, the expression of markers of mitochondrial abundance, complex 1 subunit

(NDUFB6), VDAC, β -HAD and LCAD were comparable in CAL and SHAM hearts (Fig 4.7B-E), indicative of an unchanged mitochondrial content in CAL hearts. Expression levels of CaMKII, pCaMKII, phospholamban and SERCA2 were also similar in CAL and SHAM hearts (Fig 4.7F-H), suggesting the absence of abnormalities in Ca^{2+} handling. Similarly, expression of PPAR α , PDH, hexokinase, GLUT1, GLUT4, GSK3 β , pGSK3 β , LDH and GAPDH was similar in CAL hearts supporting the lack of major changes in metabolic rates in CAL hearts compared to SHAM hearts (Fig 4.8A-I). Similarly AMPK activity (pAMPK/tAMPK) was similar in CAL and SHAM hearts at each time point (Fig 4.6). As expected, AMPK activity was higher in both SHAM and CAL hearts at the end of ischemia (Fig 4.6), but recovered during reperfusion.

4.4 Discussion

A number of major findings were demonstrated in this study. Confirming previous studies, we demonstrate that hearts remodeled following a coronary artery ligation are not energy deficient, but rather have a lower metabolic efficiency. Of importance, we provide the novel observation that hearts remodeled following coronary artery ligation exhibit less deterioration of mechanical function during post-ischemic reperfusion. Despite lower metabolic efficiency during aerobic (pre-ischemic) conditions, remodeled hearts maintain similar levels of metabolic efficiency during reperfusion. In contrast, normal hearts exhibit a marked deterioration of mechanical function and metabolic efficiency during reperfusion following ischemia. Recovery of cardiac energy metabolism was not compromised in either normal or remodeled hearts following

ischemia. However, there is a significant attenuation of glycogen utilization in remodeled hearts during ischemia, with a lower rate of proton production during ischemia in the remodeled hearts. This decrease in proton production in remodeled hearts compared to normal may explain the improved tolerance to ischemic injury in the remodeled hearts.

While there are numerous studies of energy substrate metabolism and reperfusion injury in normal hearts, few have addressed the relationships between metabolism and post-ischemic function in hearts remodeled following a myocardial infarction. In order to create an experimental model of the remodeled heart, we produced a permanent ligation of the coronary artery in mice, followed by a 4 wk post-surgical period during which a mature scar formed and LV dysfunction developed. The examination of LV mechanical and metabolic function during isolated working heart perfusion enabled comparisons of normal and remodeled hearts under controlled conditions of energy substrate availability and workload and so provided an appropriate assessment of metabolic efficiency, a measure of LV work produced per unit ATP produced (joule/ μ mol).

Post-infarction remodeled hearts exhibit a marked deterioration of mechanical function [221]. We previously showed that CAL hearts are not energy-starved since they maintain comparable adenine nucleotide contents to SHAM hearts, and the reduction in ATP production rates from fatty acid, glucose, and lactate metabolism in these hearts does not match the deterioration of mechanical function. Thus there is a significant reduction of metabolic efficiency (i.e., inefficient utilization of ATP for generation of external mechanical work) in

the CAL hearts during aerobic perfusion [221]. We also showed that this may be due to increased proton production per LV work as a result of increased mismatch between glycolytic flux and glucose oxidation rates [221] that may lead to a diversion of ATP from contractile work towards correction of ion homeostasis. The demonstration in this study that CAL hearts maintain similar metabolic rates to SHAM hearts during aerobic perfusion confirms our previous finding that CAL hearts are not energy starved [221] but instead develop metabolic inefficiency. In addition, we now demonstrate that following ischemia and reperfusion, CAL hearts maintain comparable rates of energy substrate metabolism to reperfused SHAM hearts excludes the possibility of a change in energy substrate preference as a contributor to the observed lower functional deterioration in reperfused CAL hearts. Indeed, the finding that CAL hearts maintain similar metabolic rates per LV work during reperfusion as during aerobic perfusion indicates that there is no further deterioration of metabolic efficiency in reperfused CAL hearts. These findings are in accordance with previously published reports highlighting a better ischemic tolerance in remodeled post-infarction hearts as indicated by reduced release of purines and lactate [315], less ischemic contracture and less lactate dehydrogenase release [314]. Similarly, cardiomyocytes derived from post-infarction remodeled hearts exhibit lower decreases in ATP levels and less release of lactate dehydrogenase following hypoxia re-oxygenation [316].

In contrast to CAL hearts, reperfused SHAM hearts exhibit a significant increase in glycolytic flux per LV work that is not matched by a corresponding increase in the rate of glucose oxidation, resulting in increased proton production

per LV work. This finding, together with a significant increase in reperfusion fatty acid oxidation rate per LV work, contributes to the deteriorating metabolic efficiency during reperfusion of SHAM hearts. These findings are also in accordance with previous published data showing that during post-ischemic reperfusion, normal mouse hearts exhibit a marked deterioration of oxidative metabolism. This augments the mismatch between glycolytic flux and glucose oxidation rates resulting in lactate accumulation [13, 326, 405-407]. Meanwhile, protons derived from the hydrolysis of glycolytically produced ATP accumulate, increasing intracellular acidosis [317]. The subsequent activation of the $\text{Na}^+\text{-H}^+$ exchanger causes Na^+ accumulation [333], which, in turn, activates reverse mode $\text{Na}^+\text{-Ca}^{2+}$ exchange leading to Ca^{2+} overload [185]. In order to correct Na^+ and Ca^{2+} overload, more ATP is diverted towards ionic homeostasis than to mechanical function. This is expected to lead to deterioration of metabolic efficiency associated with a significant deterioration of mechanical function (reviewed in [319])

A higher abundance of mitochondria in CAL hearts is a potential mechanism for the finding that CAL hearts, as compared to SHAM hearts, do not show further deterioration of metabolic efficiency during reperfusion. Although higher expression of PGC-1 α (which stimulates mitochondrial biogenesis) is observed in CAL hearts, this did not translate into increase in mitochondrial abundance of enzymes such as complex 1 subunit (NDUFB6), VDAC, β HAD or LCAD. Moreover, protein expression of key enzyme regulators of oxidative metabolism is similar in CAL and SHAM hearts. Nevertheless, the increased level

of PGC-1 α expression in CAL hearts may have contributed to the maintenance of mitochondrial mass and oxidative capacity in the remodeled viable tissue. Thus it is unlikely that the better functional recovery and maintained metabolic efficiency during reperfusion of remodeled hearts are due to alterations in mitochondrial abundance.

Improved calcium handling is another potential mechanism for the absence of functional deterioration during reperfusion of CAL hearts. If present, it may contribute to reduced post-ischemic contracture and more efficient utilization of ATP for external mechanical work. However, the absence of changes in the calcium handling proteins, CaMKII, phospholamban and SERCA2, suggests the presence of other contributing factors to the observed absence of post-ischemic functional deterioration in CAL hearts.

A third potential explanation of the observed better functional recovery following ischemia and maintained metabolic efficiency in CAL hearts is a decrease in intracellular acidosis and Na⁺ and Ca²⁺ overload during ischemia. A major contributor to the development of acidosis during ischemia is the incorporation of glycogenolysis-derived glucose-6-P into anaerobic glycolysis producing lactate and protons. The finding that CAL hearts exhibit significantly lower ischemic glycogenolysis as compared to SHAM hearts resulted in a lower ischemic production of lactate and protons in CAL hearts. Evidence to support this hypothesis comes from the finding that recovery of intracellular pH in reperfused hearts is delayed if the rates of glycolytic flux are not matched with glucose oxidation and that improving the coupling enhances the recovery of

intracellular pH and improves both mechanical function and cardiac efficiency [317]. In fact, many interventions that inhibit glycolytic flux during early reperfusion are cardioprotective. Omar et al [318] showed that diverting glucose metabolism towards glycogen synthesis rather than glycolytic flux reduces proton production, limits Ca^{2+} overload and improves recovery of post-ischemic mechanical function. Similarly, other cardioprotective interventions such as adenosine [340] or ischemic preconditioning [330, 408] reduce glycogen utilization and inhibit glycolytic flux. The demonstration that CAL hearts utilize less glycogen than SHAM hearts during ischemia indicates that CAL hearts have lower proton accumulation at the end of ischemia. This lower stimulus for Na^+ and Ca^{2+} accumulation during early reperfusion likely contributes to the lack of further deterioration in mechanical function and the lower deterioration in metabolic efficiency.

Attenuation of rates of glycogenolysis during ischemia has been noted with some cardioprotective interventions such as ischemic preconditioning and adenosine [328, 330] as well as with lower rates of ATP catabolism [409]. Indeed, the findings that CAL hearts have lower rates of glycogenolysis during ischemia and preserved ATP contents during reperfusion suggest that the improved ischemic tolerance of remodeled hearts may mimic some of the mechanisms involved in ischemic preconditioning. Furthermore, the demonstration that preconditioning mechanisms are already activated in remodeled hearts may explain the failure of additional preconditioning interventions to achieve functional benefits in remodeled hearts [410-412].

AMPK is a known regulator of glycogen turnover [325, 413]. A previous study by Jaswal et al [325] showed that AMPK inhibition at post-ischemic reperfusion of rat hearts shifts glucose metabolism towards glycogen synthesis. The inhibition of glycogenolysis and subsequent reduction of glycolytic flux rates improve coupling between glycolytic flux and glucose oxidation rates. This, in turn, reduces reperfusion proton production and is associated with a better functional recovery. We studied the expression and activation of AMPK at different perfusion time points. The demonstration that CAL hearts exhibit similar pattern of ischemic AMPK activation indicates that changes in AMPK are less likely to explain the observed reduction of ischemic glycogen utilization in CAL hearts.

4.5 Conclusion

In conclusion, remodeled CAL hearts exhibit impaired LV mechanical function and metabolic efficiency during baseline aerobic conditions. Following exposure to an acute ischemic episode remodeled hearts exhibit higher recovery of LV function compared to normal hearts, with no further deterioration of metabolic efficiency. Lower glycogenolysis during ischemia with subsequent less intracellular acidosis and ion dysregulation may contribute to the greater tolerance to ischemic injury in the remodeled heart. Changes in Ca²⁺ handling proteins, mitochondrial mass or AMPK activity are less likely contributors to our findings.

Figure 4.1 In vivo echocardiographic functional assessment.

Panel A shows a parasternal long axis view of a SHAM heart. Panel B shows a parasternal long axis view of a CAL heart. Notice the dilatation of the LV. Panel C shows an m-Mode capture of a SHAM heart. Panel D shows an m-Mode capture of a CAL heart. Notice the increased LV volume (panel B) and reduced wall motion (panel D) in CAL hearts as compared to SHAM hearts (panels A & C).

Figure 4.1

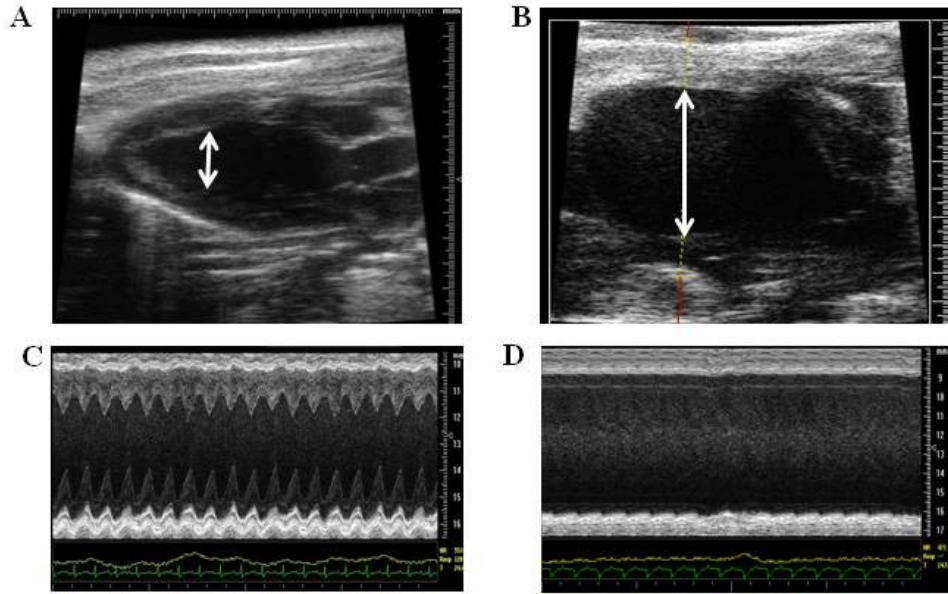


Figure 4.2 *Ex vivo* assessment of mechanical function and hemodynamic parameters.

Panel A shows time-dependent changes in LV work and Panel B shows average LV work for SHAM (N=33) and CAL (N=17) hearts during aerobic perfusion, global ischemia and reperfusion. Panel C shows % recovery of mechanical function during reperfusion. (*) refers to a significant difference ($P < 0.05$) from aerobic SHAM parameters. Data are expressed as means \pm SEM.

Figure 4.2

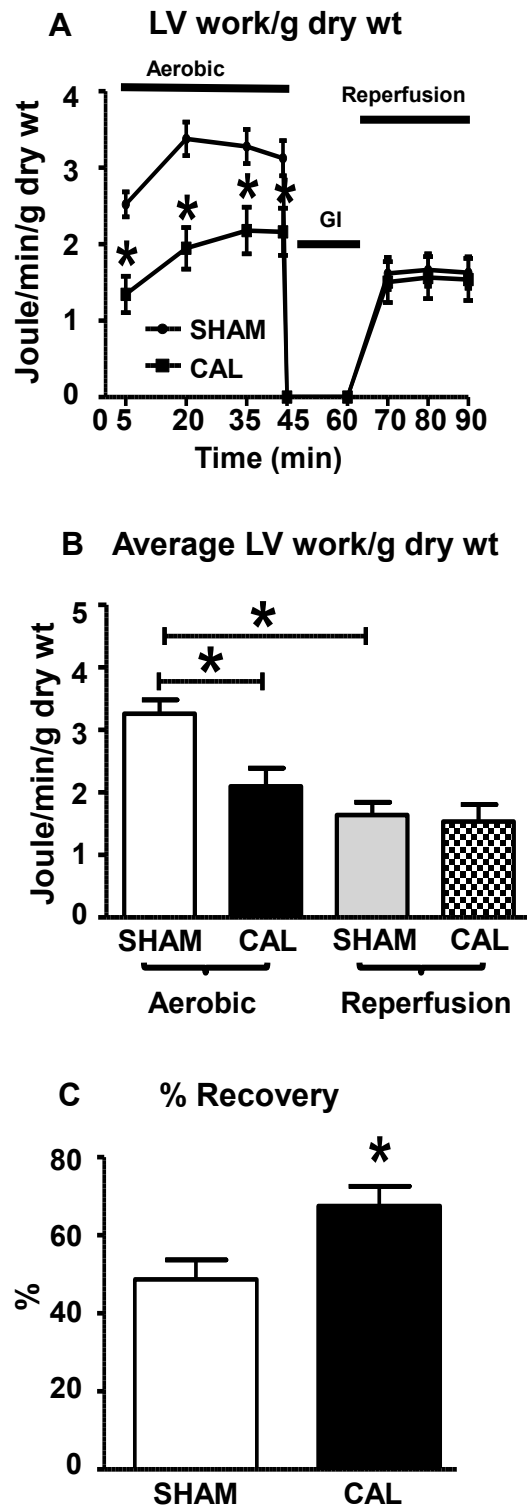


Figure 4.3 Rates of energy substrate metabolism in SHAM and CAL hearts.

Glycolysis, glucose oxidation and calculated proton production are shown in panels A-C (SHAM N=16, CAL N=7). Fatty acid oxidation (panel D, SHAM N=15, CAL N=10) and lactate oxidation (panel E, SHAM N=15, CAL N=9) are also shown. Calculated ATP production rates are shown in panel F. Since data are not normally distributed, data are presented as median \pm interquartile range (5% and 95%).. Differences are considered significant when $P < 0.05$.

Figure 4.3

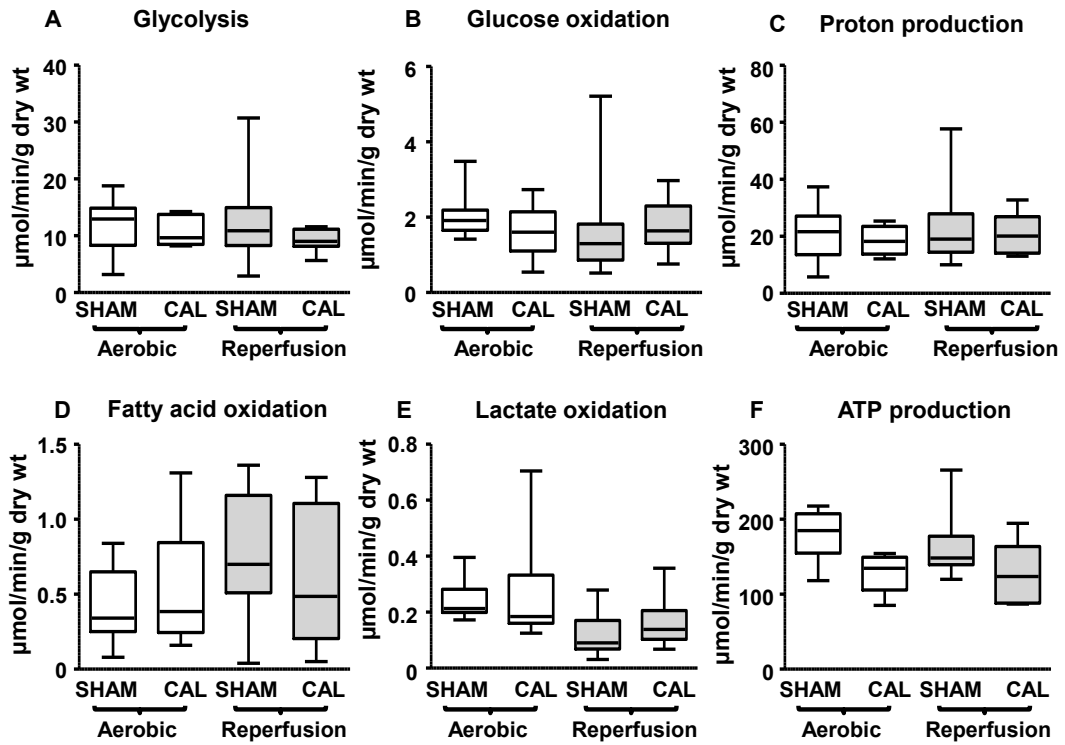


Figure 4.4 Metabolic rates per LV work of SHAM and CAL hearts.

Glycolysis, glucose oxidation and calculated proton production are shown in panels A-C (SHAM N=16, CAL N=7). Fatty acid oxidation (panel D, SHAM N=15, CAL N=10) and lactate oxidation (panel E, SHAM N=15, CAL N=9) are also shown. Values for calculated metabolic efficiency are shown in panel F.

Since data are not normally distributed, data are presented as median \pm interquartile range (5% and 95%). Differences are considered significant when $P < 0.05$. (*)

Figure 4.4

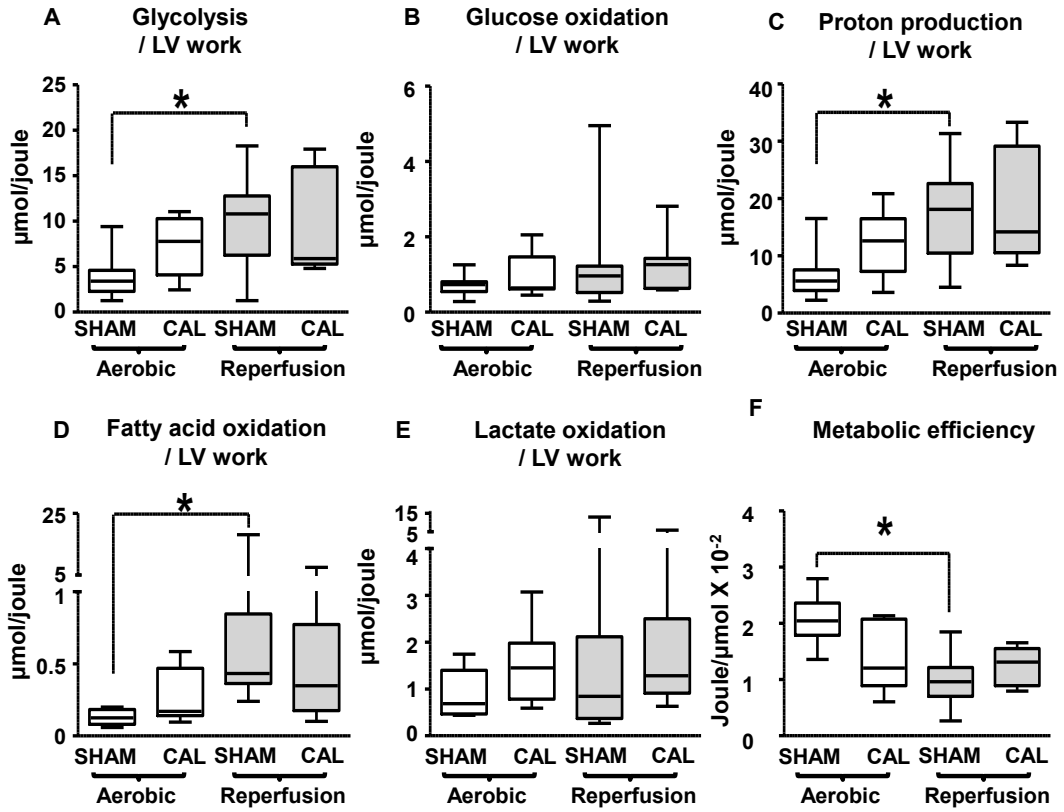


Figure 4.5 Contents and change of endogenous energy substrates in SHAM and CAL hearts.

Glycogen content is shown in panel A at the end of aerobic perfusion (SHAM N=5 and CAL N=5), end of ischemia (SHAM N=4 and CAL N=4) and end of reperfusion (SHAM N=6 and CAL N=4). Changes in glycogen content during these intervals are presented in panel B. Ischemic proton production from glycogen utilization is presented in panel C. Triglyceride (TG) content is shown in panel D at the end of aerobic perfusion (SHAM N=4 and CAL N=5), end of ischemia (SHAM N=4 and CAL N=4) and end of reperfusion (SHAM N=6 and CAL N=5). Changes in TG content during these intervals are presented in panel E. Data are presented as median \pm interquartile range (5% and 95%). Differences are considered significant when $P < 0.05$ (*).

Figure 4.5

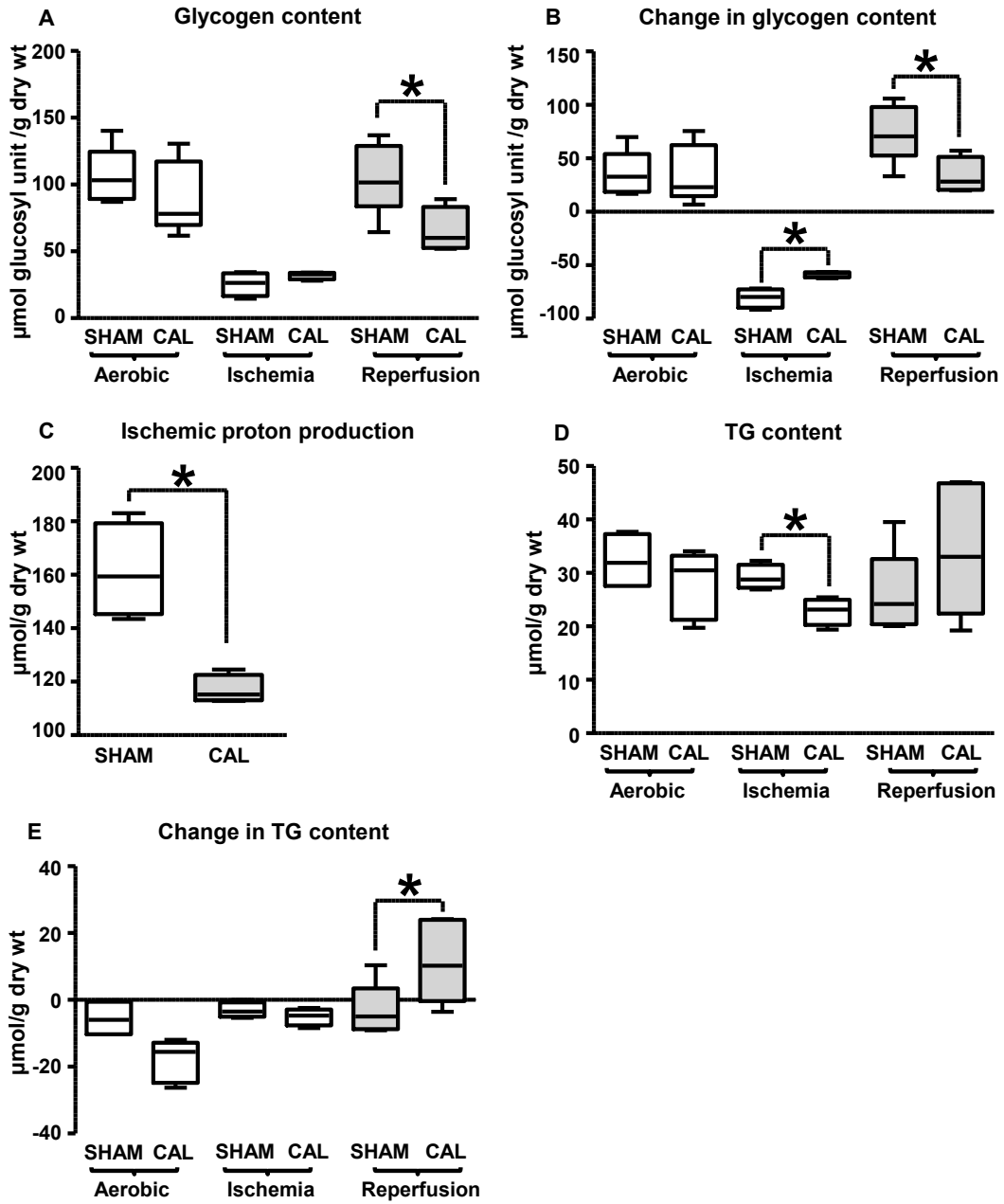


Figure 4.6 Phosphorylation status (pAMPK/tAMPK) of AMPK.

Phosphorylation of AMPK is used as an indication of activity. Data are shown for the following time points: end of aerobic perfusion, ischemia and reperfusion.

N=4. Data are expressed as mean \pm SEM. Differences are considered significant when $P < 0.05$. * Significantly different from aerobic values. # Significantly different from corresponding reperfusion values.

Figure 4.6

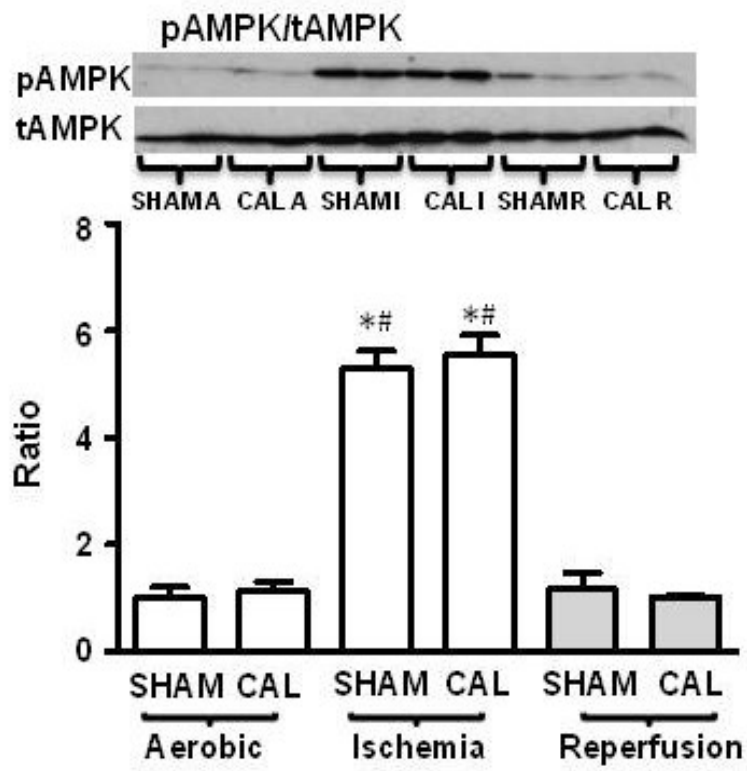


Figure 4.7 Protein expression of markers of mitochondrial biogenesis and abundance and calcium handling proteins in aerobically perfused hearts.

Protein expression of markers of stimulus for mitochondrial biogenesis (PGC1 α - panel A), markers of mitochondrial abundance (complex I subunit, NADH dehydrogenase (ubiquinone) 1 beta subcomplex (NDUFB6), voltage dependent anion channel (VDAC), β -hydroxy acyl CoA dehydrogenase (β -HAD) and long chain acyl-CoA dehydrogenase (LCAD) - panels B-E), calcium handling proteins (pCaMKII, tCaMKII and phospholamban - Panel F-H). N = 3-6. Data are expressed as mean \pm SEM. Differences are considered significant when $P < 0.05$. (*) refers to a significant difference.

Figure 4.7

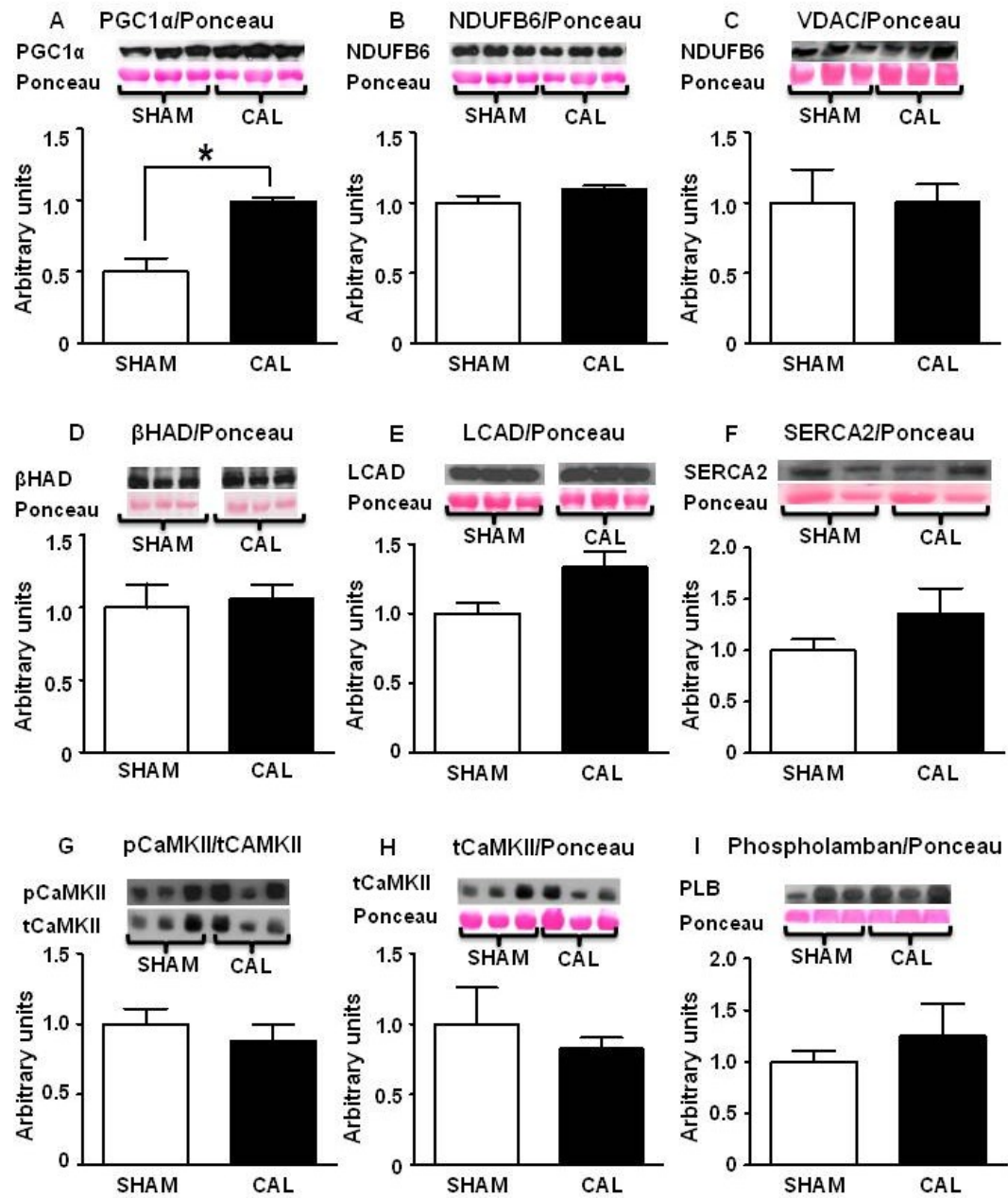


Figure 4.8 Protein expression of key metabolic enzymes

Protein expression of PPAR α , PDH, hexokinase, GLUT1, GLUT4, GSK3 β , LDH and GAPDH (Panel A-I). N = 3-6. Data are expressed as mean \pm SEM.

Differences are considered significant when $P < 0.05$. (*) refers to a significant difference.

Figure 4.8

Online supplement Figure 2

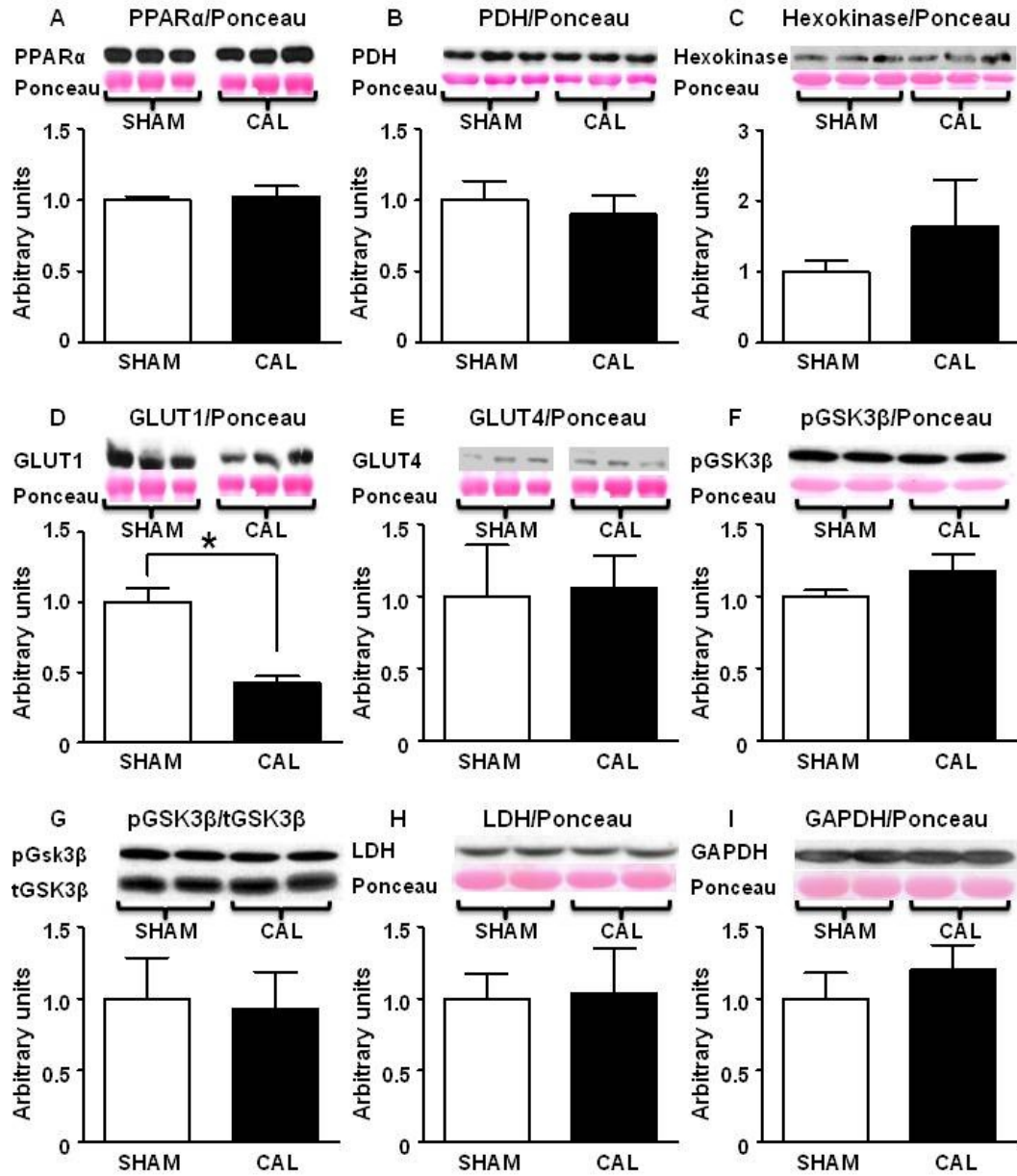


Table 4.1 Detailed echocardiographic parameters of SHAM and CAL hearts.

LV = left ventricular, LVID = LV internal dimension, LVPW = LV posterior wall thickness, IVS = interventricular septal thickness, EF = ejection fraction, FAC = fraction area change, IVRT = isovolumetric relaxation time, IVCT = isovolumetric contraction time, MVDT = mitral valve deceleration time. (*) refers to a statistically significant difference ($P < 0.05$). Data are presented as means \pm SEM.

Table 4.1

Parameter (unit)	SHAM (N)	CAL (N)
<u>M-mode measures:</u>		
Heart rate (beats/min)	422±10 (18)	418±14 (11)
Cardiac output (mL/min)	21.95±2.15 (6)	18.96±0.98 (11)
EF (%)	56.04±0.98 (18)	25.79±1.43 (11)*
FAC (%)	42.88±4.76 (6)	22.53±2.20 (11)*
<u>Wall measurements:</u>		
LV systolic volume (μL)	36±1.80 (18)	98±12.09 (11)*
LV diastolic volume (μL)	83±2.81 (18)	149±11 (11)*
LVIDs (mm)	3.02±0.06 (18)	4.55±0.22 (11)*
LVIDd (mm)	4.30±0.06 (18)	5.49±0.17 (11)*
LVPWs (mm)	1.14±0.04 (18)	1.05±0.05 (11)
LVPWd (mm)	0.77±0.02 (18)	0.85±0.05 (11)
IVSs (mm)	1.15±0.03 (18)	1.15±0.05 (11)
IVSd (mm)	0.78±0.01 (18)	0.89±0.03 (11)*
Corrected LV mass (mg)	102±3 (18)	184±16 (11)*
<u>Tissue doppler data:</u>		
IVCT (ms)	17.95±1.04 (17)	22.59±2.36 (11)
Tei index (ratio)	0.75±0.03 (17)	1.06±0.07 (11)*
E	715±97 (17)	619±130 (11)*
E`	29.5±7.6 (17)	20.4±3.8 (11)*
A	426±166 (17)	307±75 (7)
E/E` (ratio)	25±1 (17)	31±2 (11)*
E/A (ratio)	1.89±0.18 (17)	2.02±0.12 (7)
IVRT (ms)	18.13±0.75 (17)	22.83±1.11 (11)*
MV DT (ms)	19.45±2.16 (16)	19.94±2.47 (7)

Table 4.2 Detailed *ex vivo* hemodynamic parameters of SHAM and CAL hearts.

(*) refers to a significant difference (P<0.05) from aerobic SHAM parameters. Data are expressed as means ± SEM.

Parameter (unit)	SHAM (N=33)		CAL (N=17)	
	Aerobic	Reperfusion	Aerobic	Reperfusion
Body weight (g)	27.6±0.3		27.01±0.36	
Viable heart dry weight (mg)	32±1		33±2	
Viable heart dry wet ratio (ratio)	0.16±0.01		0.16±0.01	
Heart rate (bpm)	329±7	319±11	324±11	309±8
Systolic pressure (mmHg)	82.9±1.6	69.2±4.0	75.4±2.0*	71.0±3.5
Diastolic pressure (mmHg)	20.6±1.1	25.6± 1.7	29.1±1.7*	28.5±1.4
Cardiac output (mL/min)	9.7±0.3	5.9±0.6	6.3±0.5*	5.2±0.6
Aortic flow (mL/min)	7.6±0.3	3.6±0.4	4.6±0.5*	3.2±0.4
Coronary flow (mL/min)	2.1±0.3	2.2±0.3	1.8±0.2	1.9±0.3

Table 4.3 End reperfusion nucleotide, nucleoside and creatine contents.

Data are expressed as means \pm SEM. Differences are considered significant when $P < 0.05$. End aerobic nucleotide contents are presented in Table 3.3.

Parameter ($\mu\text{mol/g dry wt}$)	SHAM (N=5)	CAL (N=5)
Adenosine triphosphate (ATP)	20.02 \pm 2.30	24.27 \pm 3.10
Adenosine diphosphate (ADP)	3.86 \pm 0.37	5.05 \pm 0.74
Adenosine monophosphate	0.47 \pm 0.05	0.86 \pm 0.13
Guanosine triphosphate (GTP)	1.03 \pm 0.14	1.42 \pm 0.16
Inosine	1.75 \pm 1.12	1.91 \pm 0.68
Creatine	21.20 \pm 3.97	19.84 \pm 3.03
Creatine phosphate	32.15 \pm 3.31	39.77 \pm 5.87

**5 Study of the possible cardioprotective effect of
pharmacologic modulation of cardiac energy
substrate metabolism**

**Echocardiographic examinations were performed by Donna Becker from the
Cardiovascular Research Centre, University of Alberta.**

5.1 Introduction

In Chapter 3 we showed that hearts remodeled following infarction are metabolically inefficient possibly due, in part, to mismatched glycolytic flux rates and glucose oxidation rates. In addition, we showed that improving the match between glycolytic rates and glucose oxidation rates in mice with a chronic deficiency of MCD improves metabolic efficiency and lessens post-infarction functional deterioration. In addition, in Chapter 4 we showed that despite their metabolic inefficiency, post-infarction remodeled hearts exhibit no further deterioration of their metabolic efficiency during *ex vivo* post-ischemic reperfusion as compared to SHAM hearts. This is in contrast to the known features of IR injury, namely, slowed oxidative metabolism and an increase in glycolytic rates [318, 322, 325, 329, 414] which result in a greater mismatch between glycolytic flux rates and glucose oxidation rates with the subsequent increased proton production rates. This Chapter addresses the potential for improvement of metabolic efficiency in remodeled hearts by pharmacologic MCD inhibition using an MCD inhibitor (MCDi), CMB-0000382 as well as the possibility for further improvement in the recovery of post-ischemic functional recovery and metabolic efficiency using DCA, a known stimulator of glucose oxidation.

DCA stimulates glucose oxidation in normal healthy hearts through inhibition of PDK, an upstream inhibitor of PDH [367, 415, 416]. This results in stimulation of PDH, the rate limiting enzyme of glucose oxidation. The

accelerated rate of glucose oxidation lessens the mismatch between the rates of glycolysis and glucose oxidation and so causes less proton accumulation and less deterioration of metabolic efficiency in conditions such as reperfusion and heart failure. In *ex vivo* models of IR, DCA improves post-ischemic recovery of mechanical function in normal healthy hearts [416-418]. It also improves efficiency of these hearts through the stimulation of the oxidation of glucose, a more efficient energy substrate relative to fatty acids [367, 419]. Beneficial effects of DCA also occur in patients with heart failure where it improves exercise tolerance, hemodynamic function and mechanical efficiency [355, 420-422].

As shown in Chapter 4, the response of post-infarction remodeled hearts to *ex vivo* IR does not follow the expected pattern of healthy hearts. Instead, they maintain comparable levels of metabolic efficiency and LV function as seen during aerobic perfusion. Thus, as the response of remodeled hearts to DCA might not be similar to healthy hearts, we describe in this chapter the response of remodeled hearts to DCA when administered at the onset of post-ischemic reperfusion.

Many studies of DCA on cardiac metabolism have been performed in the absence of lactate [320, 367, 369, 373, 423, 424] since study focus was on the effects of DCA on the changes in the metabolism of glucose. Interestingly, reports about effects of DCA when examined in the presence of lactate are not consistent. Barak *et al* [418] reported limited functional recovery following ischemia that was associated with insignificant changes in glucose oxidation and fatty acid metabolism in rat hearts reperfused with 5 mM DCA. In contrast, Mazer

et al [425] reported that *in vivo* pig hearts reperfused with 3 mM DCA show the expected stimulation of carbohydrate metabolism but without improvements in systolic function. Since this thesis is addressing energy substrate metabolism in remodeled hearts, we have included lactate as an energy substrate as the heart is normally exposed to this energy substrate during similar pathologic conditions. Thus, the regular heart perfusate used throughout this thesis contains glucose, palmitate and lactate unless specified otherwise. A secondary aim of this component of the thesis is to determine whether the absence of lactate might affect the response to DCA treatment during post-ischemic reperfusion.

We have also shown (Chapter 3) that chronic MCD deficiency results in less functional deterioration and an improved cardiac metabolic efficiency following CAL surgery. This appears to be due to enhancement of the matching between glycolytic rates and glucose oxidation rates resulting in lower rates of proton production. These findings are confirmed by a recent report that cardiac-specific MCD deletion by microRNA limits functional deterioration and preserves energy stores in post-infarction remodeled rat hearts [60]. Similarly, other studies highlight the important benefit of MCD inhibition in the setting of ischemia, heart failure and insulin resistance [66, 67, 96, 221, 322, 324]. The ability of MCD inhibition to improve the matching of glycolysis to glucose oxidation, which occurs secondary to inhibition of fatty acid oxidation (Randle cycle), reduces lactate production in ischemic pig hearts following demand induced-ischemia [66]. Furthermore, MCD inhibition improves post-ischemic functional recovery in *ex vivo* perfused rat hearts [66, 67]. This benefit was associated with improved

matching of glucose metabolism, due to stimulated glucose oxidation resulting in less lactate production [66, 67].

It is known that genetic interventions such as MCD deletion in mice can result in a myriad of compensatory mechanisms that can confound experimental results. In this regard, MCD-KO mouse hearts maintain comparable energy substrate metabolic rates under normal aerobic perfusion conditions despite an increase in malonyl CoA content [96]. The authors of that study concluded that a compensatory increase in the fatty acid carrier, CD36, uncoupler protein 3 (UCP3), CPT1 or pyruvate dehydrogenase kinase 4 (PDK₄) [96] may have helped maintain normal rates of fatty acid oxidation. Thus, a second series of experiments in this chapter investigates the effect of acute MCD inhibition in remodeled CAL hearts during *ex vivo* aerobic perfusion to determine if MCD could be a useful drug target to improve metabolic efficiency in remodeled hearts.

5.2 Methods

Male C57BL/6 mice, age 12-14 weeks, were subjected to permanent coronary artery ligation (CAL, n=45) or sham operation (SHAM, n=60). Anesthesia was induced by IP pentobarbital (60 mg/kg) (See Chapter 2, Materials and Methods for details). A total of 26 CAL and 37 SHAM hearts were used for the reperfusion DCA treatment study and 19 CAL and 23 SHAM hearts were used for aerobic MCDi study.

To study the effect of an absence of lactate on DCA action, another set of C57BL/6 mice (12-14 wk of age) (N=11) were used for aerobic perfusion in the

working mode in the presence (N=5) or absence (N=6) of 1 mM lactate. In treated groups, DCA (1.5 mM) was present from time 45 min until the end of the 90-min perfusion protocol.

The protocol for the MCDi study included a 45-min aerobic perfusion and in treated groups, the MCDi, CMB-0000382 at a concentration of 50 μ M was added to the perfusate at time zero of the perfusion protocol. The choice of 50 μ M concentration is based on the IC₅₀ of CMB-0000382 for inhibition of MCD (verbal communication from Dr. Lopaschuk's lab). Please refer to Chapter 2 for details of methods.

5.2.1 Measurement of short chain CoA esters in heart tissues

Measurement of short-chain CoA esters (malonyl CoA, acetyl CoA and succinyl CoA) was performed as reported previously [322]. Briefly, frozen viable heart tissue samples (~10–20 mg, excluding infarcts in CAL hearts), were homogenized for 20 s in 300 μ L of 6% (v/v) perchloric acid. After homogenization, the samples were left on ice for 10 min followed by centrifugation at 12,000g for 5 min. Then 100 μ L of the supernatant was analyzed using an Ascentis Express C18 Column, 10 cm \times 2.1 mm and 2.7 μ m particle size from Supelco and an ACQUITY UPLC HSS system (Waters, Milford, MA, USA). Each sample was maintained at a temperature of 40 °C and run at a flow rate of 0.4 mL/min. Detection was performed at an absorbance of 260 nm. The mobile phase consisted of a mixture of buffer A (water and 0.25 M NaH₂PO₄) and buffer B (acetonitrile and 0.25 M NaH₂PO₄). The gradient-elution profile consisted of the following sequence of initial conditions: 2% B for 2–4 min, 25%

B for 4–6 min, 40% B for 6–8 min and 100% B for 10–12 min, maintained for 15 min. All gradients were linear and peaks were acquired, integrated and analyzed using the Waters Empower Software.

5.3 Results

5.3.1 Treatment with DCA at reperfusion

5.3.1.1 Pre- and post-ischemic function of untreated remodeled hearts

Confirming our previous data, CAL hearts have impaired systolic function as evidenced by lower percentage ejection fraction (%EF) and fractional shortening (%FS). Diastolic function is not much affected in this cohort as indicated by a higher Tei index and only a trending high isovolumetric relaxation time (IVRT, $P=0.08$). Other parameters such as MV DT, the ratio between early mitral inflow velocity and mitral annular early diastolic velocity (E/E') and the ratio of the early (E) to late (A) ventricular filling velocities (E/A ratio) remain similar to SHAM hearts. There is a marked dilatation of CAL hearts as evidenced by increased systolic and diastolic LV volumes and LVID. CAL hearts maintain similar LVPW and IVS despite the loss of a portion in the infarcted area, indicative of compensatory hypertrophy. See Table 5.1 for details of the aforementioned hemodynamic parameters.

During *ex vivo* aerobic perfusion, CAL hearts produce less LV mechanical work than SHAMs confirming *in vivo* findings and our previous data. During

reperfusion, LV mechanical work of untreated SHAM and CAL hearts recover to similar values as observed in aerobic CAL hearts, indicative of a better % recovery of CAL hearts. Similarly, cardiac output and systolic pressure decline significantly during reperfusion in SHAM hearts but remain similar to aerobic perfusion values in CAL hearts (Fig 5.2B-C, Table 5.2).

5.3.1.2 The effect of reperfusion DCA treatment on SHAM and CAL hearts

5.3.1.2.1 Post-ischemic functional recovery

SHAM hearts treated with DCA recover to similar LV work levels as untreated SHAM hearts (46% vs 47% - Fig 5.2B-C). Similarly, treated SHAM hearts show a similar trend of deterioration of LV work, systolic pressure, developed pressure and cardiac output during reperfusion as compared to untreated SHAM hearts (Table 5.2). However, CAL hearts treated with DCA exhibit poorer functional recovery as compared to untreated CAL hearts (25% vs 50% - Fig 5.2B-C). A similar pattern is also observed for systolic pressure, cardiac output and aortic flow that significantly deteriorated in treated reperfused CAL hearts as compared to untreated CAL hearts (Table 5.2).

5.3.1.2.2 Energy substrate metabolism and ATP production

Confirming our previous data, CAL hearts maintain comparable metabolic rates to SHAM hearts during aerobic perfusion (Fig 5.3A-E). Similarly, reperfused CAL hearts maintain similar metabolic rates to aerobic values, indicative of lack of energy starvation during both aerobic and reperfusion phases.

Apart from lower lactate oxidation rates, reperfused SHAM hearts maintain similar metabolic rates to aerobic levels. Confirming our previous published data, CAL hearts exhibit a slightly but significantly lower ATP production rate during aerobic perfusion, but this is not sufficient to explain the observed lower LV mechanical function (Fig 5.3F). During reperfusion, both untreated CAL and SHAM hearts as well as CAL hearts treated with DCA maintain similar ATP production rates to their aerobic values. Conversely, reperfused SHAM hearts treated with DCA exhibit a significant decrease in ATP production rates as compared to SHAM aerobic rates (Fig 5.3F).

5.3.1.2.3 Reperfusion metabolic efficiency

Confirming our previous data shown in Chapter 3, when expressed per LV work, CAL hearts have higher glycolytic rates (Fig 5.4A) than SHAM hearts ($P < 0.5$ - t-test). This is not associated with an increase in glucose oxidation rates (Fig 4B) resulting in a significant increase in proton production rates in CAL hearts ($P < 0.05$ - t-test) (Fig 5.4C). Fatty acid oxidation and lactate oxidation per LV work are also higher in CAL than SHAM hearts (Fig 5.4D-E). Thus the calculated metabolic efficiency of CAL hearts during aerobic perfusion is lower than SHAM hearts (Fig 5.4F).

During reperfusion, confirming our data presented in Chapter 4, untreated reperfused SHAM hearts exhibit a significant increase in glycolytic rates (Fig 5.4A), but these are not matched by a corresponding increase in glucose oxidation rates (Fig 5.4B) resulting in a significant increase in proton production rates (Fig 5.4C). Untreated reperfused SHAM hearts also exhibit higher fatty acid oxidation

per LV work than aerobic hearts (Fig 5.4D). Lactate oxidation is similar to aerobic values. Collectively these alterations result in a significant deterioration of metabolic efficiency in reperfused SHAM hearts.

In accordance with our previous data, reperfused CAL hearts maintain similar rates of glycolysis (Fig 5.4A) and glucose oxidation (Fig 5.4B) resulting in no further increase in proton production rates (Fig 5.4C). Fatty acid oxidation and lactate oxidation rates per LV work remain similar to aerobic values (Fig 5.4D-E). Thus, metabolic efficiency does not exhibit further deterioration during reperfusion (Fig 5.4E).

DCA treatment at reperfusion does not alter rates of glucose metabolism per LV work in SHAM hearts. During reperfusion, DCA-treated SHAM hearts maintain a higher glycolytic flux rate per LV work as compared to values during aerobic perfusion (Mann-Whitney test – $P < 0.05$ - Fig 5.4A). Despite higher rates of glycolysis, DCA does not increase glucose oxidation. Thus, the extent of uncoupling of the rates of glycolysis and glucose oxidation is increased (Fig 5.4B), resulting in a significant increase of the rate of proton production per LV work, as compared to aerobic perfusion values (Fig 5.4C). Thus, regardless of DCA treatment, metabolic efficiency significantly deteriorated in reperfused SHAM hearts (Fig 5.4E).

In contrast to untreated CAL hearts, DCA-treated reperfused CAL hearts exhibit a significant increase in glycolytic rate per LV work as compared to aerobic values ($P < 0.05$ – Mann-Whitney – Fig 5.4A). DCA fails to accelerate glucose oxidation per LV work over the rates observed in untreated reperfused

CAL hearts (Fig 5.4B). These rates are not sufficient to match the increased glycolytic flux rates. Thus, DCA-treated reperfused CAL hearts have a higher proton production rate per LV work as compared to aerobic values. Despite lower LV work, DCA-treated reperfused CAL hearts exhibit higher fatty acid oxidation and lactate oxidation rates per LV work than either aerobic and untreated reperfusion values ($P < 0.05$ - Kruskal Wallis - Fig 5.4D-E). Thus, DCA-treated reperfused CAL hearts exhibit a marked deterioration of metabolic efficiency (Fig 5.4E).

5.3.1.3 The effect of reperfusion DCA treatment on healthy (non-SHAM) hearts

5.3.1.3.1 Post-ischemic functional recovery

Normal healthy hearts subjected to ischemia and treated with DCA during reperfusion recover to similar work levels as untreated healthy hearts. There is no significant difference in percent recovery of LV work (50 ± 7 vs 38 ± 7 , $P > 0.05$) (Fig 5.5A-C). Also hemodynamic parameters are similar in both groups (see Table 5.3 for details).

5.3.1.3.2 Energy substrate metabolism and ATP production

Rates of glycolysis, glucose oxidation, lactate oxidation and fatty acid oxidation are similar during aerobic perfusion of untreated and DCA-treated reperfused healthy hearts, indicative of a lack of response to DCA treatment (Fig 5.6A-E). Consequently, DCA does not improve ATP production rates (Fig 5.6F).

5.3.1.3.3 Reperfusion metabolic efficiency

Hearts reperfused in the absence or presence of DCA exhibit similar patterns of metabolic rates when expressed per unit LV work (Fig 5.7A-E). DCA fails to increase the rate of glucose oxidation (Fig 5.7B) so the proton production rate is not reduced during reperfusion and remains comparable to untreated hearts (Fig 5.7C). Similarly, rates of fatty acid oxidation and lactate oxidation are not altered in the DCA-treated group. Thus, DCA-treated hearts show the same pattern of significant deterioration of metabolic efficiency at reperfusion as untreated hearts (Fig 5.7F).

5.3.1.4 Effect of absence of lactate on response to DCA treatment of healthy hearts

In order to determine if the unexpected failure of DCA to affect rates of glucose oxidation might be due to the presence of lactate, a competing substrate, we also studied the effects of DCA in hearts perfused in the absence of lactate. Comparison of values obtained in normal hearts that were perfused aerobically with or without lactate (1.5mM) indicates that the absence of lactate does not affect aerobic LV work (Fig 5.8A-B) or *ex vivo* hemodynamic parameters (Table 5.4).

Glycolytic rates (Fig 5.8C), glucose oxidation rates (Fig 5.8D) and proton production rates (Fig 5.8E) are similar for hearts perfused in the presence or absence of lactate. Furthermore, DCA does not affect glycolytic rates regardless of the presence of lactate (Fig 5.8C). However, in the absence of lactate, DCA stimulates glucose oxidation (Fig 5.8D), but the presence of lactate prevents DCA-induced stimulation of glucose oxidation (Fig 5.8D). Nevertheless, DCA

has no effect on the rate of proton production regardless of the presence of lactate (Fig 5.8E).

5.3.2 Treatment with MCDi during aerobic perfusion

5.3.2.1 LV function:

Confirming our previous results, compared to SHAM, CAL hearts have impaired *ex vivo* LV function. Average LV work during aerobic perfusion (Joule/min/g dry wt) is 30% lower than SHAM hearts and confirms *in vivo* findings (Fig 5.9A-B). See Table 5.5 for detailed *ex vivo* hemodynamic parameters. MCDi does not alter LV function in either CAL or SHAM hearts (Fig 5.9A-B).

5.3.2.2 Metabolic rates:

In SHAM hearts, MCDi increases the glycolytic rate (Fig 5.10A) and the rate of glucose oxidation (Fig 5.10B). Consequently, the rate of proton production is accelerated by MCDi (Fig 5.10C). As expected, MCDi significantly decreases the rate of fatty acid oxidation (Fig 5.10D). In marked contrast to SHAM hearts, treatment of CAL hearts with MCDi has no effect on rates of glucose or palmitate metabolism.

Lactate oxidation rates are similar in SHAM and CAL hearts and these rates are not altered by MCDi (Fig 5.10E).

5.3.2.3 Malonyl CoA content:

MCDi-treated SHAM hearts exhibit a trend towards increased malonyl CoA content (P=0.10 Fig 5.11) that was not associated with inhibition of fatty acid oxidation. Treated CAL hearts exhibit a significant increase in malonyl CoA content. However, this did not result in inhibition of fatty acid oxidation.

5.4 Discussion

5.4.1 Response to DCA during reperfusion

A major finding of this study is that 1.5 mM DCA, when present during reperfusion does not improve recovery of mechanical function of CAL, SHAM or normal healthy hearts. In addition, the presence of 1.5 mM DCA during reperfusion does not alter rates of energy substrate metabolism in CAL, SHAM or normal healthy hearts during post-ischemic reperfusion. However, DCA (1.5 mM) does stimulate glucose oxidation in normal hearts perfused aerobically in the absence of lactate but this effect does not translate into inhibition of proton production or to improved mechanical function.

There are many studies that address the beneficial effect of DCA in reducing IR-induced mechanical dysfunction and deterioration of cardiac efficiency [320, 367, 417-419]. However, the benefit of DCA in the treatment of human cardiac dysfunction such as heart failure has been a controversial issue. Some studies have reported a benefit of DCA in improving exercise tolerance [420, 421], hemodynamic function and mechanical efficiency in heart failure patients [426] while others have found no benefit of DCA in improving exercise

tolerance [427] or LV function [428]. However, the potential benefit of DCA for alleviation of IR-induced LV dysfunction in post-infarction remodeled hearts has not been addressed.

The demonstrations that CAL hearts develop systolic and diastolic dysfunction as shown by echocardiographic evaluation and LV dysfunction during *ex vivo* aerobic perfusion confirm our previous data [221] and indicates that our model is a successful model of post-infarction heart failure. The finding that aerobically-perfused CAL hearts maintain similar metabolic rates to SHAM hearts and that the reduced ATP production rate cannot explain the LV dysfunction also confirms our previous conclusion that CAL hearts are not energetically starved, but are metabolically inefficient. Moreover, the finding that reperfused CAL hearts exhibit no further deterioration of LV function of metabolic efficiency as compared to the significant deterioration of reperfused SHAM heart LV function and metabolic efficiency confirms our previous finding of maintained metabolic efficiency and a better functional recovery of CAL hearts during reperfusion.

In this section, the effects of DCA, when given at reperfusion, have been examined in CAL, SHAM and normal healthy hearts. The demonstration that DCA at reperfusion fails to improve recovery of mechanical function or to change rates of energy substrate metabolism in reperfused CAL, SHAM and normal healthy hearts indicates that the expected stimulation of glucose oxidation did not occur. Instead, CAL hearts reperfused in the presence of DCA have the worst

percent recovery and experience a significant decrease in their metabolic efficiency.

5.4.1.1 Contribution of the chemical composition of the perfusate to the sensitivity of mouse hearts to DCA

One possible explanation for the finding that DCA does not stimulate glucose oxidation in perfused mouse hearts is the chemical composition of the heart perfusate. The standard perfusate used in all experiments described so far in this thesis contains 1 mM lactate. The use of lactate in our model is based on the fact that lactate is an important energy substrate that is normally present *in vivo* and that is expected to increase in conditions of IR injury [429]. Moreover, the presence of lactate in the perfusate is important for accurate assessment of metabolic rates of an energy substrate other than glucose or palmitate [430]. Clearly, the chemical composition and the type of energy substrate provided in the perfusate may affect measured metabolic rates due to intra-substrate competition. An example of this is the ability of increased fatty acid oxidation to inhibit glucose oxidation and *vice versa* (Randle cycle - Fig 1.1). Similarly, reported glucose oxidation rates in rat hearts in the presence of lactate are less than those reported in the absence of lactate perhaps due to the feeding of lactate-derived pyruvate into the TCA cycle which reduces the glucose-derived pyruvate incorporation into the TCA cycle. Interestingly, it was reported that the presence of 1 mM lactate in the perfusate doubles fatty acid oxidation rates in isolated perfused rat hearts [430].

In contrast to the standard perfusion condition used in this thesis (1 mM lactate), many of the published reports on DCA-mediated acceleration of glucose oxidation have utilized perfusates that lack lactate [431-434] or used smaller concentration of lactate (0.5 mM) [436-438]. Thus, it is possible that lactate in the perfusate may have reduced the sensitivity of the hearts to the stimulatory effect of DCA on glucose oxidation. Indeed, a report from White *et al* indicates that addition of lactate (2.5 mM) to reperfused normal rabbit hearts prevents the functional benefits of DCA (5 mM) as compared to hearts perfused with a solution supplemented with pyruvate [435]. Those authors concluded that the presence of lactate at reperfusion limits the functional benefits of DCA-induced stimulation of PDH [435]. Similar findings were reported by Griffin *et al* 2000 [358] where post-ischemic rabbit hearts were reperfused with 5 mM DCA in presence of glucose (5 mM), pyruvate (2.5 mM) or lactate (2.5 mM). The presence of lactate yielded the least functional recovery and a delayed recovery of intracellular pH. Alternatively, the stimulation of pyruvate oxidation in their preparation may be due to the use of a higher DCA concentration (5 mM), as compared to the 1.5 mM used in this study.

To study the possibility that the presence of 1 mM lactate in our preparation could be contributing to the lack of benefit of DCA treatment at reperfusion, we treated aerobically perfused normal healthy mouse hearts with 1.5 mM DCA in the presence or absence of 1 mM lactate. The demonstration that DCA stimulates glucose oxidation in the absence of lactate confirms our hypothesis. The demonstration that DCA-induced stimulation of glucose

oxidation does not translate into an inhibition of proton production or functional benefit is possibly because only small changes in glucose oxidation are elicited by the relatively low concentration of DCA. Also, these hearts were perfused in aerobic mode. Further challenge with *ex vivo* IR that exacerbates the mismatch in glucose metabolism, as well as higher concentrations of DCA may be needed to illustrate the functional benefit of stimulating glucose oxidation and restoration of a better matched state of glucose metabolism.

5.4.1.2 Species-dependent difference in the sensitivity to DCA

The finding that DCA is able to improve cardiac efficiency [436] as well as improve functional recovery in rat hearts [437] and newborn (6 weeks) rabbit hearts [438] after IR in presence of lower concentrations of lactate (0.5 mM) indicate the possibility of species-dependent response to DCA.

One major difference in mouse heart is that PDH seems to be working at maximal activity and therefore there is no potential for further stimulation. Rat heart studies report glucose oxidation rates between 0.2-0.8 $\mu\text{mol/g dry wt/ min}$, depending on glucose concentration (5 to 11 mM) and palmitate concentration (0.4 to 1.2 mM) [318, 329, 439-443]. In the experiments reported in this thesis, glucose oxidation rates for mouse hearts perfused under similar conditions (1.2 mM palmitate and 11 mM glucose) were 2-3 $\mu\text{mol/g dry wt/ min}$ [221], values similar to those reported earlier for mouse hearts perfused with (glucose 5-11 mM and palmitate 0.4 - 1.2 mM) [244, 322, 444]. The higher baseline glucose oxidation rates in mouse hearts indicate a state of higher activity of PDH that may

be close to maximal and so less able to respond with further increases in response to treatment with DCA (1.5 mM). Measurements of PDH activity in rat and mouse hearts perfused with a range of DCA concentrations would be a useful approach to test for this possibility.

Another possible explanation of the higher baseline glucose oxidation rates in mouse hearts as compared to rat hearts is that higher baseline glycolytic rates in mouse heart supply more pyruvate as substrate for oxidative metabolism. Rates of glycolysis reported for aerobically perfused rat hearts range from 1.5 to 5 $\mu\text{mol/g dry wt/ min}$ [318, 329, 439-443]. In contrast, glycolytic rates in mouse hearts are significantly greater. Values reported in this thesis range from 13 to 25 $\mu\text{mol/g dry wt/ min}$ depending on perfusion conditions and are similar to values reported for mouse hearts by other authors (11-20 $\mu\text{mol/g dry wt/ min}$) [244, 322, 444]. Thus, higher baseline PDH activity in mouse heart might be an adaptive response of PDH to match the higher availability of pyruvate supplied through glycolysis and thereby minimize the consequences of the mismatch in glucose metabolism.

5.4.2 Response to aerobic MCD inhibition

A major finding of this part of the study is that despite acute *ex vivo* MCD inhibition in CAL and SHAM hearts, as indicated by increased malonyl CoA content in CAL and a trending increase of malonyl CoA in SHAM hearts, only SHAM hearts exhibit an inhibition of fatty acid oxidation rate, and this is accompanied by an increase in glucose oxidation (Randle cycle). However, due to a concomitant increase in the glycolytic rate in SHAM hearts, as compared to

CAL hearts, this MCDi-mediated increase in glucose oxidation does not translate into an improvement in the matching of glucose metabolism. Indeed, proton production rates are higher in the MCDi-treated SHAM hearts. Despite this, LV function in untreated and treated SHAM hearts is similar. In contrast, MCDi-treated CAL hearts do not exhibit an inhibition of fatty acid oxidation rates and maintained LV function that is comparable to untreated CAL hearts.

It has been shown previously that an increased dependence on fatty acid which is a less efficient energy substrate than glucose, contributes to the development of cardiomyopathy in diabetes and obesity [21, 397, 445]. We have also shown in Chapters 4 and Chapter 5 that post-ischemic reperfused SHAM hearts exhibit a significant increase in fatty acid oxidation rate that is associated with deterioration of LV function as compared to their pre-ischemic aerobic values. These findings highlight the potential importance of inhibiting fatty acid oxidation as an approach to reduce cardiac dysfunction in heart failure.

Several approaches have been proposed to inhibit fatty acid oxidation in heart failure (reviewed in [21, 140]). Among these approaches, MCD inhibition is an evolving and promising approach for protection against acute IR and functional consequences of post-ischemic remodeling. Data presented in Chapter 3 indicate that chronic MCD deficiency reduces post-ischemic LV dysfunction and improves metabolic efficiency. A similar report from Dyck *et al* [96] highlights the cardioprotective effect of chronic MCD deficiency against acute IR injury. However, it can be argued that these experimental scenarios do not mimic the real-life situations where the pharmacologic intervention is normally initiated

after the ischemic insult. In this regard, MCD inhibition is also reported to be protective when initiated after the ischemic injury [60]. A recent report by Wu et al [60] indicates that chronic *in vivo* cardiac-specific inhibition of MCD via microRNA intervention initiated after CAL surgery in rats limits functional deterioration and maintains energy stores. Hence, we studied the possibility of improvement of metabolic inefficiency in remodeled hearts via acute *ex vivo* MCD inhibition using CMB-0000382.

The demonstration that CMB-0000382 increases malonyl CoA content in CAL and SHAM (a trend) hearts suggests inhibition of MCD in both groups. The demonstration that fatty acid oxidation rates are inhibited only in treated SHAM, but not CAL hearts indicates that other regulators of fatty acid oxidation might have been upregulated in association with the remodeling process in CAL hearts. The finding that malonyl CoA content is increased in MCDi-treated CAL hearts excludes the possibility that a compensatory downregulation of acetyl CoA carboxylase (ACC2) [446], that produces malonyl CoA, may have contributed to the observed lack of fatty acid oxidation inhibition. However, other regulators of fatty acid oxidation may have been up-regulated in CAL hearts that prevent a response to MCD inhibition. These data are in accordance with the previous report of Dyck *et al* [96] where the lack of inhibition of fatty acid oxidation in MCD-KO hearts under aerobic perfusion conditions was suggested, but not tested, to be due to upregulation of other regulators of fatty acid oxidation such as CPT1, CD36, PDK₄ and PPAR α .

Another explanation for the lack of fatty acid oxidation inhibition in MCDi-treated CAL hearts, despite malonyl CoA accumulation, is the possibility of compartmentalization of malonyl CoA so that its concentration in the vicinity of its effector; CPT1 at the outer mitochondrial membrane is not sufficient to exert its inhibitory action leading to an unaltered fatty acid oxidation rate. In this regard, basal malonyl CoA levels in whole tissue were reported to be higher than the inhibitory concentration for CPT1 [447], suggesting compartmentalization of cardiac malonyl CoA [97]. Thus, it is possible that malonyl CoA levels in the vicinity of CPT1 could undergo changes sufficient to affect CPT1 activity accordingly. This possibility can explain the finding that a moderate increase in malonyl CoA concentrations (20% of control) in human skeletal muscles leads to a significant reduction of fatty acid oxidation (41% of control) [68]. Confirming our results, Zordoky *et al* [91] reported that accumulation of malonyl CoA in post-ischemic and high work-load perfused hearts, secondary to lack of AMPK-mediated inhibitory phosphorylation of the key regulatory enzyme ACC, is not associated with any change in the rate of fatty acid oxidation. This is indicative of possible compartmentalization of malonyl CoA as well as involvement of other regulatory mechanisms potentially including the energy demand of the hearts in the regulation of fatty acid oxidation [91].

The apparent discrepancy between the impact of MCD inhibition on glycolysis in chronic and acute settings can be explained on basis of the demand for energy which, in turn, is influenced by the metabolic efficiency status. In our MCD-KO CAL heart model, where metabolic efficiency is, in fact, improved,

MCD inhibition is associated with reduction of glycolytic rates and glucose oxidation rates with less functional deterioration following CAL surgery. Hence, there is less need for a compensatory increase in the metabolic rates of other energy substrates (Chapter 3). This is not the condition in acute *ex vivo* MCD inhibition where a compensatory increase in glycolytic flux is noted in MCDi-treated SHAM hearts (Chapter 5).

One limitation of this study is the short-term acute *ex vivo* exposure of the hearts to MCD inhibition. It remains a possibility that that chronic *in vivo* post-ischemic initiation of MCD inhibition would be more effective since it is present during the time-dependent and evolving remodeling process. This assumption is supported by our findings in Chapter 3 where chronic MCD deficiency in MCD-KO mice was associated with less functional deterioration and less metabolic inefficiency following CAL surgery. Similarly, the protective effect of post-surgical MCD inhibition via microRNA treatment of CAL rats [60] suggests the potential for a more effective response to chronic post-surgical pharmacologic MCD inhibition.

5.5 Conclusion

In conclusion, the sensitivity to DCA in mouse hearts is influenced by the chemical composition of the perfusate. In addition, mouse-specific differences in the baseline contribution of the various energy substrates to overall ATP production (higher dependence on glycolysis, less contribution of fatty acid oxidation to overall ATP production) may influence the pharmacologic response

and/or sensitivity to DCA and may explain the marked differences from the more extensively studied rat heart. Further studies are needed to study whether DCA can improve the matching in glucose metabolism using either higher DCA doses or lactate-free perfusate. Similarly, more studies are needed to understand why CAL hearts exhibit a significant deterioration of post-ischemic function in the presence of DCA. Also, more studies are needed to understand the mechanism of lactate-induced reduction of sensitivity to DCA action.

Similarly, further studies are needed to understand the regulation of fatty acid metabolism in CAL hearts. This is expected to help an understanding of the mechanisms underlying the differences in the response of chronically remodeled hearts to MCD inhibition from healthy hearts where MCD inhibition improves post-ischemic LV function [60, 61, 66, 96, 140, 176].

Figure 5.1 *In vivo* echocardiographic assessment of LV function in SHAM and CAL hearts.

Panel A shows a parasternal long axis view of a SHAM heart. Panel B shows a parasternal long axis view of a CAL heart. Notice the dilatation of the LV. Panel C shows an m-mode capture of a SHAM heart. Panel D shows an m-Mode capture of a CAL heart. Notice the increased LV volume (panel B) and reduced wall motion (panel D) in CAL hearts as compared to SHAM hearts (panels A & C).

Figure 5.1

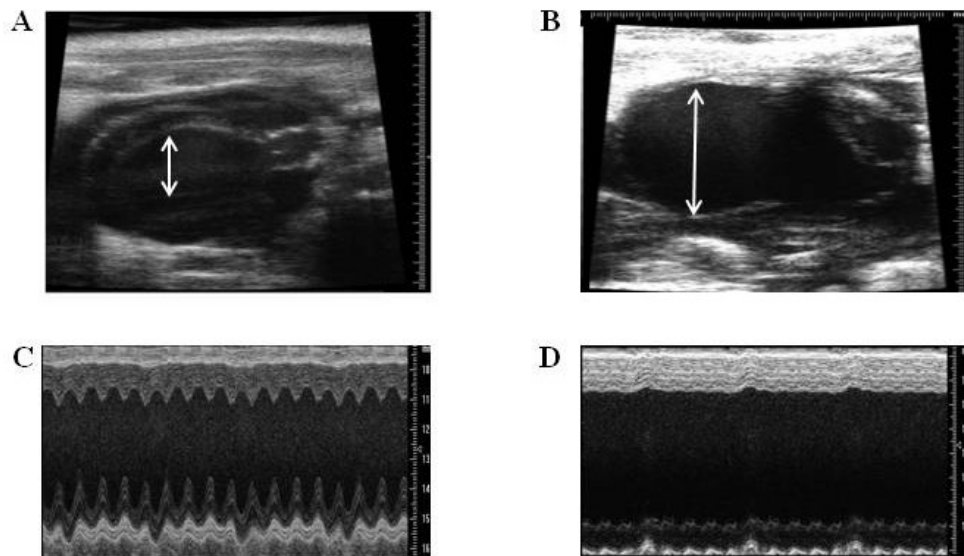


Figure 5.2 *Ex vivo* assessment of LV mechanical function of SHAM and CAL hearts.

Panel A shows time-dependent changes in LV work and Panel B shows average LV work for SHAM (N=37) and CAL (N=26) hearts during aerobic perfusion, global ischemia and reperfusion. Panel C shows % recovery of mechanical function during reperfusion. * refers to a significant difference ($P < 0.05$) from aerobic SHAM parameters. Data are expressed as means \pm SEM.

Figure 5.2

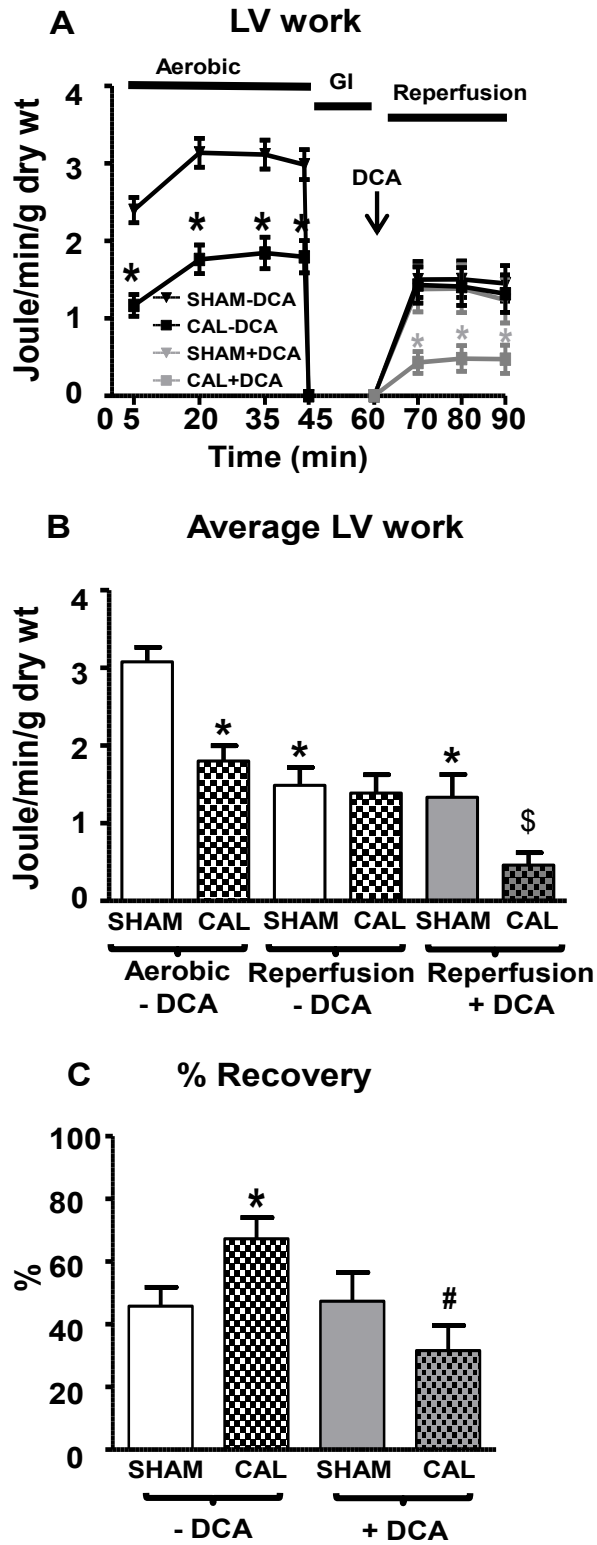


Figure 5.3 Rates of energy substrate metabolism in SHAM and CAL hearts.

Glycolysis, glucose oxidation and calculated proton production are shown in panels A-C (SHAM N=16 (12 without DCA and 6 with DCA at reperfusion), CAL N=13 (8 without DCA and 5 with DCA at reperfusion)). Fatty acid oxidation (panel D, SHAM N=19 (13 without DCA and 6 with DCA at reperfusion), CAL N=13 (7 with DCA and 6 without DCA at reperfusion) and lactate oxidation (panel E, SHAM N=19 (13 without DCA and 6 with DCA at reperfusion), CAL N=13 (7 with DCA and 6 without DCA at reperfusion) are also shown. Calculated ATP production rates are shown in panel F. Since data are not normally distributed, data are presented as median \pm interquartile range (5% and 95%). Differences are considered significant when $P < 0.05$. * refers to a significant difference from untreated aerobic SHAM values.

Figure 5.3

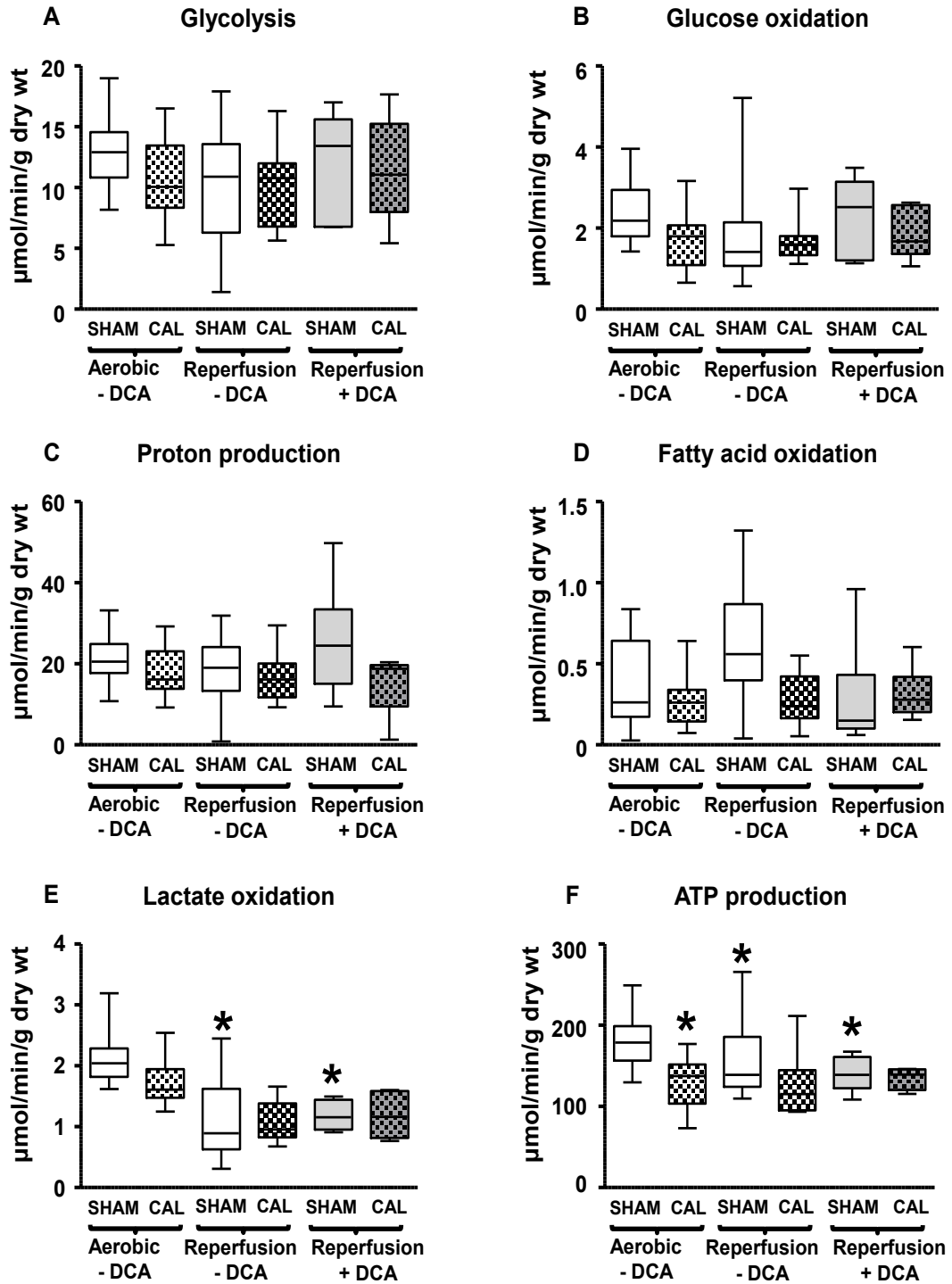


Figure 5.4 Metabolic rates per LV work of SHAM and CAL hearts.

Glycolysis, glucose oxidation and calculated proton production are shown in panels A-C (SHAM N=16 (12 without DCA and 6 with DCA at reperfusion), CAL N=13 (8 without DCA and 5 with DCA at reperfusion)). Fatty acid oxidation (panel D, SHAM N=19 (13 without DCA and 6 with DCA at reperfusion), CAL N=13 (7 with DCA and 6 without DCA at reperfusion) and lactate oxidation (panel E, SHAM N=19 (13 without DCA and 6 with DCA at reperfusion), CAL N=13 (7 with DCA and 6 without DCA at reperfusion) are also shown. Calculated metabolic efficiencies are shown in panel F. Since data are not normally distributed, data are presented as median \pm interquartile range (5% and 95%). Differences are considered significant when $P < 0.05$. (*) refers to a significant difference from aerobic SHAM values. # refers to a significant difference from untreated aerobic CAL values.

Figure 5.4

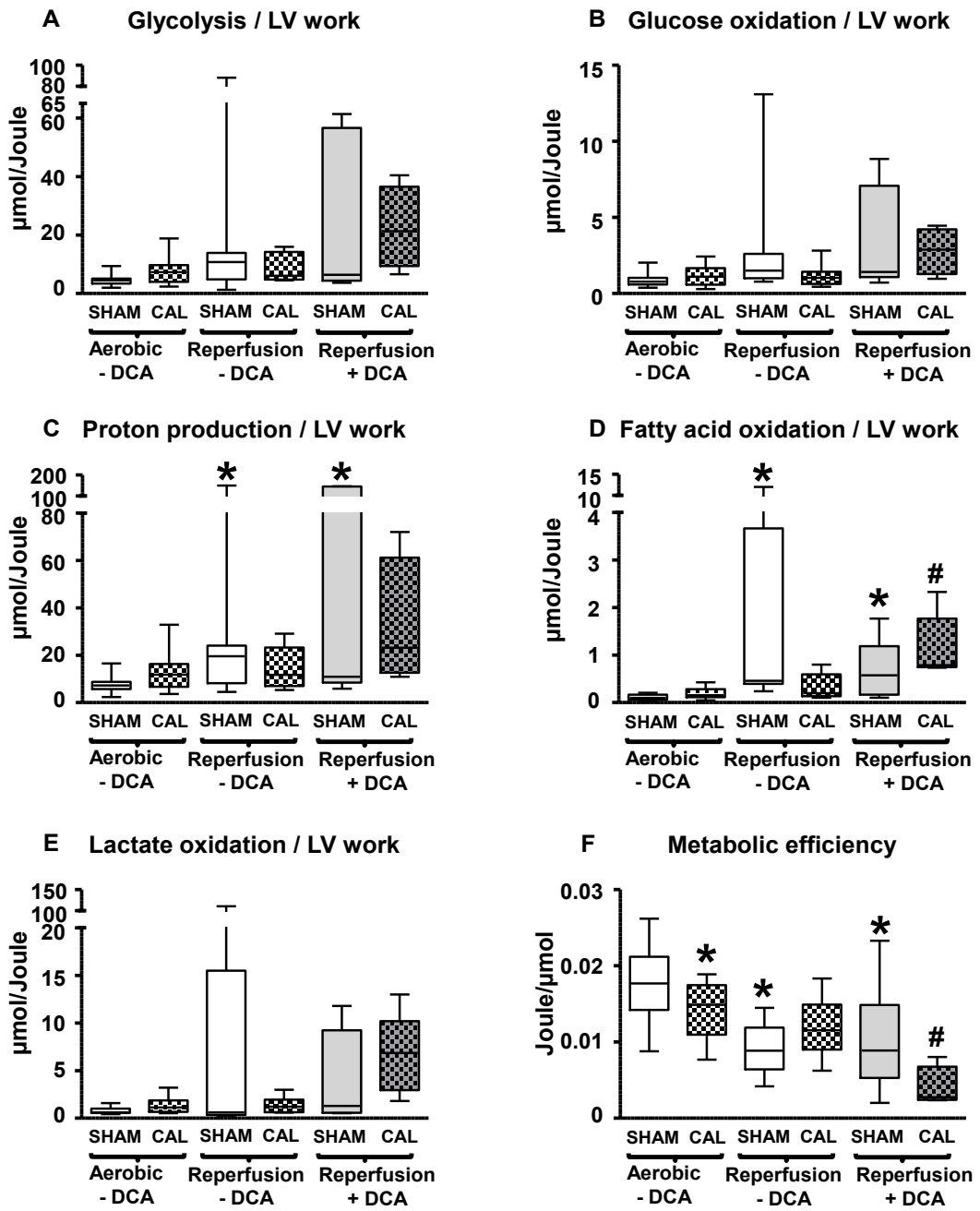


Figure 5.5 *Ex vivo* assessment of LV mechanical function of normal healthy hearts.

Panel A shows time-dependent changes in LV work and Panel B shows average LV work for normal hearts (Aerobic (N=28), reperfusion without DCA (N=17) and reperfusion with DCA (1.5mM, N=11)). Panel C shows % recovery of mechanical function during reperfusion. * refers to a significant difference (P<0.05) from untreated aerobic SHAM hearts. Data are expressed as means ± SEM.

Figure 5.5

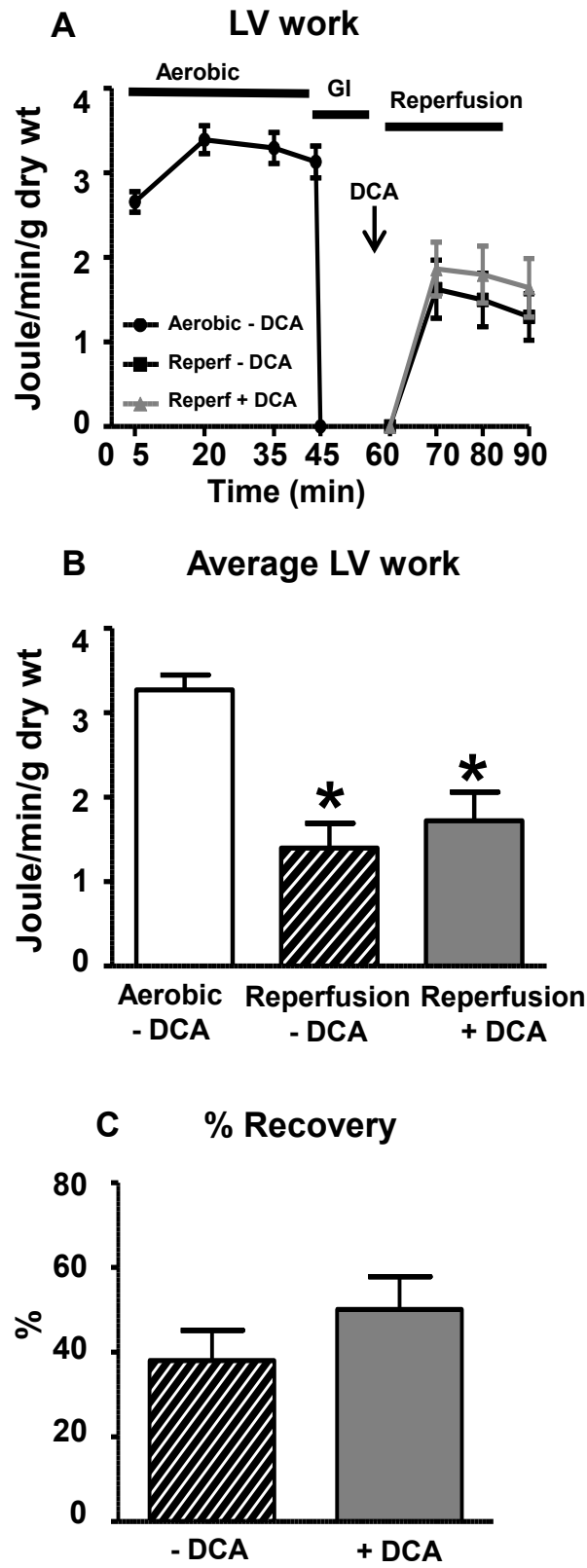


Figure 5.6 Rates of energy substrate metabolism in unremodeled hearts treated with DCA at reperfusion.

Glycolysis, glucose oxidation and calculated proton production are shown in panels A-C (Aerobic, N=14 (8 without DCA and 6 with DCA at reperfusion)). Fatty acid oxidation (panel D, aerobic N=12 (7 without DCA and 5 with DCA at reperfusion) and lactate oxidation (panel E, aerobic, N=14 (9 without DCA and 5 with DCA at reperfusion) are also shown. Calculated ATP production rates are shown in panel F. Since data are not normally distributed, data are presented as median \pm interquartile range (5% and 95%). Differences are considered significant when $P < 0.05$. * refers to a significant difference from aerobic values.

Figure 5.6

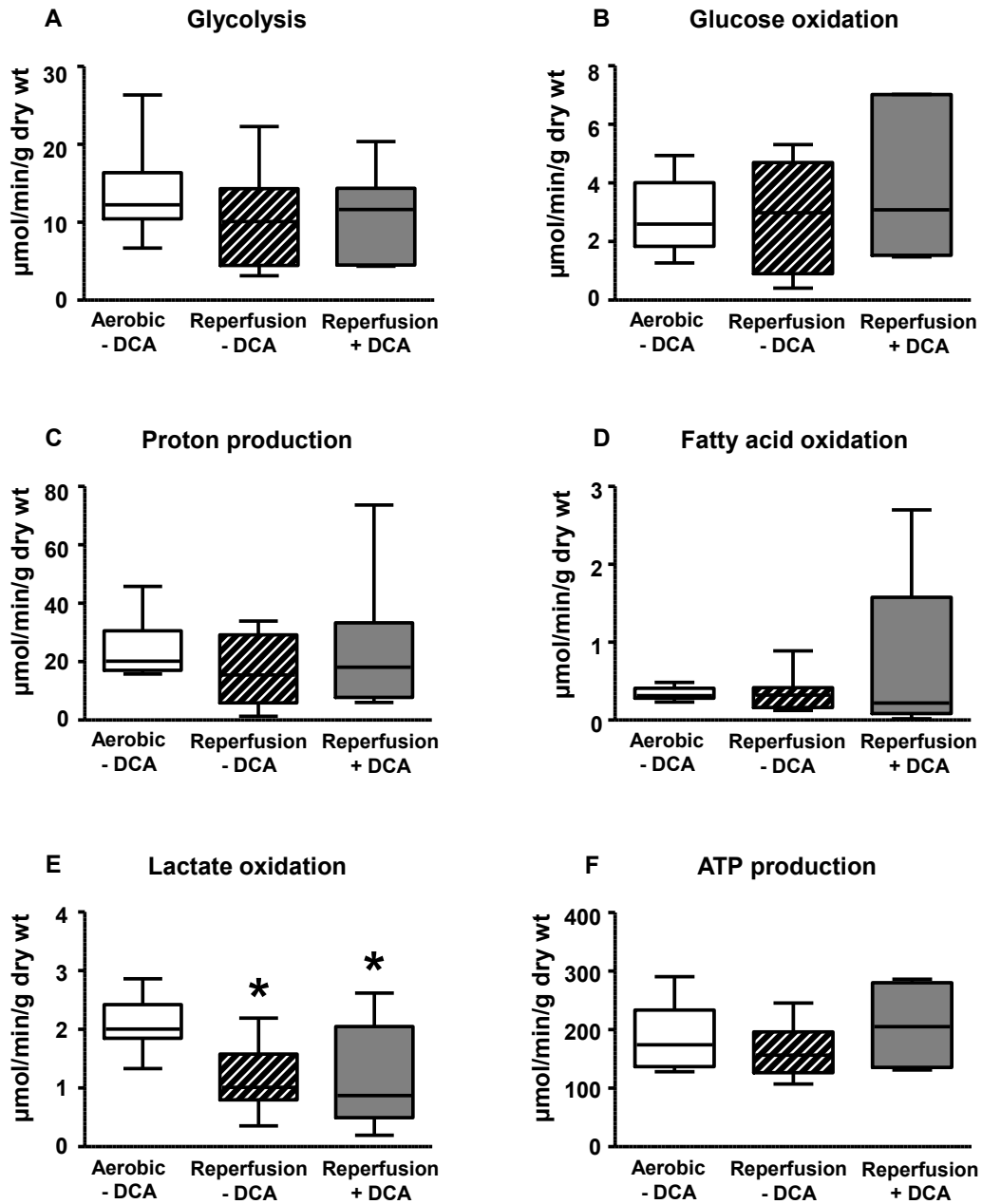


Figure 5.7 Rates of energy substrate metabolism per LV work in normal healthy hearts.

Glycolysis, glucose oxidation and calculated proton production are shown in panels A-C (Aerobic, N=14 (8 without DCA and 6 with DCA at reperfusion)). Fatty acid oxidation (panel D, aerobic N=12 (7 without DCA and 5 with DCA at reperfusion) and lactate oxidation (panel E, aerobic, N=14 (9 without DCA and 5 with DCA at reperfusion) are also shown. Calculated metabolic efficiencies are shown in panel F. Since data are not normally distributed, data are presented as median \pm interquartile range (5% and 95%). Differences are considered significant when $P < 0.05$. * refers to a significant difference from aerobic values.

Figure 5.7

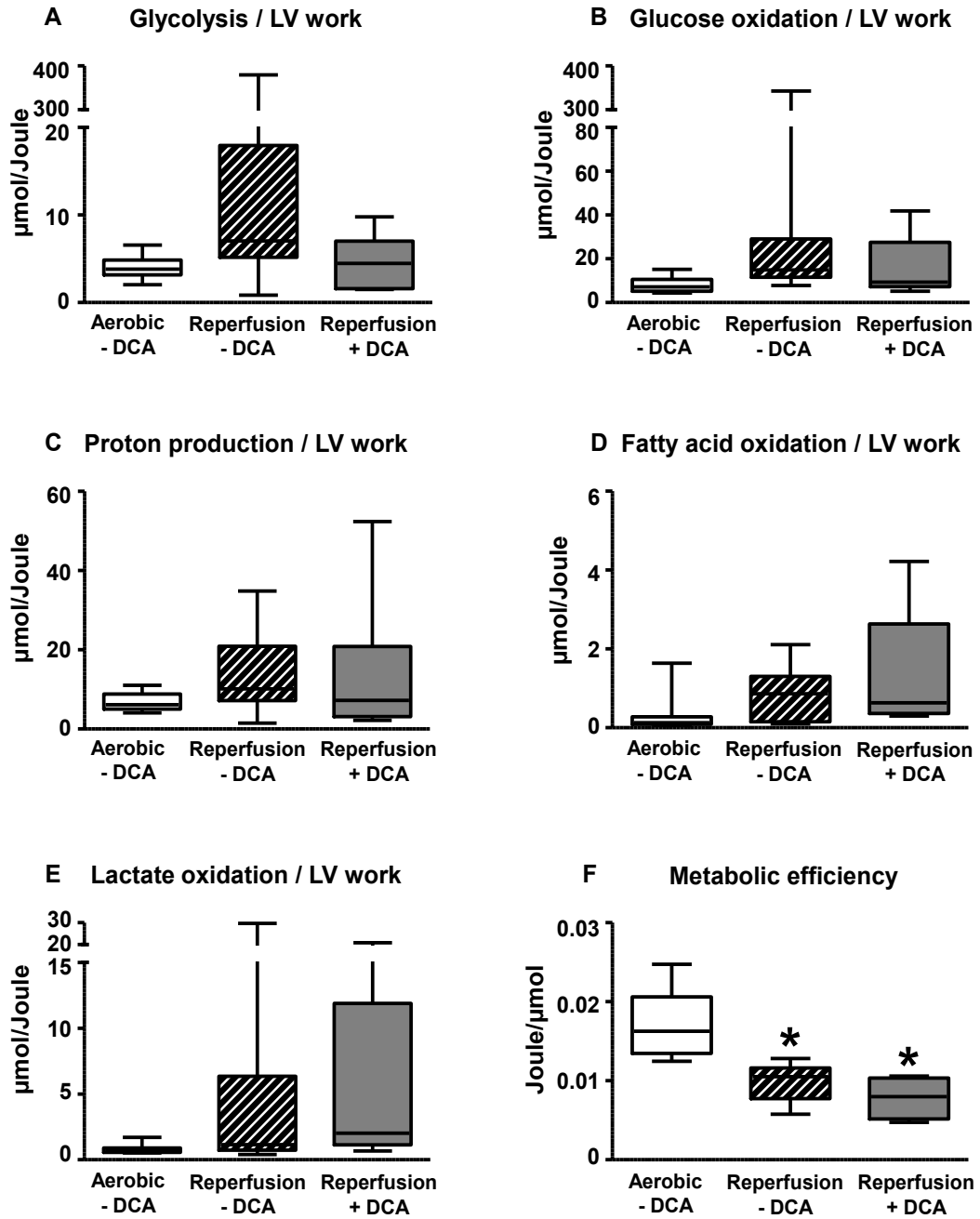


Figure 5.8 *Ex vivo* assessment of LV mechanical function and metabolic rates of aerobically-perfused normal healthy hearts: Effect of DCA in presence or absence of lactate

Panel A shows time-dependent changes in LV work and Panel B shows average LV work for normal hearts (5 with lactate and 6 without lactate). Glycolysis, glucose oxidation and proton production rates are shown in panels C-E (5 with lactate and 6 without lactate). Since data are normally distributed, they are expressed as means \pm SEM. (*) refers to a significant difference from aerobic counterpart values.

Figure 5.8

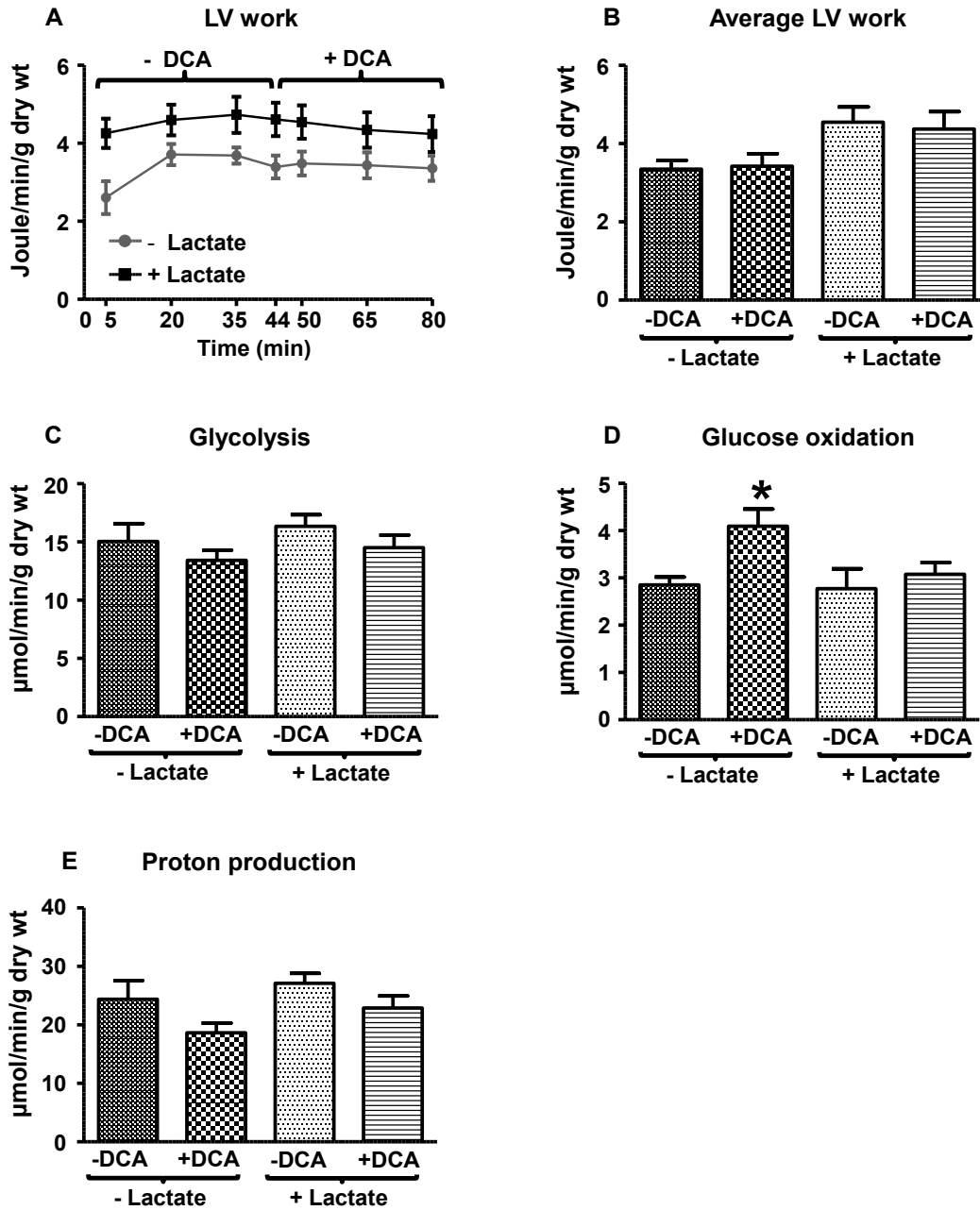
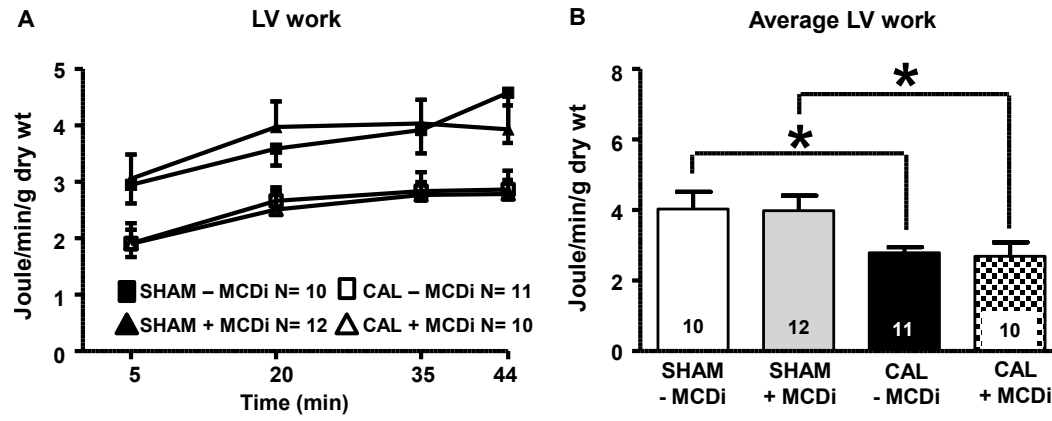


Figure 5.9 *Ex vivo* assessment of LV mechanical function of aerobically-perfused CAL and SHAM hearts: Effect of MCDi.

Panel A shows time-dependent changes in LV work and Panel B shows average LV work for SHAM hearts (10 without MCDi and 12 with MCDi) and CAL hearts (11 without MCDi and 10 with MCDi). Data are normally distributed and are expressed as means \pm SEM. (*) refers to a significant difference.

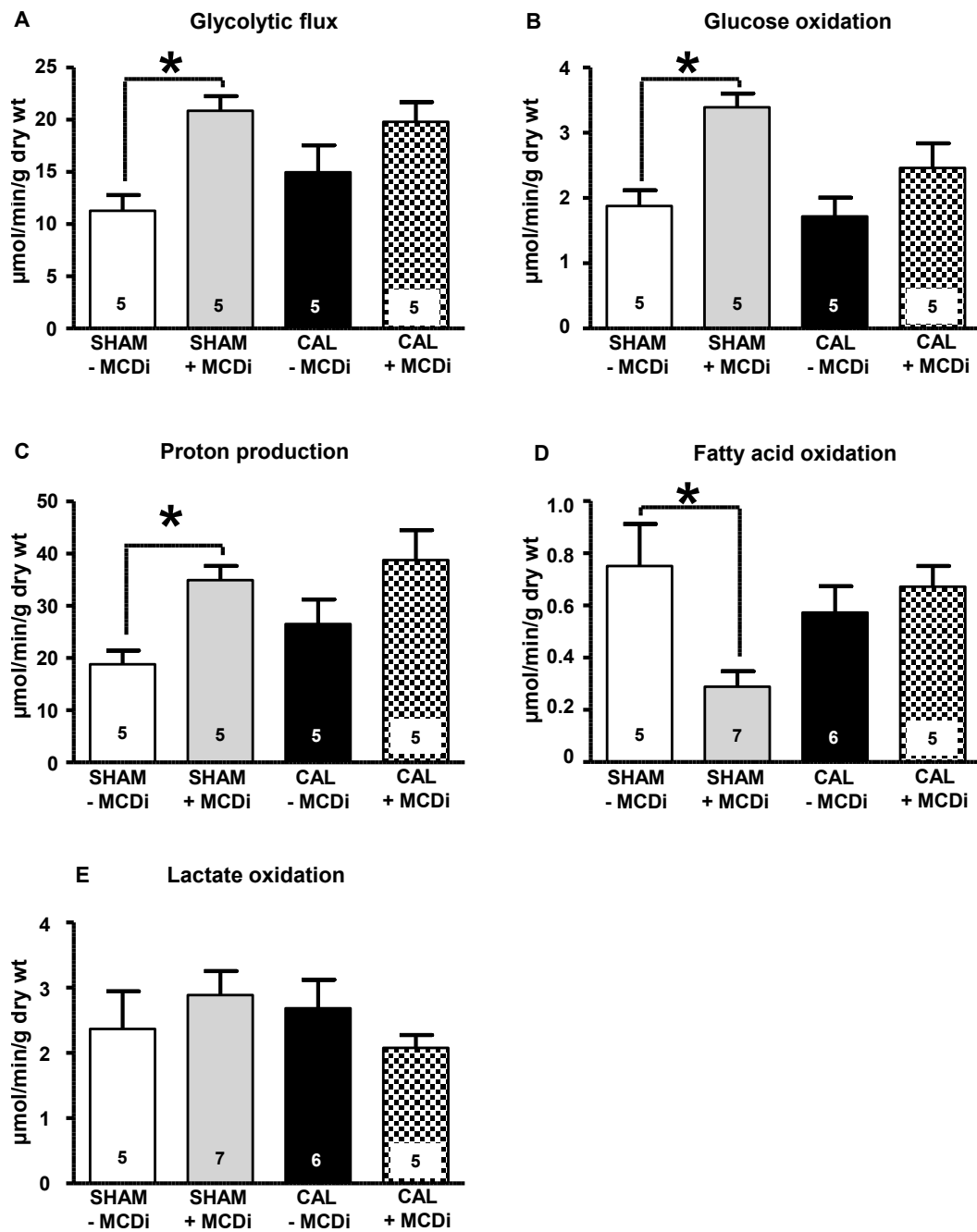
Figure 5.9



5.10 Rates of energy substrate metabolism in SHAM and CAL hearts: Effect of MCDi.

Glycolysis, glucose oxidation and calculated proton production rates are shown in panels A-C (SHAM, N=10 (5 without MCDi and 5 with 50 μ M MCDi) and CAL, N=10 (5 without MCDi and 5 with 50 μ M MCDi). Fatty acid oxidation and lactate oxidation (panels D and E, SHAM N=12 (5 without MCDi and 7 with 50 μ M MCDi and CAL N=11 (5 without MCDi and 7 with 50 μ M MCDi)) are also shown. Since data are normally distributed, data are presented as mean \pm SEM. Differences are considered significant when $P < 0.05$. (*) refers to a significant difference.

Figure 5.10



5.11 Change in cardiac malonyl CoA content in SHAM and CAL hearts: Effect of MCDi.

Cardiac malonyl CoA contents of SHAM, N=8 (4 without MCDi and 4 with MCDi) and CAL hearts, N=8 (4 without MCDi and 4 with MCDi). Data are normally distributed and are presented as mean \pm SEM. One way ANOVA was used. Differences are considered significant when $P < 0.05$. (*) refers to a significant difference.

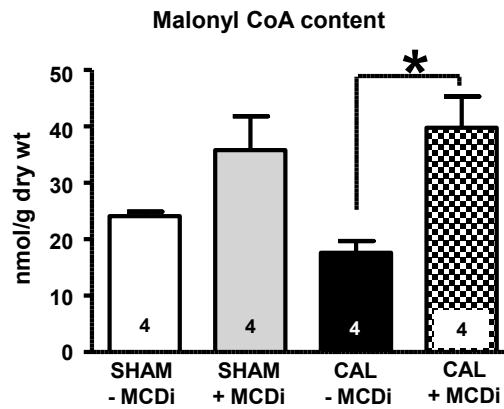


Table 5.1 *In vivo* echocardiographic assessment of function of SHAM and CAL hearts.

Detailed echocardiographic parameters are shown for both SHAM (n=6) and CAL (n=10) hearts. * refers to a statistically significant difference (P<0.05). Data are presented as means \pm SEM. **Abbreviations:** LV = left ventricular, LVID = LV internal dimension, LVPW = LV posterior wall thickness, IVS = interventricular septal thickness, EF = ejection fraction, FAC = fraction area change, IVRT = isovolumetric relaxation time, IVCT = isovolumetric contraction time, MVDT = mitral valve deceleration time.

Table 5.1

Parameter (unit)	SHAM (N)	CAL (N)
<u>M-mode measures:</u>		
Heart rate (beats/min)	449±20 (6)	454±11 (10)
Cardiac output (mL/min)	17.59±1.63 (6)	16.14±0.89 (10)
EF (%)	53.24±1.18 (6)	27.34±2.21 (10)*
FS (%)	28.65±2.04 (6)	15.60±1.57 (11)*
<u>Wall measurements:</u>		
LV systolic volume (μL)	36±5 (6)	131± 22 (8)*
LV diastolic volume (μL)	78±6 (6)	188±26 (8)*
LVIDs (mm)	2.99±0.18 (6)	5.12±0.37 (8)*
LVIDd (mm)	4.16±0.14 (6)	6.04±0.35 (8)*
LVPWs (mm)	1.10±0.04 (6)	1.25±0.17 (8)
LVPWd (mm)	0.77±0.03 (6)	0.93±0.10 (8)
IVSs (mm)	1.12±0.03 (6)	1.18±0.18 (4)
IVSd (mm)	0.79±0.02 (6)	0.84±0.09 (4)
Corrected LV mass (mg)	97±5 (6)	168±22 (4)*
<u>Tissue doppler data:</u>		
IVCT (ms)	16.65±1.04 (6)	26.88±2.41 (10)*
Tei index (ratio)	0.74±0.04 (6)	1.24±0.10 (10)*
E	777±96 (6)	712±186 (8)
E'	33.7±10 (6)	23.7± 3.4 (8)
		P=0.07
A	449±135 (6)	260±187 (8)
		P=0.07
E/E' (ratio)	24.39±2.73 (6)	32.57±4.09 (8)
E/A (ratio)	1.81±0.13 (6)	3.82±1.51 (7)
IVRT (ms)	17.53±1.10 (6)	21.90±1.71 (10)
MV DT (ms)	16.18±1.32 (6)	13.65±2.65 (4)

Table 5.2 *Ex vivo* hemodynamic parameters of SHAM and CAL hearts.

Detailed *ex vivo* hemodynamic parameters are shown for SHAM and CAL hearts.

(*) refers to a significant difference ($P<0.05$) from aerobic SHAM parameters. (#)

refers to a significant difference ($P<0.05$) from aerobic CAL parameters. (§) refers

to a significant difference ($P<0.05$) from reperfused CAL - DCA parameters. Data

are expressed as means \pm SEM.

Parameter (unit)	SHAM (N=37)			CAL (N=26)		
	Aerobic	Reperfusion	Reperfusion	Aerobic	Reperfusion	Reperfusion
	N=37	- DCA N=25	+ DCA N=12	N=26	- DCA N=15	+ DCA N=11
Body weight (g)		27.62 \pm 0.30			27.45 \pm 0.31	
Viable heart dry weight (mg)		32 \pm 1			34 \pm 1	
Viable heart dry wet ratio		0.162 \pm 0.004			0.161 \pm 0.006	
Heart rate (bpm)	332 \pm 8	331 \pm 8	287 \pm 15*	300 \pm 12	315 \pm 8	303 \pm 16
Systolic pressure (mmHg)	78 \pm 1	67 \pm 5*	59 \pm 5*	71 \pm 2	68 \pm 4	46 \pm 5 ^{#§}
Diastolic pressure (mmHg)	20 \pm 1	24 \pm 2	26 \pm 3	27 \pm 1*	26 \pm 2	28 \pm 3
Cardiac output (mL/min)	10.0 \pm 0.4	6.1 \pm 0.7*	6.2 \pm 1.0*	6.4 \pm 0.5*	5.4 \pm 0.7	2.6 \pm 0.6 [#]
Aortic flow (mL/min)	7.3 \pm 0.3	3.5 \pm 0.5*	2.2 \pm 0.6*	4.0 \pm 0.4*	3.2 \pm 0.5	0.7 \pm 0.3 ^{#§}
Coronary flow (mL/min)	2.7 \pm 0.2	2.6 \pm 0.4	4.0 \pm 0.9	2.4 \pm 0.3	2.2 \pm 0.3	1.9 \pm 0.4

Table 5.3 *Ex vivo* hemodynamic parameters of normal healthy hearts.

Detailed *ex vivo* hemodynamic parameters are shown for normal healthy control hearts. (*) refers to a significant difference ($P < 0.05$) from aerobic control parameters. Data are expressed as means \pm SEM.

Parameter (unit)	Control (N=28)		
	Aerobic (N=28)	Reperfusion - DCA (N=17)	Reperfusion + DCA (N=11)
Body weight (g)		27.2 \pm 0.5	
Viable heart dry weight (mg)		27.2 \pm 1.2	
Viable heart dry wet ratio		0.172 \pm 0.006	
Heart rate (bpm)	317 \pm 10	304 \pm 17	318 \pm 24
Systolic pressure (mmHg)	80 \pm 2	62 \pm 5*	65 \pm 6*
Diastolic pressure (mmHg)	20 \pm 1	26 \pm 2*	28 \pm 3*
Cardiac output (mL/min)	11.1 \pm 0.6	6.8 \pm 1.1*	7.7 \pm 1.6*
Aortic flow (mL/min)	6.5 \pm 0.5	4.0 \pm 0.8*	5.6 \pm 1.5
Coronary flow (mL/min)	4.7 \pm 0.6	2.8 \pm 0.6*	2.1 \pm 0.6*

Table 5.4 *Ex vivo* hemodynamic parameters of aerobically-perfused normal healthy hearts.

Detailed *ex vivo* hemodynamic parameters are shown for normal healthy control hearts. Since data are normally distributed, they are expressed as means \pm SEM.

Parameter (unit)	- Lactate (N=5)		+ Lactate (N=6)	
	- DCA	+ DCA	- DCA	+ DCA
Body weight (g)	26.9 \pm 1.0		25.8 \pm 0.5	
Viable heart dry weight (mg)	27 \pm 1		25 \pm 1	
Viable heart dry wet ratio	0.141 \pm 0.006		0.143 \pm 0.008	
Heart rate (bpm)	359 \pm 10	360 \pm 12	328 \pm 12	329 \pm 9
Systolic pressure (mmHg)	78 \pm 2	79 \pm 3	86 \pm 3	84 \pm 3
Diastolic pressure (mmHg)	23 \pm 2	26 \pm 2	23 \pm 2	22 \pm 1
Cardiac output (mL/min)	10.1 \pm 0.3	10.1 \pm 0.5	11.5 \pm 0.6	11.3 \pm 0.8
Aortic flow (mL/min)	7.3 \pm 0.4	7.2 \pm 0.6	8.5 \pm 0.4	8.2 \pm 0.5
Coronary flow (mL/min)	2.8 \pm 0.2	2.9 \pm 0.3	3.1 \pm 0.3	3.0 \pm 0.4

Table 5.5 *Ex vivo* hemodynamic parameters of aerobically-perfused SHAM and CAL hearts: Effect of MCDi.

Detailed *ex vivo* hemodynamic parameters are shown for normal healthy hearts.

Since data are normally distributed, they are expressed as means±SEM. (*) refers to a significant difference (P<0.05) from aerobic SHAM - MCDi parameters.

Parameter (unit)	SHAM		CAL	
	- MCDi (N=10)	+ MCDi (N=12)	-MCDi (N=11)	+ MCDi (N=10)
Body weight (g)	27.9±0.6	27.9±0.4	27.5±0.5	28.6±0.7
Viable heart dry weight (mg)	26±1	26±1	28±1	26±1
Viable heart dry wet ratio	0.14±0.01	0.13±0.01	0.15±0.01	0.13±0.01
Heart rate (bpm)	300±24	282±14	289±1	326±9
Systolic pressure (mmHg)	85.7±4.7	83.7±1.4	82.2±3.2	74.1±2.9
Diastolic pressure (mmHg)	15.2±1.6	13.3±1.1	21.6±1.7*	24.6±1.6*
Cardiac output (mL/min)	9.4±0.4	9.7±0.5	7.5±0.4*	6.9±0.7*
Aortic flow (mL/min)	7.4±0.4	7.3±0.3	5.8±0.3*	4.6±0.6*
Coronary flow (mL/min)	1.9±0.2	2.4±0.4	1.7±0.3	2.3±0.4

6 General Discussion and Conclusions

In Canada, cardiovascular disease is a major health problem that results in serious morbidity and mortality. According to a Heart and Stroke Foundation of Canada report in 2014, each year there are 50,000 new heart failure cases diagnosed and 70,000 heart attacks occur [448]. Due to advances in diagnosis and treatments, the numbers of cardiovascular disease survivors are on the rise. In 2013, there were 165,000 Canadian survivors of heart and stroke diseases [448]. This group of patients needs special medical attention which adds more expenses in the health care sector. Earlier statistics from Health Canada indicate that cardiovascular disease represents 11.6% of the total Canadian cost of illness classifiable by diagnostic category. This was estimated to be about \$21.2 billion in direct and indirect annual costs [449]. Thus, it is important to invest in research that aims at discovering new modalities of treatment not only to manage the acute attacks of ischemic heart disease but also to improve the quality of life and performance of the increasingly growing group of cardiovascular disease survivors.

One step to discover new treatments of cardiac diseases is to better understand the nature of changes that occur as the disease evolves and progresses. Currently, it is established that both heart failure and ischemic heart disease are associated with changes in energy substrate metabolism. Yet, there is no agreement on the nature of these changes. However, there are two main themes that attempt to explain the nature of these metabolic changes. One theme considers the failing heart as an engine out of fuel implying reduced rates of energy substrate metabolism and scarcity of resources. The other theme considers

the failing heart an inefficient machine where the available energy resources are inefficiently used for external mechanical work. The first study of this thesis has investigated the nature of metabolic changes in a post-infarction model of heart failure. It also studied the changes of metabolic efficiency which reflects the LV work generated per ATP produced. The second part of that study used a genetic metabolic intervention, MCD deletion, to study the potential of functional improvement through indirect improvement of glucose metabolism.

Since post-infarction heart failure patients are more susceptible to subsequent ischemic attacks, the second study of this thesis addressed the response of remodeled hearts to an *ex vivo* IR insult. Changes in exogenous and endogenous energy substrate metabolism before and during IR injury were studied. This included characterization of the accompanying changes in metabolic efficiency and how they relate to the observed functional responses in remodeled and healthy control hearts.

Finally, the last group of studies in this thesis investigated the potential for improving functional recovery following *ex vivo* ischemic injury using pharmacologic interventions such as DCA. Based on our findings that remodeled hearts are metabolically inefficient due, in part, to mismatched glucose metabolism, DCA, a known stimulator of glucose oxidation, was used to study the potential for improvement of functional recovery by minimizing mismatched glucose metabolism with the resultant reduction of proton production. Since chronic MCD deficiency limits functional deterioration and metabolic inefficiency after CAL surgery, another set of experiments was performed to

study whether MCD is a potential target for acute pharmacologic inhibition to improve metabolic inefficiency in remodeled hearts using an MCDi administered during *ex vivo* aerobic perfusion of remodeled hearts.

This penultimate chapter will discuss the rationale for the methods used in this thesis, justification of their use, advantages over other methods used for the same purpose and potential limitations. It will also discuss the results of the studies described in this thesis and how they fit into the current knowledge and literature, in addition to the main conclusions summarized in each experimental chapter. The discussion will focus on the contribution of the new research findings to our current understanding of the nature of metabolic changes in post-ischemic heart failure and those accompanying exposure of the failing heart to subsequent IR.

6.1 Experimental model and methods

6.1.1 Coronary artery ligation in the mouse

The use of mice in this thesis provided the advantage of the use of genetic interventions such as MCD-KO. In addition, the short life cycle and a more economic cost of care provided an additional advantage. The availability of a research core equipped with tools for *in vivo* functional evaluation and validation of the surgical model made it possible to validate the model *in vivo* before proceeding to the *ex vivo* heart perfusions.

Since the focus of this thesis is on a well-established heart failure model rather than an evolving one, we chose the coronary artery ligation model. Other

models such as transverse aortic ligation allow the stratified development of variable degrees of hypertrophy which eventually mount to full blown heart failure. Such models are more suitable for studies with a focus on the hypertrophic process and interventions aiming to alter the development or progression of cardiac hypertrophy (reviewed in [450-454]).

The coronary artery ligation model of heart failure was first described about 36 years ago [455]. Nowadays, it is a well-established and widely-used model of post-infarction heart failure [381, 382, 450, 452-454, 456-458]. This model can be used for either permanent ischemia that mimics an unresolved ischemic attack or an IR insult that mimics an ischemic attack that was resolved using revascularization interventions. In the latter, cardioprotective interventions can be used to rescue the area at risk and reduce the overall infarct size.

For the purpose of this thesis, the permanent ischemia intervention was chosen to allow the development of a predictable post-infarction scar following a permanent ligation with limited variability. The recovering hearts eventually develop LV dysfunction where the remaining viable myocardium undergoes remodeling and hypertrophy with accompanying metabolic alterations. For quality control, a SHAM procedure was performed to exclude any cardiac dysfunction that might develop as a result of the surgical procedure itself. We adhered to the peri-operative use of analgesia and antibiotics to minimize confounders in the etiology of heart failure in this model.

Being aware of the second window of inhalational anesthetic-induced preconditioning [459, 460], a three-day interval was allowed before the hearts of echoed mice were taken for *ex vivo* perfusion in the working mode. The choice of a 4-week postoperative period before *ex vivo* perfusion allowed the development of a mature scar which guarantees that the measured metabolic rates are attributed to metabolic activity of the remaining viable remodeled tissue that are not confounded by any contribution from the infarct tissue.

In general, our mouse model is not typically representative of human pathologic conditions. In human ischemic attacks, a common scenario is an immediate therapeutic medical or surgical intervention which alters the natural course of the remodeling process. In the CAL model, interventions were initiated either before the ischemic insult via the use of MCD deficiency or 4 weeks after the coronary artery ligation. However, both interventions contribute to our understanding of how a pharmacologic intervention can affect the normal course of metabolic remodeling following an ischemic insult. Another potential disadvantage is the fact that mice are not an exact replicate of human response to a disease process [461]. Moreover, different mouse strains exhibit different metabolic profiles. To further complicate the matter, metabolic profiles of the same strain of mice differ according to the various experimental conditions [462]. The latter adds emphasis on the importance of keeping standardized experimental conditions throughout the experimental protocol, a fact that we strictly followed.

6.1.2 Isolated working mouse heart perfusions

The isolated working heart preparation is a well-established model for *ex vivo* study of heart mechanical function and metabolic rates under well-controlled physiologic conditions of workloads and energy substrate concentrations [5, 386, 463]. Standardizing cardiac workloads to near physiologic levels allows a more reliable measurement of energy substrate metabolic rates since they are greatly influenced by the work level [464] and *vice versa* [465]. In contrast, other models, such as the Langendorff preparation, are considered less physiologic since levels of external cardiac work during perfusion cannot be maintained at physiologic levels [5, 466]. In addition, the isolated working heart preparation allows profiling of cardiac energy substrate metabolism without the influence of changes in autonomic regulation, circulating hormones or the influence of other organs.

The isolated working heart preparation is an ideal method to study changes in energy substrate metabolism since it guarantees adequate supply of oxygen and energy substrates to the working heart under controlled physiologic workloads. The fact that these materials reach the heart via the normal coronary perfusion route guarantees access of all parts of the heart to the required energy substrates and oxygen, hence more reliable values of metabolic rates can be measured. In contrast, Langendorff perfusion renders the heart under limited energy demand since physiologic workloads are not maintained. Besides, the retrograde aortic perfusion in this preparation and the use of low viscosity perfusate allows a minor degree of aortic valve incompetence. This builds up the intraventricular pressure to values more than perfusion pressure. Thus, metabolic

rates may be underestimated [5]. Similarly, isolated muscle preparations, such as isolated papillary muscle, can underestimate metabolic rates since these preparations depend on superfusion which does not guarantee adequate supply of oxygen to the deep muscle layers [467]. This limitation applies also to isolated cardiomyocyte preparations where the cells are not beating and are thus under a low metabolic demand [468]. Even when these cells are induced to beat, they beat under zero load which again render them under a low energy demand, hence underestimating metabolic rates [469].

In order to guarantee adequate energy substrate supply to our preparation, exogenous energy substrates were added to the perfusate in adequate amounts. With the exception of the MCD-KO mouse study, all the experiments were performed with 11 mM glucose, 1.2 mM palmitate and 1 mM lactate. Insulin (100 μ U/mL) was added in all experiments. An aerobic perfusion for a minimum of 40 min was used to replenish glycogen stores which are depleted during dissection and connection of the isolated hearts to the apparatus. Previous data from isolated working rat heart preparations indicated that aerobic perfusion for a period of 45-60 minute is needed to rebuild glycogen stores and hence increase the reliability of the measured metabolic rates [470, 471].

The choice of 1.2 mM concentration of palmitate may be considered higher than physiologic levels if compared to reported normal human non-esterified fatty acids (NEFA) levels (0.2 - 0.8 mM) [472, 473] that in turn vary according the fasting status. However, reported mouse NEFA levels vary from 0.4 mM [474] to 2.5 mM [475]. Thus, 1.2 mM palmitate is a reasonable average

value. Moreover, in conditions of stress such as ischemic attacks and in high cardiovascular risk groups, circulating NEFA levels are elevated [476-478].

Similar issues can arise regarding the use of 11 mM glucose. The normal fasting human glucose levels are defined as values below 6.1 mM [479]. However, considering conditions of metabolic stress such as ischemic attacks and post-infarction heart failure where cardiovascular risk factors exist, 11 mM is also a reasonable choice. Moreover, reported mouse non-diabetic fasting glucose level are 8 mM [480] which make 11 mM a close value to *in vivo* levels under stressful conditions. The exception is the choice of 5 mM glucose and 0.4 mM palmitate in the MCD-KO study to mimic perfusion conditions where MCD-KO mice were found to exhibit a lower proton production rate during reperfusion [322].

To comply with the commonly used experimental conditions for isolated mouse heart perfusions, perfusate in all experiments contained 100 $\mu\text{U}/\text{mL}$ insulin. Despite this value appearing higher than the reported normal diet-fed mouse plasma insulin levels of 20 - 40 $\mu\text{U}/\text{mL}$ according to age [481], the chosen higher concentration guarantees adequate free circulating insulin levels as a great portion of insulin adheres to the glass walls and tubing of the perfusion apparatus.

Oxygen is delivered to isolated mouse heart preparation via oxygenation of a crystalloid perfusate. Despite the fact that such a perfusate has less oxygen carrying capacity as compared to blood, adequate oxygen supply is secured through gassing of the perfusate with a carbogen mixture (95% O_2 and 5% CO_2) that results in a high partial pressure of oxygen ($p\text{O}_2$) [482]. This method of

oxygen delivery was shown previously to maintain oxygen supply to the preparation [482]. Moreover, reducing pO_2 of the perfusate by gassing with only 70% O_2 is associated with a similar contractile performance. Also the stability of mechanical function, after an initial period of adaptation, confirms adequate O_2 supply. Besides, the preparation is able to respond to positive inotropic drug treatment by increasing work without development of ischemic injury, indicative of a plentiful O_2 supply. Finally, the measured coronary venous pO_2 was found to remain high, indicative of sufficient oxygen reserve [482].

Despite the fact that the isolated mouse heart preparation can remain functioning for hours, a maximum perfusion time of 90 min was used to guarantee reliability of results and stability of function. Hearts were immersed in the perfusate to maintain adequate physiologic temperatures throughout the perfusion protocol. Since isolated mouse hearts were maintained under physiologic temperatures, they maintained an adequate spontaneous heart rate and electrical pacing was unnecessary.

For the study of IR injury in the second and third studies of this thesis, a global no-flow ischemia was used. In this approach, the inflow of perfusate to the whole heart is stopped for 15 min by clamping both the left atrial inflow and aortic outflow lines leading to ischemia to the entire preparation. Reperfusion is achieved by removal of the clamps; a reperfusion period of 30 min was used. This approach is slightly different from what happens *in vivo* where a coronary branch is blocked by a thrombus leading to a regional ischemia in the area supplied by this branch while the remaining heart is normally supplied by the uninterrupted

coronary blood flow. However, our experimental approach provides an ideal way of measuring changes in energy substrate metabolism where the observed changes can be attributed to the entire ischemic myocardium. Should a regional ischemia be produced, distinction of metabolic changes attributed to healthy and ischemic tissue would be impossible.

6.1.3 Measurement of energy substrate metabolism

Rates of energy substrate metabolism were assessed by measuring $^{14}\text{CO}_2$ and $^3\text{H}_2\text{O}$ released by the metabolism of radiolabeled glucose added to the perfusate. With the knowledge of specific activities of the radiolabeled substrates used, rates of flux through individual metabolic pathways can be directly measured [419, 483]. All experiments were done in two sets, one with [5- ^3H]glucose and [U- ^{14}C]glucose for measurement of glycolytic flux and glucose oxidation, respectively. In the other set, [9,10- ^3H]palmitate and [U- ^{14}C]lactate were added to measure palmitate and lactate oxidation, respectively. Details of the methods and interpretation are mentioned in Chapter 2. This section will focus on the advantages and disadvantages of this method in comparison to other methods used for the same purpose.

The use of radiolabeled isotopes for direct *ex vivo* measurement of energy substrate metabolism is well characterized in hearts from other experimental animals such as rats [368, 484-487]. Efforts of Belke *et al* 1999 [488] showed that energy substrate metabolism can be directly measured mouse hearts and that it compares to results from other models such as rat hearts. Since then, many studies have been performed characterizing energy substrate metabolism in *ex vivo* mouse

hearts under different pathologic conditions [221, 334, 489-491]. As our knowledge grows, more differences between mouse and rat heart energy substrate metabolism are being characterized.

6.1.4 Pros and cons of the use of ^3H - and ^{14}C - radiolabeled substrates

This method allows the measurement of metabolic end products, $^3\text{H}_2\text{O}$ and $^{14}\text{CO}_2$, which implies a direct steady state rate that can be maintained throughout the perfusion protocol. Since metabolic rates of glucose oxidation, lactate oxidation and palmitate oxidation are directly measured, tricarboxylic acid cycle activity can be assessed since the acetyl CoA yield from each metabolic pathway can be calculated (8 from palmitate, 2 from glucose and 1 from lactate). Moreover, ATP production rates can be assessed by quantification of the ATP yield of glycolytic flux (2 ATP), glucose oxidation (31 ATP), lactate oxidation (17.5 ATP) and palmitate oxidation (104 ATP).

Another advantage is the direct measurement of the end products of the metabolic pathways which does not require complex mathematical assumptions, calculations and kinetic modeling. This method is also relatively inexpensive compared to other alternative methods (see below). Moreover, no sophisticated expensive instruments are needed in this approach.

The use of [5- ^3H]glucose for measurement of glycolytic flux was claimed by Goodwin et al. [492] to overestimate the actual rates of glycolytic flux since

the rates calculated from detritiation of [5-³H]glucose were higher than the rates calculated from the sum of glucose oxidation rates and rates of accumulation of pyruvate and lactate in the perfusate which, according to the authors, may be due to non-glycolytic detritiation of [5-³H]glucose by the non-oxidative branch of pentose phosphate shunt. However, it is important to mention that reported glucose oxidation rates in that study were very low which may underestimate glycolytic rates calculated using the authors' suggested method. This evidence is further supported by reports from Leong et al. [493] who found glycolytic flux rates to be similar to rates calculated by either method with minimal contribution from the pentose phosphate shunt.

Claims about the inability of [U-¹⁴C]glucose to account for other specific pathways such as the pentose phosphate shunt since it measures the end product of oxidative glucose metabolism can be seen as an advantage since the portion of glucose that goes through the pentose phosphate shunt will end up in the TCA cycle. Thus this method is a better option to study the ultimate fate of glucose metabolism, regardless of intermediary pathways.

The *ex vivo* isolated heart preparation has advantages as well as disadvantages. *Ex vivo* isolated hearts do not reflect hormonal and autonomic influences that are important players in modulating cardiac metabolism under different physiologic and pathologic conditions. However, the isolated preparation can be seen as a focused approach to study isolated cardiac responses and direct cardiac effects of pharmacologic agents excluding confounding effects of the complex *in vivo* responses. Similarly, despite efforts to represent most of energy

substrates such as palmitate, glucose and lactate in the perfusate, many other substrates are not represented in the *ex vivo* isolated heart perfusate including other fatty acids, different carbohydrates, amino acids and ketone bodies. (See Barr RL and Lopaschuk GD [494] for details regarding other available methods of assessment of energy substrate metabolic rates).

6.2 Aerobic metabolic profiling of CAL hearts

As discussed in the Introduction, there is no agreement on the nature of metabolic changes in heart failure. Currently it is explained by two themes. The first one describes the failing heart as an engine out of fuel. This implies a generalized deterioration in energy substrate uptake and utilization [245, 246], oxidative phosphorylation for ATP production [270, 271], and/or transfer of high energy phosphate to creatine, via CK activity [400]. While this holds true in advanced cases of heart failure, we hypothesize that failing hearts are inefficient and that inefficient energy utilization can play a major role in the evolving heart failure. This is of great importance since interventions that aim to improve functional performance of the failing hearts should be initiated early in the disease process before a well-established impairment supervenes.

The fact that a decline in energy substrate metabolism is not uniformly present in all heart failure models [239, 401] suggests that alternate etiologies are involved. Interestingly, evidence used to support the energy starvation theory can be subject to alternate interpretations that actually support the inefficiency concept. An inefficient heart uses more energy to perform an equivalent workload, so providing more ATP, whether via external supply of energy

substrates, increasing rates of energy substrate metabolism, or enhancing ATP flux through CK, can improve contractility. Improved mechanical function in failing rat hearts by DCA-induced stimulation of glucose oxidation [214] reduces mismatched glucose metabolism. Thus, heart function improves, not only due to increased ATP generation, but also by less dysregulation of ionic homeostasis.

We have shown in the first study of this thesis that CAL hearts do not have depressed rates of glycolysis, glucose oxidation or fatty acid oxidation. Moreover, total rates of ATP production were only 25% lower in CAL hearts, not sufficient to explain the marked depression in LV work (46%). Similarly, endogenous energy substrate turnover, glycogen and TG synthesis and degradation, were similar in CAL and SHAM hearts. Besides, CAL hearts maintain similar contents of adenine nucleotides and creatine. These findings provide strong evidence against energy starvation and support metabolic inefficiency in these hearts. Thus, the calculated metabolic efficiency for exogenous energy substrate utilization (external LV work done per ATP produced) was significantly lower in CAL hearts (two thirds of SHAM values). Similarly, the metabolic efficiency for endogenous energy substrate utilization in CAL hearts tended to be lower than in SHAM hearts ($P=0.07$).

Alterations in energy substrate preference occur in hearts following acute ischemia [403] and have the potential to decrease efficiency [21, 319], but based on similar percentage contributions of energy substrates to overall ATP production in SHAM and CAL hearts (Fig 3.4H), it appears that substrate preference is unaltered in the infarct-remodeled heart. Instead, CAL hearts exhibit

an increase in glycolysis rate per unit LV work that is not matched by a sufficient increase in glucose oxidation rate per unit LV work causing a significant increase in proton production per unit LV work and suggests that mismatched glucose metabolism may be a contributor to inefficiency. This mismatch has also been reported in other Heart failure models [9, 236, 325, 404].

6.3 Improved coupling of glucose metabolism limits metabolic inefficiency and mechanical dysfunction in CAL hearts

MCD-KO mice were chosen because their hearts were previously shown to exhibit lower reperfusion proton production rates associated with better post-ischemic functional recovery [322]. These hearts have unaltered rates of glucose and fatty acid oxidation when perfused aerobically. However, when challenged by IR they show a preference for glucose oxidation over fatty acid oxidation which improves coupling between glycolysis and glucose oxidation, lessens intracellular acidosis and improves recovery of contractility [322]. Using this model, we studied the potential for enhancing mechanical function in remodeled hearts via improvement in the efficiency of exogenous substrate utilization. Confirming what is expected in our permanent coronary artery ligation model, infarct weights (both actual and as % of whole heart weight) are similar in WT CAL and MCD-KO CAL hearts. This indicates that functional effects are due to actions on the surviving viable tissue.

MCD-KO CAL hearts exhibit improved cardiac function and a reduction in the rates of glycolysis, glucose oxidation, lactate oxidation and ATP production. The improved mechanical function in presence of lower energy substrate metabolic rates indicates improved metabolic efficiency. These changes persist after normalization for LV work. In accordance with the study by Dyck *et al* [96], MCD-KO CAL hearts have unaltered fatty acid oxidation rates. That study showed that fatty acid oxidation regulating genes that code for fatty acid transporter (CD36), CPT1, acyl CoA thioesterase, and uncoupling protein-3 are upregulated in MCD-KO healthy hearts [96] resulting in maintained aerobic fatty acid oxidation despite the lack of MCD. We speculate that the upregulated genes are also responsible for the lack of significant change in fatty acid oxidation rates in remodeled MCD-KO CAL hearts. The improved metabolic efficiency and maintained fatty acid oxidation rates in these hearts may explain why lower rates of glucose metabolism were observed.

In that part of the thesis, we showed that MCD-KO CAL hearts have improved coupling between glycolysis and glucose oxidation, lower proton production and improved total LV work. This indicates that enhancing the matching of glucose metabolism is beneficial in this model of heart failure. While this does not prove a cause-effect relationship between metabolic inefficiency and cardiac function, it supports such a relationship.

6.4 Remodeled hearts exhibit no further deterioration of mechanical function and metabolic efficiency following *ex vivo* ischemia reperfusion

IR injury is associated with changes in energy substrate preferences, deterioration of cardiac efficiency and mechanical dysfunction [342, 405]. During post-ischemic reperfusion, normal mouse hearts exhibit a marked deterioration of oxidative metabolism. This augments the mismatch between glycolytic flux and glucose oxidation rates resulting in lactate accumulation [13, 326, 405-407]. Meanwhile, protons derived from the hydrolysis of glycolytically produced ATP accumulate, increasing intracellular acidosis [317]. The subsequent activation of the $\text{Na}^+\text{-H}^+$ exchanger causes Na^+ accumulation [333], which, in turn, activates reverse mode $\text{Na}^+\text{-Ca}^{2+}$ exchange leading to Ca^{2+} overload [185]. In order to correct Na^+ and Ca^{2+} overload, more ATP is diverted towards ionic homeostasis and away from mechanical function. This is expected to lead to deterioration of metabolic efficiency associated with a significant deterioration of mechanical function. It is thus expected that CAL hearts being metabolically inefficient and functionally impaired, would experience severe functional deterioration following *ex vivo* IR. However, we confirmed in the second study of this thesis previous evidence that remodeled hearts actually exhibit a better tolerance to IR injury [314-316].

That study extended measurements of energy substrate metabolism and metabolic efficiency to reperfused hearts. The demonstration that reperfused CAL hearts maintain comparable rates of energy substrate metabolism to reperfused SHAM hearts excludes the possibility of a change in energy substrate preference as a contributor to the observed lower functional deterioration in reperfused CAL hearts. Indeed, the finding that CAL hearts maintain similar metabolic rates per LV work during reperfusion as during aerobic perfusion indicates that there is no further deterioration of metabolic efficiency in reperfused CAL hearts. This contrasts with reperfused SHAM hearts that experience a significant deterioration in function and metabolic efficiency associated with increased reperfusion proton production per LV work due a marked mismatch between glycolytic flux and glucose oxidation rates. Also reperfused SHAM hearts exhibit a significantly increased utilization of the less efficient energy substrate, fatty acid, as indicated by a significant increase in fatty acid oxidation per LV work.

We also studied potential contributors to the observed better ischemic tolerance and maintained metabolic efficiency in CAL hearts. We studied two possibilities, higher mitochondrial abundance and improved calcium handling. However, there was no difference in the expression of markers of either mitochondrial abundance or key metabolic enzymes. Similarly, there were no changes in the calcium handling proteins, SERCA2, CaMKII and phospholamban, suggesting that it is unlikely that the better functional recovery and maintained

metabolic efficiency during reperfusion of remodeled hearts are due to alterations in mitochondrial abundance or improved calcium handling.

A third potential explanation is a lower stimulus to develop intracellular acidosis and Na^+ and Ca^{2+} overload. The finding that CAL hearts exhibit significantly lower ischemic glycogenolysis as compared to SHAM hearts implies lower ischemic production of lactate and protons in CAL hearts. Hence, accumulation of protons during ischemia is expected to be lower in CAL hearts. In support of our hypothesis, recovery of intracellular pH in reperfused hearts is delayed if the rates of glycolytic flux are not matched with glucose oxidation. Similarly, improving the coupling enhances the recovery of intracellular pH and improves both mechanical function and cardiac efficiency [317]. In fact, diverting glucose metabolism towards glycogen synthesis rather than glycolytic flux reduces proton production, limits Ca^{2+} overload and improves recovery of post-ischemic mechanical function [318]. Similarly, cardioprotection by adenosine [340] or ischemic preconditioning [330, 408] reduce glycogen utilization and inhibit glycolytic flux. Indeed, the findings that CAL hearts have lower rates of glycogenolysis during ischemia and preserved ATP contents during reperfusion suggest that the improved ischemic tolerance of remodeled hearts mimics some of the mechanisms of ischemic preconditioning. The possibility that preconditioning mechanisms are already activated in remodeled hearts may explain the failure of additional preconditioning interventions to achieve functional benefits in remodeled hearts [410-412].

6.5 Reperfusion DCA administration does not stimulate glucose oxidation or improve functional recovery

Many studies have addressed the cardioprotective effect of DCA against IR injury in normal hearts [364, 367, 416, 418, 419]. Meanwhile, the benefit of DCA in the treatment of heart failure patients has been a controversial issue. As indicated in Chapter 5, some studies reported the benefit of DCA in improving hemodynamic function and cardiac mechanical efficiency in heart failure patients [426]. Others found no benefit of DCA in improving exercise tolerance [427] or LV function in heart failure patients [428]. However, the potential benefit of DCA for alleviation of IR-induced LV dysfunction in post-infarction remodeled hearts has not been addressed. Since CAL hearts are metabolically inefficient with a mismatch between rates of glycolytic flux and glucose oxidation, it was hypothesized that these hearts would benefit from improving the matching of glucose metabolism during reperfusion with a potential of improved functional recovery.

We demonstrated in Chapter 5 that DCA treatment at reperfusion failed to improve functional recovery or to induce metabolic changes in reperfused CAL, SHAM and normal control hearts indicative of failure to stimulate glucose oxidation. Below are the potential contributors to the reduced sensitivity of mouse hearts to DCA treatment.

6.5.1 Contribution of the chemical composition of the perfusate to the sensitivity of mouse hearts to DCA

As indicated in Chapter 5, our standard perfusate contains 1 mM lactate which is an important energy substrate normally present *in vivo* and is expected to increase in conditions of IR injury [429]. Moreover, the presence of lactate in the perfusate is important for accurate assessment of metabolic rates of energy substrates [430]. In contrast, many of the published reports on DCA-mediated acceleration of glucose oxidation have utilized perfusates that lack lactate [431-434] or used smaller concentrations (0.5 mM) of lactate [436-438]. Thus, it is possible that lactate in the perfusate may have contributed to the reduced sensitivity of mouse hearts to the stimulatory effect of DCA on glucose oxidation. As detailed in Chapter 5, reports from White *et al* 1999 [435] and Griffin *et al* [358] indicated that presence of lactate in the perfusate prevented the functional benefits of DCA and delayed recovery of intracellular pH or reperfused rabbit hearts. Similarly, we demonstrated that DCA stimulated glucose oxidation in mouse hearts in absence of lactate, indicative of lactate-induced reduced sensitivity to DCA.

Since the aim of this thesis was to characterize energy substrate metabolism under physiologic and pathologic IR conditions, studies required the use of lactate in the perfusate [429]. Moreover, the presence of lactate in the perfusate is important for accurate assessment of metabolic rates of energy substrates [430].

6.5.2 Species-dependent difference in the response to DCA

The finding that DCA is able to improve cardiac efficiency [436] as well as improve functional recovery in rat hearts [437] and newborn (6 weeks) rabbit hearts [438] after IR in presence of lower concentrations of lactate (0.5 mM) indicate the possibility of species-dependent difference in sensitivity to DCA.

One major difference in mouse heart is that PDH seems to be working at maximal activity and therefore there is no potential for further stimulation. As detailed in Chapter 5, rat heart studies report lower baseline glucose oxidation rates (0.2-0.8 $\mu\text{mol/g dry wt/ min}$) [318, 329, 439-443]. We report in this thesis glucose oxidation rates in mouse hearts of 2-3 $\mu\text{mol/g dry wt/ min}$ [221], which are similar to previously reported mouse heart data [244, 322, 444]. The higher baseline glucose oxidation rates in mouse hearts can be an indication of higher baseline activity of PDH that may be close to maximal and so unable to respond to DCA stimulation. Measurements of PDH activity in rat and mouse hearts would be a useful approach to test for this possibility.

Another possible explanation of the higher baseline glucose oxidation rates in mouse hearts as compared to rat hearts is that higher baseline glycolytic rates in mouse heart supply more pyruvate as substrate for oxidative metabolism. Rates of glycolysis reported for aerobically perfused rat hearts range from 1.5 to 5 $\mu\text{mol/g dry wt/ min}$ [318, 329, 439-443]. In contrast, glycolytic rates in mouse hearts are significantly greater. Values reported in this thesis range from 13 to 25 $\mu\text{mol/g dry wt/ min}$ depending on perfusion conditions and are similar to values reported for mouse hearts by other authors (11-20 $\mu\text{mol/g dry wt/ min}$) [244, 322,

444]. Thus, higher baseline PDH activity in mouse heart might be an adaptive response of PDH to match the higher availability of pyruvate supplied through glycolysis and thereby minimize the consequences of the mismatch in glucose metabolism.

6.6 Despite effective MCD inhibition, metabolic inefficiency is not improved in MCDi-treated CAL hearts

MCD inhibition is an evolving and promising approach for protection against acute IR injury and functional consequences of post-ischemic remodeling. We have shown in Chapter 3 that chronic MCD deficiency reduces post-ischemic LV dysfunction and improves metabolic efficiency. Similar reports from Dyck *et al* [96] highlighted the cardioprotective effect of chronic MCD deficiency against acute IR injury. It can be claimed that these scenarios do not mimic real life situations where the intervention is normally initiated after the ischemic insult. In a scenario more similar to the clinical scenario where treatment is usually initiated after the ischemic insult, cardiac-specific inhibition of MCD via microRNA intervention *in vivo* initiated after CAL surgery in rats limits functional deterioration and maintains energy stores in treated hearts. Hence, to probe further the potential benefit of acute MCD inhibition, we studied the consequences of acute *ex vivo* MCD inhibition using an MCDi (CMB-0000382) on metabolic efficiency in remodeled hearts.

The demonstration that CMB-0000382 increases malonyl CoA content in CAL and trends to increase it in SHAM hearts confirms inhibition of MCD in both groups. Thus it was unexpected that fatty acid oxidation rates were inhibited by CMB-0000382 only in SHAM hearts and not in CAL hearts. This indicates that other regulators of fatty acid oxidation might have been altered in remodeled CAL hearts, but the finding that malonyl CoA content was increased in treated CAL hearts excludes the possibility of a compensatory downregulation of acetyl CoA carboxylase (ACC) [446], that produces malonyl CoA, could have contributed to the lack of inhibition of fatty acid oxidation in treated CAL hearts. However, other regulators of fatty acid oxidation could be altered in our CAL model, thereby preventing any response to MCD inhibition. These data are in accordance with previous reports from Dyck *et al* [96] where the lack of fatty acid oxidation in MCD-KO hearts under aerobic perfusion conditions was associated with upregulation of CPT1, CD36, PDK4 and PPAR α .

Another explanation for the lack of fatty acid oxidation inhibition in MCDi-treated CAL hearts despite malonyl CoA accumulation is the possibility of compartmentalization of malonyl CoA so that its concentration in the vicinity of CPT1 at the outer mitochondrial membrane, where it competes with acyl CoA for intramitochondrial transport by CPT1, is not sufficient to inhibit transport and so fatty acid oxidation rates remain unchanged. In support, previous reports that basal malonyl CoA levels in tissues are in excess of those required to inhibit CPT1 [447] have also suggested possible compartmentalization of cardiac malonyl CoA [97]. In this way, a lower malonyl CoA concentration exists in the vicinity of

CPT1, hence CPT1 remains active despite the higher overall malonyl CoA content. Thus, it is possible that malonyl CoA levels in the vicinity of CPT1 could undergo changes sufficient to affect CPT1 activity accordingly. This possibility may explain the finding that a moderate increase in malonyl CoA concentrations (20% of control) in human skeletal muscles led to significant reduction of fatty acid oxidation (41% of control) [68].

Further studies are needed to understand the regulation of fatty acid metabolism in CAL hearts. This is expected to help understand the response of chronically remodeled hearts to fatty acid oxidation inhibitors that are known to be effective in improving function in acute settings such as acute ischemia reperfusion in healthy hearts [61, 66, 96, 140, 176].

One limitation of this study is the short-term acute *ex vivo* exposure of the heart to the MCDi. It is possible that longer-term *in vivo* post-ischemic exposure to MCDi would be more effective since MCD inhibition would occur during the remodeling process. This assumption is supported by our findings in Chapter 3 where chronic MCD deficiency in MCD-KO mice was associated with less functional deterioration and less metabolic inefficiency following CAL surgery. Similarly, the protective effect of post-surgical MCD inhibition via microRNA treatment of CAL rats [60] suggests the possibility of a better response to chronic post-surgical pharmacologic MCD inhibition in CAL hearts.

6.7 Conclusion

Post-infarction remodeled failing mouse hearts are inefficient in the utilization of energy substrates for mechanical work. Mismatched glucose metabolism (glycolysis vs glucose oxidation) and the resulting accelerated proton production per unit LV work may be a contributor to inefficiency and the deterioration of LV mechanical function. The prevention of inefficiency by a metabolic intervention (chronic MCD deficiency) that lessens mismatched glucose metabolism and improves mechanical function supports the view that inefficiency is a major contributor to HF in the infarct-remodeled heart and is amenable for improvement by metabolic interventions.

Remodeled CAL hearts exhibit impaired LV mechanical function and metabolic efficiency during baseline aerobic conditions. They exhibit higher recovery of LV function and no further deterioration of metabolic efficiency following exposure to *ex vivo* IR injury. Lower glycogenolysis during ischemia with subsequent less intracellular acidosis and ion dysregulation may contribute to the greater tolerance to ischemic injury in the remodeled heart.

Extreme caution is warranted when generalizing the responses to cardioprotective metabolic interventions from normal to remodeled hearts. For example, while the presence of DCA during reperfusion of normal hearts is associated with functional benefits and maintenance of cardiac efficiency [367, 416, 495], the response of remodeled hearts to the same metabolic intervention appears more complex and potentially different from normal healthy hearts. More studies are needed to understand why CAL hearts exhibit a significant

deterioration of post-ischemic function following the DCA exposure. Also, more studies are needed to understand the mechanism of lactate-induced inhibition of the effects of DCA on glucose oxidation. Also species differences may partly explain why mouse hearts do not exhibit a similar response to DCA as rat hearts. This is extremely important and should be considered when applying animal-derived data to human studies.

Similarly, while MCD inhibition is protective against acute IR injury and chronic MCD inhibition, whether by MCD-KO [221] or by microRNA approaches initiated after CAL surgery [60], is protective against post-ischemic functional and metabolic efficiency deterioration, acute *ex vivo* MCD inhibition was not sufficient to produce similar beneficial effects in CAL hearts. A study employing chronic *in vivo* pharmacologic MCD inhibition is needed to test the potential benefit of MCD inhibition in terms of improving mechanical function and metabolic efficiency in remodeled CAL hearts.

7 Future directions

7.1 Limiting metabolic inefficiency and mechanical dysfunction following CAL surgery via chronic MCD inhibition

We have shown in Chapter 3 that chronic MCD deficiency is associated with less deterioration of metabolic efficiency and less cardiac dysfunction. This is associated with better matching of glycolytic flux and glucose oxidation rates which results in lower proton production rates. These findings confirm our hypothesis that CAL hearts are metabolically inefficient and that this state of inefficiency is amenable to correction, at least partially, by metabolic interventions. Similar benefits are obtained by microRNA-induced silencing of MCD expression in rat hearts [60]. However, genetic interventions can result in a myriad of compensatory mechanisms that can confound the observed findings. Moreover, the initiation of the intervention before the ischemic insult does not recapitulate the actual clinical real-life sequence of events where interventions are usually initiated after the ischemic insult.

One approach to dissect the actual consequence of MCD inhibition from any other confounding factors is to inhibit pharmacologically MCD after the initiation of the ischemic event. As mentioned in the second part of Chapter 5, acute *ex vivo* administration of MCDi at time zero of the perfusion protocol does not improve *ex vivo* function of CAL hearts despite a significant increase in malonyl CoA levels. An alternative approach to better address this issue is to

initiate chronic MCD inhibition *in vivo* immediately after CAL surgery. This would allow a sufficient treatment period that is initiated at the start of the remodeling process where there is a higher possibility of causing a reversal or at least a diminution of the adverse events. Preliminary data (personal communication from Lopaschuk's lab) indicate that CAL rats treated with oral MCDi initiated after the surgery have better treadmill performance indicative of improved exercise tolerance as compared to untreated rats.

7.2 Study of the acetylation control of fatty acid oxidation in remodeled hearts

Acetylation/deacetylation control of metabolic enzymes is an emerging field of research. In general, lysine acetylation is an important reversible post-translational modification that modifies activity of proteins involved in many cellular processes, including nuclear transcription, cell survival, apoptosis and mitochondrial function [496-501]. Lysine acetylation is achieved via the activity of a group of enzymes called histone acetyl transferases and involves the transfer of an acetyl moiety from acetyl CoA to lysine resulting in neutralization of the lysine positive charge and subsequent alterations in protein configuration and activity [496, 498, 501]. The deacetylation process is carried out by a group of histone deacetylases of which sirtuins (SIRTs) are of particular interest [499, 500, 502-504].

Currently, there is no agreement about the consequences of acetylation of fatty acid β -oxidation enzymes. Reports from Hirschey *et al* [505, 506] suggest that deacetylation of LCAD by SIRT3 accelerates fatty acid oxidation in the liver. Moreover, chemical acetylation of LCAD on lysine 318 and lysine 322 reduces enzymatic activity, while deacetylation with recombinant SIRT3 restored catalytic activity [507]. In contrast, Zhao *et al* [508] reports that acetylation activates β -HAD in muscle cells. Similarly, mitochondria from hindlimb muscles of fasted mice have an increased acetylation associated with increased fatty acid oxidation rates [509]. Moreover, diaphragm muscle of SIRT3-KO mice exhibit increased acetylation and increased fatty acid oxidation rates [509]. Furthermore, obese dam offsprings exhibit a significant decrease in SIRT3 expression and activity associated with increased LCAD acetylation [510]. Recently, Abo Alrob *et al* [511] reports that decrease in SIRT3 seen following chronic high fat feeding or chronic SIRT3 deficiency enhances acetylation of β -HAD and LCAD. This induces a switch in cardiac energy substrate utilization from glucose to fatty acid oxidation.

Similarly, acetylation is reported to regulate glucose and lactate oxidation through modification of the rate limiting PDH activity. As mentioned in chapter 1, PDH is regulated by substrate/product ratios and by covalent modifications [20]. The latter includes phosphorylation and acetylation [509, 512, 513]. Acetylation of lysine residues in the E1 α subunit of PDH inhibits the enzyme [509]. Similarly, inhibition of SIRT3 in skeletal muscles and myoblasts induces acetylation resulting in inactivation of PDH [509]. In the heart, treatment with angiotensin II

leads to a reduction in SIRT3 protein levels as well as increased acetylation and inactivation of PDH [514]. A recent study by Fan *et al* [512] suggested that acetylation at lysine 321 of PDH is an important regulator of PDH activity in human cancer cells. Similar to fatty acid regulation, there is no agreement regarding the impact of acetylation. Recently, acetylation of lysine 254 is reported to activate GAPDH in response to glucose signals [515]. In contrast, a report from Wang *et al* [516] indicates that G-6-PD is inactivated by acetylation of lysine 403 increasing the susceptibility of the cell to oxidative stress secondary to reduced pentose phosphate pathway-derived NADPH. The subsequent reduction of intracellular reduced glutathione that is the main intracellular reducing agent increases the susceptibility to oxidative stress [516].

Considering the complexity of metabolic changes that develop in remodeled hearts and the lack of agreement regarding the role of acetylation in the control of the key metabolic regulatory enzymes, it is warranted to examine the acetylation status of key enzymes such as PDH, G-6-PD, LCAD and β -HAD as an initial step towards the understanding of the regulation of these pathways which helps in the identification of potential targets for the improvement of the function of remodeled hearts through improvement of their metabolic efficiency.

7.3 Stimulation of pentose phosphate pathway to lessen cardiac post-infarction functional and metabolic deterioration

The pentose phosphate pathway (PPP) is an important accessory glucose metabolism pathway that can be divided into oxidative PPP and non-oxidative PPP [517, 518]. The main function of the oxidative PPP is the production of NADPH which plays an essential role in regulating oxidative stress via replenishing reduced glutathione levels. Meanwhile NADPH is required for the production of cytosolic reactive oxygen species that, at low levels, are involved in proliferation and survival signaling [519]. Besides, NADPH is also required for lipogenesis [520, 521] and anaplerosis [522-526]. The oxidative PPP utilizes G-6-P created from the initial reaction of glycolysis as a substrate through the action of G-6-PD [518, 520, 521]. In the non-oxidative PPP, formation of ribose-5-phosphate and xylulose-5-phosphate is important in nucleotide or nucleic acid synthesis or as a possible transcriptional signaling molecule, respectively [527, 528].

Currently, there is no agreement regarding the occurrence of PPP stimulation in heart failure models. While earlier reports indicated that PPP is not upregulated in heart failure [529], many other reports confirm its stimulation [530-533]. Moreover, the consequences of PPP stimulation are not agreed upon. In canine model of pacing-induced heart failure, increased activity of G-6-PD is associated with increased levels of superoxide [533]. The consequences of

increased superoxide production depend on whether its level exceeds the threshold for harmful oxidative damage of cellular organelles and disruption of ionic homeostasis. Similarly, proteomic analysis of hearts from Dahl salt sensitive rats reveals activation of PPP and the functional benefits of DCA treatment is associated with further activation of PPP [259]. Furthermore, chronic deficiency of G-6-PD in mice increases oxidative stress and functional deterioration following myocardial infarction and transverse aortic constriction [534]. In contrast, recent reports indicate that excessive NADPH derived from the oxidative PPP contributes to cardiomyopathy and heart failure [533, 535]. Taken together, the current evidence suggests that a certain degree of PPP stimulation is a protective compensatory mechanism in heart failure and that further stimulation may be protective.

One approach to stimulate PPP is the treatment with benfotiamine which is a thiamine derivative that activates transketolase and directs glucose to PPP [536-541]. Treatment with benfotiamine is reported to protect against acute streptozotocin-induced diabetes reducing oxidative stress and rescuing cardiomyocyte contractile function [541]. Similarly, treatment of normal and streptozotocin-induced diabetic mice with benfotiamine is reported to stimulate PPP leading to reduction of oxidative stress and activation of G-6-PD/akt prosurvival pathway leading to improved post-infarction survival, functional recovery and neovascularization and reduced cardiomyocyte apoptosis and neurohormonal activation in normal and diabetic mice [540]. Benfotiamine is also reported to stimulate glucose oxidation in differentiated human skeletal muscle

cells under normoglycemic and hyperglycemic conditions [542] perhaps through enhancement of NADPH-dependent anaplerotic generation of TCA cycle intermediates.

We showed in this thesis that CAL hearts have mismatched glucose metabolism where the increase in glycolytic rates is not associated with sufficient increase in glucose oxidation. It is important to study the changes in PPP and the subsequent changes in oxidative stress in CAL hearts which can contribute to the observed functional deterioration. Chronic post-infarction treatment with benfotiamine can add insights regarding the potential benefits of further stimulation of PPP in our model.

8 References

1. MacIver DH, Dayer MJ, Harrison AJ (2013) A general theory of acute and chronic heart failure. *Int J Cardiol* 165:25-34.
2. Francis GS, McDonald KM, Cohn JN (1993) Neurohumoral activation in preclinical heart failure. Remodeling and the potential for intervention. *Circulation* 87:IV90-96.
3. Kemp CD, Conte JV (2012) The pathophysiology of heart failure. *Cardiovasc Pathol* 21:365-371.
4. Houser SR, Margulies KB, Murphy AM, Spinale FG, Francis GS, Prabhu SD, Rockman HA, Kass DA, Molkentin JD, Sussman MA, Koch WJ, American Heart Association Council on Basic Cardiovascular Sciences, Council on Clinical Cardiology, and Council on Functional Genomics and Translational Biology (2012) Animal models of heart failure: a scientific statement from the American Heart Association. *Circ Res* 111:131-150.
5. Neely JR, Morgan HE (1974) Relationship between carbohydrate and lipid metabolism and the energy balance of heart muscle. *Annu Rev Physiol* 36:413-459.
6. Opie LH (1968) Metabolism of the heart in health and disease. I. *Am Heart J* 76:685-698.
7. Opie LH (1969) Metabolism of the heart in health and disease. II. *Am Heart J* 77:100-22 contd.
8. Opie LH (1969) Metabolism of the heart in health and disease. 3. *Am Heart J* 77:383-410.
9. Lei B, Lionetti V, Young ME, Chandler MP, d'Agostino C, Kang E, Altarejos M, Matsuo K, Hintze TH, Stanley WC, Recchia FA (2004) Paradoxical downregulation of the glucose oxidation pathway despite enhanced flux in severe heart failure. *J Mol Cell Cardiol* 36:567-576.
10. Osorio JC, Stanley WC, Linke A, Castellari M, Diep QN, Panchal AR, Hintze TH, Lopaschuk GD, Recchia FA (2002) Impaired myocardial fatty acid oxidation and reduced protein expression of retinoid X receptor-alpha in pacing-induced heart failure. *Circulation* 106:606-612.
11. Dodd MS, Ball DR, Schroeder MA, Le Page LM, Atherton HJ, Heather LC, Seymour AM, Ashrafian H, Watkins H, Clarke K, Tyler DJ (2012) In vivo alterations in cardiac metabolism and function in the spontaneously hypertensive rat heart. *Cardiovasc Res* 95:69-76.

12. Xu J, Nie HG, Zhang XD, Tian Y, Yu B (2011) Down-regulated energy metabolism genes associated with mitochondria oxidative phosphorylation and fatty acid metabolism in viral cardiomyopathy mouse heart. *Mol Biol Rep* 38:4007-4013.
13. Li X, Arslan F, Ren Y, Adav SS, Poh KK, Sorokin V, Lee CN, de Kleijn D, Lim SK, Sze SK (2012) Metabolic adaptation to a disruption in oxygen supply during myocardial ischemia and reperfusion is underpinned by temporal and quantitative changes in the cardiac proteome. *J Proteome Res* 11:2331-2346.
14. Gertz EW, Wisneski JA, Stanley WC, Neese RA (1988) Myocardial substrate utilization during exercise in humans. Dual carbon-labeled carbohydrate isotope experiments. *J Clin Invest* 82:2017-2025.
15. Stanley WC, Lopaschuk GD, Hall JL, McCormack JG (1997) Regulation of myocardial carbohydrate metabolism under normal and ischaemic conditions. Potential for pharmacological interventions. *Cardiovasc Res* 33:243-257.
16. Wisneski JA, Gertz EW, Neese RA, Gruenke LD, Craig JC (1985) Dual carbon-labeled isotope experiments using D-[6-¹⁴C] glucose and L-[1,2,3-¹³C₃] lactate: a new approach for investigating human myocardial metabolism during ischemia. *J Am Coll Cardiol* 5:1138-1146.
17. Wisneski JA, Gertz EW, Neese RA, Gruenke LD, Morris DL, Craig JC (1985) Metabolic fate of extracted glucose in normal human myocardium. *J Clin Invest* 76:1819-1827.
18. Wisneski JA, Stanley WC, Neese RA, Gertz EW (1990) Effects of acute hyperglycemia on myocardial glycolytic activity in humans. *J Clin Invest* 85:1648-1656.
19. Neubauer S (2007) The failing heart--an engine out of fuel . *N Engl J Med* 356:1140-1151.
20. Jaswal JS, Keung W, Wang W, Ussher JR, Lopaschuk GD (2011) Targeting fatty acid and carbohydrate oxidation--a novel therapeutic intervention in the ischemic and failing heart. *Biochim Biophys Acta* 1813:1333-1350.
21. Lopaschuk GD, Ussher JR, Folmes CD, Jaswal JS, Stanley WC (2010) Myocardial fatty acid metabolism in health and disease. *Physiol Rev* 90:207-258.
22. Postic C, Leturque A, Printz RL, Maulard P, Loizeau M, Granner DK, Girard J (1994) Development and regulation of glucose transporter and hexokinase expression in rat. *Am J Physiol* 266:E548-559.

23. Becker C, Sevilla L, Tomas E, Palacin M, Zorzano A, Fischer Y (2001) The endosomal compartment is an insulin-sensitive recruitment site for GLUT4 and GLUT1 glucose transporters in cardiac myocytes. *Endocrinology* 142:5267-5276.
24. Kerner J, Hoppel C (2000) Fatty acid import into mitochondria. *Biochim Biophys Acta* 1486:1-17.
25. Murthy MS, Pande SV (1990) Characterization of a solubilized malonyl-CoA-sensitive carnitine palmitoyltransferase from the mitochondrial outer membrane as a protein distinct from the malonyl-CoA-insensitive carnitine palmitoyltransferase of the inner membrane. *Biochem J* 268:599-604.
26. Pande SV, Parvin R (1976) Characterization of carnitine acylcarnitine translocase system of heart mitochondria. *J Biol Chem* 251:6683-6691.
27. Pande SV, Parvin R (1980) Carnitine-acylcarnitine translocase catalyzes an equilibrating unidirectional transport as well. *J Biol Chem* 255:2994-3001.
28. Murthy MS, Pande SV (1984) Mechanism of carnitine acylcarnitine translocase-catalyzed import of acylcarnitines into mitochondria. *J Biol Chem* 259:9082-9089.
29. Murthy MS, Pande SV (1987) Some differences in the properties of carnitine palmitoyltransferase activities of the mitochondrial outer and inner membranes. *Biochem J* 248:727-733.
30. Murthy MS, Pande SV (1987) Malonyl-CoA binding site and the overt carnitine palmitoyltransferase activity reside on the opposite sides of the outer mitochondrial membrane. *Proc Natl Acad Sci U S A* 84:378-382.
31. Stanley WC, Chandler MP (2002) Energy metabolism in the normal and failing heart: potential for therapeutic interventions. *Heart Fail Rev* 7:115-130.
32. Wolff AA, Rotmensch HH, Stanley WC, Ferrari R (2002) Metabolic approaches to the treatment of ischemic heart disease: the clinicians' perspective. *Heart Fail Rev* 7:187-203.
33. McGarry JD, Sen A, Esser V, Woeltje KF, Weis B, Foster DW (1991) New insights into the mitochondrial carnitine palmitoyltransferase enzyme system. *Biochimie* 73:77-84.
34. McGarry JD (1995) The mitochondrial carnitine palmitoyltransferase system: its broadening role in fuel homeostasis and new insights into its molecular features. *Biochem Soc Trans* 23:321-324.

35. McGarry JD, Brown NF (1997) The mitochondrial carnitine palmitoyltransferase system. From concept to molecular analysis. *Eur J Biochem* 244:1-14.
36. Cotter DG, Schugar RC, Crawford PA (2013) Ketone body metabolism and cardiovascular disease. *Am J Physiol Heart Circ Physiol* 304:H1060-1076.
37. Drake KJ, Sidorov VY, McGuinness OP, Wasserman DH, Wikswo JP (2012) Amino acids as metabolic substrates during cardiac ischemia. *Exp Biol Med* (Maywood) 237:1369-1378.
38. Marazzi G, Rosanio S, Caminiti G, Dioguardi FS, Mercurio G (2008) The role of amino acids in the modulation of cardiac metabolism during ischemia and heart failure. *Curr Pharm Des* 14:2592-2604.
39. Brodan V, Fabian J, Andel M, Pechar J (1978) Myocardial amino acid metabolism in patients with chronic ischemic heart disease. *Basic Res Cardiol* 73:160-170.
40. Wanders RJ, Vreken P, Ferdinandusse S, Jansen GA, Waterham HR, van Roermund CW, Van Grunsven EG (2001) Peroxisomal fatty acid alpha- and beta-oxidation in humans: enzymology, peroxisomal metabolite transporters and peroxisomal diseases. *Biochem Soc Trans* 29:250-267.
41. Wanders RJ, Ferdinandusse S, Brites P, Kemp S (2010) Peroxisomes, lipid metabolism and lipotoxicity. *Biochim Biophys Acta* 1801:272-280.
42. Alexander JJ, Snyder A, Tongsard JH (1998) Omega-oxidation of monocarboxylic acids in rat brain. *Neurochem Res* 23:227-233.
43. Muller M, Sorrell TC (1992) Leukotriene B4 omega-oxidation by human polymorphonuclear leukocytes is inhibited by pyocyanin, a phenazine derivative produced by *Pseudomonas aeruginosa*. *Infect Immun* 60:2536-2540.
44. Kam W, Kumaran K, Landau BR (1978) Contribution of omega-oxidation to fatty acid oxidation by liver of rat and monkey. *J Lipid Res* 19:591-600.
45. Wanders RJ, Vreken P, Ferdinandusse S, Jansen GA, Waterham HR, van Roermund CW, Van Grunsven EG (2001) Peroxisomal fatty acid alpha- and beta-oxidation in humans: enzymology, peroxisomal metabolite transporters and peroxisomal diseases. *Biochem Soc Trans* 29:250-267.
46. Eldjarn L, Stokke O, Try K (1966) Alpha-oxidation of branched chain fatty acids in man and its failure in patients with Refsum's disease showing phytanic acid accumulation. *Scand J Clin Lab Invest* 18:694-695.

47. Depre C, Rider MH, Hue L (1998) Mechanisms of control of heart glycolysis. *Eur J Biochem* 258:277-290.
48. King LM, Opie LH (1998) Glucose and glycogen utilisation in myocardial ischemia--changes in metabolism and consequences for the myocyte. *Mol Cell Biochem* 180:3-26.
49. Stanley WC, Recchia FA, Lopaschuk GD (2005) Myocardial substrate metabolism in the normal and failing heart. *Physiol Rev* 85:1093-1129.
50. Chandler MP, Kerner J, Huang H, Vazquez E, Reszko A, Martini WZ, Hoppel CL, Imai M, Rastogi S, Sabbah HN, Stanley WC (2004) Moderate severity heart failure does not involve a downregulation of myocardial fatty acid oxidation. *Am J Physiol Heart Circ Physiol* 287:H1538-543.
51. Lopaschuk GD (2001) Malonyl CoA control of fatty acid oxidation in the diabetic rat heart. *Adv Exp Med Biol* 498:155-165.
52. Dyck JR, Lopaschuk GD (2002) Malonyl CoA control of fatty acid oxidation in the ischemic heart. *J Mol Cell Cardiol* 34:1099-1109.
53. Cuthbert KD, Dyck JR (2005) Malonyl-CoA decarboxylase is a major regulator of myocardial fatty acid oxidation. *Curr Hypertens Rep* 7:407-411.
54. Kudo N, Barr AJ, Barr RL, Desai S, Lopaschuk GD (1995) High rates of fatty acid oxidation during reperfusion of ischemic hearts are associated with a decrease in malonyl-CoA levels due to an increase in 5'-AMP-activated protein kinase inhibition of acetyl-CoA carboxylase. *J Biol Chem* 270:17513-17520.
55. Hue L, Taegtmeyer H (2009) The Randle cycle revisited: a new head for an old hat. *Am J Physiol Endocrinol Metab* 297:E578-591.
56. Randle PJ (1998) Regulatory interactions between lipids and carbohydrates: the glucose fatty acid cycle after 35 years. *Diabetes Metab Rev* 14:263-283.
57. Randle PJ, Garland PB, Hales CN, Newsholme EA (1963) The glucose fatty-acid cycle. Its role in insulin sensitivity and the metabolic disturbances of diabetes mellitus. *Lancet* 1:785-789.
58. Balligand JL (2000) Beta 3 adrenergic receptor: physiologic role and potential therapeutic applications. *Bull Mem Acad R Med Belg* 155:311-317; discussion 317-319.
59. Fillmore N, Lopaschuk GD (2014) Malonyl CoA: A promising target for the treatment of cardiac disease. *IUBMB Life*. doi: 10.1002/iub.1253. [Epub ahead of print].

60. Wu H, Zhu Q, Cai M, Tong X, Liu D, Huang J, Yang G, Jiang Y (2014) Effect of Inhibiting Malonyl-CoA Decarboxylase on Cardiac Remodeling after Myocardial Infarction in Rats. *Cardiology* 127:236-244.
61. Ussher JR, Lopaschuk GD (2009) Targeting malonyl CoA inhibition of mitochondrial fatty acid uptake as an approach to treat cardiac ischemia/reperfusion. *Basic Res Cardiol* 104:203-210.
62. Ussher JR, Lopaschuk GD (2008) The malonyl CoA axis as a potential target for treating ischaemic heart disease. *Cardiovasc Res* 79:259-268.
63. Dyck JR, Hopkins TA, Bonnet S, Michelakis ED, Young ME, Watanabe M, Kawase Y, Jishage K, Lopaschuk GD (2006) Absence of malonyl coenzyme A decarboxylase in mice increases cardiac glucose oxidation and protects the heart from ischemic injury. *Circulation* 114:1721-1728.
64. Lopaschuk GD, Stanley WC (2006) Malonyl-CoA decarboxylase inhibition as a novel approach to treat ischemic heart disease. *Cardiovasc Drugs Ther* 20:433-439.
65. Roepstorff C, Halberg N, Hillig T, Saha AK, Ruderman NB, Wojtaszewski JF, Richter EA, Kiens B (2005) Malonyl-CoA and carnitine in regulation of fat oxidation in human skeletal muscle during exercise. *Am J Physiol Endocrinol Metab* 288:E133-142.
66. Stanley WC, Morgan EE, Huang H, McElfresh TA, Sterk JP, Okere IC, Chandler MP, Cheng J, Dyck JR, Lopaschuk GD (2005) Malonyl-CoA decarboxylase inhibition suppresses fatty acid oxidation and reduces lactate production during demand-induced ischemia. *Am J Physiol Heart Circ Physiol* 289:H2304-2309.
67. Dyck JR, Cheng JF, Stanley WC, Barr R, Chandler MP, Brown S, Wallace D, Arrhenius T, Harmon C, Yang G, Nadzan AM, Lopaschuk GD (2004) Malonyl coenzyme a decarboxylase inhibition protects the ischemic heart by inhibiting fatty acid oxidation and stimulating glucose oxidation. *Circ Res* 94:e78-84.
68. Bavenholm PN, Pigon J, Saha AK, Ruderman NB, Efendic S (2000) Fatty acid oxidation and the regulation of malonyl-CoA in human muscle. *Diabetes* 49:1078-1083.
69. Dyck JR, Barr AJ, Barr RL, Kolattukudy PE, Lopaschuk GD (1998) Characterization of cardiac malonyl-CoA decarboxylase and its putative role in regulating fatty acid oxidation. *Am J Physiol* 275:H2122-129.
70. Hardie DG (1992) Regulation of fatty acid and cholesterol metabolism by the AMP-activated protein kinase. *Biochim Biophys Acta* 1123:231-238.

71. Li J, Hu X, Selvakumar P, Russell RR,3rd, Cushman SW, Holman GD, Young LH (2004) Role of the nitric oxide pathway in AMPK-mediated glucose uptake and GLUT4 translocation in heart muscle. *Am J Physiol Endocrinol Metab* 287:E834-841.
72. Shearer J, Fueger PT, Rottman JN, Bracy DP, Martin PH, Wasserman DH (2004) AMPK stimulation increases LCFA but not glucose clearance in cardiac muscle in vivo. *Am J Physiol Endocrinol Metab* 287:E871-877.
73. Rutter GA, Da Silva Xavier G, Leclerc I (2003) Roles of 5'-AMP-activated protein kinase (AMPK) in mammalian glucose homeostasis. *Biochem J* 375:1-16.
74. Xing Y, Musi N, Fujii N, Zou L, Luptak I, Hirshman MF, Goodyear LJ, Tian R (2003) Glucose metabolism and energy homeostasis in mouse hearts overexpressing dominant negative alpha2 subunit of AMP-activated protein kinase. *J Biol Chem* 278:28372-28377.
75. Burcelin R, Crivelli V, Perrin C, Da Costa A, Mu J, Kahn BB, Birnbaum MJ, Kahn CR, Vollenweider P, Thorens B (2003) GLUT4, AMP kinase, but not the insulin receptor, are required for hepatoportal glucose sensor-stimulated muscle glucose utilization. *J Clin Invest* 111:1555-1562.
76. Russell RR,3rd, Li J, Coven DL, Pypaert M, Zechner C, Palmeri M, Giordano FJ, Mu J, Birnbaum MJ, Young LH (2004) AMP-activated protein kinase mediates ischemic glucose uptake and prevents postischemic cardiac dysfunction, apoptosis, and injury. *J Clin Invest* 114:495-503.
77. Bertrand L, Ginion A, Beauloye C, Hebert AD, Guigas B, Hue L, Vanoverschelde JL (2006) AMPK activation restores the stimulation of glucose uptake in an in vitro model of insulin-resistant cardiomyocytes via the activation of protein kinase B. *Am J Physiol Heart Circ Physiol* 291:H239-250.
78. Jing M, Cheruvu VK, Ismail-Beigi F (2008) Stimulation of glucose transport in response to activation of distinct AMPK signaling pathways. *Am J Physiol Cell Physiol* 295:C1071-1082.
79. Samovski D, Su X, Xu Y, Abumrad NA, Stahl PD (2012) Insulin and AMPK regulate FA translocase/CD36 plasma membrane recruitment in cardiomyocytes via Rab GAP AS160 and Rab8a Rab GTPase. *J Lipid Res* 53:709-717.
80. Bijland S, Mancini SJ, Salt IP (2013) Role of AMP-activated protein kinase in adipose tissue metabolism and inflammation. *Clin Sci (Lond)* 124:491-507.
81. Lee-Young RS, Bonner JS, Mayes WH, Iwueke I, Barrick BA, Hasenour CM, Kang L, Wasserman DH (2013) AMP-activated protein kinase (AMPK)alpha2

- plays a role in determining the cellular fate of glucose in insulin-resistant mouse skeletal muscle. *Diabetologia* 56:608-617.
82. Nagendran J, Waller TJ, Dyck JR (2013) AMPK signalling and the control of substrate use in the heart. *Mol Cell Endocrinol* 366:180-193.
83. Horman S, Beauloye C, Vanoverschelde JL, Bertrand L (2012) AMP-activated protein kinase in the control of cardiac metabolism and remodeling. *Curr Heart Fail Rep* 9:164-173.
84. Hardie DG, Ross FA, Hawley SA (2012) AMPK: a nutrient and energy sensor that maintains energy homeostasis. *Nat Rev Mol Cell Biol* 13:251-262.
85. Hardie DG (2011) AMP-activated protein kinase: an energy sensor that regulates all aspects of cell function. *Genes Dev* 25:1895-1908.
86. Hardie DG (2011) AMP-activated protein kinase: a cellular energy sensor with a key role in metabolic disorders and in cancer. *Biochem Soc Trans* 39:1-13.
87. Hardie DG (2011) Energy sensing by the AMP-activated protein kinase and its effects on muscle metabolism. *Proc Nutr Soc* 70:92-99.
88. Hardie DG, Ashford ML (2014) AMPK: regulating energy balance at the cellular and whole body levels. *Physiology (Bethesda)* 29:99-107.
89. Gowans GJ, Hardie DG (2014) AMPK: a cellular energy sensor primarily regulated by AMP. *Biochem Soc Trans* 42:71-75.
90. Hardie DG (2014) AMP-activated protein kinase: maintaining energy homeostasis at the cellular and whole-body levels. *Annu Rev Nutr* 34:31-55.
91. Zordoky BN, Nagendran J, Pulinilkunnil T, Kienesberger PC, Masson G, Waller TJ, Kemp BE, Steinberg GR, Dyck JR (2014) AMPK-Dependent Inhibitory Phosphorylation of ACC Is Not Essential for Maintaining Myocardial Fatty Acid Oxidation. *Circ Res* 115:518-524.
92. Poirier M, Vincent G, Reszko AE, Bouchard B, Kelleher JK, Brunengraber H, Des Rosiers C (2002) Probing the link between citrate and malonyl-CoA in perfused rat hearts. *Am J Physiol Heart Circ Physiol* 283:H1379-386.
93. Munday MR (2002) Regulation of mammalian acetyl-CoA carboxylase. *Biochem Soc Trans* 30:1059-1064.
94. Abo Alrob O, Lopaschuk GD (2014) Role of CoA and acetyl-CoA in regulating cardiac fatty acid and glucose oxidation. *Biochem Soc Trans* 42:1043-1051.

95. Samokhvalov V, Ussher JR, Fillmore N, Armstrong IK, Keung W, Moroz D, Lopaschuk DG, Seubert J, Lopaschuk GD (2012) Inhibition of malonyl-CoA decarboxylase reduces the inflammatory response associated with insulin resistance. *Am J Physiol Endocrinol Metab* 303:E1459-468.
96. Dyck JR, Hopkins TA, Bonnet S, Michelakis ED, Young ME, Watanabe M, Kawase Y, Jishage K, Lopaschuk GD (2006) Absence of malonyl coenzyme A decarboxylase in mice increases cardiac glucose oxidation and protects the heart from ischemic injury. *Circulation* 114:1721-1728.
97. Sambandam N, Steinmetz M, Chu A, Altarejos JY, Dyck JR, Lopaschuk GD (2004) Malonyl-CoA decarboxylase (MCD) is differentially regulated in subcellular compartments by 5'AMP-activated protein kinase (AMPK). Studies using H9c2 cells overexpressing MCD and AMPK by adenoviral gene transfer technique. *Eur J Biochem* 271:2831-2840.
98. Poole RC, Halestrap AP (1993) Transport of lactate and other monocarboxylates across mammalian plasma membranes. *Am J Physiol* 264:C761-782.
99. Herzig S, Raemy E, Montessuit S, Veuthey JL, Zamboni N, Westermann B, Kunji ER, Martinou JC (2012) Identification and functional expression of the mitochondrial pyruvate carrier. *Science* 337:93-96.
100. Panchal AR, Comte B, Huang H, Dudar B, Roth B, Chandler M, Des Rosiers C, Brunengraber H, Stanley WC (2001) Acute hibernation decreases myocardial pyruvate carboxylation and citrate release. *Am J Physiol Heart Circ Physiol* 281:H1613-1620.
101. Panchal AR, Comte B, Huang H, Kerwin T, Darvish A, des Rosiers C, Brunengraber H, Stanley WC (2000) Partitioning of pyruvate between oxidation and anaplerosis in swine hearts. *Am J Physiol Heart Circ Physiol* 279:H2390-2398.
102. Pound KM, Sorokina N, Ballal K, Berkich DA, Fasano M, Lanoue KF, Taegtmeier H, O'Donnell JM, Lewandowski ED (2009) Substrate-enzyme competition attenuates upregulated anaplerotic flux through malic enzyme in hypertrophied rat heart and restores triacylglyceride content: attenuating upregulated anaplerosis in hypertrophy. *Circ Res* 104:805-812.
103. Sugden MC, Holness MJ (2003) Recent advances in mechanisms regulating glucose oxidation at the level of the pyruvate dehydrogenase complex by PDKs. *Am J Physiol Endocrinol Metab* 284:E855-862.

104. Kolobova E, Tuganova A, Boulatnikov I, Popov KM (2001) Regulation of pyruvate dehydrogenase activity through phosphorylation at multiple sites. *Biochem J* 358:69-77.
105. Karpova T, Danchuk S, Kolobova E, Popov KM (2003) Characterization of the isozymes of pyruvate dehydrogenase phosphatase: implications for the regulation of pyruvate dehydrogenase activity. *Biochim Biophys Acta* 1652:126-135.
106. Patel MS, Korotchkina LG (2006) Regulation of the pyruvate dehydrogenase complex. *Biochem Soc Trans* 34:217-222.
107. Connaughton S, Chowdhury F, Attia RR, Song S, Zhang Y, Elam MB, Cook GA, Park EA (2010) Regulation of pyruvate dehydrogenase kinase isoform 4 (PDK4) gene expression by glucocorticoids and insulin. *Mol Cell Endocrinol* 315:159-167.
108. Attia RR, Sharma P, Janssen RC, Friedman JE, Deng X, Lee JS, Elam MB, Cook GA, Park EA (2011) Regulation of pyruvate dehydrogenase kinase 4 (PDK4) by CCAAT/enhancer-binding protein beta (C/EBPbeta). *J Biol Chem* 286:23799-23807.
109. Korotchkina LG, Patel MS (2001) Site specificity of four pyruvate dehydrogenase kinase isoenzymes toward the three phosphorylation sites of human pyruvate dehydrogenase. *J Biol Chem* 276:37223-37229.
110. Holness MJ, Sugden MC (2003) Regulation of pyruvate dehydrogenase complex activity by reversible phosphorylation. *Biochem Soc Trans* 31:1143-1151.
111. Peters SJ (2003) Regulation of PDH activity and isoform expression: diet and exercise. *Biochem Soc Trans* 31:1274-1280.
112. St Amand TA, Spriet LL, Jones NL, Heigenhauser GJ (2000) Pyruvate overrides inhibition of PDH during exercise after a low-carbohydrate diet. *Am J Physiol Endocrinol Metab* 279:E275-283.
113. Spriet LL, Heigenhauser GJ (2002) Regulation of pyruvate dehydrogenase (PDH) activity in human skeletal muscle during exercise. *Exerc Sport Sci Rev* 30:91-95.
114. Kimber NE, Heigenhauser GJ, Spriet LL, Dyck DJ (2003) Skeletal muscle fat and carbohydrate metabolism during recovery from glycogen-depleting exercise in humans. *J Physiol* 548:919-927.

115. Peters SJ (2003) Regulation of PDH activity and isoform expression: diet and exercise. *Biochem Soc Trans* 31:1274-1280.
116. Watt MJ, Heigenhauser GJ, LeBlanc PJ, Inglis JG, Spriet LL, Peters SJ (2004) Rapid upregulation of pyruvate dehydrogenase kinase activity in human skeletal muscle during prolonged exercise. *J Appl Physiol* (1985) 97:1261-1267.
117. Pehleman TL, Peters SJ, Heigenhauser GJ, Spriet LL (2005) Enzymatic regulation of glucose disposal in human skeletal muscle after a high-fat, low-carbohydrate diet. *J Appl Physiol* (1985) 98:100-107.
118. Kiilerich K, Birk JB, Damsgaard R, Wojtaszewski JF, Pilegaard H (2008) Regulation of PDH in human arm and leg muscles at rest and during intense exercise. *Am J Physiol Endocrinol Metab* 294:E36-42.
119. Gurd BJ, Peters SJ, Heigenhauser GJ, LeBlanc PJ, Doherty TJ, Paterson DH, Kowalchuk JM (2009) Prior heavy exercise elevates pyruvate dehydrogenase activity and muscle oxygenation and speeds O₂ uptake kinetics during moderate exercise in older adults. *Am J Physiol Regul Integr Comp Physiol* 297:R877-884.
120. Kiilerich K, Gudmundsson M, Birk JB, Lundby C, Taudorf S, Plomgaard P, Saltin B, Pedersen PA, Wojtaszewski JF, Pilegaard H (2010) Low muscle glycogen and elevated plasma free fatty acid modify but do not prevent exercise-induced PDH activation in human skeletal muscle. *Diabetes* 59:26-32.
121. Kiilerich K, Ringholm S, Bienso RS, Fisher JP, Iversen N, van Hall G, Wojtaszewski JF, Saltin B, Lundby C, Calbet JA, Pilegaard H (2011) Exercise-induced pyruvate dehydrogenase activation is not affected by 7 days of bed rest. *J Appl Physiol* (1985) 111:751-757.
122. Pilegaard H, Neuffer PD (2004) Transcriptional regulation of pyruvate dehydrogenase kinase 4 in skeletal muscle during and after exercise. *Proc Nutr Soc* 63:221-226.
123. Stanley WC, Recchia FA, Lopaschuk GD (2005) Myocardial substrate metabolism in the normal and failing heart. *Physiol Rev* 85:1093-1129.
124. Halestrap AP, Poole RC, Cranmer SL (1990) Mechanisms and regulation of lactate, pyruvate and ketone body transport across the plasma membrane of mammalian cells and their metabolic consequences. *Biochem Soc Trans* 18:1132-1135.
125. Halestrap AP, Price NT (1999) The proton-linked monocarboxylate transporter (MCT) family: structure, function and regulation. *Biochem J* 343 Pt 2:281-299.

126. Poole RC, Halestrap AP (1993) Transport of lactate and other monocarboxylates across mammalian plasma membranes. *Am J Physiol* 264:C761-782.
127. Dennis SC, Gevers W, Opie LH (1991) Protons in ischemia: where do they come from; where do they go to?. *J Mol Cell Cardiol* 23:1077-1086.
128. Robergs RA, Ghiasvand F, Parker D (2004) Biochemistry of exercise-induced metabolic acidosis. *Am J Physiol Regul Integr Comp Physiol* 287:R502-516.
129. Lysiak W, Toth PP, Suelter CH, Bieber LL (1986) Quantitation of the efflux of acylcarnitines from rat heart, brain, and liver mitochondria. *J Biol Chem* 261:13698-13703.
130. Calvani M, Reda E, Arrigoni-Martelli E (2000) Regulation by carnitine of myocardial fatty acid and carbohydrate metabolism under normal and pathological conditions. *Basic Res Cardiol* 95:75-83.
131. Ingwall JS (2009) Energy metabolism in heart failure and remodelling. *Cardiovasc Res* 81:412-419.
132. Strumia E, Pelliccia F, D'Ambrosio G (2012) Creatine phosphate: pharmacological and clinical perspectives. *Adv Ther* 29:99-123.
133. Guzun R, Timohhina N, Tepp K, Gonzalez-Granillo M, Shevchuk I, Chekulayev V, Kuznetsov AV, Kaambre T, Saks VA (2011) Systems bioenergetics of creatine kinase networks: physiological roles of creatine and phosphocreatine in regulation of cardiac cell function. *Amino Acids* 40:1333-1348.
134. Sahlin K, Harris RC (2011) The creatine kinase reaction: a simple reaction with functional complexity. *Amino Acids* 40:1363-1367.
135. Boehm E, Chan S, Monfared M, Wallimann T, Clarke K, Neubauer S (2003) Creatine transporter activity and content in the rat heart supplemented by and depleted of creatine. *Am J Physiol Endocrinol Metab* 284:E399-406.
136. Rossi AM, Eppenberger HM, Volpe P, Cotrufo R, Wallimann T (1990) Muscle-type MM creatine kinase is specifically bound to sarcoplasmic reticulum and can support Ca²⁺ uptake and regulate local ATP/ADP ratios. *J Biol Chem* 265:5258-5266.
137. Wallimann T, Wyss M, Brdiczka D, Nicolay K, Eppenberger HM (1992) Intracellular compartmentation, structure and function of creatine kinase isoenzymes in tissues with high and fluctuating energy demands: the

- 'phosphocreatine circuit' for cellular energy homeostasis. *Biochem J* 281 (Pt 1):21-40.
138. Ventura-Clapier R, Garnier A, Veksler V, Joubert F (2011) Bioenergetics of the failing heart. *Biochim Biophys Acta* 1813:1360-1372.
139. Tuunanen H, Knuuti J (2011) Metabolic remodelling in human heart failure. *Cardiovasc Res* 90:251-257.
140. Jaswal JS, Keung W, Wang W, Ussher JR, Lopaschuk GD (2011) Targeting fatty acid and carbohydrate oxidation - A novel therapeutic intervention in the ischemic and failing heart . *Biochim Biophys Acta* 1813(7):1333-13350.
141. Ohte N, Narita H, Iida A, Wakami K, Asada K, Fukuta H, Kato T, Hyano J, Kimura G (2009) Impaired myocardial oxidative metabolism in the remote normal region in patients in the chronic phase of myocardial infarction and left ventricular remodeling. *J Nucl Cardiol* 16:73-81.
142. Hasegawa S, Yamamoto K, Sakata Y, Takeda Y, Kajimoto K, Kanai Y, Hori M, Hatazawa J (2008) Effects of cardiac energy efficiency in diastolic heart failure: assessment with positron emission tomography with ¹¹C-acetate. *Hypertens Res* 31:1157-1162.
143. van Bilsen M, van Nieuwenhoven FA, van der Vusse GJ (2009) Metabolic remodelling of the failing heart: beneficial or detrimental?. *Cardiovasc Res* 81:420-428.
144. Schulz TJ, Westermann D, Isken F, Voigt A, Laube B, Thierbach R, Kuhlow D, Zarse K, Schomburg L, Pfeiffer AF, Tschope C, Ristow M (2010) Activation of mitochondrial energy metabolism protects against cardiac failure. *Aging (Albany NY)* 2:843-853.
145. Jullig M, Hickey AJ, Chai CC, Skea GL, Middleditch MJ, Costa S, Choong SY, Philips AR, Cooper GJ (2008) Is the failing heart out of fuel or a worn engine running rich? A study of mitochondria in old spontaneously hypertensive rats. *Proteomics* 8:2556-2572.
146. Ingwall JS, Weiss RG (2004) Is the failing heart energy starved? On using chemical energy to support cardiac function. *Circ Res* 95:135-145.
147. Ingwall JS (2006) Energetics of the failing heart: new insights using genetic modification in the mouse. *Arch Mal Coeur Vaiss* 99:839-847.
148. Taegtmeyer H, Wilson CR, Razeghi P, Sharma S (2005) Metabolic energetics and genetics in the heart. *Ann N Y Acad Sci* 1047:208-218.

149. BING RJ, HAMMOND MM (1949) The measurement of coronary blood flow, oxygen consumption, and efficiency of the left ventricle in man. *Am Heart J* 38:1-24.
150. Suga H (2003) Cardiac energetics: from E(max) to pressure-volume area. *Clin Exp Pharmacol Physiol* 30:580-585.
151. Suga H (1990) Ventricular energetics. *Physiol Rev* 70:247-277.
152. Burkhoff D, Weiss RG, Schulman SP, Kalil-Filho R, Wannenburg T, Gerstenblith G (1991) Influence of metabolic substrate on rat heart function and metabolism at different coronary flows. *Am J Physiol* 261:H741-750.
153. Korvald C, Elvenes OP, Myrnes T (2000) Myocardial substrate metabolism influences left ventricular energetics in vivo. *Am J Physiol Heart Circ Physiol* 278:H1345-351.
154. Lammerant J, Huynh-Thu T, Kolanowski J (1985) Inhibitory effects of the D(-) isomer of 3-hydroxybutyrate on cardiac non-esterified fatty acid uptake and oxygen demand induced by norepinephrine in the intact dog. *J Mol Cell Cardiol* 17:421-433.
155. Mjos OD (1971) Effect of free fatty acids on myocardial function and oxygen consumption in intact dogs. *J Clin Invest* 50:1386-1389.
156. Mjos OD (1971) Effect of inhibition of lipolysis on myocardial oxygen consumption in the presence of isoproterenol. *J Clin Invest* 50:1869-1873.
157. Mjos OD, Kjekshus J (1971) Increased local metabolic rate by free fatty acids in the intact dog heart. *Scand J Clin Lab Invest* 28:389-393.
158. Simonsen S, Kjekshus JK (1978) The effect of free fatty acids on myocardial oxygen consumption during atrial pacing and catecholamine infusion in man. *Circulation* 58:484-491.
159. Hinkle PC (2005) P/O ratios of mitochondrial oxidative phosphorylation. *Biochim Biophys Acta* 1706:1-11.
160. Kadenbach B (2003) Intrinsic and extrinsic uncoupling of oxidative phosphorylation. *Biochim Biophys Acta* 1604:77-94.
161. Bouillaud F, Combes-George M, Ricquier D (1983) Mitochondria of adult human brown adipose tissue contain a 32 000-Mr uncoupling protein. *Biosci Rep* 3:775-780.

162. Enerback S (2010) Brown adipose tissue in humans. *Int J Obes (Lond)* 34 Suppl 1:S43-46.
163. McLeod CJ, Aziz A, Hoyt RF, Jr, McCoy JP, Jr, Sack MN (2005) Uncoupling proteins 2 and 3 function in concert to augment tolerance to cardiac ischemia. *J Biol Chem* 280:33470-33476.
164. Boehm EA, Jones BE, Radda GK, Veech RL, Clarke K (2001) Increased uncoupling proteins and decreased efficiency in palmitate-perfused hyperthyroid rat heart. *Am J Physiol Heart Circ Physiol* 280:H977-983.
165. Cole MA, Murray AJ, Cochlin LE, Heather LC, McAleese S, Knight NS, Sutton E, Jamil AA, Parassol N, Clarke K (2011) A high fat diet increases mitochondrial fatty acid oxidation and uncoupling to decrease efficiency in rat heart. *Basic Res Cardiol* 106:447-457.
166. Laskowski KR, Russell RR, 3rd (2008) Uncoupling proteins in heart failure. *Curr Heart Fail Rep* 5:75-79.
167. Li N, Wang J, Gao F, Li AM, Song R, Tian Y, Zhu SJ (2009) The relationship between uncoupling protein 2 expression and myocardial high energy phosphates content in abdominal aorta constriction induced heart failure rats. *Zhonghua Xin Xue Guan Bing Za Zhi* 37:1108-1112.
168. Turner JD, Gaspers LD, Wang G, Thomas AP (2010) Uncoupling protein-2 modulates myocardial excitation-contraction coupling. *Circ Res* 106:730-738.
169. Murray AJ, Cole MA, Lygate CA, Carr CA, Stuckey DJ, Little SE, Neubauer S, Clarke K (2008) Increased mitochondrial uncoupling proteins, respiratory uncoupling and decreased efficiency in the chronically infarcted rat heart. *J Mol Cell Cardiol* 44:694-700.
170. Ingwall JS (2009) Energy metabolism in heart failure and remodelling. *Cardiovasc Res* 81:412-419.
171. Saddik M, Lopaschuk GD (1991) Myocardial triglyceride turnover and contribution to energy substrate utilization in isolated working rat hearts. *J Biol Chem* 266:8162-8170.
172. Saddik M, Lopaschuk GD (1992) Myocardial triglyceride turnover during reperfusion of isolated rat hearts subjected to a transient period of global ischemia. *J Biol Chem* 267:3825-3831.
173. Himms-Hagen J, Harper ME (2001) Physiological role of UCP3 may be export of fatty acids from mitochondria when fatty acid oxidation predominates: an hypothesis. *Exp Biol Med (Maywood)* 226:78-84.

174. Schrauwen P, Hoeks J, Hesselink MK (2006) Putative function and physiological relevance of the mitochondrial uncoupling protein-3: involvement in fatty acid metabolism?. *Prog Lipid Res* 45:17-41.
175. Rame JE, Barouch LA, Sack MN, Lynn EG, Abu-Asab M, Tsokos M, Kern SJ, Barb JJ, Munson PJ, Halushka MK, Miller KL, Fox-Talbot K, Zhang J, Hare JM, Solomon MA, Danner RL (2011) Caloric restriction in leptin deficiency does not correct myocardial steatosis: failure to normalize PPAR α /PGC1 α and thermogenic glycerolipid/fatty acid cycling. *Physiol Genomics* 43:726-738.
176. Oka T, Lam VH, Zhang L, Keung W, Cadete VJ, Samokhvalov V, Tanner BA, Beker DL, Ussher JR, Huqi A, Jaswal JS, Rebeyka IM, Lopaschuk GD (2012) Cardiac hypertrophy in the newborn delays the maturation of fatty acid beta-oxidation and compromises postischemic functional recovery. *Am J Physiol Heart Circ Physiol* 302:H1784-794.
177. Razeghi P, Young ME, Alcorn JL, Moravec CS, Frazier OH, Taegtmeyer H (2001) Metabolic gene expression in fetal and failing human heart. *Circulation* 104:2923-2931.
178. Rajabi M, Kassiotis C, Razeghi P, Taegtmeyer H (2007) Return to the fetal gene program protects the stressed heart: a strong hypothesis. *Heart Fail Rev* 12:331-343.
179. Taegtmeyer H, Sen S, Vela D (2010) Return to the fetal gene program: a suggested metabolic link to gene expression in the heart. *Ann N Y Acad Sci* 1188:191-198.
180. Dodd MS, Ball DR, Schroeder MA, Le Page LM, Atherton HJ, Heather LC, Seymour AM, Ashrafian H, Watkins H, Clarke K, Tyler DJ (2012) In Vivo Alterations in Cardiac Metabolism and Function in the Spontaneously Hypertensive Rat Heart. *Cardiovasc Res* 95(1):69-76.
181. Dai DF, Hsieh EJ, Liu Y, Chen T, Beyer RP, Chin MT, MacCoss MJ, Rabinovitch PS (2012) Mitochondrial proteome remodeling in pressure overload-induced heart failure: the role of mitochondrial oxidative stress. *Cardiovasc Res* 93:79-88.
182. Moravec J, El Alaoui-Talibi Z, Moravec M, Guendouz A (1996) Control of oxidative metabolism in volume-overloaded rat hearts: effect of pretreatment with propionyl-L-carnitine. *Adv Exp Med Biol* 388:205-212.
183. El Alaoui-Talibi Z, Guendouz A, Moravec M, Moravec J (1997) Control of oxidative metabolism in volume-overloaded rat hearts: effect of propionyl-L-carnitine. *Am J Physiol* 272:H1615-1624.

184. Wang J, Bai L, Li J, Sun C, Zhao J, Cui C, Han K, Liu Y, Zhuo X, Wang T, Liu P, Fan F, Guan Y, Ma A (2009) Proteomic analysis of mitochondria reveals a metabolic switch from fatty acid oxidation to glycolysis in the failing heart. *Sci China C Life Sci* 52:1003-1010.
185. Baartscheer A, Schumacher CA, Coronel R, Fiolet JW (2011) The Driving Force of the Na/Ca-Exchanger during Metabolic Inhibition. *Front Physiol* 2:10.
186. Madrazo JA, Kelly DP (2008) The PPAR trio: regulators of myocardial energy metabolism in health and disease. *J Mol Cell Cardiol* 44:968-975.
187. Smeets PJ, Teunissen BE, Willemsen PH, van Nieuwenhoven FA, Brouns AE, Janssen BJ, Cleutjens JP, Staels B, van der Vusse GJ, van Bilsen M (2008) Cardiac hypertrophy is enhanced in PPAR alpha^{-/-} mice in response to chronic pressure overload. *Cardiovasc Res* 78:79-89.
188. Watanabe K, Fujii H, Takahashi T, Kodama M, Aizawa Y, Ohta Y, Ono T, Hasegawa G, Naito M, Nakajima T, Kamijo Y, Gonzalez FJ, Aoyama T (2000) Constitutive regulation of cardiac fatty acid metabolism through peroxisome proliferator-activated receptor alpha associated with age-dependent cardiac toxicity. *J Biol Chem* 275:22293-22299.
189. Campbell FM, Kozak R, Wagner A, Altarejos JY, Dyck JR, Belke DD, Severson DL, Kelly DP, Lopaschuk GD (2002) A role for peroxisome proliferator-activated receptor alpha (PPARalpha) in the control of cardiac malonyl-CoA levels: reduced fatty acid oxidation rates and increased glucose oxidation rates in the hearts of mice lacking PPARalpha are associated with higher concentrations of malonyl-CoA and reduced expression of malonyl-CoA decarboxylase. *J Biol Chem* 277:4098-4103.
190. Sarma S, Ardehali H, Gheorghide M (2012) Enhancing the metabolic substrate: PPAR-alpha agonists in heart failure. *Heart Fail Rev* 17:35-43.
191. Young ME, Laws FA, Goodwin GW, Taegtmeyer H (2001) Reactivation of peroxisome proliferator-activated receptor alpha is associated with contractile dysfunction in hypertrophied rat heart. *J Biol Chem* 276:44390-44395.
192. Morgan EE, Rennison JH, Young ME, McElfresh TA, Kung TA, Tserng KY, Hoit BD, Stanley WC, Chandler MP (2006) Effects of chronic activation of peroxisome proliferator-activated receptor-alpha or high-fat feeding in a rat infarct model of heart failure. *Am J Physiol Heart Circ Physiol* 290:H1899-1904.
193. Labinsky V, Bellomo M, Chandler MP, Young ME, Lionetti V, Qanud K, Bigazzi F, Sampietro T, Stanley WC, Recchia FA (2007) Chronic activation of peroxisome proliferator-activated receptor-alpha with fenofibrate prevents alterations in cardiac metabolic phenotype without changing the onset of

decompensation in pacing-induced heart failure. *J Pharmacol Exp Ther* 321:165-171.

194. Brigadeau F, Gele P, Wibaux M, Marquie C, Martin-Nizard F, Torpier G, Fruchart JC, Staels B, Duriez P, Lacroix D (2007) The PPARalpha activator fenofibrate slows down the progression of the left ventricular dysfunction in porcine tachycardia-induced cardiomyopathy. *J Cardiovasc Pharmacol* 49:408-415.

195. Ogata T, Miyauchi T, Sakai S, Takanashi M, Irukayama-Tomobe Y, Yamaguchi I (2004) Myocardial fibrosis and diastolic dysfunction in deoxycorticosterone acetate-salt hypertensive rats is ameliorated by the peroxisome proliferator-activated receptor-alpha activator fenofibrate, partly by suppressing inflammatory responses associated with the nuclear factor-kappa-B pathway. *J Am Coll Cardiol* 43:1481-1488.

196. Alvarez-Guardia D, Palomer X, Coll T, Serrano L, Rodriguez-Calvo R, Davidson MM, Merlos M, El Kochairi I, Michalik L, Wahli W, Vazquez-Carrera M (2011) PPARbeta/delta activation blocks lipid-induced inflammatory pathways in mouse heart and human cardiac cells. *Biochim Biophys Acta* 1811:59-67.

197. Cheng L, Ding G, Qin Q, Huang Y, Lewis W, He N, Evans RM, Schneider MD, Brako FA, Xiao Y, Chen YE, Yang Q (2004) Cardiomyocyte-restricted peroxisome proliferator-activated receptor-delta deletion perturbs myocardial fatty acid oxidation and leads to cardiomyopathy. *Nat Med* 10:1245-1250.

198. Opie LH, Sack MN (2002) Metabolic plasticity and the promotion of cardiac protection in ischemia and ischemic preconditioning. *J Mol Cell Cardiol* 34:1077-1089.

199. Mitra B, Panja M (2005) Myocardial metabolism: pharmacological manipulation in myocardial ischaemia. *J Assoc Physicians India* 53:552-560.

200. Lopaschuk GD (1998) Treating ischemic heart disease by pharmacologically improving cardiac energy metabolism. *Presse Med* 27:2100-2104.

201. Liu J, Wang P, He L, Li Y, Luo J, Cheng L, Qin Q, Brako LA, Lo WK, Lewis W, Yang Q (2011) Cardiomyocyte-Restricted Deletion of PPARbeta/delta in PPARalpha-Null Mice Causes Impaired Mitochondrial Biogenesis and Defense, but No Further Depression of Myocardial Fatty Acid Oxidation. *PPAR Res* 2011:372854.

202. Ingwall JS (2006) On the hypothesis that the failing heart is energy starved: lessons learned from the metabolism of ATP and creatine. *Curr Hypertens Rep* 8:457-464.

203. Hearse DJ (1979) Oxygen deprivation and early myocardial contractile failure: a reassessment of the possible role of adenosine triphosphate. *Am J Cardiol* 44:1115-1121.
204. Whitman GJ, Kieval RS, Seeholzer S, McDonald G, Simson MB, Harken AH (1985) Recovery of left ventricular function after graded cardiac ischemia as predicted by myocardial P-31 nuclear magnetic resonance. *Surgery* 97:428-435.
205. Ye Y, Gong G, Ochiai K, Liu J, Zhang J (2001) High-energy phosphate metabolism and creatine kinase in failing hearts: a new porcine model. *Circulation* 103:1570-1576.
206. Edwards LM, Ashrafian H, Korzeniewski B (2011) In silico studies on the sensitivity of myocardial PCr/ATP to changes in mitochondrial enzyme activity and oxygen concentration. *Mol Biosyst* 7:3335-3342.
207. Fragasso G, Perseghin G, De Cobelli F, Esposito A, Palloschi A, Lattuada G, Scifo P, Calori G, Del Maschio A, Margonato A (2006) Effects of metabolic modulation by trimetazidine on left ventricular function and phosphocreatine/adenosine triphosphate ratio in patients with heart failure. *Eur Heart J* 27:942-948.
208. Winter JL, Castro P, Meneses L, Chalhub M, Verdejo H, Greig D, Gabrielli L, Chiong M, Concepcion R, Mellado R, Hernandez C, Uribe S, Lavandero S (2010) Myocardial lipids and creatine measured by magnetic resonance spectroscopy among patients with heart failure. *Rev Med Chil* 138:1475-1479.
209. Hardy CJ, Weiss RG, Bottomley PA, Gerstenblith G (1991) Altered myocardial high-energy phosphate metabolites in patients with dilated cardiomyopathy. *Am Heart J* 122:795-801.
210. Neubauer S, Krahe T, Schindler R, Horn M, Hillenbrand H, Entzeroth C, Mader H, Kromer EP, Riegger GA, Lackner K (1992) ³¹P magnetic resonance spectroscopy in dilated cardiomyopathy and coronary artery disease. Altered cardiac high-energy phosphate metabolism in heart failure. *Circulation* 86:1810-1818.
211. Weiss RG, Bottomley PA, Hardy CJ, Gerstenblith G (1990) Regional myocardial metabolism of high-energy phosphates during isometric exercise in patients with coronary artery disease. *N Engl J Med* 323:1593-1600.
212. Yabe T, Mitsunami K, Inubushi T, Kinoshita M (1995) Quantitative measurements of cardiac phosphorus metabolites in coronary artery disease by ³¹P magnetic resonance spectroscopy. *Circulation* 92:15-23.

213. Tuunanen H, Engblom E, Naum A, Scheinin M, Nagren K, Airaksinen J, Nuutila P, Iozzo P, Ukkonen H, Knuuti J (2006) Decreased myocardial free fatty acid uptake in patients with idiopathic dilated cardiomyopathy: evidence of relationship with insulin resistance and left ventricular dysfunction. *J Card Fail* 12:644-652.
214. Bersin RM, Wolfe C, Kwasman M, Lau D, Klinski C, Tanaka K, Khorrami P, Henderson GN, de Marco T, Chatterjee K (1994) Improved hemodynamic function and mechanical efficiency in congestive heart failure with sodium dichloroacetate. *J Am Coll Cardiol* 23:1617-1624.
215. Hermann HP, Pieske B, Schwarzmuller E, Keul J, Just H, Hasenfuss G (1999) Haemodynamic effects of intracoronary pyruvate in patients with congestive heart failure: an open study. *Lancet* 353:1321-1323.
216. Liao R, Jain M, Cui L, D'Agostino J, Aiello F, Luptak I, Ngoy S, Mortensen RM, Tian R (2002) Cardiac-specific overexpression of GLUT1 prevents the development of heart failure attributable to pressure overload in mice. *Circulation* 106:2125-2131.
217. Ong HT, Ong LM, Kow FP (2012) Beta-blockers for heart failure: an evidence based review answering practical therapeutic questions. *Med J Malaysia* 67:7-11.
218. Dery AS, Hamilton LA, Starr JA (2011) Nebivolol for the treatment of heart failure. *Am J Health Syst Pharm* 68:879-886.
219. Riva N, Lip GY (2011) Nebivolol for the treatment of heart failure. *Expert Opin Investig Drugs* 20:1733-1746.
220. Klapholz M (2009) Beta-blocker use for the stages of heart failure. *Mayo Clin Proc* 84:718-729.
221. Masoud WG, Ussher JR, Wang W, Jaswal JS, Wagg CS, Dyck JR, Lygate CA, Neubauer S, Clanachan AS, Lopaschuk GD (2014) Failing mouse hearts utilize energy inefficiently and benefit from improved coupling of glycolysis and glucose oxidation. *Cardiovasc Res* 101:30-38.
222. Zhu P, Lu L, Xu Y, Schwartz GG (2000) Troglitazone improves recovery of left ventricular function after regional ischemia in pigs. *Circulation* 101:1165-1171.
223. Yue TL, Bao W, Gu JL, Cui J, Tao L, Ma XL, Ohlstein EH, Jucker BM (2005) Rosiglitazone treatment in Zucker diabetic Fatty rats is associated with ameliorated cardiac insulin resistance and protection from ischemia/reperfusion-induced myocardial injury. *Diabetes* 54:554-562.

224. Sidell RJ, Cole MA, Draper NJ, Desrois M, Buckingham RE, Clarke K (2002) Thiazolidinedione treatment normalizes insulin resistance and ischemic injury in the Zucker Fatty rat heart. *Diabetes* 51:1110-1117.
225. Schmitz FJ, Rosen P, Reinauer H (1995) Improvement of myocardial function and metabolism in diabetic rats by the carnitine palmitoyl transferase inhibitor Etomoxir. *Horm Metab Res* 27:515-522.
226. Abozguia K, Elliott P, McKenna W, Phan TT, Nallur-Shivu G, Ahmed I, Maher AR, Kaur K, Taylor J, Henning A, Ashrafian H, Watkins H, Frenneaux M (2010) Metabolic modulator perhexiline corrects energy deficiency and improves exercise capacity in symptomatic hypertrophic cardiomyopathy. *Circulation* 122:1562-1569.
227. Horowitz JD, Chirkov YY (2010) Perhexiline and hypertrophic cardiomyopathy: a new horizon for metabolic modulation. *Circulation* 122:1547-1549.
228. Lee L, Campbell R, Scheuermann-Freestone M, Taylor R, Gunaruwan P, Williams L, Ashrafian H, Horowitz J, Fraser AG, Clarke K, Frenneaux M (2005) Metabolic modulation with perhexiline in chronic heart failure: a randomized, controlled trial of short-term use of a novel treatment. *Circulation* 112:3280-3288.
229. Zhang L, Lu Y, Jiang H, Zhang L, Sun A, Zou Y, Ge J (2012) Additional use of trimetazidine in patients with chronic heart failure: a meta-analysis. *J Am Coll Cardiol* 59:913-922.
230. Fragasso G, Salerno A, Lattuada G, Cuko A, Calori G, Scollo A, Ragona F, Arioli F, Bassanelli G, Spoladore R, Luzi L, Margonato A, Perseghin G (2011) Effect of partial inhibition of fatty acid oxidation by trimetazidine on whole body energy metabolism in patients with chronic heart failure. *Heart* 97:1495-1500.
231. Gao D, Ning N, Niu X, Hao G, Meng Z (2011) Trimetazidine: a meta-analysis of randomised controlled trials in heart failure. *Heart* 97:278-286.
232. Wenmeng W, Qizhu T (2011) Early administration of trimetazidine may prevent or ameliorate diabetic cardiomyopathy. *Med Hypotheses* 76:181-183.
233. Gunes Y, Guntekin U, Tuncer M, Sahin M (2009) Improved left and right ventricular functions with trimetazidine in patients with heart failure: a tissue Doppler study. *Heart Vessels* 24:277-282.
234. Sisakian AS, Torgomian AL, Barkhudarian AL (2006) The effects of trimetazidine on left ventricular function and physical exercise tolerance in patients with ischemic cardiomyopathy. *Klin Med (Mosk)* 84:55-58.

235. Kolwicz SC, Jr, Olson DP, Marney LC, Garcia-Menendez L, Synovec RE, Tian R (2012) Cardiac-specific deletion of acetyl CoA carboxylase 2 prevents metabolic remodeling during pressure-overload hypertrophy. *Circ Res* 111:728-738.
236. Mori J, Basu R, McLean BA, Das SK, Zhang L, Patel VB, Wagg CS, Kassiri Z, Lopaschuk GD, Oudit GY (2012) Agonist-induced hypertrophy and diastolic dysfunction are associated with selective reduction in glucose oxidation: a metabolic contribution to heart failure with normal ejection fraction. *Circ Heart Fail* 5:493-503.
237. Herrmann G DG (1939) The chemical nature of heart failure. *Ann Intern Med* 12:1233-1244.
238. Gong G, Liu J, Liang P, Guo T, Hu Q, Ochiai K, Hou M, Ye Y, Wu X, Mansoor A, From AH, Ugurbil K, Bache RJ, Zhang J (2003) Oxidative capacity in failing hearts. *Am J Physiol Heart Circ Physiol* 285:H541-548.
239. Chandler MP, Kerner J, Huang H, Vazquez E, Reszko A, Martini WZ, Hoppel CL, Imai M, Rastogi S, Sabbah HN, Stanley WC (2004) Moderate severity heart failure does not involve a downregulation of myocardial fatty acid oxidation. *Am J Physiol Heart Circ Physiol* 287:H1538-543.
240. Degens H, de Brouwer KF, Gilde AJ, Lindhout M, Willemsen PH, Janssen BJ, van der Vusse GJ, van Bilsen M (2006) Cardiac fatty acid metabolism is preserved in the compensated hypertrophic rat heart. *Basic Res Cardiol* 101:17-26.
241. Garcia-Rua V, Otero MF, Lear PV, Rodriguez-Penas D, Feijoo-Bandin S, Noguera-Moreno T, Calaza M, Alvarez-Barredo M, Mosquera-Leal A, Parrington J, Brugada J, Portoles M, Rivera M, Gonzalez-Juanatey JR, Lago F (2012) Increased expression of Fatty-Acid and calcium metabolism genes in failing human heart. *PLoS One* 7:e37505.
242. Remondino A, Rosenblatt-Velin N, Montessuit C, Tardy I, Papageorgiou I, Dorsaz PA, Jorge-Costa M, Lerch R (2000) Altered expression of proteins of metabolic regulation during remodeling of the left ventricle after myocardial infarction. *J Mol Cell Cardiol* 32:2025-2034.
243. Nascimben L, Ingwall JS, Lorell BH, Pinz I, Schultz V, Tornheim K, Tian R (2004) Mechanisms for increased glycolysis in the hypertrophied rat heart. *Hypertension* 44:662-667.
244. Zhabyeyev P, Gandhi M, Mori J, Basu R, Kassiri Z, Clanachan A, Lopaschuk GD, Oudit GY (2013) Pressure-overload-induced heart failure induces

a selective reduction in glucose oxidation at physiological afterload. *Cardiovasc Res* 97:676-685.

245. Razeghi P, Young ME, Alcorn JL, Moravec CS, Frazier OH, Taegtmeier H (2001) Metabolic gene expression in fetal and failing human heart. *Circulation* 104:2923-2931.

246. Taylor M, Wallhaus TR, Degrado TR, Russell DC, Stanko P, Nickles RJ, Stone CK (2001) An evaluation of myocardial fatty acid and glucose uptake using PET with [18F]fluoro-6-thia-heptadecanoic acid and [18F]FDG in Patients with Congestive Heart Failure. *J Nucl Med* 42:55-62.

247. Fujii S (2013) Insulin resistance and heart failure: underlying molecular mechanisms and potential pharmacological solutions. *J Cardiovasc Pharmacol* 62:379-380.

248. Wong AK, Symon R, AlZadjali MA, Ang DS, Ogston S, Choy A, Petrie JR, Struthers AD, Lang CC (2012) The effect of metformin on insulin resistance and exercise parameters in patients with heart failure. *Eur J Heart Fail* 14:1303-1310.

249. Taegtmeier H, Beauloye C, Harmancey R, Hue L (2013) Insulin resistance protects the heart from fuel overload in dysregulated metabolic states. *Am J Physiol Heart Circ Physiol* 305:H1693-697.

250. Dutka DP, Pitt M, Pagano D, Mongillo M, Gathercole D, Bonser RS, Camici PG (2006) Myocardial glucose transport and utilization in patients with type 2 diabetes mellitus, left ventricular dysfunction, and coronary artery disease. *J Am Coll Cardiol* 48:2225-2231.

251. Amorim PA, Nguyen TD, Shingu Y, Schwarzer M, Mohr FW, Schrepper A, Doenst T (2010) Myocardial infarction in rats causes partial impairment in insulin response associated with reduced fatty acid oxidation and mitochondrial gene expression. *J Thorac Cardiovasc Surg* 140:1160-1167.

252. Doenst T, Pytel G, Schrepper A, Amorim P, Farber G, Shingu Y, Mohr FW, Schwarzer M (2010) Decreased rates of substrate oxidation ex vivo predict the onset of heart failure and contractile dysfunction in rats with pressure overload. *Cardiovasc Res* 86:461-470.

253. Bugger H, Schwarzer M, Chen D, Schrepper A, Amorim PA, Schoepe M, Nguyen TD, Mohr FW, Khalimonchuk O, Weimer BC, Doenst T (2010) Proteomic remodelling of mitochondrial oxidative pathways in pressure overload-induced heart failure. *Cardiovasc Res* 85:376-384.

254. Qanud K, Mamdani M, Pepe M, Khairallah RJ, Gravel J, Lei B, Gupte SA, Sharov VG, Sabbah HN, Stanley WC, Recchia FA (2008) Reverse changes in

- cardiac substrate oxidation in dogs recovering from heart failure. *Am J Physiol Heart Circ Physiol* 295:H2098-2105.
255. Lei B, Lionetti V, Young ME, Chandler MP, d'Agostino C, Kang E, Altarejos M, Matsuo K, Hintze TH, Stanley WC, Recchia FA (2004) Paradoxical downregulation of the glucose oxidation pathway despite enhanced flux in severe heart failure. *J Mol Cell Cardiol* 36:567-576.
256. Neglia D, De Caterina A, Marraccini P, Natali A, Ciardetti M, Vecoli C, Gastaldelli A, Ciociaro D, Pellegrini P, Testa R, Menichetti L, L'Abbate A, Stanley WC, Recchia FA (2007) Impaired myocardial metabolic reserve and substrate selection flexibility during stress in patients with idiopathic dilated cardiomyopathy. *Am J Physiol Heart Circ Physiol* 293:H3270-3278.
257. Tuunanen H, Engblom E, Naum A, Nagren K, Hesse B, Airaksinen KE, Nuutila P, Iozzo P, Ukkonen H, Opie LH, Knuuti J (2006) Free fatty acid depletion acutely decreases cardiac work and efficiency in cardiomyopathic heart failure. *Circulation* 114:2130-2137.
258. Degens H, de Brouwer KF, Gilde AJ, Lindhout M, Willemsen PH, Janssen BJ, van der Vusse GJ, van Bilsen M (2006) Cardiac fatty acid metabolism is preserved in the compensated hypertrophic rat heart. *Basic Res Cardiol* 101:17-26.
259. Kato T, Niizuma S, Inuzuka Y, Kawashima T, Okuda J, Tamaki Y, Iwanaga Y, Narazaki M, Matsuda T, Soga T, Kita T, Kimura T, Shioi T (2010) Analysis of metabolic remodeling in compensated left ventricular hypertrophy and heart failure. *Circ Heart Fail* 3:420-430.
260. de Brouwer KF, Degens H, Aartsen WM, Lindhout M, Bitsch NJ, Gilde AJ, Willemsen PH, Janssen BJ, van der Vusse GJ, van Bilsen M (2006) Specific and sustained down-regulation of genes involved in fatty acid metabolism is not a hallmark of progression to cardiac failure in mice. *J Mol Cell Cardiol* 40:838-845.
261. O'Donnell JM, Fields AD, Sorokina N, Lewandowski ED (2008) The absence of endogenous lipid oxidation in early stage heart failure exposes limits in lipid storage and turnover. *J Mol Cell Cardiol* 44:315-322.
262. Perrone-Filardi P, Bacharach SL, Dilsizian V, Panza JA, Maurea S, Bonow RO (1993) Regional systolic function, myocardial blood flow and glucose uptake at rest in hypertrophic cardiomyopathy. *Am J Cardiol* 72:199-204.
263. Grover-McKay M, Schwaiger M, Krivokapich J, Perloff JK, Phelps ME, Schelbert HR (1989) Regional myocardial blood flow and metabolism at rest in mildly symptomatic patients with hypertrophic cardiomyopathy. *J Am Coll Cardiol* 13:317-324.

264. Lommi J, Kupari M, Yki-Jarvinen H (1998) Free fatty acid kinetics and oxidation in congestive heart failure. *Am J Cardiol* 81:45-50.
265. Paolisso G, Gambardella A, Galzerano D, D'Amore A, Rubino P, Verza M, Teasuro P, Varricchio M, D'Onofrio F (1994) Total-body and myocardial substrate oxidation in congestive heart failure. *Metabolism* 43:174-179.
266. Taylor M, Wallhaus TR, Degrado TR, Russell DC, Stanko P, Nickles RJ, Stone CK (2001) An evaluation of myocardial fatty acid and glucose uptake using PET with [18F]fluoro-6-thia-heptadecanoic acid and [18F]FDG in Patients with Congestive Heart Failure. *J Nucl Med* 42:55-62.
267. Leong HS, Brownsey RW, Kulpa JE, Allard MF (2003) Glycolysis and pyruvate oxidation in cardiac hypertrophy--why so unbalanced?. *Comp Biochem Physiol A Mol Integr Physiol* 135:499-513.
268. Wang Y, Li C, Chuo W, Liu Z, Ouyang Y, Li D, Han J, Wu Y, Guo S, Wang W (2013) Integrated proteomic and metabolomic analysis reveals the NADH-mediated TCA cycle and energy metabolism disorders based on a new model of chronic progressive heart failure. *Mol Biosyst* 9:3135-3145.
269. Osterholt M, Nguyen TD, Schwarzer M, Doenst T (2013) Alterations in mitochondrial function in cardiac hypertrophy and heart failure. *Heart Fail Rev* 18:645-656.
270. Quigley AF, Kapsa RM, Esmore D, Hale G, Byrne E (2000) Mitochondrial respiratory chain activity in idiopathic dilated cardiomyopathy. *J Card Fail* 6:47-55.
271. Casademont J, Miro O (2002) Electron transport chain defects in heart failure. *Heart Fail Rev* 7:131-139.
272. Murray AJ, Anderson RE, Watson GC, Radda GK, Clarke K (2004) Uncoupling proteins in human heart. *Lancet* 364:1786-1788.
273. Taegtmeyer H (2000) Genetics of energetics: transcriptional responses in cardiac metabolism. *Ann Biomed Eng* 28:871-876.
274. Davies MJ (2000) The pathophysiology of acute coronary syndromes. *Heart* 83:361-366.
275. Haeck JD, Verouden NJ, Henriques JP, Koch KT (2009) Current status of distal embolization in percutaneous coronary intervention: mechanical and pharmacological strategies. *Future Cardiol* 5:385-402.

276. Ghadri JR, Ruschitzka F, Luscher TF, Templin C (2014) Prinzmetal angina. *QJM* 107:375-377.
277. Safi AM, Rachko M, Tang A, Ketosugbo A, Kwan T, Afflu E (2001) Anomalous origin of the left main coronary artery from the right sinus of Valsalva: disabling angina and syncope with noninterarterial courses case report of two patients. *Heart Dis* 3:24-27.
278. Vianna CB, Gonzalez MM, Dallan LA, Shiozaki AA, Medeiros FM, Britto PC, Cesar LA (2007) Anomalous coronary artery causing transmural ischaemia and ventricular tachycardia in a high school athlete. *Resuscitation* 74:183-186.
279. Karim S, Young T, Reilly JR, Delaney P (2013) Anomalous left main coronary artery causing a myocardial infarction in a 14-year-old boy. *J La State Med Soc* 165:319-323.
280. Bainey KR, Armstrong PW (2014) Clinical perspectives on reperfusion injury in acute myocardial infarction. *Am Heart J* 167:637-645.
281. Duicu OM, Angoulvant D, Muntean DM (2013) Cardioprotection against myocardial reperfusion injury: successes, failures, and perspectives. *Can J Physiol Pharmacol* 91:657-662.
282. Vander Heide RS, Steenbergen C (2013) Cardioprotection and myocardial reperfusion: pitfalls to clinical application. *Circ Res* 113:464-477.
283. Raedschelders K, Ansley DM, Chen DD (2012) The cellular and molecular origin of reactive oxygen species generation during myocardial ischemia and reperfusion. *Pharmacol Ther* 133:230-255.
284. Clanachan AS (2006) Contribution of protons to post-ischemic Na⁽⁺⁾ and Ca⁽²⁺⁾ overload and left ventricular mechanical dysfunction. *J Cardiovasc Electrophysiol* 17 Suppl 1:S141-S148.
285. Andrews DT, Royse C, Royse AG (2012) The mitochondrial permeability transition pore and its role in anaesthesia-triggered cellular protection during ischaemia-reperfusion injury. *Anaesth Intensive Care* 40:46-70.
286. Murphy E, Steenbergen C (2008) Ion transport and energetics during cell death and protection. *Physiology (Bethesda)* 23:115-123.
287. Gabel SA, Cross HR, London RE, Steenbergen C, Murphy E (1997) Decreased intracellular pH is not due to increased H⁺ extrusion in preconditioned rat hearts. *Am J Physiol* 273:H2257-2262.

288. Murphy E, Steenbergen C (2008) Mechanisms underlying acute protection from cardiac ischemia-reperfusion injury. *Physiol Rev* 88:581-609.
289. Murphy E, Perlman M, London RE, Steenbergen C (1991) Amiloride delays the ischemia-induced rise in cytosolic free calcium. *Circ Res* 68:1250-1258.
290. Vaughan-Jones RD, Spitzer KW (2002) Role of bicarbonate in the regulation of intracellular pH in the mammalian ventricular myocyte. *Biochem Cell Biol* 80:579-596.
291. Light PE, Wallace CH, Dyck JR (2003) Constitutively active adenosine monophosphate-activated protein kinase regulates voltage-gated sodium channels in ventricular myocytes. *Circulation* 107:1962-1965.
292. Wagner S, Ruff HM, Weber SL, Bellmann S, Sowa T, Schulte T, Anderson ME, Grandi E, Bers DM, Backs J, Belardinelli L, Maier LS (2011) Reactive oxygen species-activated Ca/calmodulin kinase II δ is required for late I(Na) augmentation leading to cellular Na and Ca overload. *Circ Res* 108:555-565.
293. Song Y, Shryock JC, Wagner S, Maier LS, Belardinelli L (2006) Blocking late sodium current reduces hydrogen peroxide-induced arrhythmogenic activity and contractile dysfunction. *J Pharmacol Exp Ther* 318:214-222.
294. Ward CA, Giles WR (1997) Ionic mechanism of the effects of hydrogen peroxide in rat ventricular myocytes. *J Physiol* 500 (Pt 3):631-642.
295. Belardinelli L, Shryock JC, Fraser H (2006) Inhibition of the late sodium current as a potential cardioprotective principle: effects of the late sodium current inhibitor ranolazine. *Heart* 92 Suppl 4:iv6-iv14.
296. Imahashi K, Pott C, Goldhaber JJ, Steenbergen C, Philipson KD, Murphy E (2005) Cardiac-specific ablation of the Na⁺-Ca²⁺ exchanger confers protection against ischemia/reperfusion injury. *Circ Res* 97:916-921.
297. Dong Z, Saikumar P, Weinberg JM, Venkatachalam MA (2006) Calcium in cell injury and death. *Annu Rev Pathol* 1:405-434.
298. Robertson RP, Porte D, Jr (1973) Adrenergic modulation of basal insulin secretion in man. *Diabetes* 22:1-8.
299. Lerner RL, Porte D, Jr (1971) Epinephrine: selective inhibition of the acute insulin response to glucose. *J Clin Invest* 50:2453-2457.
300. Christensen NJ, Videbaek J (1974) Plasma catecholamines and carbohydrate metabolism in patients with acute myocardial infarction. *J Clin Invest* 54:278-286.

301. Rizza RA, Mandarino LJ, Gerich JE (1982) Cortisol-induced insulin resistance in man: impaired suppression of glucose production and stimulation of glucose utilization due to a postreceptor defect of insulin action. *J Clin Endocrinol Metab* 54:131-138.
302. Mueller HS, Ayres SM (1980) Propranolol decreases sympathetic nervous activity reflected by plasma catecholamines during evolution of myocardial infarction in man. *J Clin Invest* 65:338-346.
303. Renstrom B, Liedtke AJ, Nellis SH (1990) Mechanisms of substrate preference for oxidative metabolism during early myocardial reperfusion. *Am J Physiol* 259:H317-323.
304. Liedtke AJ, Nellis SH, Mjos OD (1984) Effects of reducing fatty acid metabolism on mechanical function in regionally ischemic hearts. *Am J Physiol* 247:H387-394.
305. Lloyd SG, Wang P, Zeng H, Chatham JC (2004) Impact of low-flow ischemia on substrate oxidation and glycolysis in the isolated perfused rat heart. *Am J Physiol Heart Circ Physiol* 287:H351-362.
306. Wang P, Lloyd SG, Zeng H, Bonen A, Chatham JC (2005) Impact of altered substrate utilization on cardiac function in isolated hearts from Zucker diabetic fatty rats. *Am J Physiol Heart Circ Physiol* 288:H2102-2110.
307. Folmes CD, Sowah D, Clanachan AS, Lopaschuk GD (2009) High rates of residual fatty acid oxidation during mild ischemia decrease cardiac work and efficiency. *J Mol Cell Cardiol* 47:142-148.
308. Whitmer JT, Idell-Wenger JA, Rovetto MJ, Neely JR (1978) Control of fatty acid metabolism in ischemic and hypoxic hearts. *J Biol Chem* 253:4305-4309.
309. Neely JR, Feuvray D (1981) Metabolic products and myocardial ischemia. *Am J Pathol* 102:282-291.
310. Lopaschuk GD, Saddik M (1992) The relative contribution of glucose and fatty acids to ATP production in hearts reperfused following ischemia. *Mol Cell Biochem* 116:111-116.
311. Lopaschuk GD, Saddik M, Barr R, Huang L, Barker CC, Muzyka RA (1992) Effects of high levels of fatty acids on functional recovery of ischemic hearts from diabetic rats. *Am J Physiol* 263:E1046-1053.
312. Idell-Wenger JA, Grotyohann LW, Neely JR (1978) Coenzyme A and carnitine distribution in normal and ischemic hearts. *J Biol Chem* 253:4310-4318.

313. Jennings RB, Reimer KA (1991) The cell biology of acute myocardial ischemia. *Annu Rev Med* 42:225-246.
314. Pantos C, Mourouzis I, Dimopoulos A, Markakis K, Panagiotou M, Xinaris C, Tzeis S, Kokkinos AD, Cokkinos DV (2007) Enhanced tolerance of the rat myocardium to ischemia and reperfusion injury early after acute myocardial infarction. *Basic Res Cardiol* 102:327-333.
315. Kalkman EA, Saxena PR, Schoemaker RG (1996) Sensitivity to ischemia of chronically infarcted rat hearts; effects of long-term captopril treatment. *Eur J Pharmacol* 298:121-128.
316. Sharikabad MN, Aronsen JM, Haugen E, Pedersen J, Moller AS, Mork HK, Aass HC, Sejersted OM, Sjaastad I, Brors O (2009) Cardiomyocytes from postinfarction failing rat hearts have improved ischemia tolerance. *Am J Physiol Heart Circ Physiol* 296:H787-795.
317. Liu Q, Docherty JC, Rendell JC, Clanachan AS, Lopaschuk GD (2002) High levels of fatty acids delay the recovery of intracellular pH and cardiac efficiency in post-ischemic hearts by inhibiting glucose oxidation. *J Am Coll Cardiol* 39:718-725.
318. Omar MA, Wang L, Clanachan AS (2010) Cardioprotection by GSK-3 inhibition: role of enhanced glycogen synthesis and attenuation of calcium overload. *Cardiovasc Res* 86:478-486.
319. Masoud WT, Clanachan A, Lopaschuk G (2013) The Failing Heart: Is It an Inefficient Engine or an Engine Out of Fuel?. In: Jugdutt BI, Dhalla NS (eds) *Cardiac Remodeling*. Springer New York, pp 65-84.
320. Skierczynska A, Beresewicz A (2010) Demand-induced ischemia in volume expanded isolated rat heart; the effect of dichloroacetate and trimetazidine. *J Physiol Pharmacol* 61:153-162.
321. Belardinelli R, Cianci G, Gigli M, Mazzanti M, Lacalaprice F (2008) Effects of trimetazidine on myocardial perfusion and left ventricular systolic function in type 2 diabetic patients with ischemic cardiomyopathy. *J Cardiovasc Pharmacol* 51:611-615.
322. Ussher JR, Wang W, Gandhi M, Keung W, Samokhvalov V, Oka T, Wagg CS, Jaswal JS, Harris RA, Clanachan AS, Dyck JR, Lopaschuk GD (2012) Stimulation of glucose oxidation protects against acute myocardial infarction and reperfusion injury. *Cardiovasc Res* 94:359-369.

323. Fillmore N, Mori J, Lopaschuk GD (2014) Mitochondrial fatty acid oxidation alterations in heart failure, ischaemic heart disease and diabetic cardiomyopathy. *Br J Pharmacol* 171:2080-2090.
324. Ussher JR, Koves TR, Jaswal JS, Zhang L, Ilkayeva O, Dyck JR, Muoio DM, Lopaschuk GD (2009) Insulin-stimulated cardiac glucose oxidation is increased in high-fat diet-induced obese mice lacking malonyl CoA decarboxylase. *Diabetes* 58:1766-1775.
325. Jaswal JS, Gandhi M, Finegan BA, Dyck JR, Clanachan AS (2007) Inhibition of p38 MAPK and AMPK restores adenosine-induced cardioprotection in hearts stressed by antecedent ischemia by altering glucose utilization. *Am J Physiol Heart Circ Physiol* 293:H1107-1114.
326. Rosano GM, Fini M, Caminiti G, Barbaro G (2008) Cardiac metabolism in myocardial ischemia. *Curr Pharm Des* 14:2551-2562.
327. Aasum E, Hafstad AD, Larsen TS (2003) Changes in substrate metabolism in isolated mouse hearts following ischemia-reperfusion. *Mol Cell Biochem* 249:97-103.
328. Finegan BA, Lopaschuk GD, Gandhi M, Clanachan AS (1996) Inhibition of glycolysis and enhanced mechanical function of working rat hearts as a result of adenosine A1 receptor stimulation during reperfusion following ischaemia. *Br J Pharmacol* 118:355-363.
329. Liu B, Clanachan AS, Schulz R, Lopaschuk GD (1996) Cardiac efficiency is improved after ischemia by altering both the source and fate of protons. *Circ Res* 79:940-948.
330. Finegan BA, Lopaschuk GD, Gandhi M, Clanachan AS (1995) Ischemic preconditioning inhibits glycolysis and proton production in isolated working rat hearts. *Am J Physiol* 269:H1767-1775.
331. Finegan BA, Lopaschuk GD, Coulson CS, Clanachan AS (1993) Adenosine alters glucose use during ischemia and reperfusion in isolated rat hearts. *Circulation* 87:900-908.
332. Madonna R, De Caterina R (2013) Sodium-hydrogen exchangers (NHE) in human cardiovascular diseases: interfering strategies and their therapeutic applications. *Vascul Pharmacol* 59:127-130.
333. Wakabayashi S, Hisamitsu T, Nakamura TY (2013) Regulation of the cardiac Na⁽⁺⁾/H⁽⁺⁾ exchanger in health and disease. *J Mol Cell Cardiol* 61:68-76.

334. Mraiche F, Wagg CS, Lopaschuk GD, Fliegel L (2011) Elevated levels of activated NHE1 protect the myocardium and improve metabolism following ischemia/reperfusion injury. *J Mol Cell Cardiol* 50:157-164.
335. Liu H, Cala PM, Anderson SE (2010) Na/H exchange inhibition protects newborn heart from ischemia/reperfusion injury by limiting Na⁺-dependent Ca²⁺ overload. *J Cardiovasc Pharmacol* 55:227-233.
336. MacDonald AC, Howlett SE (2008) Differential effects of the sodium calcium exchange inhibitor, KB-R7943, on ischemia and reperfusion injury in isolated guinea pig ventricular myocytes. *Eur J Pharmacol* 580:214-223.
337. Wei GZ, Zhou JJ, Wang B, Wu F, Bi H, Wang YM, Yi DH, Yu SQ, Pei JM (2007) Diastolic Ca²⁺ overload caused by Na⁺/Ca²⁺ exchanger during the first minutes of reperfusion results in continued myocardial stunning. *Eur J Pharmacol* 572:1-11.
338. Yeung HM, Kravtsov GM, Ng KM, Wong TM, Fung ML (2007) Chronic intermittent hypoxia alters Ca²⁺ handling in rat cardiomyocytes by augmented Na⁺/Ca²⁺ exchange and ryanodine receptor activities in ischemia-reperfusion. *Am J Physiol Cell Physiol* 292:C2046-2056.
339. Clanachan AS, Jaswal JS, Gandhi M, Bottorff DA, Coughlin J, Finegan BA, Stone JC (2003) Effects of inhibition of myocardial extracellular-responsive kinase and P38 mitogen-activated protein kinase on mechanical function of rat hearts after prolonged hypothermic ischemia. *Transplantation* 75:173-180.
340. Fraser H, Lopaschuk GD, Clanachan AS (1999) Alteration of glycogen and glucose metabolism in ischaemic and post-ischaemic working rat hearts by adenosine A1 receptor stimulation. *Br J Pharmacol* 128:197-205.
341. Liu B, el Alaoui-Talibi Z, Clanachan AS, Schulz R, Lopaschuk GD (1996) Uncoupling of contractile function from mitochondrial TCA cycle activity and MVO₂ during reperfusion of ischemic hearts. *Am J Physiol* 270:H72-80.
342. Paiva MA, Rutter-Locher Z, Goncalves LM, Providencia LA, Davidson SM, Yellon DM, Mocanu MM (2011) Enhancing AMPK activation during ischemia protects the diabetic heart against reperfusion injury. *Am J Physiol Heart Circ Physiol* 300:H2123-2134.
343. Saeedi R, Grist M, Wambolt RB, Bescond-Jacquet A, Lucien A, Allard MF (2005) Trimetazidine normalizes postischemic function of hypertrophied rat hearts. *J Pharmacol Exp Ther* 314:446-454.
344. Vitale C, Wajngaten M, Sposato B, Gebara O, Rossini P, Fini M, Volterrani M, Rosano GM (2004) Trimetazidine improves left ventricular function and

quality of life in elderly patients with coronary artery disease. *Eur Heart J* 25:1814-1821.

345. Fragasso G, Piatti Md PM, Monti L, Palloshi A, Setola E, Puccetti P, Calori G, Lopaschuk GD, Margonato A (2003) Short- and long-term beneficial effects of trimetazidine in patients with diabetes and ischemic cardiomyopathy. *Am Heart J* 146:E18.

346. Rosano GM, Vitale C, Sposato B, Mercurio G, Fini M (2003) Trimetazidine improves left ventricular function in diabetic patients with coronary artery disease: a double-blind placebo-controlled study. *Cardiovasc Diabetol* 2:16.

347. Belardinelli R (2000) Trimetazidine and the contractile response of dysfunctional myocardium in ischaemic cardiomyopathy. *Rev Port Cardiol* 19 Suppl 5:V35-39.

348. Kantor PF, Lucien A, Kozak R, Lopaschuk GD (2000) The antianginal drug trimetazidine shifts cardiac energy metabolism from fatty acid oxidation to glucose oxidation by inhibiting mitochondrial long-chain 3-ketoacyl coenzyme A thiolase. *Circ Res* 86:580-588.

349. Lu C, Dabrowski P, Fragasso G, Chierchia SL (1998) Effects of trimetazidine on ischemic left ventricular dysfunction in patients with coronary artery disease. *Am J Cardiol* 82:898-901.

350. Lopaschuk GD, McNeil GF, McVeigh JJ (1989) Glucose oxidation is stimulated in reperfused ischemic hearts with the carnitine palmitoyltransferase 1 inhibitor, Etomoxir. *Mol Cell Biochem* 88:175-179.

351. Whitehouse S, Cooper RH, Randle PJ (1974) Mechanism of activation of pyruvate dehydrogenase by dichloroacetate and other halogenated carboxylic acids. *Biochem J* 141:761-774.

352. Denton RM, Randle PJ, Bridges BJ, Cooper RH, Kerbey AL, Pask HT, Severson DL, Stansbie D, Whitehouse S (1975) Regulation of mammalian pyruvate dehydrogenase. *Mol Cell Biochem* 9:27-53.

353. Kerbey AL, Randle PJ, Cooper RH, Whitehouse S, Pask HT, Denton RM (1976) Regulation of pyruvate dehydrogenase in rat heart. Mechanism of regulation of proportions of dephosphorylated and phosphorylated enzyme by oxidation of fatty acids and ketone bodies and of effects of diabetes: role of coenzyme A, acetyl-coenzyme A and reduced and oxidized nicotinamide-adenine dinucleotide. *Biochem J* 154:327-348.

354. Matsuoka S, Toshima K, Naito E, Nakatsu T, Miyauchi Y, Kuroda Y, Miyao M (1987) Effects of dichloroacetate on the mechanical function of the isolated ischemic heart. *Jpn Heart J* 28:531-537.
355. Racey-Burns LA, Burns AH, Summer WR, Shepherd RE (1989) The effect of dichloroacetate on the isolated no flow arrested rat heart. *Life Sci* 44:2015-2023.
356. Burns AH, Summer WR, Burns LA, Shepherd RE (1988) Inotropic interactions of dichloroacetate with amrinone and ouabain in isolated hearts from endotoxin-shocked rats. *J Cardiovasc Pharmacol* 11:379-386.
357. Neely JR, Grotyohann LW (1984) Role of glycolytic products in damage to ischemic myocardium. Dissociation of adenosine triphosphate levels and recovery of function of reperfused ischemic hearts. *Circ Res* 55:816-824.
358. Griffin JL, White LT, Lewandowski ED (2000) Substrate-dependent proton load and recovery of stunned hearts during pyruvate dehydrogenase stimulation. *Am J Physiol Heart Circ Physiol* 279:H361-367.
359. Orchard CH, Kentish JC (1990) Effects of changes of pH on the contractile function of cardiac muscle. *Am J Physiol* 258:C967-981.
360. Schaefer S, Schwartz GG, Gober JR, Wong AK, Camacho SA, Massie B, Weiner MW (1990) Relationship between myocardial metabolites and contractile abnormalities during graded regional ischemia. Phosphorus-31 nuclear magnetic resonance studies of porcine myocardium in vivo. *J Clin Invest* 85:706-713.
361. Allard MF, Emanuel PG, Russell JA, Bishop SP, Digerness SB, Anderson PG (1994) Preischemic glycogen reduction or glycolytic inhibition improves postischemic recovery of hypertrophied rat hearts. *Am J Physiol* 267:H66-74.
362. Burns AH, Giaimo ME, Summer WR (1986) Dichloroacetic acid improves in vitro myocardial function following in vivo endotoxin administration. *J Crit Care* 1:11-17.
363. Schofield RS, Hill JA (2001) Role of metabolically active drugs in the management of ischemic heart disease. *Am J Cardiovasc Drugs* 1:23-35.
364. Wahr JA, Childs KF, Bolling SF (1994) Dichloroacetate enhances myocardial functional and metabolic recovery following global ischemia. *J Cardiothorac Vasc Anesth* 8:192-197.
365. Mizushima M (1990) Effects of dichloroacetate in the ischemic heart. Analysis of hemodynamics, myocardial energy metabolism and myocardial pH. *Hokkaido Igaku Zasshi* 65:298-310.

366. Opie LH (1975) Metabolism of free fatty acids, glucose and catecholamines in acute myocardial infarction. Relation to myocardial ischemia and infarct size. *Am J Cardiol* 36:938-953.
367. Taniguchi M, Wilson C, Hunter CA, Pehowich DJ, Clanachan AS, Lopaschuk GD (2001) Dichloroacetate improves cardiac efficiency after ischemia independent of changes in mitochondrial proton leak. *Am J Physiol Heart Circ Physiol* 280:H1762-1769.
368. McVeigh JJ, Lopaschuk GD (1990) Dichloroacetate stimulation of glucose oxidation improves recovery of ischemic rat hearts. *Am J Physiol* 259:H1079-1085.
369. Gandhi M, Finegan BA, Clanachan AS (2008) Role of glucose metabolism in the recovery of postischemic LV mechanical function: effects of insulin and other metabolic modulators. *Am J Physiol Heart Circ Physiol* 294:H2576-2586.
370. Lopaschuk GD, Wambolt RB, Barr RL (1993) An imbalance between glycolysis and glucose oxidation is a possible explanation for the detrimental effects of high levels of fatty acids during aerobic reperfusion of ischemic hearts. *J Pharmacol Exp Ther* 264:135-144.
371. Saddik M, Gamble J, Witters LA, Lopaschuk GD (1993) Acetyl-CoA carboxylase regulation of fatty acid oxidation in the heart. *J Biol Chem* 268:25836-25845.
372. Latipaa PM, Hiltunen JK, Peuhkurinen KJ, Hassinen IE (1983) Regulation of fatty acid oxidation in heart muscle. Effects of pyruvate and dichloroacetate. *Biochim Biophys Acta* 752:162-171.
373. McAllister A, Allison SP, Randle PJ (1973) Effects of dichloroacetate on the metabolism of glucose, pyruvate, acetate, 3-hydroxybutyrate and palmitate in rat diaphragm and heart muscle in vitro and on extraction of glucose, lactate, pyruvate and free fatty acids by dog heart in vivo. *Biochem J* 134:1067-1081.
374. Mjos OD, Miller NE, Riemersma RA, Oliver MF (1976) Effects of dichloroacetate on myocardial substrate extraction, epicardial ST-segment elevation, and ventricular blood flow following coronary occlusion in dogs. *Cardiovasc Res* 10:427-436.
375. Stacpoole PW, Felts JM (1970) Diisopropylammonium dichloroacetate (DIPA) and sodium dichloroacetate (DCA): effect on glucose and fat metabolism in normal and diabetic tissue. *Metabolism* 19:71-78.

376. Forsey RG, Reid K, Brosnan JT (1987) Competition between fatty acids and carbohydrate or ketone bodies as metabolic fuels for the isolated perfused heart. *Can J Physiol Pharmacol* 65:401-406.
377. Sakai K, Ichihara K, Nasa Y, Kamigaki M, Abiko Y (1990) Dichloroacetate attenuates myocardial acidosis and metabolic changes induced by partial occlusion of the coronary artery in dogs. *Arch Int Pharmacodyn Ther* 307:92-108.
378. Ludvik B, Peer G, Berzlanovich A, Stifter S, Graf H (1991) Effects of dichloroacetate and bicarbonate on haemodynamic parameters in healthy volunteers. *Clin Sci (Lond)* 80:47-51.
379. Wargovich TJ, MacDonald RG, Hill JA, Feldman RL, Stacpoole PW, Pepine CJ (1988) Myocardial metabolic and hemodynamic effects of dichloroacetate in coronary artery disease. *Am J Cardiol* 61:65-70.
380. Kato M, Li J, Chuang JL, Chuang DT (2007) Distinct structural mechanisms for inhibition of pyruvate dehydrogenase kinase isoforms by AZD7545, dichloroacetate, and radicicol. *Structure* 15:992-1004.
381. Kolk MV, Meyberg D, Deuse T, Tang-Quan KR, Robbins RC, Reichenspurner H, Schrepfer S (2009) LAD-ligation: a murine model of myocardial infarction. *J Vis Exp* (32). pii: 1438. doi:10.3791/1438.
382. Virag JA, Lust RM (2011) Coronary artery ligation and intramyocardial injection in a murine model of infarction. *J Vis Exp* (52). pii: 2581. doi:10.3791/2581.
383. Stasiak KL, Maul D, French E, Hellyer PW, VandeWoude S (2003) Species-specific assessment of pain in laboratory animals. *Contemp Top Lab Anim Sci* 42:13-20.
384. Ommen SR, Nishimura RA, Appleton CP, Miller FA, Oh JK, Redfield MM, Tajik AJ (2000) Clinical utility of Doppler echocardiography and tissue Doppler imaging in the estimation of left ventricular filling pressures: A comparative simultaneous Doppler-catheterization study. *Circulation* 102:1788-1794.
385. Nagueh SF, Mikati I, Kopelen HA, Middleton KJ, Quinones MA, Zoghbi WA (1998) Doppler estimation of left ventricular filling pressure in sinus tachycardia. A new application of tissue doppler imaging. *Circulation* 98:1644-1650.
386. Barr RL, Lopaschuk GD (1997) Direct measurement of energy metabolism in the isolated working rat heart. *J Pharmacol Toxicol Methods* 38:11-17.

387. Folmes CD, Clanachan AS, Lopaschuk GD (2006) Fatty acids attenuate insulin regulation of 5'-AMP-activated protein kinase and insulin cardioprotection after ischemia. *Circ Res* 99:61-68.
388. Jaswal JS, Gandhi M, Finegan BA, Dyck JR, Clanachan AS (2006) Effects of adenosine on myocardial glucose and palmitate metabolism after transient ischemia: role of 5'-AMP-activated protein kinase. *Am J Physiol Heart Circ Physiol* 291:H1883-892.
389. Atkinson LL, Kozak R, Kelly SE, Onay Besikci A, Russell JC, Lopaschuk GD (2003) Potential mechanisms and consequences of cardiac triacylglycerol accumulation in insulin-resistant rats. *Am J Physiol Endocrinol Metab* 284:E923-930.
390. Laemmli UK (1970) Cleavage of structural proteins during the assembly of the head of bacteriophage T4. *Nature* 227:680-685.
391. Romero-Calvo I, Ocon B, Martinez-Moya P, Suarez MD, Zarzuelo A, Martinez-Augustin O, de Medina FS (2010) Reversible Ponceau staining as a loading control alternative to actin in Western blots. *Anal Biochem* 401:318-320.
392. Sikk, P., Käämbre, T., Vija, H., Tepp, K., Tiivel, T., Nutt, A., Saks, V. (2009) Ultra performance liquid chromatography analysis of adenine nucleotides and creatine derivatives for kinetic studies. *Proceedings of the Estonian Academy of Science* 58 (2):122-131.
393. Idikio HA (2011) Postmyocardial infarct remodeling and heart failure: potential contributions from pro- and antiaging factors. *Cardiol Res Pract* 2011:836806.
394. Rolande DM, Fantini JP, Cardinalli Neto A, Cordeiro JA, Bestetti RB (2012) Prognostic determinants of patients with chronic systolic heart failure secondary to systemic arterial hypertension. *Arq Bras Cardiol* 98:76-84.
395. Takeda Y, Sakata Y, Mano T, Ohtani T, Kamimura D, Tamaki S, Omori Y, Tsukamoto Y, Aizawa Y, Komuro I, Yamamoto K (2011) Competing risks of heart failure with preserved ejection fraction in diabetic patients. *Eur J Heart Fail* 13:664-669.
396. Kemi OJ, Arbo I, Hoydal MA, Loennechen JP, Wisloff U, Smith GL, Ellingsen O (2006) Reduced pH and contractility in failing rat cardiomyocytes. *Acta Physiol (Oxf)* 188:185-193.
397. Ussher JR, Koves TR, Jaswal JS, Zhang L, Ilkayeva O, Dyck JR, Muoio DM, Lopaschuk GD (2009) Insulin-stimulated cardiac glucose oxidation is

increased in high-fat diet-induced obese mice lacking malonyl CoA decarboxylase. *Diabetes* 58:1766-1775.

398. Rubin SA, Fishbein MC, Swan HJ (1983) Compensatory hypertrophy in the heart after myocardial infarction in the rat. *J Am Coll Cardiol* 1:1435-1441.

399. Herrmann G, Decherd G (1939) The chemical nature of heart failure. *Ann Int Med* 12(8):1233-1244.

400. Weiss RG, Gerstenblith G, Bottomley PA (2005) ATP flux through creatine kinase in the normal, stressed, and failing human heart. *Proc Natl Acad Sci U S A* 102:808-813.

401. Lionetti V, Linke A, Chandler MP, Young ME, Penn MS, Gupte S, d'Agostino C, Hintze TH, Stanley WC, Recchia FA (2005) Carnitine palmitoyl transferase-I inhibition prevents ventricular remodeling and delays decompensation in pacing-induced heart failure. *Cardiovasc Res* 66:454-461.

402. Shimizu J, Yamashita D, Misawa H, Tohne K, Matsuoka S, Kim B, Takeuchi A, Nakajima-Takenaka C, Takaki M (2009) Increased O₂ consumption in excitation-contraction coupling in hypertrophied rat heart slices related to increased Na⁺-Ca²⁺ exchange activity. *J Physiol Sci* 59:63-74.

403. Zoll J, Ponsot E, Doutreleau S, Mettauer B, Piquard F, Mazzucotelli JP, Diemunsch P, Geny B (2005) Acute myocardial ischaemia induces specific alterations of ventricular mitochondrial function in experimental pigs. *Acta Physiol Scand* 185:25-32.

404. Harmancey R, Lam TN, Lubrano GM, Guthrie PH, Vela D, Taegtmeyer H (2012) Insulin resistance improves metabolic and contractile efficiency in stressed rat heart. *FASEB J* 26:3118-3126.

405. Sanada S, Komuro I, Kitakaze M (2011) Pathophysiology of myocardial reperfusion injury: preconditioning, postconditioning, and translational aspects of protective measures. *Am J Physiol Heart Circ Physiol* 301:H1723-741.

406. Ofir M, Arad M, Porat E, Freimark D, Chepurko Y, Vidne BA, Seidman CE, Seidman JG, Kemp BE, Hochhauser E (2008) Increased glycogen stores due to gamma-AMPK overexpression protects against ischemia and reperfusion damage. *Biochem Pharmacol* 75:1482-1491.

407. Barillas R, Friehs I, Cao-Danh H, Martinez JF, del Nido PJ (2007) Inhibition of glycogen synthase kinase-3beta improves tolerance to ischemia in hypertrophied hearts. *Ann Thorac Surg* 84:126-133.

408. Weiss RG, de Albuquerque CP, Vandegaer K, Chacko VP, Gerstenblith G (1996) Attenuated glycogenolysis reduces glycolytic catabolite accumulation during ischemia in preconditioned rat hearts. *Circ Res* 79:435-446.
409. Vogt AM, Elsasser A, Pott-Beckert A, Ackermann C, Vetter SY, Yildiz M, Schoels W, Fell DA, Katus HA, Kubler W (2005) Myocardial energy metabolism in ischemic preconditioning and cardioplegia: a metabolic control analysis. *Mol Cell Biochem* 278:223-232.
410. Miki T, Miura T, Tanno M, Sakamoto J, Kuno A, Genda S, Matsumoto T, Ichikawa Y, Shimamoto K (2003) Interruption of signal transduction between G protein and PKC-epsilon underlies the impaired myocardial response to ischemic preconditioning in postinfarct remodeled hearts. *Mol Cell Biochem* 247:185-193.
411. Miki T, Miura T, Tsuchida A, Nakano A, Hasegawa T, Fukuma T, Shimamoto K (2001) Cardioprotective mechanism of ischemic preconditioning is impaired by postinfarct ventricular remodeling through angiotensin II type 1 receptor activation. *J Cardiol* 37:112-113.
412. Miki T, Miura T, Tanno M, Nishihara M, Naitoh K, Sato T, Takahashi A, Shimamoto K (2007) Impairment of cardioprotective PI3K-Akt signaling by postinfarct ventricular remodeling is compensated by an ERK-mediated pathway. *Basic Res Cardiol* 102:163-170.
413. Lopaschuk GD (2008) AMP-activated protein kinase control of energy metabolism in the ischemic heart. *Int J Obes (Lond)* 32 Suppl 4:S29-35.
414. Heather LC, Pates KM, Atherton HJ, Cole MA, Ball DR, Evans RD, Glatz JF, Luiken JJ, Griffin JL, Clarke K (2013) Differential translocation of the fatty acid transporter, FAT/CD36, and the glucose transporter, GLUT4, coordinates changes in cardiac substrate metabolism during ischemia and reperfusion. *Circ Heart Fail* 6:1058-1066.
415. Lewandowski ED, White LT (1995) Pyruvate dehydrogenase influences postischemic heart function. *Circulation* 91:2071-2079.
416. Skierczynska A, Beresewicz A (2010) Demand-induced ischemia in volume expanded isolated rat heart; the effect of dichloroacetate and trimetazidine. *J Physiol Pharmacol* 61:153-162.
417. Wahr JA, Childs KF, Bolling SF (1994) Dichloroacetate enhances myocardial functional and metabolic recovery following global ischemia. *J Cardiothorac Vasc Anesth* 8:192-197.
418. Barak C, Reed MK, Maniscalco SP, Sherry AD, Malloy CR, Jessen ME (1998) Effects of dichloroacetate on mechanical recovery and oxidation of

physiologic substrates after ischemia and reperfusion in the isolated heart. *J Cardiovasc Pharmacol* 31:336-344.

419. Liu B, Clanachan AS, Schulz R, Lopaschuk GD (1996) Cardiac efficiency is improved after ischemia by altering both the source and fate of protons. *Circ Res* 79:940-948.

420. Calvert LD, Shelley R, Singh SJ, Greenhaff PL, Bankart J, Morgan MD, Steiner MC (2008) Dichloroacetate enhances performance and reduces blood lactate during maximal cycle exercise in chronic obstructive pulmonary disease. *Am J Respir Crit Care Med* 177:1090-1094.

421. Koshkarian GM (1995) Congestive heart failure and sodium dichloroacetate. *J Am Coll Cardiol* 25:804-805.

422. Bersin RM, Wolfe C, Kwasman M, Lau D, Klinski C, Tanaka K, Khorrami P, Henderson GN, de Marco T, Chatterjee K (1994) Improved hemodynamic function and mechanical efficiency in congestive heart failure with sodium dichloroacetate. *J Am Coll Cardiol* 23:1617-1624.

423. Lopaschuk GD, Barr R, Thomas PD, Dyck JR (2003) Beneficial effects of trimetazidine in ex vivo working ischemic hearts are due to a stimulation of glucose oxidation secondary to inhibition of long-chain 3-ketoacyl coenzyme a thiolase. *Circ Res* 93:e33-37.

424. Aasum E, Steigen TK, Larsen TS (1997) Stimulation of carbohydrate metabolism reduces hypothermia-induced calcium load in fatty acid-perfused rat hearts. *J Mol Cell Cardiol* 29:527-534.

425. Mazer CD, Cason BA, Stanley WC, Shnier CB, Wisneski JA, Hickey RF (1995) Dichloroacetate stimulates carbohydrate metabolism but does not improve systolic function in ischemic pig heart. *Am J Physiol* 268:H879-885.

426. Bersin RM, Wolfe C, Kwasman M, Lau D, Klinski C, Tanaka K, Khorrami P, Henderson GN, de Marco T, Chatterjee K (1994) Improved hemodynamic function and mechanical efficiency in congestive heart failure with sodium dichloroacetate. *J Am Coll Cardiol* 23:1617-1624.

427. Wilson JR, Mancini DM, Ferraro N, Egler J (1988) Effect of dichloroacetate on the exercise performance of patients with heart failure. *J Am Coll Cardiol* 12:1464-1469.

428. Lewis JF, DaCosta M, Wargowich T, Stacpoole P (1998) Effects of dichloroacetate in patients with congestive heart failure. *Clin Cardiol* 21:888-892.

429. Levy B, Mansart A, Montemont C, Gibot S, Mallie JP, Regnault V, Lecompte T, Lacolley P (2007) Myocardial lactate deprivation is associated with decreased cardiovascular performance, decreased myocardial energetics, and early death in endotoxic shock. *Intensive Care Med* 33:495-502.
430. Onay-Besikci A (2007) Impact of lactate in the perfusate on function and metabolic parameters of isolated working rat heart. *Mol Cell Biochem* 296:121-127.
431. Lopaschuk GD, Wambolt RB, Barr RL (1993) An imbalance between glycolysis and glucose oxidation is a possible explanation for the detrimental effects of high levels of fatty acids during aerobic reperfusion of ischemic hearts. *J Pharmacol Exp Ther* 264:135-144
432. Lewandowski ED, White LT (1995) Pyruvate dehydrogenase influences postischemic heart function. *Circulation* 91:2071-2079
433. Wahr JA, Olszanski D, Childs KF, Bolling SF (1996) Dichloroacetate enhanced myocardial functional recovery post-ischemia : ATP and NADH recovery. *J Surg Res* 63:220-224
434. Taniguchi M, Wilson C, Hunter CA, Pehowich DJ, Clanachan AS, Lopaschuk GD (2001) Dichloroacetate improves cardiac efficiency after ischemia independent of changes in mitochondrial proton leak. *Am J Physiol Heart Circ Physiol* 280:H1762-1769
435. White LT, O'Donnell JM, Griffin J, Lewandowski ED (1999) Cytosolic redox state mediates postischemic response to pyruvate dehydrogenase stimulation . *Am J Physiol* 277:H626-634.
436. Liu B, Clanachan AS, Schulz R, Lopaschuk GD (1996) Cardiac efficiency is improved after ischemia by altering both the source and fate of protons. *Circ Res* 79:940-948
437. Wambolt RB, Lopaschuk GD, Brownsey RW, Allard MF (2000) Dichloroacetate improves postischemic function of hypertrophied rat hearts. *J Am Coll Cardiol* 36:1378-1385
438. Itoi T, Huang L, Lopaschuk GD (1993) Glucose use in neonatal rabbit hearts reperfused after global ischemia. *Am J Physiol* 265:H427-433
439. Onay-Besikci A, Wagg C, Lopaschuk TP, Keung W, Lopaschuk GD (2007) Alpha-lipoic acid increases cardiac glucose oxidation independent of AMP-activated protein kinase in isolated working rat hearts. *Basic Res Cardiol* 102:436-444.

440. Omar MA, Verma S, Clanachan AS (2012) Adenosine-mediated inhibition of 5'-AMP-activated protein kinase and p38 mitogen-activated protein kinase during reperfusion enhances recovery of left ventricular mechanical function. *J Mol Cell Cardiol* 52:1308-1318.
441. Jaswal JS, Gandhi M, Finegan BA, Dyck JR, Clanachan AS (2007) Inhibition of p38 MAPK and AMPK restores adenosine-induced cardioprotection in hearts stressed by antecedent ischemia by altering glucose utilization. *Am J Physiol Heart Circ Physiol* 293:H1107-114.
442. Jaswal JS, Gandhi M, Finegan BA, Dyck JR, Clanachan AS (2007) p38 mitogen-activated protein kinase mediates adenosine-induced alterations in myocardial glucose utilization via 5'-AMP-activated protein kinase. *Am J Physiol Heart Circ Physiol* 292:H1978-985.
443. Dyck JR, Lopaschuk GD (1998) Glucose metabolism, H⁺ production and Na⁺/H⁺-exchanger mRNA levels in ischemic hearts from diabetic rats. *Mol Cell Biochem* 180:85-93.
444. Zhang L, Jaswal JS, Ussher JR, Sankaralingam S, Wagg C, Zaugg M, Lopaschuk GD (2013) Cardiac insulin-resistance and decreased mitochondrial energy production precede the development of systolic heart failure after pressure-overload hypertrophy. *Circ Heart Fail* 6:1039-1048.
445. Finck BN, Lehman JJ, Leone TC, Welch MJ, Bennett MJ, Kovacs A, Han X, Gross RW, Kozak R, Lopaschuk GD, Kelly DP (2002) The cardiac phenotype induced by PPAR α overexpression mimics that caused by diabetes mellitus. *J Clin Invest* 109:121-130.
446. O'Neill HM, Lally JS, Galic S, Thomas M, Azizi PD, Fullerton MD, Smith BK, Pulinilkunnil T, Chen Z, Samaan MC, Jorgensen SB, Dyck JR, Holloway GP, Hawke TJ, van Denderen BJ, Kemp BE, Steinberg GR (2014) AMPK phosphorylation of ACC2 is required for skeletal muscle fatty acid oxidation and insulin sensitivity in mice. *Diabetologia* 57(8):1693-1702.
447. Eaton S (2002) Control of mitochondrial beta-oxidation flux. *Prog Lipid Res* 41:197-239.
448. Heart and Stroke Foundation Canada (2014) . In: 2014 Report on Health - Creating survivors. Heart and Stroke Foundation of Canada. http://www.heartandstroke.com/atf/cf/%7B99452D8B-E7F1-4BD6-A57D-B136CE6C95BF%7D/HSF_HMReport2014E_web.pdf?_ga=1.144435893.1483929827.1383060350. Accessed October 10 2014.

449. Tarride JE, Lim M, DesMeules M, Luo W, Burke N, O'Reilly D, Bowen J, Goeree R (2009) A review of the cost of cardiovascular disease. *Can J Cardiol* 25:e195-202.
450. Patten RD, Hall-Porter MR (2009) Small animal models of heart failure: development of novel therapies, past and present. *Circ Heart Fail* 2:138-144.
451. Ou L, Li W, Liu Y, Zhang Y, Jie S, Kong D, Steinhoff G, Ma N (2010) Animal models of cardiac disease and stem cell therapy. *Open Cardiovasc Med J* 4:231-239.
452. Zaragoza C, Gomez-Guerrero C, Martin-Ventura JL, Blanco-Colio L, Lavin B, Mallavia B, Tarin C, Mas S, Ortiz A, Egido J (2011) Animal models of cardiovascular diseases. *J Biomed Biotechnol* 2011:497841.
453. Gomes AC, Falcao-Pires I, Pires AL, Bras-Silva C, Leite-Moreira AF (2013) Rodent models of heart failure: an updated review. *Heart Fail Rev* 18:219-249.
454. Milani-Nejad N, Janssen PM (2014) Small and large animal models in cardiac contraction research: advantages and disadvantages. *Pharmacol Ther* 141:235-249.
455. Zolotareva AG, Kogan ME (1978) Production of experimental occlusive myocardial infarction in mice. *Cor Vasa* 20:308-314.
456. Lancaster JJ, Juneman E, Arnce SA, Johnson NM, Qin Y, Witte R, Thai H, Kellar RS, Ek Vitorin J, Burt J, Gaballa MA, Bahl JJ, Goldman S (2013) An electrically coupled tissue-engineered cardiomyocyte scaffold improves cardiac function in rats with chronic heart failure. *J Heart Lung Transplant* 33(4):438-445.
457. Wildgruber M, Bielicki I, Aichler M, Kosanke K, Feuchtinger A, Settles M, Onthank DC, Cesati RR, Robinson SP, Huber AM, Rummeny EJ, Walch AK, Botnar RM (2014) Assessment of myocardial infarction and postinfarction scar remodeling with an elastin-specific magnetic resonance agent. *Circ Cardiovasc Imaging* 7:321-329.
458. Kolseth SM, Rolim NP, Salvesen O, Nordhaug DO, Wahba A, Hoydal MA (2014) Levosimendan improves contractility in vivo and in vitro in a rodent model of post-myocardial infarction heart failure. *Acta Physiol (Oxf)* 210:865-874.
459. Hausenloy DJ, Yellon DM (2010) The second window of preconditioning (SWOP) where are we now?. *Cardiovasc Drugs Ther* 24:235-254.
460. Baxter GF, Ferdinandy P (2001) Delayed preconditioning of myocardium: current perspectives. *Basic Res Cardiol* 96:329-344.

461. Couzin-Frankel J (2013) When mice mislead. *Science* 342:922-3, 925.
462. Vaillant F, Lauzier B, Poirier I, Gelinas R, Rivard ME, Robillard Frayne I, Thorin E, Des Rosiers C (2014) Mouse strain differences in metabolic fluxes and function of ex vivo working hearts. *Am J Physiol Heart Circ Physiol* 306:H78-87.
463. Larsen TS, Belke DD, Sas R, Giles WR, Severson DL, Lopaschuk GD, Tyberg JV (1999) The isolated working mouse heart: methodological considerations. *Pflugers Arch* 437:979-985.
464. Takala TE, Hassinen IE (1981) Effect of mechanical work load on the transmural distribution of glucose uptake in the isolated perfused rat heart, studied by regional deoxyglucose trapping. *Circ Res* 49:62-69.
465. Burkhoff D, Weiss RG, Schulman SP, Kalil-Filho R, Wannenburg T, Gerstenblith G (1991) Influence of metabolic substrate on rat heart function and metabolism at different coronary flows. *Am J Physiol* 261:H741-50.
466. Bell RM, Mocanu MM, Yellon DM (2011) Retrograde heart perfusion: The Langendorff technique of isolated heart perfusion. *J Mol Cell Cardiol* 50(6):940-950.
467. Widen C, Barclay CJ (2005) Resting metabolism of mouse papillary muscle. *Pflugers Arch* 450:209-216.
468. Berry MN, Friend DS, Scheuer J (1970) Morphology and metabolism of intact muscle cells isolated from adult rat heart. *Circ Res* 26:679-687.
469. Haworth RA, Hunter DR, Berkoff HA, Moss RL (1983) Metabolic cost of the stimulated beating of isolated adult rat heart cells in suspension. *Circ Res* 52:342-351.
470. Finegan BA, Lopaschuk GD, Gandhi M, Clanachan AS (1995) Ischemic preconditioning inhibits glycolysis and proton production in isolated working rat hearts. *Am J Physiol* 269:H1767-775.
471. Fraser H, Lopaschuk GD, Clanachan AS (1998) Assessment of glycogen turnover in aerobic, ischemic, and reperfused working rat hearts. *Am J Physiol* 275:H1533-541.
472. Carlsson M, Wessman Y, Almgren P, Groop L (2000) High levels of nonesterified fatty acids are associated with increased familial risk of cardiovascular disease. *Arterioscler Thromb Vasc Biol* 20:1588-1594.

473. Jouven X, Charles MA, Desnos M, Ducimetiere P (2001) Circulating nonesterified fatty acid level as a predictive risk factor for sudden death in the population. *Circulation* 104:756-761.
474. Singh U, Zhong S, Xiong M, Li TB, Sniderman A, Teng BB (2004) Increased plasma non-esterified fatty acids and platelet-activating factor acetylhydrolase are associated with susceptibility to atherosclerosis in mice. *Clin Sci (Lond)* 106:421-432.
475. Goncalves de Albuquerque CF, Burth P, Younes Ibrahim M, Garcia DG, Bozza PT, Castro Faria Neto HC, Castro Faria MV (2012) Reduced plasma nonesterified fatty acid levels and the advent of an acute lung injury in mice after intravenous or enteral oleic acid administration. *Mediators Inflamm* 2012:601032.
476. Riemersma RA (1987) Raised plasma non-esterified fatty acids (NEFA) during ischaemia: implications for arrhythmias. *Basic Res Cardiol* 82 Suppl 1:177-186.
477. Oliver MF (2002) Metabolic causes and prevention of ventricular fibrillation during acute coronary syndromes. *Am J Med* 112:305-311.
478. Rowe MJ, Neilson JM, Oliver MF (1975) Control of ventricular arrhythmias during myocardial infarction by antilipolytic treatment using a nicotinic-acid analogue. *Lancet* 1:295-300.
479. Ritzel RA, Butler AE, Rizza RA, Veldhuis JD, Butler PC (2006) Relationship between beta-cell mass and fasting blood glucose concentration in humans. *Diabetes Care* 29:717-718.
480. Parker JC, VanVolkenburg MA, Levy CB, Martin WH, Burk SH, Kwon Y, Giragossian C, Gant TG, Carpino PA, McPherson RK, Vestergaard P, Treadway JL (1998) Plasma glucose levels are reduced in rats and mice treated with an inhibitor of glucose-6-phosphate translocase. *Diabetes* 47:1630-1636.
481. Ahren B (1999) Plasma leptin and insulin in C57BI/6J mice on a high-fat diet: relation to subsequent changes in body weight. *Acta Physiol Scand* 165:233-240.
482. Sutherland FJ, Hearse DJ (2000) The isolated blood and perfusion fluid perfused heart. *Pharmacol Res* 41:613-627.
483. Liu B, el Alaoui-Talibi Z, Clanachan AS, Schulz R, Lopaschuk GD (1996) Uncoupling of contractile function from mitochondrial TCA cycle activity and MVO₂ during reperfusion of ischemic hearts. *Am J Physiol* 270:H72-80.

484. Kantor PF, Lucien A, Kozak R, Lopaschuk GD (2000) The antianginal drug trimetazidine shifts cardiac energy metabolism from fatty acid oxidation to glucose oxidation by inhibiting mitochondrial long-chain 3-ketoacyl coenzyme A thiolase. *Circ Res* 86:580-588.
485. McCormack JG, Baracos VE, Barr R, Lopaschuk GD (1996) Effects of ranolazine on oxidative substrate preference in epitrochlearis muscle. *J Appl Physiol* (1985) 81:905-910.
486. Broderick TL, Quinney HA, Lopaschuk GD (1992) Carnitine stimulation of glucose oxidation in the fatty acid perfused isolated working rat heart. *J Biol Chem* 267:3758-3763.
487. Schonekess BO, Allard MF, Lopaschuk GD (1995) Propionyl L-carnitine improvement of hypertrophied heart function is accompanied by an increase in carbohydrate oxidation. *Circ Res* 77:726-734.
488. Belke DD, Larsen TS, Lopaschuk GD, Severson DL (1999) Glucose and fatty acid metabolism in the isolated working mouse heart. *Am J Physiol* 277:R1210-1217.
489. Zhabyeyev P, Gandhi M, Mori J, Basu R, Kassiri Z, Clanachan A, Lopaschuk GD, Oudit GY (2013) Pressure-overload-induced heart failure induces a selective reduction in glucose oxidation at physiological afterload. *Cardiovasc Res* 97:676-685.
490. Jessen N, Koh HJ, Folmes CD, Wagg C, Fujii N, Lofgren B, Wolf CM, Berul CI, Hirshman MF, Lopaschuk GD, Goodyear LJ (2010) Ablation of LKB1 in the heart leads to energy deprivation and impaired cardiac function. *Biochim Biophys Acta* 1802:593-600.
491. Shan L, Li J, Wei M, Ma J, Wan L, Zhu W, Li Y, Zhu H, Arnold JM, Peng T (2010) Disruption of Rac1 signaling reduces ischemia-reperfusion injury in the diabetic heart by inhibiting calpain. *Free Radic Biol Med* 49:1804-1814.
492. Goodwin GW, Cohen DM, Taegtmeyer H (2001) 5-3H]glucose overestimates glycolytic flux in isolated working rat heart: role of the pentose phosphate pathway. *Am J Physiol Endocrinol Metab* 280:E502-508.
493. Leong HS, Grist M, Parsons H, Wambolt RB, Lopaschuk GD, Brownsey R, Allard MF (2002) Accelerated rates of glycolysis in the hypertrophied heart: are they a methodological artifact?. *Am J Physiol Endocrinol Metab* 282:E1039-1045.
494. Barr RL, Lopaschuk GD (2000) Methodology for measuring in vitro/ex vivo cardiac energy metabolism. *J Pharmacol Toxicol Methods* 43:141-152.

495. Lloyd S, Brocks C, Chatham JC (2003) Differential modulation of glucose, lactate, and pyruvate oxidation by insulin and dichloroacetate in the rat heart. *Am J Physiol Heart Circ Physiol* 285:H163-172.
496. Xiong Y, Guan KL (2012) Mechanistic insights into the regulation of metabolic enzymes by acetylation. *J Cell Biol* 198:155-164.
497. Sack MN, Finkel T (2012) Mitochondrial metabolism, sirtuins, and aging. *Cold Spring Harb Perspect Biol* 4: doi 10.1101/cshperspect.a013102 [epub ahead of print].
498. Pillai VB, Sundaesan NR, Gupta MP (2014) Regulation of Akt signaling by sirtuins: its implication in cardiac hypertrophy and aging. *Circ Res* 114:368-378.
499. Newman JC, He W, Verdin E (2012) Mitochondrial protein acylation and intermediary metabolism: regulation by sirtuins and implications for metabolic disease. *J Biol Chem* 287:42436-42443.
500. Anderson KA, Hirschey MD (2012) Mitochondrial protein acetylation regulates metabolism. *Essays Biochem* 52:23-35.
501. Shaw BF, Schneider GF, Bilgicer B, Kaufman GK, Neveu JM, Lane WS, Whitelegge JP, Whitesides GM (2008) Lysine acetylation can generate highly charged enzymes with increased resistance toward irreversible inactivation. *Protein Sci* 17:1446-1455.
502. Verdin E (2014) The many faces of sirtuins: Coupling of NAD metabolism, sirtuins and lifespan. *Nat Med* 20:25-27.
503. Fiorino E, Giudici M, Ferrari A, Mitro N, Caruso D, De Fabiani E, Crestani M (2014) The sirtuin class of histone deacetylases: regulation and roles in lipid metabolism. *IUBMB Life* 66:89-99.
504. Chang HC, Guarente L (2014) SIRT1 and other sirtuins in metabolism. *Trends Endocrinol Metab* 25:138-145.
505. Hirschey MD, Shimazu T, Goetzman E, Jing E, Schwer B, Lombard DB, Grueter CA, Harris C, Biddinger S, Ilkayeva OR, Stevens RD, Li Y, Saha AK, Ruderman NB, Bain JR, Newgard CB, Farese RV, Jr, Alt FW, Kahn CR, Verdin E (2010) SIRT3 regulates mitochondrial fatty-acid oxidation by reversible enzyme deacetylation. *Nature* 464:121-125.
506. Hirschey MD, Shimazu T, Jing E, Grueter CA, Collins AM, Aouizerat B, Stancakova A, Goetzman E, Lam MM, Schwer B, Stevens RD, Muehlbauer MJ, Kakar S, Bass NM, Kuusisto J, Laakso M, Alt FW, Newgard CB, Farese RV, Jr, Kahn CR, Verdin E (2011) SIRT3 deficiency and mitochondrial protein

hyperacetylation accelerate the development of the metabolic syndrome. *Mol Cell* 44:177-190.

507. Bharathi SS, Zhang Y, Mohsen AW, Uppala R, Balasubramani M, Schreiber E, Uechi G, Beck ME, Rardin MJ, Vockley J, Verdin E, Gibson BW, Hirschey MD, Goetzman ES (2013) Sirtuin 3 (SIRT3) protein regulates long-chain acyl-CoA dehydrogenase by deacetylating conserved lysines near the active site. *J Biol Chem* 288:33837-33847.

508. Zhao S, Xu W, Jiang W, Yu W, Lin Y, Zhang T, Yao J, Zhou L, Zeng Y, Li H, Li Y, Shi J, An W, Hancock SM, He F, Qin L, Chin J, Yang P, Chen X, Lei Q, Xiong Y, Guan KL (2010) Regulation of cellular metabolism by protein lysine acetylation. *Science* 327:1000-1004.

509. Jing E, O'Neill BT, Rardin MJ, Kleinridders A, Ilkeyeva OR, Ussar S, Bain JR, Lee KY, Verdin EM, Newgard CB, Gibson BW, Kahn CR (2013) Sirt3 regulates metabolic flexibility of skeletal muscle through reversible enzymatic deacetylation. *Diabetes* 62:3404-3417.

510. Borengasser SJ, Lau F, Kang P, Blackburn ML, Ronis MJ, Badger TM, Shankar K (2011) Maternal obesity during gestation impairs fatty acid oxidation and mitochondrial SIRT3 expression in rat offspring at weaning. *PLoS One* 6:e24068.

511. Alrob OA, Sankaralingam S, Ma C, Wagg CS, Fillmore N, Jaswal JS, Sack MN, Lehner R, Gupta MP, Michelakis ED, Padwal RS, Johnstone DE, Sharma AM, Lopaschuk GD (2014) Obesity-induced lysine acetylation increases cardiac fatty acid oxidation and impairs insulin signalling. *Cardiovasc Res* 103:485-497

512. Fan J, Shan C, Kang HB, Elf S, Xie J, Tucker M, Gu TL, Aguiar M, Lonning S, Chen H, Mohammadi M, Britton LM, Garcia BA, Aleckovic M, Kang Y, Kaluz S, Devi N, Van Meir EG, Hitosugi T, Seo JH, Lonial S, Gaddh M, Arellano M, Khoury HJ, Khuri FR, Boggon TJ, Kang S, Chen J (2014) Tyr phosphorylation of PDP1 toggles recruitment between ACAT1 and SIRT3 to regulate the pyruvate dehydrogenase complex. *Mol Cell* 53:534-548.

513. Milne JC, Lambert PD, Schenk S, Carney DP, Smith JJ, Gagne DJ, Jin L, Boss O, Perni RB, Vu CB, Bemis JE, Xie R, Disch JS, Ng PY, Nunes JJ, Lynch AV, Yang H, Galonek H, Israelian K, Choy W, Iffland A, Lavu S, Medvedik O, Sinclair DA, Olefsky JM, Jirousek MR, Elliott PJ, Westphal CH (2007) Small molecule activators of SIRT1 as therapeutics for the treatment of type 2 diabetes. *Nature* 450:712-716.

514. Mori J, Alrob OA, Wagg CS, Harris RA, Lopaschuk GD, Oudit GY (2013) ANG II causes insulin resistance and induces cardiac metabolic switch and

inefficiency: a critical role of PDK4. *Am J Physiol Heart Circ Physiol* 304:H1103-1113.

515. Li T, Liu M, Feng X, Wang Z, Das I, Xu Y, Zhou X, Sun Y, Guan KL, Xiong Y, Lei QY (2014) Glyceraldehyde-3-phosphate dehydrogenase is activated by lysine 254 acetylation in response to glucose signal. *J Biol Chem* 289:3775-3785.

516. Wang YP, Zhou LS, Zhao YZ, Wang SW, Chen LL, Liu LX, Ling ZQ, Hu FJ, Sun YP, Zhang JY, Yang C, Yang Y, Xiong Y, Guan KL, Ye D (2014) Regulation of G6PD acetylation by SIRT2 and KAT9 modulates NADPH homeostasis and cell survival during oxidative stress. *EMBO J* 33:1304-1320.

517. Horecker BL, Mehler AH (1955) Carbohydrate metabolism. *Annu Rev Biochem* 24:207-274.

518. Kolwicz SC, Jr, Tian R (2011) Glucose metabolism and cardiac hypertrophy. *Cardiovasc Res* 90:194-201.

519. Burgoyne JR, Mongue-Din H, Eaton P, Shah AM (2012) Redox signaling in cardiac physiology and pathology. *Circ Res* 111:1091-1106.

520. Ussher JR, Jaswal JS, Lopaschuk GD (2012) Pyridine nucleotide regulation of cardiac intermediary metabolism. *Circ Res* 111:628-641.

521. Doenst T, Nguyen TD, Abel ED (2013) Cardiac metabolism in heart failure: implications beyond ATP production. *Circ Res* 113:709-724.

522. Pound KM, Sorokina N, Ballal K, Berkich DA, Fasano M, Lanoue KF, Taegtmeyer H, O'Donnell JM, Lewandowski ED (2009) Substrate-enzyme competition attenuates upregulated anaplerotic flux through malic enzyme in hypertrophied rat heart and restores triacylglyceride content: attenuating upregulated anaplerosis in hypertrophy. *Circ Res* 104:805-812.

523. Mallet RT, Sun J (2003) Antioxidant properties of myocardial fuels. *Mol Cell Biochem* 253:103-111.

524. Russell RR, 3rd, Taegtmeyer H (1991) Pyruvate carboxylation prevents the decline in contractile function of rat hearts oxidizing acetoacetate. *Am J Physiol* 261:H1756-1762.

525. Sundqvist KE, Heikkila J, Hassinen IE, Hiltunen JK (1987) Role of NADP⁺ (corrected)-linked malic enzymes as regulators of the pool size of tricarboxylic acid-cycle intermediates in the perfused rat heart. *Biochem J* 243:853-857.

526. Peuhkurinen KJ (1984) Regulation of the tricarboxylic acid cycle pool size in heart muscle. *J Mol Cell Cardiol* 16:487-495.
527. Nishimura M, Uyeda K (1995) Purification and characterization of a novel xylulose 5-phosphate-activated protein phosphatase catalyzing dephosphorylation of fructose-6-phosphate,2-kinase:fructose-2,6-bisphosphatase. *J Biol Chem* 270:26341-26346.
528. Doiron B, Cuif MH, Chen R, Kahn A (1996) Transcriptional glucose signaling through the glucose response element is mediated by the pentose phosphate pathway. *J Biol Chem* 271:5321-5324.
529. Leong HS, Grist M, Parsons H, Wambolt RB, Lopaschuk GD, Brownsey R, Allard MF (2002) Accelerated rates of glycolysis in the hypertrophied heart: are they a methodological artifact?. *Am J Physiol Endocrinol Metab* 282:E1039-1045.
530. Chess DJ, Khairallah RJ, O'Shea KM, Xu W, Stanley WC (2009) A high-fat diet increases adiposity but maintains mitochondrial oxidative enzymes without affecting development of heart failure with pressure overload. *Am J Physiol Heart Circ Physiol* 297:H1585-1593.
531. Zimmer HG, Ibel H, Steinkopff G (1980) Studies on the hexose monophosphate shunt in the myocardium during development of hypertrophy. *Adv Myocardiol* 1:487-492.
532. Meerson FZ, Spiritchev VB, Pshennikova MG, Djachkova LV (1967) The role of the pentose-phosphate pathway in adjustment of the heart to a high load and the development of myocardial hypertrophy. *Experientia* 23:530-532.
533. Gupte SA, Levine RJ, Gupte RS, Young ME, Lionetti V, Labinsky V, Floyd BC, Ojaimi C, Bellomo M, Wolin MS, Recchia FA (2006) Glucose-6-phosphate dehydrogenase-derived NADPH fuels superoxide production in the failing heart. *J Mol Cell Cardiol* 41:340-349.
534. Hecker PA, Lionetti V, Ribeiro RF, Jr, Rastogi S, Brown BH, O'Connell KA, Cox JW, Shekar KC, Gamble DM, Sabbah HN, Leopold JA, Gupte SA, Recchia FA, Stanley WC (2013) Glucose 6-phosphate dehydrogenase deficiency increases redox stress and moderately accelerates the development of heart failure. *Circ Heart Fail* 6:118-126.
535. Rajasekaran NS, Connell P, Christians ES, Yan LJ, Taylor RP, Orosz A, Zhang XQ, Stevenson TJ, Peshock RM, Leopold JA, Barry WH, Loscalzo J, Odelberg SJ, Benjamin IJ (2007) Human alpha B-crystallin mutation causes oxido-reductive stress and protein aggregation cardiomyopathy in mice. *Cell* 130:427-439.

536. Joseph D, Kimar C, Symington B, Milne R, Essop MF (2014) The detrimental effects of acute hyperglycemia on myocardial glucose uptake. *Life Sci* 105:31-42.
537. Mapanga RF, Joseph D, Symington B, Garson KL, Kimar C, Kelly-Laubscher R, Essop MF (2014) Detrimental effects of acute hyperglycaemia on the rat heart. *Acta Physiol (Oxf)* 210:546-564.
538. Katare R, Oikawa A, Cesselli D, Beltrami AP, Avolio E, Muthukrishnan D, Munasinghe PE, Angelini G, Emanuelli C, Madeddu P (2013) Boosting the pentose phosphate pathway restores cardiac progenitor cell availability in diabetes. *Cardiovasc Res* 97:55-65.
539. Du Y, Kowluru A, Kern TS (2010) PP2A contributes to endothelial death in high glucose: inhibition by benfotiamine. *Am J Physiol Regul Integr Comp Physiol* 299:R1610-1617.
540. Katare R, Caporali A, Emanuelli C, Madeddu P (2010) Benfotiamine improves functional recovery of the infarcted heart via activation of pro-survival G6PD/Akt signaling pathway and modulation of neurohormonal response. *J Mol Cell Cardiol* 49:625-638.
541. Ceylan-Isik AF, Wu S, Li Q, Li SY, Ren J (2006) High-dose benfotiamine rescues cardiomyocyte contractile dysfunction in streptozotocin-induced diabetes mellitus. *J Appl Physiol* (1985) 100:150-156.
542. Fraser DA, Hessvik NP, Nikolic N, Aas V, Hanssen KF, Bohn SK, Thoresen GH, Rustan AC (2012) Benfotiamine increases glucose oxidation and downregulates NADPH oxidase 4 expression in cultured human myotubes exposed to both normal and high glucose concentrations. *Genes Nutr* 7:459-469.